

FORM-FINDING FRAMEWORK FOR FRP SHELLS

A MULTI-STEP STRUCTURAL OPTIMIZATION TOOL FOR PRELIMINARY FRP DESIGNS

MASTER THESIS
BUILDING ENGINEERING // STRUCTURAL DESIGN TRACK
TU DELFT // FACULTY OF CIVIL ENGINEERING (CiTG)

AUTHOR

Mohamad Tuffaha
mohamad.h.tuffaha@gmail.com

October 18th, 2019

GRADUATION COMMITTEE:

Prof. ir. Rob Nijse (Chair)	CiTG // Applied Mechanics - Building Engineering
Dr. Marko Pavlovic	CiTG // Engineering Structures -Steel and Composite Structures
ir. Lennert van der Linden (Supervisor)	CiTG // Applied Mechanics - Building Engineering

ACKNOWLEDGEMENT

I would like to thank the members of my committee for their counsel throughout this research. I am particularly grateful to Professor R.Nijse, who agreed to chair my thesis committee. Professor Nijse's commitment to his students and his passion for structural design have enriched my thesis experience in particular, and my time at TU Delft, in general.

I am especially grateful for Lennert van der Linden's supervision of my graduation project. His guidance, practical help, and insightful feedback were instrumental to this research. Always available to discuss my work, he challenged me to venture into new grounds and explore the boundaries of my topic.

Furthermore, I appreciate Dr. M. Pavlovic's involvement from the research's earliest formulation. His expertise in FRP and general input were pivotal to framing and guiding my scope of work.

I would like to extend a special message of gratitude to Laurent Ney for his availability and involvement throughout. His firm's project, the Wilhelminaberg Viewpoint, served as the case-study to my research. I appreciate the opportunity to work with such an innovative and challenging structure and to be entrusted with the necessary information to propose this new tool. I would also like to thank Bart Bols, project engineer at Ney & Partners, for answering all my questions regarding the case-study.

I am very grateful for my time at TU Delft. I thank my professors and colleagues who made these two years an invaluable experience.

Finally, I am greatly indebted to my family and friends for their support and encouragement throughout this process.

Fibre reinforced polymers, or FRP, are increasingly used in structural engineering applications. Permeating the construction field from the aerospace industry, FRP are applied in both the rehabilitation of existing degrading structures as well as the conception of new projects such as pedestrian and traffic bridges or building facades. The increase of interest and use in FRP in recent decades is driven by the material's advantageous properties. Its tailorable mechanical properties, long-term durability, customizable free-form design, and its light-weight feature have engrained FRP as a noteworthy alternative to traditional construction materials such as concrete, steel, or timber. This is of paramount importance in light of the climate change challenge facing structural engineers today. While the material properties have been extensively investigated over the past decades, the structural use in FRP have remained limited to specific applications. As such, FRP, material of the future, has fallen short of its aspirations, disappointing its most ardent proponents. A rift is identified between the academic setting of laboratory testing and the pragmatic essence of the construction industry. This research situates itself as part of the efforts interrogating the industry limits and attempting to bridge these two spheres. It proposes to answer the following research question:

What strategies capitalize on FRP's favorable mechanical properties in order to promote formal exploration with the material in the preliminary phase of a design considering its durable and sustainable potential?

This research proposes a tool that capitalizes on the advantageous mechanical properties of FRP and encourages formal exploration in FRP at the conception phase of a design. Considering the climate change threat, the stakes of such a catalyst framework are high. The Wilhelminaberg Viewpoint, a landmark project in Landgraaf (NL) designed by Ney & Partners, is used as case-study to implement the proposed framework. It also allows to draw a contrast between what is structurally feasible in FRP and what is realistically buildable in FRP.

To develop such a tool, the research starts with a literature review of FRP's mechanical properties, durable and sustainable performance, and the general elaboration around modern form-finding. As a composite material, FRP combines reinforcement (fiber) with a matrix (resin) as its main constituents to form a lamina. Mechanical properties of a laminate can then be derived from the properties of its constitutive laminae using the Classical Lamination Theory (CLT). Examining the available optimization methods, classical form-finding methods have clearly inherited many limitations of the physical methods on which they are based: isotropy, constant material properties, and uniform stresses. In contrast, modern form-finding tools allow to investigate new frontiers such as the orthotropic nature of FRP. This research extrapolates from the lesson learned from FRP optimization techniques, adapting the strategies used in aerospace applications to the construction industry.

With modern form-finding, shape resistant structures in composites that transfer their loads dominantly through in-plane forces can be derived. These correspond to structure exhibiting shell-like behavior. As such, formal exploration in FRP will capitalize on the material's strength (in-plane stiffness) with minimal and efficient use of the materials (weight). This optimization framework first limits the form-finding to two main objectives: maximizing the structural stiffness to generate shape resistant structure and minimizing the weight of the geometry for efficient material use. Considering this framework will require both material and geometric parameters, evolutionary algorithms (EA) are chosen as a tool to generate optimal structures. Despite their disadvantages, EA offer significant benefits in converging to an optimum solution in large and complex search spaces. Following an empirical exploration of the available tools for designers, specifically plug-ins in Grasshopper, an optimization framework is developed.

A multi-step single-objective optimization is proposed. First, stiffness for a certain design boundary is maximized. Using a brute force algorithm, the first level iterates through all the possible laminate layup combinations to find the combination which generates the stiffest structure. The second level of the optimization finds the lightest geometries using a genetic algorithm. This suggested framework offers an answer to the research question, mentioned hereinabove. Completely integrated in one interface (Grasshopper 3D), the developed tool stimulates formal exploration in FRP structures exhibiting shell-like behavior. The user defines the design boundaries, design constraints, load-cases, and material properties and implements the framework.

In this research, the tool is applied for the Wilhelminaberg Viewpoint case-study, and run with eight different geometric scenarios. These eight geometric scenarios are the combination of three different aspects: triangular vs quadrilateral cross-section, symmetric vs. asymmetric geometries, and fixed-deck and cantilevering deck. Implementing the tool on the case-study, the following observations are made:

- In the first level of the optimization, the stiffest laminate layup combination found reduces the strain energy by a factor of 1.2 or a relative difference of 20% when compared to the least stiff laminate combination. Similarly, the deflection is reduced by a factor of 2.2 (or a relative decrease of 69%) between the stiffest and least stiff laminate layup combination.
- The second level optimization finds the lightest geometry that verifies the design constraints. In comparing the eight FRP scenarios suggested for the case-study, a weight saving of 35% can be achieved between the best and the worst performing structure. Most importantly, the generated FRP structure are about 70% lighter than their steel counterparts, highlighting the potential of weight savings with FRP.

Once run, the research offers a critical post-optimality assessment of the geometries, comparing their performance on three distinct levels: computational efficiency, material efficiency, and their production efficiency. This allows to address the general production considerations and assess the landscape of the FRP industry. Assessing production efficiency proves to be challenging; it requires to work out a construction logic for the structure from production to assembly. Thus, a close collaboration with a specialized contractor from the early stages can prove to be beneficial: it allows to incorporate manufacturing constraints in the optimization process, rather than only in the post-optimality analysis. Other measures are suggested as means to strive towards integrated designs.

This research ends with critical reflections on larger themes relating to the developed tool such as integration in structural design, parametric modeling, and free-form architecture in FRP as well as recommendations to users and further investigations to improve the proposed tool.

key words: fiber reinforced polymers - FRP // form-finding // structural optimization // evolutionary algorithm - EA // genetic algorithm - GA // alternative materials.

TABLE OF CONTENTS

INTRODUCTION	1. Research Motivation	1
	1.1 On Sustainability	1
	1.2 On Alternative Construction Materials	2
	2. Research Question	2
	3. Objectives	2
	4. Research Methodology	3
I. LITERATURE REVIEW	<u>Chapter 1: FRP, from Constituents to Production</u>	5
	1. FRP, A Composite Material	6
	1.1 Matrix	7
	i. Thermoplastic Polymers	7
	ii. Thermoset Polymers	7
	1.2 Reinforcement	8
	2. Production Methods	9
	2.1 Open-mould	9
	2.2 Closed-mould: Vacuum infusion	9
	3. Practical Limitations	10
	4. Conclusion	11
	<u>Chapter 2: Mechanical Properties of FRP composites</u>	13
	1. FRP, an Anisotropic Material	14
	1.1 Stress-Strain Relationship of a lamina	14
	1.2 Transformation of stresses and strains	15
	2. Classical Lamination Theory (CLT)	16
	2.1 CLT Steps	16
	2.2 Rules of Thumb and Recommendations for Designing in FRP	18
	3. Failure Mechanisms	19
	3.1 Intralaminar Failure	19
	i. Maximum Stress Criterion	19
	ii. Maximum Strain Criterion	20
	iii. Tsai-Wu Criterion	20
	3.2 Discussions of Lamina Failure Criteria	20
	3.3 Failure Analysis of a Laminate	21
	4. Conclusion	22

<u>Chapter 3: Durability and Sustainability of FRP</u>	23
1. Sustainability in Structural Design	24
1.1 Solutions for Today	24
1.2 Challenges for the Future	24
1.3 The Research within the Larger Context	25
2. Sustainability of FRP, Framework and Evaluation	25
2.1 Sustainability Framework: Life-Cycle Analysis	25
2.2 Sustainability of Composites	26
2.3 A Nuanced Picture	26
3. Durability of FRP	28
3.1 Mechanical Properties of FRP	28
i. Intralaminar and interlaminar failure mechanisms	28
ii. Fatigue	29
iii. Creep	29
3.2 Environmental Degradation of FRP	30
i. Moisture	30
ii. Corrosion	30
iii. Thermal effects	30
iv. Fire	31
4. Conclusion	32
<u>Chapter 4: From Form-finding to Structural Optimization</u>	33
1. Form-Finding, from Physical to Numerical Methods	34
1.1 Physical Models	34
1.2 Modern Form-Finding	34
1.3 Form-Finding Numerical Methods and their Limitations	36
2. Structural Optimization	36
2.1 Optimization Types	36
2.2 Single Optimization	38
2.3 Multi-Objective Optimization	38
3. Structural Optimization in FRP	40
3.1 Parameters and Objectives	40
3.2 Evaluating the Landscape	42
4. Formal Exploration in FRP	44
4.1 Framework Ambitions	44
4.2 Complex Search Spaces	44
4.3 Evolutionary Algorithms	45
4.4 Available Plug-ins	46
5. Conclusion	47

1. Case-Study	50
1.1 The IBA Context	50
1.2 The IBA Parkstad	51
1.3 The Wilhelminaberg Viewpoint	51
1.4 Wilhelminaberg Viewpoint Renders	52
1.5 An FRP Manifesto?	53
2. Tool Development	54
2.1 Optimization Objectives	54
i. Stiffness Maximization	54
ii. Weight Minimization	54
2.2 From a Multi-Objective to a Single-Objective Design	54
2.3 Multi-Step Single Objective Optimization	56
3. The Proposed Framework	56
3.1 Design Boundary	58
3.2 Geometric Parameters	59
i. Defined Scenarios	60
ii. Geometry Generation	62
3.3 Material Parameters	64
3.4 Load-Cases and Applied-Loads	66
i. Load-Cases	66
ii. Applied Load-Areas	66
iii. Pre-Stressed Cables	68
3.5 Design Constraints	68
i. FRP stress criterion for laminae and laminate	69
ii. Deflection	69
iii. Buckling Load-Factor	69
3.6 Stiffness Optimization	70
i. Modeling the Orthotropic Material in Grasshopper and Karamba3D	71
3.7 Weight Optimization	72
i. Fitness Function and Penalty	72
ii. GA Algorithm: Galapagos	73
4. Limitations	75
4.1 Genetic Algorithm Limitations	75
4.2 Generative Modeling	76
i. On Mesh Size	76
ii. On Mesh Type	76
5. Conclusion	77

1.Results

80

1.1 Level of the Optimization: Maximizing Stiffness

80

1.2 Level 2 of the Optimization: Minimizing Weight

83

i. Triangular Symmetric Fixed-width Deck

84

ii. Triangular Symmetric Cantilevering Deck

86

iii. Triangular Asymmetric Fixed-width Deck

88

iv. Triangular Asymmetric Cantilevering Deck

90

v. Quadrilateral Symmetric Fixed-width Deck

92

vi. Quadrilateral Symmetric Cantilevering Deck

94

vii. Quadrilateral Asymmetric Fixed-width Deck

96

viii. Quadrilateral Asymmetric Cantilevering Deck

98

2. Post-optimality Study

100

2.1 Computational Efficiency

101

i. Framework

101

ii. Results

101

iii. Discussion

102

2.2 Material Efficiency

103

i. Framework

103

ii. Results

103

iii. Discussion

104

iv. Comparison with Steel

104

2.3 Production efficiency

106

i. Construction

108

ii. Production Efficiency

108

iii. Manufacturing

108

iv. Connections

110

3. Integrated Design

114

3.1 Towards an Integrated Design

114

3.2 Post-Optimality Assessment

116

4. Conclusion

118

DISCUSSIONS

1. Answer to the research question

119

2. Critical Reflections

120

2.1 On the developed Framework and its Limitations

120

2.2 On Integration in Structural Design

121

2.3 On Parametric Modeling

121

2.4 On Free-Form Architecture in FRP

122

2.5 On the Case-Study

122

3. Conclusions

124

3.1 On the Proposed Framework

124

3.2 On the Case-Study

124

i. Qualitative Conclusions

124

ii. Quantitative Conclusions

125

4. Recommendations

126

4.1 Structural Designers, Architects, and Contractors

126

	4.2 Researchers and Educators	126
	4.3 The construction Industry	126
	5. Further Investigations	127
BIBLIOGRAPHY	1. Main Report Bibliography	129
	2. Appendices Bibliography	136
APPENDICES	<u>Appendix A.</u>	138
	A1. Thermoset Polymers	138
	A2. Fibers Types	139
	A3. Manufacturing Processes	141
	<u>Appendix B.</u>	142
	B1. Thermal Effects on FRP	142
	B2. Sustainability of Constituent Materials	143
	<u>Appendix C.</u>	144
	C1. Micro-Mechanics of a Lamina	144
	<u>Appendix D</u>	145
	D1. Pareto Optimality	145
	<u>Appendix E</u>	146
	E1. Lamination Parameters	146
	<u>Appendix F</u>	148
	F1. Tool Development: Multi-objective Optimization	148
	<u>Appendix G</u>	150
	G1. Parameters of Scenario 1: Triangular Symmetric Fixed-width Deck	150
	G2. Parameters of Scenario 2: Triangular Symmetric Cantilevering Deck	151
	G3. Parameters of Scenario 3: Triangular Asymmetric Fixed-width Deck	152
	G4. Parameters of Scenario 1: Triangular Asymmetric Cantilevering Deck	153
	G5. Parameters of Scenario 1: Quadrilateral Symmetric Fixed-width Deck	154
	G6. Parameters of Scenario 1: Quadrilateral Symmetric Cantilevering Deck	155
	G7. Parameters of Scenario 1: Quadrilateral Asymmetric Fixed-width Deck	156
	G8. Parameters of Scenario 1: Quadrilateral Asymmetric Cantilevering Deck	157
	<u>Appendix H</u>	158
	H1. Material Properties: Summary	158
	H2. Material Properties: Derivation	160
	<u>Appendix I</u>	164
	I1. Determining Load-Areas	164
	I2. Approximating Cable-effect in the case study	168
	<u>Appendix K</u>	170
	K1. Determining Mesh Size	170
	<u>Appendix L</u>	174
	L1. Search Spaces for the 8 Scenarios	174
	L2. Convergence of Graphs	177
	L3. Natural Frequency of the 8 structures.	178
	L4. Cost Estimates	178
	L5. Production Methods	179
	L6. Joint Design	180
	<u>Appendix M</u>	182
	M1. Performance Graphs	182
	M2. Performance Graphs, using improvement factor	184

LIST OF SYMBOLS

Lamina Properties

E_1	Longitudinal (fibre direction) elastic modulus of the lamina
E_2	Transverse (perpendicular to fibre direction) elastic modulus of the lamina
G_{12}	In-plane shear modulus of the lamina
ν_{12}	Longitudinal Poisson's ratio of a lamina
ν_{23}	Transverse Poisson's ratio of a lamina

Angle

θ	Angle measured counter clock-wise from the global coordinate system to the local coordinate system.
----------	---

Stresses and Strains

σ_1	Normal stress in the longitudinal direction
σ_2	Normal stress in the transverse direction
τ_{12}	In-plane shear stress
ε_1	Normal strain in the longitudinal direction
ε_2	Normal strain in the transverse direction
γ_{12}	In-plane shear strain
ε_{1t}^u	Ultimate tensile strain in the longitudinal direction
ε_{1c}^u	Ultimate compressive strain in the transverse direction
γ_{12}^u	Ultimate in-plane shear strain

Material Properties

f_{1t}	Tensile strength in the fibre direction
f_{2t}	Tensile strength in the transverse direction
f_{1c}	Compressive strength in the fibre direction
f_{2c}	Compressive strength in the transverse direction
f_{12}	In-plane shear strength
σ_1	Normal stress in the longitudinal direction
σ_2	Normal stress in the transverse direction
τ_{12}	In-plane shear stress in the principal material coordinate system

CLT

Q	Stiffness matrix
N	External line loads
M	Resultant moments
A	Extensional stiffness matrix
B	Bending-extension coupling stiffness matrix
D	Flexural stiffness matrix

Optimization

U	Total strain energy
$[E]$	Material stiffness
$\{D\}$	Global degree of freedom vector of the finite element structure
$[K]$	Structural stiffness matrix
$\{R\}$	Consistent global nodal vector

1. Research Motivation

1.1. On Sustainability

Climate change is a prominent challenge facing humanity in the 21st century. Rising sea levels, dramatic increase in global temperatures, and alarming rates of resource depletion have marked the last 30 years. Today, studies predicting the inevitable catastrophic consequences of climate change have become numerous. The timeline to reverse them is all but shortening with every published study. And yet, we can still reverse it [1].

With the dire consequences already underway, tackling the climate threat requires concerted actions from policy makers, researchers, engineers, designers, and educators. Achieving sustainability will require all professionals to challenge their existing framework and work holistically beyond their industry limits. The construction industry, in particular, has the unique opportunity to assume a central role in challenging the *status quo*. Recent studies estimate the contribution of the construction industry to nearly 36% of global final energy use and nearly 40% of energy related carbon emissions [2]. With this significant global impact, the construction industry has the responsibility to evaluate its practices and offer solutions, both on the short and long term.

Numerous challenges face structural engineers today. The environmental concern of climate change must however be addressed as a priority for the profession. So far, efforts to address climate change have materialized through improving the life-cycle performance of our infrastructure, integrating new technologies to reduce buildings' energy consumption, and exploring alternative materials. Nonetheless, mitigating the environmental impact of the construction industry will require a wide-scope questioning of the education, principles, and common practices of structural engineers. Engineers must be involved in every stage of the design process to enact environmental, economic, and social sustainability [3].

1.2 On Alternative Construction Materials

Fiber reinforced polymers, or FRP, have permeated the field of construction from the aerospace industry in the last decades of the 20th century. In recent times, its performance properties, particularly its claims for durability and sustainability, have engrained FRP as the material of the future with its increasing use in infrastructure applications such as bridge decks, facade panels, and fiberglass pipes. While the material's properties have been extensively investigated over the past decades in laboratory settings, their applications have remained limited. As such, FRP, material of the future, has fallen short of its aspirations, disappointing its most ardent proponents [4], [5], and [6]. Significant research is required to fill the divide between laboratory testing and the construction industry. Further research in the following area is required to propel FRP in becoming a prominent and viable material in the construction field:

1. structural optimization methods proper to FRP
2. manufacturing processes
3. durability and sustainability of the material
4. joint design (FRP/FRP joints or FRP/other material joints).

This research positions itself at the boundaries between the pragmatism of the construction industry and the innovation of academic investigation, questioning what has limited FRP's proliferation. Examining available structural optimization methods, it becomes evident that form-finding numerical methods have inherited their corresponding physical experiments limitations of isotropy, constant material properties, and uniform stresses [7], [8]. Designers, such as Ney & Partners, echoed these concerns. Developing a framework for FRP form-finding can lead to more exploration with this alternative material in the preliminary stage and use this material's untapped potential. With FRP's beneficial environmental properties in-mind, the stakes of such a catalyst framework are high. This becomes the point of departure for the research.

Recent trends of digital form-finding coupled with the aforementioned sense of environmental awareness has revealed new horizons for the built environment. This research situates itself as part of the broad effort interrogating the industry's limits, questioning these new horizons. In particular, the research examines the potential of alternative materials, such as fiber reinforced polymers FRP, that have witnessed increased interests in recent decades. Through this investigation, the research lends a critical look at the computational tools and digital architecture, prominent features in today's landscape of structural design.

2. Research Question

What strategies capitalize on FRP's favorable mechanical properties in order to promote formal exploration with the material in the preliminary phase of a design considering its durable and sustainable potential?

3. Objectives

Considering FRP's durable properties and the urgent threat of climate change, this research exists within the profession's efforts to achieve sustainability. Aiming to highlight the influence of FRP material on the design process, this research aims to develop a tool that capitalizes on the mechanical properties of FRP. Developing such a framework can lead to more formal exploration with this alternative material. The framework will be implemented with a chosen case-study. While practical issue will still need to be resolved, this case study provides insight on efficient structural forms in FRP. The research thus highlights the possibilities and ambitions the material has to offer while drawing a contrast between what is structurally feasible and what is realistically buildable in FRP. This research allows to reflect on additional venues of questioning from computational tools that have become prevalent in modern-day structural design and the trends of parametric "free-form" design in general, and in FRP in particular. Ultimately, conclusions and recommendations will be given to structural designers looking to design in FRP.

4. Research Methodology

Figure I. displays the outline of this research showcasing the adopted methodology. The content of each section is then briefly summarized hereinafter.

Introduction	Research Motivation, Research Question, Methodology
I-Literature Review	<ol style="list-style-type: none">1. FRP, from Constituents to Production2. Mechanical Properties of FRP3. Durability and Sustainability of FRP4. From Form-Finding to Optimization
II-Optimization tool	Case-Study Context & Optimization Framework Definition of framework: parameters and their scenarios, boundary conditions, material properties, load cases, design constraints, objective functions, and the chosen optimization algorithms.
III- Results & Post-Optimality Analysis	Results of the optimization for the eight different scenarios Post-Optimality Study: Evaluating the solutions according to different perspectives (computational efficiency, material efficiency, and production efficiency) and decides on an optimal design.
Discussions	Answer to the research questions, critical reflection on the thesis' main themes, recommendations, shortcomings.,etc.

Figure I. Outline of this research showing the research framework and the adopted methodology.

PART I. LITERATURE REVIEW

Chapter 1: FRP, from Constituents to Production

Chapter 1 reviews the state-of-the-art on fiber reinforced polymers in terms of knowledge of fibers/reinforcement. matrix-resin systems, and the most important production methods. The chapter aims to answer the following sub-questions:

- What is a composite material?
- What are FRP's main constituents and properties?
- What are its main production methods?
- What are practical limitations?

Chapter 2: Mechanical Properties of FRP Composites

Chapter 2 provides a framework to understand the anisotropic behavior of FRP through explaining the classical lamination theory (CLT) and the failure mechanisms dominating laminae and laminates. The chapter aims to answer the following sub-questions:

- How to define FRP's anisotropic material?
- What are rules of thumb for designing in FRP?
- What are FRP's failure mechanisms?

Chapter 3: Durability & Sustainability of FRP

Chapter 3 highlights the environmental challenges facing structural engineers today and what action courses can be taken. It then discusses the sustainability ambitions of FRP in particular and focuses on the in-service properties of the composite material (impact, fire resistance, etc.). The chapter aims to answer the following sub-questions:

- What is the environmental challenge facing structural engineers?
- What is a proper framework to study sustainability?
- What is the definition of durability?
- What are the mechanical failure mechanisms of FRP?
- What environmental conditions cause degradation of FRP?

Chapter 4: From Form-finding to Structural Optimization

Chapter 4 reviews the state-of-the art on the optimization methods available for form-finding and then focus on methods applied for FRP structures particularly those applied at the macroscale (shape and geometry). The chapter aims to answer the following sub-questions:

- What physical methods of form-finding are available for engineers? What are their limitations?
- What is structural optimization and how can it solve those limitations?
- What specific strategies can be applied for design in FRP?

PART II. OPTIMIZATION TOOL

Case-Study Context and Optimization Framework

Chapter 5 establishes the context of the chosen case-study. It then defines the framework of the developed tool, specifying its important aspects: parameters and their scenarios, boundary conditions, material properties, load cases, design constraints, objective functions, and the chosen optimization algorithms. The chapter ends with recounting the step of the tool development from choosing objectives to deciding on mesh size.

PART III. RESULTS AND POST-OPTIMALITY ANALYSIS

Chapter 6 presents the results of the optimizations run for the described scenarios of the case-study. After presenting the results, a post-optimality study evaluates the generated geometries from different perspectives and chooses the most integrated structures.

DISCUSSIONS

The final chapter answers the research question. It then offers critical reflection on the developed optimization tool as well as the broader themes of the research such as the role of computational tools in today's industry, integration in architecture, and free-form architecture in FRP. Lastly, it proposes recommendation for structural engineers to adopt for designing in FRP. The thesis ends with possible applications of the tool and future investigations with respect to the limitations of the design approach.

PART I. LITERATURE REVIEW

CHAPTER 1

FRP, FROM CONSTITUENTS TO PRODUCTION

In recent years, fiber-reinforced polymers have increasingly permeated the civil engineering field from the aerospace and maritime industries. This increasing interest has been driven by innovations in FRP systems and the committed involvement of civil engineers to build more efficiently and, most importantly, more durably.

Designing and optimizing FRP structural elements requires a baseline understanding of the composite material, particularly the properties of its constituents. As such, this chapter introduces composite materials and the necessary knowledge to lay the grounds for the optimization process that will follow. The chapter outlines the constituents of composite materials (both fiber and matrix systems), their respective roles, types, and properties. Brief descriptions of the main manufacturing processes of FRP are also presented, already eliciting boundaries for the production phase.

The chapter aims to answer the following sub-questions:

- What is a composite material?
- What are FRP's main constituents and properties?
- What are its main production methods?
- What are practical limitations?

1. FRP, A Composite Material

Composite materials are defined as a combination of two or more materials that together present better properties than those of the individual components. As such, fiber-reinforced polymers are a composite material, made of two principal constituents: the matrix and the reinforcement. This two-phase composite material is produced by dispersing the reinforcement (primary phase) in the polymer (secondary phase). This combination results in many advantages: a higher specific strength, a higher specific stiffness in one direction, and a lighter material density that results in lightweight elements [4], [5], [6], [9].

An account of the advantages and disadvantages is presented in table 1.1:

Advantages	Disadvantages
<ul style="list-style-type: none">- Light density resulting in weight saving.- Tailorable layup for optimal strength and stiffness for the desired application.- Long-durability properties lending to a sustainable material.- Non-corrosive properties (water and chemical resistance) resulting in low total maintenance costs.- Available automated manufacturing processes that can reduce assembly time.- Customizable production for free-form shape.- High degree of service integration possible.	<ul style="list-style-type: none">- High costs of raw materials.- Advanced computational methods often required (finite element analysis) for complex load paths.- Limited knowledge of long-term durability properties: the material is not fully recyclable.- Undesirable in-service properties, such as risk of delamination or low resistance to impact, temperatures, or fire.- Non-competitive means for non-repetitive production processes.

Table 1.1: Advantages and disadvantages of fiber-reinforced polymers.

The properties of composite material depend on the properties of its constituents:

- The types of used fibers and resin and their respective properties.
- The orientation of the fibers in respect to the direction of loading.
- The adhesion between the fiber and resin, particularly at the interface between the two constituents.
- It then becomes important to give an overview of the properties and types of FRP's constituents.

FRP's two main constituents are the matrix and reinforcement, as shown in figure 1.1.

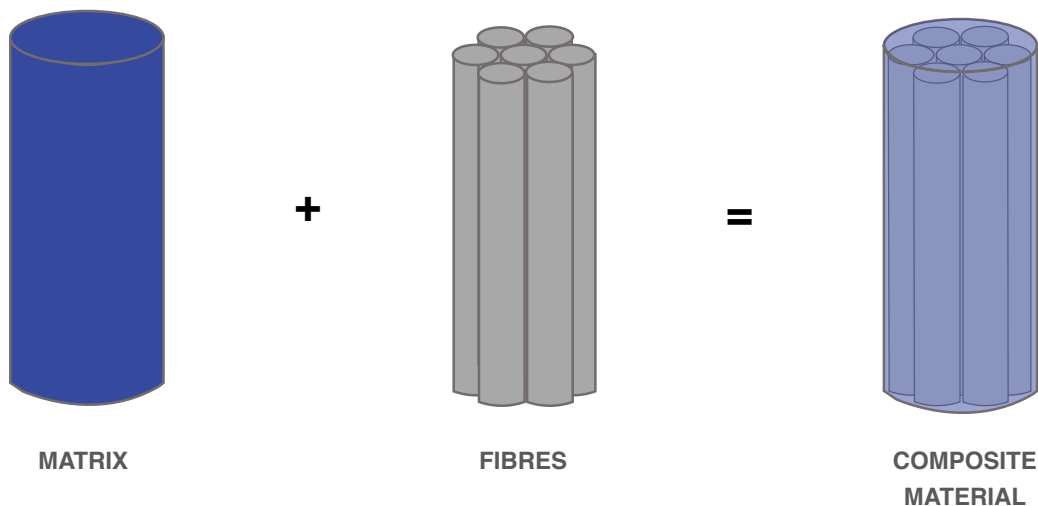


Figure 1.1 FRP's two main constituents [10].

1.1 Matrix

The polymer provides the continuous phase of the composite material. Surrounding the fibers, the polymer is also referred to as the matrix and is required to fulfill the following functions:

- Fixing the fibers in the required geometrical arrangement (orientation);
- transferring the stresses to the fibers efficiently by adhesion and friction;
- Preventing premature failure due to micro-buckling of fibers, in terms of compression;
- Protecting the fibers from environmental impact (corrosion, temperature, UV radiation, moisture, etc.); and
- Providing the composite with appropriate fire resistance, toughness, impact and abrasion tolerance.

All polymers resins are long chain molecules formed through polymerization, a chemical reaction that combines identical structural units (monomers) with covalent bonds. While there are many different polymer matrices that can be utilized for composite materials, polymeric matrices are classified in two categories, as either thermoplastic or thermosetting polymers [11], [12].

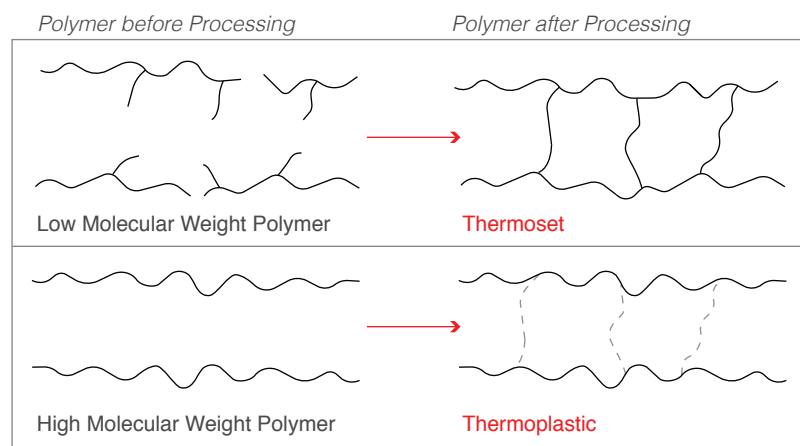


Figure 1.2 Thermoset and Thermoplastic Molecular Chains [10].

i. Thermoplastic Polymers

Thermoplastic polymer resins do not form any cross-link upon curing; their chains are rather held together by weak secondary bonds. With a high-viscosity and high melting points, thermoplastics require considerably high temperatures and pressure for curing. They offer however the advantage of short processing cycles as they are not chemically crosslinked.

With no crosslinks, they soften every time they are heated above their melting temperature and regain their solid shapes when cooled down. As such, thermoplastic polymers are tolerant to damage and resistant to low-velocity impact; they are good candidates for recycling or repair. As a general class of polymers, thermosets account for the majority of polymers produced. However, their behavior prone to creep and their very low-fire resistance have hindered their widespread in structural applications.

ii. Thermoset Polymers

Thermosets start as low molecular weight and low viscosity monomers that are converted into a three-dimensional rigid cross-linked structure during the curing process. The curing process is driven by heat generated either externally or by the reaction itself (exothermically). They mostly require a longer processing time to form the additional crosslinks, needed to form a fully cured resin [4], [6], [13].

As thermoset resins form during curing an intractable solid, they cannot be reprocessed by heating. At high temperatures, thermosets disintegrate; their mechanical properties worsen considerably. Due to the high cross-link densities needed for high-performance thermosets, they are brittle and additional steps are needed to enhance their

toughness. With the improved toughening approaches available today, thermoset exhibit toughness comparable to that of thermoplastic systems. The better performance of thermosets in creep and fire-resistance than thermoplastic resins has rendered them widely used in the civil engineering industry. Most common types of thermosets are polyester resins, vinyl ester resins, epoxy resins, and phenolic resins. A closer attention to each resin is discussed in appendix A1.

1.2 Reinforcement

The reinforcement constituents of composite materials can be particles, whiskers, or fibers. Without a preferred orientation, particles provide minimal reinforcement and only a slight in mechanical properties. Small in both length and diameter, whiskers are strong reinforcement but are more difficult to disperse uniformly in the polymer phase. As such, fibers become the predominant reinforcement for advanced composites due to their high ultimate strength and relatively high stiffness. With a longer axis compared to particles and whiskers and mostly circular, fibers can supply the main load-bearing and stiffness functions of an FRP structure [4], [6], [13].

Fibers are often processed into other product such as strands, yarns, or textiles. A single filament can be compactly bundled into a strand. Fibers can be compactly bundled into a parallel strand with twisting, a yarn, or without twisting, a roving. Rovings can be chopped into short fiber segments for molding and exhibit higher mechanical properties than yarn. Fibers are available in multiple products such as glass fibers, carbon or graphite fibers, aramid fibers, and woven fabrics. The application of each depend on a compromise between structural properties, available budget, and durability. A more extensive discussion of each of the available fiber type in discussed in appendix A2.

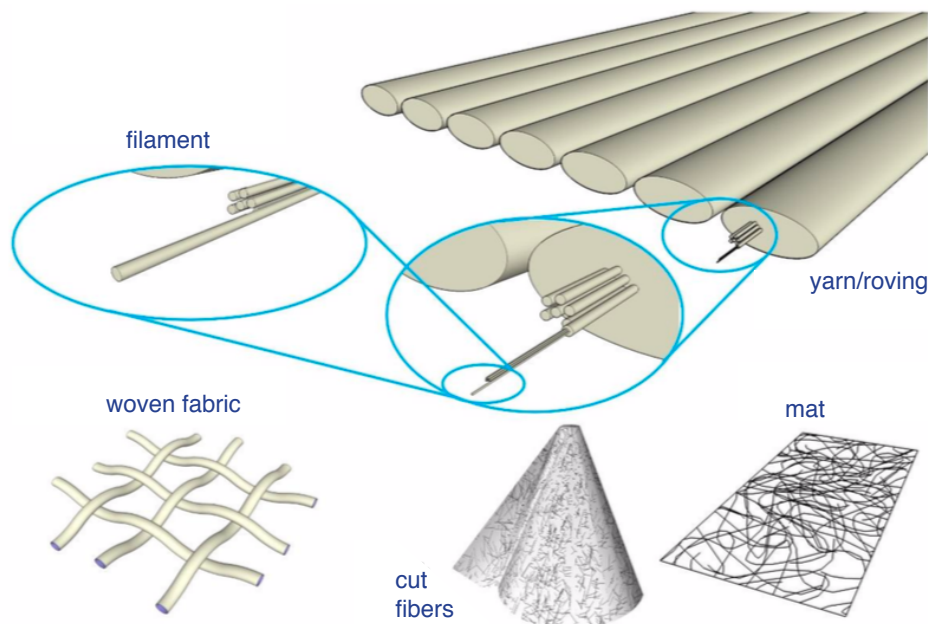


Figure 1.3 Types of reinforcement, from fiber to textile [4].

2. Production Methods

The choice of a production methods or a combination of multiple production methods is of paramount importance. For each product, there exists a delicate balance between knowledge, available technologies, and expected outcome. As such, the main criteria driving the choice of production methods are numerous: temperature, pressure, curing rate, materials and tools utilized, single or serial production, desired surface quality, used materials, and costs.

With the numerous technologies available for composite sections, the choice of production method becomes a challenging one. Each of these techniques presents its specific areas of applications as well as its limitations, its advantages and disadvantages. Accordingly, an overview of the most commonly used techniques is discussed hereinafter, with a specific attention to vacuum infusion, deemed most useful for this form-form structure. The production processes are classified in two categories: open and closed-mold technologies [4], [11].

2.1 Open-mold

As its name indicates, open-mold processes only involved a mold on which the product is made without the need to be covered by a second mold or vacuum film during the impregnation. As it is not possible to control the pressure during impregnation, emissions of volatile substance are more common in open-mold processes. The two most common open-mold processes are two of the simplest production methods, spray-up and hand layup. These two methods are considered cost-effective and even low-tech as they only require simple tools and a small number of materials. These methods are very labor intensive and can result in resin-starved areas as the impregnation is done by hand.

Other open mold processes include filament winding for bodies of revolution. Compression molding or pultrusion are other methods of production often use for mass production of components. More extensive descriptions of open-mold processes are presented in appendix A3.

2.2 Closed-mold: Vacuum infusion

Vacuum infusion is a closed-mold production method. As such, vacuum-infusion can only be performed with a closed-off and air-tight setting: the workpiece is impregnated at atmospheric pressure and air is extracted by a vacuum pump. With the process rather simple, large products can be produced with vacuum-infusion.

In the production process, the workpiece is supported on one side by a mold to avoid any creasing (compressing on its plane). A release layer can be added to allow an easy removal after the mold curing. Fibers are then arranged out according to specifications. The built-up the laminate structure is then sealed with a vacuum film, applying a vacuum at one or multiple side of the workpiece. Resin is then infused into the workpiece from a bucket at atmospheric pressure. It flows through the dry fiber reinforcement layup. Once the product is fully impregnated, the flow of resin is stopped and the product is left to cure.

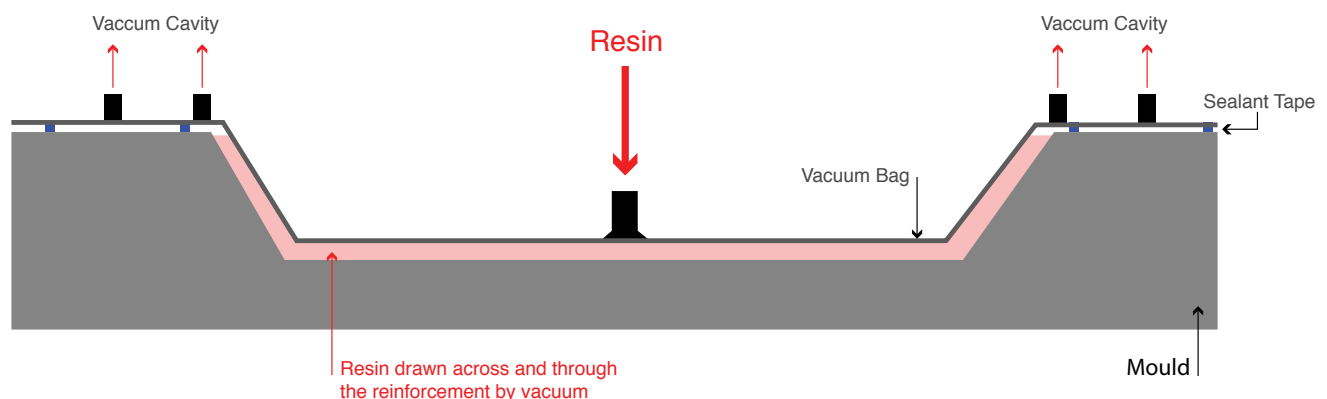


Figure 1.4 Vacuum infusion technique [10].

This production technique can achieve high volume fraction of fibers, up to 55%. However, multiple criteria must be closely controlled during the production in order to obtain a successful. That include resin infusion, resin flow, pressure, and air discharge. Furthermore, these production methods are also heavy on manual labor. It is also costly to prepare the molding of the part to be built. It is thus important to adopt strategies that can minimize production costs, as will be explained in the design process chapter 5. An obvious strategy includes making the structure symmetric limiting the molding to be able to re-use it.



Figure 1.5 (left) Pont y Ddraig, or Dragon Bridge, at Sandown, Isle of Wight, UK.
(right) FRP decks for Pont y Ddraig under construction at AM Structures, Sandown, Isle of Wight [14].

3. Practical Limitations

The limits of the produced parts are often dictated by the production costs of the components and their transportation. The transportation of these components can be done by water, land, or even water. This requirement is sometimes circumvented by having a temporary factory by the construction site to limit the transportation.

A vehicle in Dutch roads is limited by law to the following dimensions: a maximum width of 3.00 m, a maximum height of 4.00m, and a length of 22.00m and maximal mass of 50,000 kg [15]. Larger vehicles require exceptional transport and might need additional permit. In order to prevent damages to the road, it is more practical to not exceed the weight conditions. Exceeding the width and height requirements of the structure is not recommended. However, a larger length is less of a problem as long as the weight is acceptable.

Exceptional sizes can require innovative means of transportation. The Pontresina Bridge in Switzerland is an example of structures transported by helicopter. Long spans can also be transported in cargo through canals. The Dutch company Fibercore has adopted such means for its bridges. They produced spans as long as 51m but their most competitive bridges remain 15-16m in length.



Figure 1.6 Temporary lightweight pedestrian bridge in Pontresina (Switzerland), installed each fall and removed in the spring (1997) [16].

4. Conclusion

This chapter provides answers to the following questions:

- What is a composite material?
- What are FRP's main constituents and properties?
- What are its main production methods?
- What are practical limitations?

This chapter offers an introduction to fiber-reinforced polymers as a composite material. FRP is a composite material, made of two principal constituents: the matrix and the reinforcement. The properties of the composite material depend closely on the properties of its constituents.

The matrix refers to the polymeric resin providing the continuous phase of the composite material. An extensive list of the matrix's role is explored in the previous chapter. The distinction between thermoplastic and thermoset polymers is clearly delineated. The better performance of thermosets in creep and fire-resistance than their thermoplastic counterparts has rendered them widely used in the civil engineering industry.

Reinforcement provide the main load-bearing and stiffness of functions of an FRP structure. It is available in many products such as strands, yarns, and textiles. The applications of each type is thus dependent on a compromise between structural properties, defined needs, and available budget. In this research, reinforcement will be fibers can supply the main load-bearing and stiffness functions of the designed FRP structure.

The choice of production methods is an important and challenging decision. Each techniques presents specific applications, benefits, and limitations. Production methods can be classified in two categories: open and closed-mold technologies. The research focuses on vacuum infusion, a closed-mold technique, considered most appropriate for free-form elements in FRP, the focus of the rest of the research. A taxonomy of the different techniques of production is discussed in appendix A3. Concluding, the opportunities offered by the free-form production of vacuum infusion are complemented with the limitations brought by cost and transportation.

The following chapters 2 and 3 delve deeper into the material's mechanical and durable properties.

CHAPTER 2:

MECHANICAL PROPERTIES OF FRP COMPOSITES

As discussed in the previous chapter, the mechanical properties of FRP depend not only on the properties of its two main constituents, the fibers and the matrix system, but also on the directions and volume of the fibers. As such, FRP structure offer the possibility to be optimized and their mechanical properties tailored for specific applications.

The failure mechanism of fiber-reinforced polymer composites is complex; it depends on multiple factors: the stress state due to the applied loading, the properties of the fiber and matrix, and the mesoscale structure of the composite (orientation of the fibers and stacking sequence). To better understand the limits of this tailorable behavior, this chapter describes the procedures used to predict the macroscopic mechanical properties of FRP composite. At first, it illustrates the procedures to predict the stiffness and strength of a lamina from its constituent's properties (the matrix and fibers) and the volume fraction. Then, the classical laminate theory (CLT) is explained as the tool to predict the mechanical properties from the laminates and their stacking sequences. Having examined the classical laminate theory to approximate the stresses and strains, the failure criteria of a unidirectional laminae and then multidirectional laminate are explored.

This chapter answers the following sub-questions

- How to define FRP's anisotropic material?
- What are rules of thumb for designing in FRP?
- What are FRP's failure mechanisms?

1. FRP, an Anisotropic Material

As established in chapter 1, composite material consists of fibers embedded in a polymeric matrix. An FRP composite can be studied at three levels: the microscale, the mesoscale, and macroscale [17]. The microscale outlines the properties of the reinforcement (fibers) and the matrix (the resin) that constitute a ply (lamina). The mesoscale characterizes the behavior of FRP at the ply level, distinguishing between the multiple plies of a laminate. The macroscale is related to the behavior of FRP at the laminate level.

As a composite material, FRP presents a heterogeneous behavior at the mesoscale: its constituents, fibers and matrix, have different properties. The content of this chapter is limited to the properties of laminated composite materials: it first establishes the knowledge of lamina in order to then explain the behavior of laminates. A unidirectional lamina (figure 2.1.a) consists of a unidirectional fibers embedded in a matrix while a laminate (figure 2.1.b) consists of multiple lamina stacked together.

A unidirectional (UD) FRP lamina is often considered homogenous. Unlike other engineering materials such as steel or concrete, a unidirectional lamina is however not isotropic. The unidirectional ply material usually is often treated as an orthotropic material: fibers are stiffer than the polymeric matrix lending the material to be stiffer in the fiber direction.

1.1 Stress-Strain Relationship of a lamina

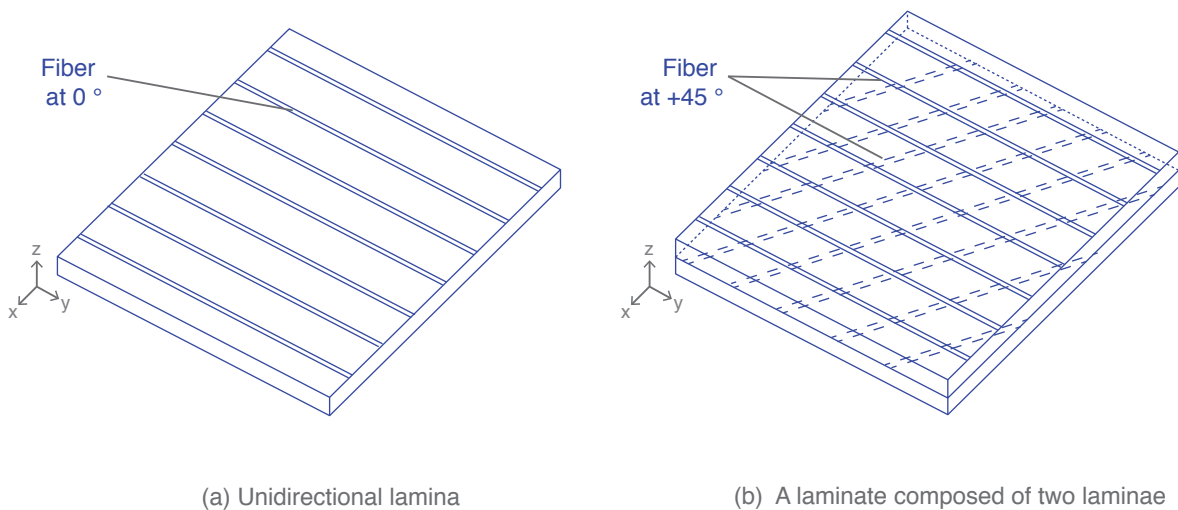


Figure 2.1 Unidirectional lamina and laminate

General orthotropic materials have three principal orthogonal axes; their behavior can be defined by 9 independent elastic parameters. In the case of UD, the three directions are the fiber or longitudinal direction (axis 1), the transverse or width direction (axis 2), and the through-thickness direction (axis 3). The elastic behavior of the transverse and through-thickness directions (axes 2 and 3) is assumed to be equal. A unidirectional FRP lamina is assumed to be a transversely quasi-isotropic material at the macroscopic level.

Behaving as a transversely isotropic material, UD composites present a more simplified behavior than general orthotropic materials with one principal direction, the fiber direction. This reduces the number of elastic parameters to five: E_1 , E_2 , G_{12} , G_{23} , ν_{12} , and ν_{23} . Due to the laminates' plates planar form, plane stress conditions can be assumed. The in-plane stress-strain relationship of an FRP lamina is then represented by the following constitutive equation, with only five elastic parameters [10].

$$\begin{pmatrix} \sigma_1 \\ \sigma_2 \\ \tau_{12} \end{pmatrix} = \begin{bmatrix} Q_{11} & Q_{12} & 0 \\ Q_{21} & Q_{22} & 0 \\ 0 & 0 & Q_{66} \end{bmatrix} \begin{pmatrix} \varepsilon_1 \\ \varepsilon_2 \\ \gamma_{12} \end{pmatrix} \quad (1)$$

$$\bar{Q} = \begin{bmatrix} Q_{11} & Q_{12} & 0 \\ Q_{21} & Q_{22} & 0 \\ 0 & 0 & Q_{66} \end{bmatrix} \quad (2a)$$

$$\bar{Q} = \begin{bmatrix} \frac{E_1}{1 - \nu_{12}\nu_{21}} & \frac{\nu_{12}E_2}{1 - \nu_{12}\nu_{21}} & 0 \\ \frac{\nu_{21}E_1}{1 - \nu_{12}\nu_{21}} & \frac{E_2}{1 - \nu_{12}\nu_{21}} & 0 \\ 0 & 0 & G_{12} \end{bmatrix} \quad (2b)$$

$$\text{with} \quad Q_{21} = Q_{12} = \frac{\nu_{21}E_1}{1 - \nu_{12}\nu_{21}} = \frac{\nu_{21}E_1}{1 - \nu_{12}\nu_{21}} \quad (2c)$$

1.2 Transformation of stresses and strains

In a unidirectional ply, the fibers' main orientation does not always coincide with the load direction: if the lamina is loaded in an arbitrary direction or the global coordinate system does not coincide with the material's local coordinate system. The ply is in a "rotated" direction in the laminate plane; transformation of stresses is required through the transformation matrix, also referred to as rotation matrix T [10]. There are two formulations of the transformation matrix: one for stresses and another for strains as shown in equation (3).

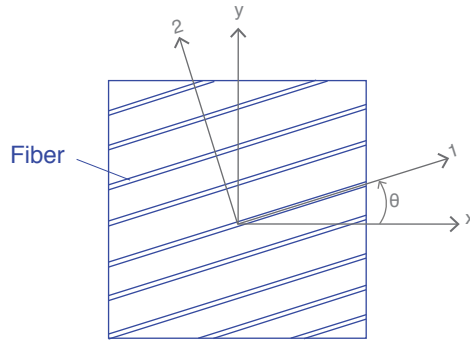


Figure 2.2 Material coordinate system (1-2) and global coordinate system (x-y).

$$T = \begin{bmatrix} \cos^2 \theta & \sin^2 \theta & -2\sin\theta\cos\theta \\ \sin^2 \theta & \cos^2 \theta & 2\sin\theta\cos\theta \\ \sin\theta\cos\theta & -\sin\theta\cos\theta & \cos^2 \theta - \sin^2 \theta \end{bmatrix} \quad (3)$$

$$\bar{\sigma} = \bar{Q} \bar{\varepsilon} \quad (4a)$$

$$\bar{\sigma} = T^{-1} \sigma \quad \bar{\varepsilon} = T^T \varepsilon \quad (4b)$$

2. Classical Lamination Theory (CLT)

A laminate is built up from different plies; each with its own set of properties as shown in section 1. The stress-strain relationship of laminates with plies the same orientation can be derived with simple calculations. However, calculations become more complex when plies are stacked in different directions: the stiffness in a particular direction differs per each ply. The differences in the elastic modulus of each ply result in varying stresses caused by the same applied strain [4]. Furthermore, due to the material's layered nature and the orthotropic nature of the plies, torsional deformation coupling effects may occur if subjected to axial loading. This coupling results from a mismatch between the load direction and the deformation in other directions.

Classical lamination theory (CLT) was introduced to better estimate the mechanical properties of multidirectional laminates from those of its composing laminae and their corresponding stacking sequence. Using extensive linear algebra, CLT is useful to compute stresses and strains for each ply under certain loading, calculate the stiffness of a laminates, check the elongations, and estimate the coupling effects. CLT is also useful to ultimately check if the structure is at risk of failure by comparing the occurring stresses and strains to the respective permitted values, by the defined failure criterion. As the strain and stresses depend on the stiffness of a laminate, it is important to calculate the stiffness of the laminate.

Assumptions surrounding the classical lamination theory formulation are [4], [18]:

- The laminate and the corresponding laminae are in a state of plane stress (the hypothesis of the Kirchhoff–Love plate theory).
- The composing laminae are perfectly bonded together. The theory is not valid for delamination.
- The properties of the ply are considered “smeared”: their microscopic behavior is not modelled. Theory is only valid for macroscopic behavior.
- The thickness of the laminate is constant and significantly smaller than its other dimensions. The theory is not valid for variation of thicknesses (ply-drops or other thickness jumps).
- The laminate is undisturbed. The theory is not valid at corners, edges, or near holes.
- The theory is linear-elastic. The displacements are sufficiently small so that second order effects or any non-linear behavior are ignored.

2.1 CLT Steps

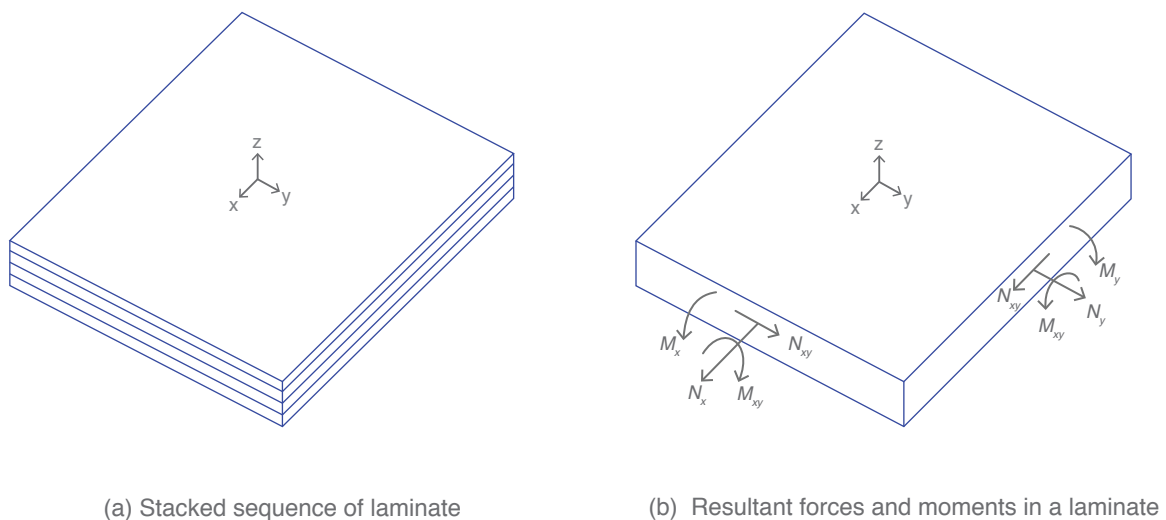


Figure 2.3 Typical n-ply laminate in the global x-y-z coordinate system.

The central assumption of the classical lamination theory is that the deformation of the laminate can be written like that of a thin plate. At any point of the laminate, the strains can be defined by [10]:

$$\varepsilon_z = \gamma_{xz} = \gamma_{yz} = 0 \quad (5a)$$

$$\begin{pmatrix} \varepsilon_x \\ \varepsilon_y \\ \gamma_{xy} \end{pmatrix} = \begin{pmatrix} \varepsilon_x^0 \\ \varepsilon_y^0 \\ \gamma_{xy}^0 \end{pmatrix} + z \begin{pmatrix} \kappa_x \\ \kappa_y \\ \kappa_{xy} \end{pmatrix} \quad (5b)$$

In a laminate formed of stacked plies, the external forces in the plane have to be in equilibrium with the total ply forces. The elongation of each ply is determined by the curvature of the laminate. Behaving like a plate, the stress resultants can be computed as distributed membrane forces N and distributed bending moments M . The matrix relating the external normal loads N and bending moments M to the strains and curvatures in the laminate is called the ABD matrix, shown in equation (6) [10].

$$\begin{pmatrix} N \\ M \end{pmatrix} = \begin{bmatrix} A & B \\ B & D \end{bmatrix} \begin{pmatrix} \varepsilon \\ \kappa \end{pmatrix} \quad (6a)$$

$$\begin{pmatrix} N_x \\ N_y \\ N_{xy} \\ M_x \\ M_y \\ M_{xy} \end{pmatrix} = \begin{bmatrix} A_{11} & A_{12} & A_{16} & B_{11} & B_{12} & B_{16} \\ A_{12} & A_{22} & A_{26} & B_{12} & B_{22} & B_{26} \\ A_{16} & A_{26} & A_{66} & B_{16} & B_{26} & B_{66} \\ B_{11} & B_{12} & B_{16} & D_{11} & D_{12} & D_{16} \\ B_{12} & B_{22} & B_{26} & D_{12} & D_{22} & D_{26} \\ B_{16} & B_{26} & B_{66} & D_{16} & D_{26} & D_{66} \end{bmatrix} \begin{pmatrix} \varepsilon_x^0 \\ \varepsilon_y^0 \\ \gamma_{xy}^0 \\ \kappa_x \\ \kappa_y \\ \kappa_{xy} \end{pmatrix} \quad (6b)$$

- N represents external line loads; it is the resultant normal forces in the global coordinate system.
- M represents the resultant moments.
- A is the extensional stiffness matrix; it describes the relation between the in-plane forces and the in-plane strains.
- B is the bending-extension coupling stiffness matrix; it describes the relation between the in-plane forces and the curvatures as well as moments to in-plane strains.
- D is the flexural stiffness matrix; it describes the relation between the bending moments and the curvatures and strains.

The behavior of a homogenous plate is simpler to calculate because of the absence of coupling between bending moment and membrane action. The $[B]$ matrix is equal to 0: in-plane deformation causes membrane forces only and pure curvature causes bending moments only.

Multidirectional laminates exhibit a more complicated behavior. If made from the same material, the plies then present the same matrix in their local coordinate frame. Because of the transformation matrix, the plies thus end up with different matrix Q in the global coordinate system. In such a multidirectional laminate, $[A]$, $[B]$, and $[D]$ matrices can be calculated with the equations (7 a, b, and c) with the layer number that stretches from thickness coordinate and the total number of laminae composing the laminate [10].

$$A = \sum_{j=1}^n Q_j (z_j - z_{j-1}) \quad (7a)$$

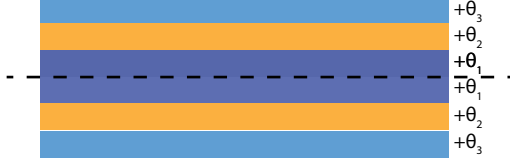
$$B = \frac{1}{2} \sum_{j=1}^n Q_j (z_j^2 - z_{j-1}^2) \quad (7b)$$

$$D = \frac{1}{3} \sum_{j=1}^n Q_j (z_j^3 - z_{j-1}^3) \quad (7c)$$

2.2 Rules of Thumb and Recommendations for Designing in FRP

While laminates present more complicated behavior than typical construction material, designers have developed guidelines to simplify their behavior and equate their behavior to regular construction material [4], [10].

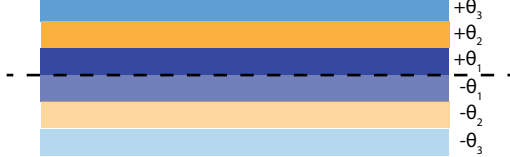
- *Symmetric laminates* exhibit no bending/membrane coupling effect. To set the matrix [B] equal to zero shown in equation (8), for each ply of lamina on one side of the middle plane, there is an identical ply (same thickness) stacked at the same orientation and at an equal distance to the mid-plane (figure 2.4).



$$\begin{pmatrix} N_x \\ N_y \\ N_{xy} \\ M_x \\ M_y \\ M_{xy} \end{pmatrix} = \begin{bmatrix} A_{11} & A_{12} & A_{16} & 0 & 0 & 0 \\ A_{12} & A_{22} & A_{26} & 0 & 0 & 0 \\ A_{16} & A_{26} & A_{66} & 0 & 0 & 0 \\ 0 & 0 & 0 & D_{11} & D_{12} & D_{16} \\ 0 & 0 & 0 & D_{12} & D_{22} & D_{26} \\ 0 & 0 & 0 & D_{16} & D_{26} & D_{66} \end{bmatrix} \begin{pmatrix} \epsilon_x^0 \\ \epsilon_y^0 \\ \gamma_{xy}^0 \\ \kappa_x \\ \kappa_y \\ \kappa_{xy} \end{pmatrix} \quad (8)$$

Figure 2.4 Symmetric laminate.

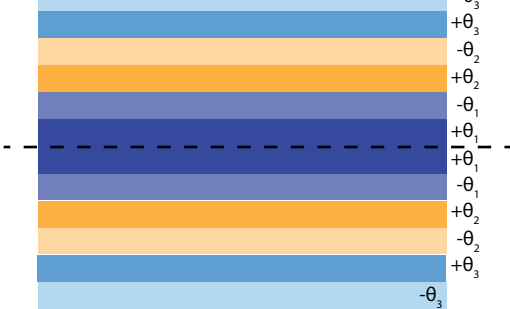
- *Balanced laminates* exhibit no shear/normal coupling: . To set the matrix and to zero, for each ply at an angle , there is an identical ply stacked at an angle as shown in equation 9. Unlike symmetric laminates, the distances to the mid-plane do not need to be equal. A balanced material is only valid for a certain global coordinate material; a transformation to another coordinate system may render it unbalanced (



$$\begin{pmatrix} N_x \\ N_y \\ N_{xy} \\ M_x \\ M_y \\ M_{xy} \end{pmatrix} = \begin{bmatrix} A_{11} & A_{12} & 0 & B_{11} & B_{12} & B_{16} \\ A_{12} & A_{22} & 0 & B_{12} & B_{22} & B_{26} \\ 0 & 0 & A_{66} & B_{16} & B_{26} & B_{66} \\ B_{11} & B_{12} & B_{16} & D_{11} & D_{12} & D_{16} \\ B_{12} & B_{22} & B_{26} & D_{12} & D_{22} & D_{26} \\ B_{16} & B_{26} & B_{66} & D_{16} & D_{26} & D_{66} \end{bmatrix} \begin{pmatrix} \epsilon_x^0 \\ \epsilon_y^0 \\ \gamma_{xy}^0 \\ \kappa_x \\ \kappa_y \\ \kappa_{xy} \end{pmatrix} \quad (9)$$

Figure 2.5 Balanced laminate.

- Laminates can be both balanced and symmetric as shown in figure 2.6 and related in equation 10.



$$\begin{pmatrix} N_x \\ N_y \\ N_{xy} \\ M_x \\ M_y \\ M_{xy} \end{pmatrix} = \begin{bmatrix} A_{11} & A_{12} & 0 & 0 & 0 & 0 \\ A_{12} & A_{22} & 0 & 0 & 0 & 0 \\ 0 & 0 & A_{66} & 0 & 0 & 0 \\ 0 & 0 & 0 & D_{11} & D_{12} & D_{16} \\ 0 & 0 & 0 & D_{12} & D_{22} & D_{26} \\ 0 & 0 & 0 & D_{16} & D_{26} & D_{66} \end{bmatrix} \begin{pmatrix} \epsilon_x^0 \\ \epsilon_y^0 \\ \gamma_{xy}^0 \\ \kappa_x \\ \kappa_y \\ \kappa_{xy} \end{pmatrix} \quad (10)$$

Figure 2.6 Symmetric and balanced laminate.

- Multidirectional laminates should not exhibit stiffness jumps between plies or sudden thickness jumps. Stiffness variation can be limited by restricting the difference between any two plies' angle orientation to 60° or by making sure the adhesive is applied to plies at 45° from the main direction.
- Designers often use *quasi-isotropic laminates* if possible. Quasi-isotropic behavior is achieved by equal behavior in three different directions. While often heavy, quasi-isotropic behavior is often invariant to transformation of coordinate systems.

3. Failure Mechanisms

The failure mechanisms of a multidirectional laminate are harder to predict; there has been continuous effort, experiments, and research into the formulation of failure models for composite materials. The failure analysis of a laminate requires first evaluating the stresses and strains in each composing lamina of a laminate under the given loading conditions (section 2), before evaluating them against the lamina failure criterion (section 3.1 and 3.2) and then against the defined laminate failure (section 3.3).

Damage in FRP refers to many failure mechanisms with varying degrees of urgency: fiber cracks, fiber micro-buckling, matrix cracks, matrix debonding, and delaminations. Defining what a “safe” structure is thus very important. Some factors to define the “safety” of a structure or alternatively its “failure” are [19]:

- *The service life of a structure*: more conservative failure stress levels are applied to structures intended for long period of service, compared to structures with a singular usage or short service life.
- *The cyclical nature of the applied loading*: more conservative failure stress levels are applied to structures that experience cyclical loads (fatigue or creep) in their service lives, compared to structures that are only subjected to static loads.
- *The consequences of structural failure*: more conservative failure stress levels are applied to structures whose failure will cause catastrophic consequences in loss of lives or damage of property, compared to structures will less serious consequences.
-

Depending on the three mentioned factors, a consequence class is determined for the structure in question.

3.1 Intralaminar Failure

The directionality of a unidirectional lamina is paramount in the formulation of the unidirectional laminate’s failure criteria. Unlike an isotropic material, a unidirectional lamina does not behave similarly in all directions. Principal stresses cannot thus be used for its failure mode as they assume that the material’s behavior is uniform in all directions. Consequently, the single expression interactive characterizing the material’s behavior (i.e: Von Mises for steel) must be replaced with multiple parameters. Multiple failure criteria have been developed for composite laminae. Three methods will be described in-depth hereafter: (1) maximum stress criterion, (2) maximum strain criterion, and (3) the Tsai-Wu Criterion [18], [20].

Under in-plane loading, a lamina’s failure criteria are based on the following strength parameters:

- The tensile strength in the fiber direction as well as the transverse direction .
- The compressive strength in the fiber direction as well as the transverse direction .
- The in-plane shear strength .

i. Maximum Stress Criterion

According to the maximum stress criterion, failure occurs if the stress in either the material’s principal directions (longitudinal or transverse directions) exceed the corresponding maximum strengths. The maximum stress criterion can be written as follows:

$$\sigma_1 = \begin{cases} f_{1t} & \text{for } \sigma_1 > 0 \\ -f_{1c} & \text{for } \sigma_1 < 0 \end{cases} \quad (11)$$

$$\sigma_2 = \begin{cases} f_{2t} & \text{for } \sigma_2 > 0 \\ -f_{2c} & \text{for } \sigma_2 < 0 \end{cases} \quad (12)$$

$$|\tau_{12}| = F_{12} \quad (13)$$

ii. Maximum Strain Criterion

According to the maximum strain criterion, failure occurs if stress in either the material's principal directions (longitudinal or transverse directions) exceed the corresponding ultimate strain. The maximum strain criterion can be written as follows:

$$\varepsilon_1 = \begin{cases} \varepsilon_{1t}^u & \text{for } \varepsilon_1 > 0 \\ -\varepsilon_{1c}^u & \text{for } \varepsilon_1 < 0 \end{cases} \quad (14)$$

$$\varepsilon_2 = \begin{cases} \varepsilon_{2t}^u & \text{for } \varepsilon_2 > 0 \\ -\varepsilon_{2c}^u & \text{for } \varepsilon_2 < 0 \end{cases} \quad (15)$$

$$|\gamma_{12}| = \gamma_{12}^u \quad (16)$$

with

In a linear elastic lamina,

$$\sigma_1 = -\nu_{12}\sigma_2 = \begin{cases} f_{1t} & \text{for } \varepsilon_1 > 0 \\ -f_{1c} & \text{for } \varepsilon_1 < 0 \end{cases} \quad (17)$$

$$\sigma_2 = -\nu_{21}\sigma_1 = \begin{cases} f_{2t} & \text{for } \varepsilon_2 > 0 \\ -f_{2c} & \text{for } \varepsilon_2 < 0 \end{cases} \quad (18)$$

$$|\tau_{12}| = F_{12} \quad (19)$$

iii. Tsai-Wu Criterion

The Tsai-Wu interactive criterion is the earliest failure criterion proposed for composite materials. It can be formulated as follows:

$$\sigma_1 \left(\frac{1}{f_{1t}} - \frac{1}{f_{1c}} \right) + \sigma_2 \left(\frac{1}{f_{2t}} - \frac{1}{f_{2c}} \right) + \frac{\sigma_1^2}{f_{1t}f_{1c}} + \frac{\sigma_2^2}{f_{2t}f_{2c}} + \frac{\tau_{12}}{f_{12}^2} - \frac{\sigma_1\sigma_2}{\sqrt{f_{1t}f_{1c}f_{2t}f_{2c}}} = 1 \quad (20)$$

The Von Mises criterion for steel can be retrieved from the Tsai-Wu criterion if $\nu_{12} = \nu_{21} = 0$ and $f_{1t} = f_{1c} = f_{2t} = f_{2c} = F$. The Tsai-Wu criterion can also be formulated in the three-dimensional space but becomes quite lengthy.

3.2 Discussions of Lamina Failure Criteria

Both the maximum stress criterion and the maximum strain criterion are conceptually straightforward: comparing occurring stresses or strains to their respective ultimate limits. However, they are both computationally inconvenient because each criterion relies on multiple sub-criteria. Furthermore, the interaction between the different stresses is not considered in the maximum stress criterion and only reflected by the Poisson's ratio in the maximum strain criterion. The Tsai-Wu criterion considers the interaction through a single equation that defines the failure state. The comparison of the discussed criteria is shown in figure 2.7.

Since the Tsai-Wu criterion, numerous failure criteria have been developed and tested for fiber-reinforced composites. In 1980, Hashin develops a failure criterion that separates the different failure modes. It states that no single expression can accurately cover all stress states. The Hashin criteria defines four failure mechanisms: fiber failure (FF) and inter-fiber failure (IFF matrix fiber) in tension and compression. As Hashin's criteria proved to be not too accurate, Puck established an improved failure-mode based criteria, the Puck criterion, following the assumptions brought by Hashin's failure theory here is continuous effort to develop failure theories that cover all stress states of unidirectional composite behavior [20], [21], [22]. These failure theories such as the Camanho criterion (2015) often involve more complex expressions. Nonetheless, with always room for improvement, the Tsai-Wu criterion remains the most popular interactive criterion.

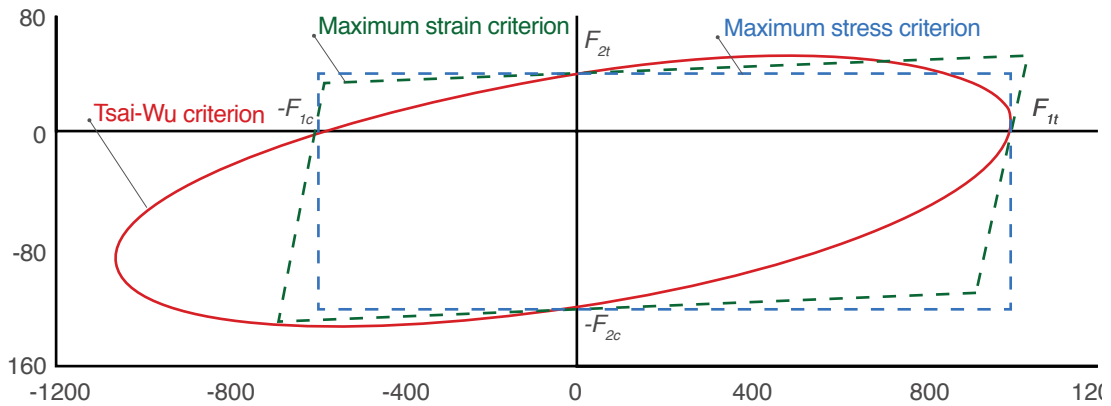


Figure 2.7 Comparison of the discussed failure criteria: maximum stress, maximum strain, and Tsai Wu criteria.

3.3 Failure Analysis of a Laminate

There are two limiting design strategies to address the failure of a laminate: the first-ply failure stress or last-ply failure stress.

- **First-ply failure** is a conservative design criterion. With the first-ply approach, the laminate failure stress is defined as the effective stress level that initiates a ply failure of any kind. Ply failure results from fiber yielding or fracturing in one or more plies. However, through internal force redistribution, the forces taken by the failed lamina can be distributed by other laminae. The failed lamina also retains some stiffness due to the constraints offered by adjacent plies [23]. Furthermore, the ultimate load-capacity of multi-directional laminates is higher than the first-ply failure load as new generation composite materials become more ductile. This underscores that the first-ply failure criterion is thus overly conservative [19]. However, its use is found appropriate for composite structures whose failure will have serious consequences in lives lost and ensuing damage.
- **Last-ply failure** is a far less conservative criterion. With the last-ply failure, the laminate failure stress is defined as the effective stress that leads to the ultimate fracture and failure of the composite structure. It is evident that the failure of a lamina reduces its elastic properties: this is due to the fracturing or yielding of the ply. The best way to approximate the contribution of the failed laminae is still debated; the traditional approach has remained a discrete reduction of the ply's stiffness. The procedures following a last-ply failure analyses, while widely discussed and available, have been met with a certain degree of skepticism. A first factor of this skepticism is the ductile nature of modern composite material systems being often not properly modeled. Furthermore, and most importantly, the continuous cracking or delamination render the classical lamination theory's hypothesis invalid (Kirchhoff–Love plate theory) [19]. The last-ply failure criterion is evidently a less conservative approach and should be used with caution. Any structural design based on the last-ply failure criterion must incorporate generous safety factors.

4. Conclusion

This chapter answers the following sub-questions

- How to define FRP's anisotropic material?
- What are rules of thumb for designing in FRP?
- What are FRP's failure mechanisms?

While composite materials offer significant advantages, learning to design efficiently in FRP requires an understanding of its behavior. The chapter expands on the two-steps the analysis required to determine the properties of laminated FPR. The first step consists of determining the behavior of a unidirectional laminae while the second step computes the properties of the laminate using the classical lamination theory (CLT). The classical lamination theory is introduced to better estimate the mechanical properties, stresses, and strains of multidirectional laminates from those of its composing laminae.

After providing the framework to understand the anisotropic behavior of FRP, rules of thumb to simplify the design process with FRP are presented. These rules of thumb will guide the optimization framework, developed in chapter 5 of this research.

Lastly, failure mechanisms are explored in order to design safely in the composite material, both at the lamina and laminate level. At the laminae level, the most important intralaminar failure criteria are explored: the maximum stress criterion, the maximum strain criterion, and the Tsai-Wu criterion. While both the maximum stress or strain are conceptually straightforward, they are computational inconvenient. In contrast, the Tsai-Wu criterion is straightforward to compute with a single equation defining the failure state. At the laminate level, two main design strategies are considered: the first-ply failure and the last-ply failure strategies. The first-ply failure is the more conservative design strategy while the last-ply failure must be used with caution. This chapter's discussion of FRP's behavior, failure criteria at the laminae and laminate levels is important to define the design criteria of any optimization framework.

The following chapter contextualizes the discussion around the sustainability and durability of FRP.

CHAPTER 3

DURABILITY AND SUSTAINABILITY OF FRP

Since the end of the twentieth century, fiber-reinforced polymers have witnessed an increased interest in civil engineering applications. However, their use has been primarily in strengthening and rehabilitations of old structure. In new structures, the use of FRP composites has remained limited to a few typologies, principally bridge structures. These limitations are seen as the consequence of a widespread design approach that doesn't exploit the material's most advantageous properties and render it not cost competitive with traditional construction materials.

The following chapter contains a brief overview of the generic form-finding methods, from physical model to structural optimization. The inherent limitations of these techniques are then discussed in order to broaden the scope of structural shape optimization. An overview of the optimization landscape for FRP is then explored in order to uncover this thesis' focus.

The chapter aims to tackle the following sub-questions:

- What is the environmental challenge facing structural engineers?
- What is a proper framework to study sustainability?
- What is the definition of durability?
- What are the mechanical failure mechanisms of FRP?
- What environmental conditions cause degradation of FRP?

1. Sustainability in Structural Design

Human-caused climate change represents one of the greatest environmental challenges of our time. Affecting all regions of the world, climate change's consequences have been underway for many decades now: rising sea-levels, rising global temperatures, and the ever more common extreme weather conditions (drought, floods, heat waves, etc.). Since the 1960s, studies have warned of the effect of climate change [24]. On a planet with finite resources and ever-increasing resource consumption rate per person, the situation is unbalanced [3]. In 1987, the Brundtland report defines sustainability as meeting the “needs of the present without compromising the ability of future generations to meet their own needs” [25]. Since the framework of sustainability was established, the reports and studies eliciting the effects of climate change have multiplied. Today, the need to address this closing threat have become widely accepted across professions and governments but the caliber of the response has not matched the urgency of the crisis.

An important sector contributing significantly to climate change is the construction industry. Recent studies estimate this contribution to nearly 36% of global final energy use and near 40% of energy related carbon emissions [2]. This important impact has been mainly driven by the non-sustainable practices entrenched in the profession. The industry's dependence on traditional building materials, most notably steel and cement, drives the important greenhouse gases emissions. Future projections models predict a rapid increase in the consumption of steel and cement over the next decades if climate policies are not enacted [26].

Despite the lacking leadership in the field, the urgency of the situation has required structural engineers to assume the responsibility of addressing climate change in their practices. Throughout the years, the profession has gradually modified the role of the structural engineer manifesting an awareness to the climate change challenged. It was only in 1991 that Chrimes defined civil engineering as “directing the great sources of power in Nature for the use and convenience of Man” [3], [27]. Since then, structural engineers have become “custodians of the built and natural environment” [3] [28] with the American Society of Civil Engineering (ASCE) urging engineers to assume their responsibility in the political and public arena. Civil engineers' societies have increasingly anchored their role in creating a sustainable world and enhancing the global quality of life [29].

1.1 Solutions for Today

There exist many opportunities for structural engineers to address the global impact of the construction industry. Considerable efforts have been mounted in recent years, particularly in the following fields of research [3]:

- **Improving life-cycle performance** is an important avenue of research. Today's landscape within the field prioritizes minimal initial costs rather than focusing on the whole in-service life of projects. In fact, reframing the discussion around costs allows for significant gains in terms of sustainability. A small increase in initial costs can reduce life-cycle costs making structures more sustainable [3].
- **Recovering materials from constructions and reusing existing structures** have witnessed significant traction in recent years. As the finite elements of our planet are depleted, it becomes essential for engineers to recover materials. It is essential for the profession to address its role within the current economy which exploits non-renewable resources, consumes them, and then discards them. The introduction of circular frameworks has become prevalent in recent years with countries, such as the Netherlands, aiming to achieve a circular economy by 2050 [30], [31]. Circular building agendas are defined as “the development, use, and reuse of buildings, areas, and infrastructures, without avoidable depletion of natural resources, pollution of the environment or negatively impacting resources” [30]. Structural engineers have a central role to play in establishing this circular framework, and its eventual success.
- **New buildings materials** are increasingly accepted as potential alternatives for the traditional building materials such as steel and cement. Steel and cement will most likely remain the primary construction materials. However, structural engineers must continue to investigate alternative building materials with enhanced durable and sustainable properties.

1.2 Challenges for the Future

These proposed solutions are indispensable to address the important global impact of the construction industry. However, a systemic questioning of our practices must occur if the profession is to meet the gravity of the environmental challenge. Such measures must consider the challenges in three areas: practice, research, and education [3].

In practice, the primary challenge facing the construction industry remains the current incentive structure of the sector. Without the introduction of any climate policies, minimizing initiative costs will remain the driving force in decision making rather than the overall life cycle costs. Fundamental changes in the practices of structural design will require the concerted efforts of governments, researchers, educators, and structural designers at every scale: global, national, and regional. As with the circular vision for the Dutch economy by 2050 [31], construction costs must reflect the entirety of the picture. They must include the environmental impact of non-renewable resource depletion.

The reform to our practices must be coupled with an investment in research and a questioning of a structural engineer's education. Research's role is central to fuel the agents of changes through new policies and sustainable design. This, of course, comes in addition to the conventional research in structural and computational mechanics. In educational settings, curriculums must reflect the new roles of structural engineers: they should value adaptability over convention. Any structural analysis of a design must be coupled with an awareness to its social and economic impact.

1.3 The Research within the Larger Context

First and foremost, this research attempts to catalyze the use of alternative materials, encouraging formal exploration with FRP. In applying FRP, a material with enhanced sustainable and durable properties, this case-study allows to improve life-cycle performance of structures. By implication, the research allows to reflect on the most-common practices in structural design today, such as computational optimization methods.

2. Sustainability of FRP, Framework and Evaluation

As established, sustainability is a prominent challenge for today's construction industry. The importance of such a challenges has led to an increased interest in understanding building's sustainability performance.

Recent years has witnessed the rise of sustainability assessment tools. However, quantifying a construction's level of sustainability remains challenging. The most prominent assessment tools on the market today are the Building Research Establishment Environmental Assessment Method or BREEAM, the Leadership in Energy and Environmental Design (LEED), or German Sustainable Building Council's standard (DGNB) [30]. Integrating economic, social, and environmental standards, each of these standards offer their advantages and limitations. With extensive literature comparing these standards in detail, defining sustainability and durability in FRP is paramount [32].

2.1 Sustainability Framework: Life-Cycle Analysis

With multiple frameworks defined in recent years, sustainable construction is one that applies the principles of sustainable development to the field of building. First framed in the 1987 World Commission on Environment and Development, sustainability in the construction aims to sustain and embody the general principles of sustainability in all phases of a construction: from mining raw material through the production of construction material, construction through execution and usage, destruction through recycling and waste management [25].

Some criteria to assess a construction material's sustainability are mainly: a minimum resource use, a low environmental impact, a low human and environmental health risks, sustainable site design strategies, and a higher material performance. The ideal sustainable material presents a closed circular life, with minimal impacts on all three spheres of sustainability: economic, environmental, and social spheres. As such, a life-cycle assessment or

analysis (LCA) is an approach used to examine the impact of structure in all phases: production, use, and then end of life. Beyond sustainability assessment tool, it includes the inputs and outputs for all phases of material life: raw materials acquisition, fabrication/processing/ construction, recycling/ disposal [23], [33].

- During **production**, LCA methods determine how much energy, material, water is consumed per component.
- During its **use**, a structure is regularly inspected and maintained accordingly, consuming further energy and materials.
- At **end of its life cycle**, the structure must find new applications or be demolished/recycled.

Life-cycle assessment are expressed in multiple ways, in tons of CO₂ or combined indicators such as Eco and MKI score. The energy consumed or harmful substances released during fabrication can be clearly measured. However, LCA methods are in large parts based on assumptions to estimate the environmental impacts of a structure. For that purpose, life-cycle inventories, a database specifying the environmental impact of each material per structure, are often used.

2.2 Sustainability of Composites

The advantages of FRP are well understood. The specific environmental impacts include concerns over health, safety, energy consumption, and emissions of volatile organic compounds. The use of crude oil for the fiber-matrix constituents of FRP sheds a doubtful light on the sustainability of FRP; nevertheless, when examined over the structure's entire cycle (LCA methods), the sustainable performance of FRP significantly improves. FRP requires less energy and present a lower need for replacement. A study by Daniel and Nagtetaal [33] provides evidence for the competitiveness of FRP composites in specific applications. Five materials (structural steel, stainless steel, glass FRP composites, aluminum, and concrete) were analyzed and compared in terms of energy consumption, emissions of air, emissions of water. While structural steel is found to be the least expensive, FRP has the least environmental impact in terms of emissions of water and air.

In general, FRP offers multiple behavioral advantages:

- 1.As long as FRP composites exists no fossil derived CO₂ is admitted.
 - 2.Little water is needed during manufacturing.
 - 3.The freedom of production allows for lighter structure. In turn, this generally minimizes the need for heavy equipment and thus minimizing fuel consumption.
- In **production**, FRP's sustainability depends more closely on the performance of each of its constituents. A closer look at the sustainability of each of its constituents is proposed in appendix B2.
 - 3During FRP's **service life**, composite materials require significantly less maintenance than steel or timber structure due to their resistance to environmental conditions. For that reason, FRP has been extensively used to extend the life cycle of structure or rehabilitate their damaged parts. Such repairs often entail the removal of the damaged parts and applying new layers of reinforcing composite materials. Often done in-situ, such repairs are referred to as "cosmetic"; their ability to restore the original strength of a structure is rather limited.
 - After its **service life**, there exists limited to no market for recycling and re-using FRP. There is however an increased interest in reducing components easily disassembled, reused, and recycling at the end of their product life [34].

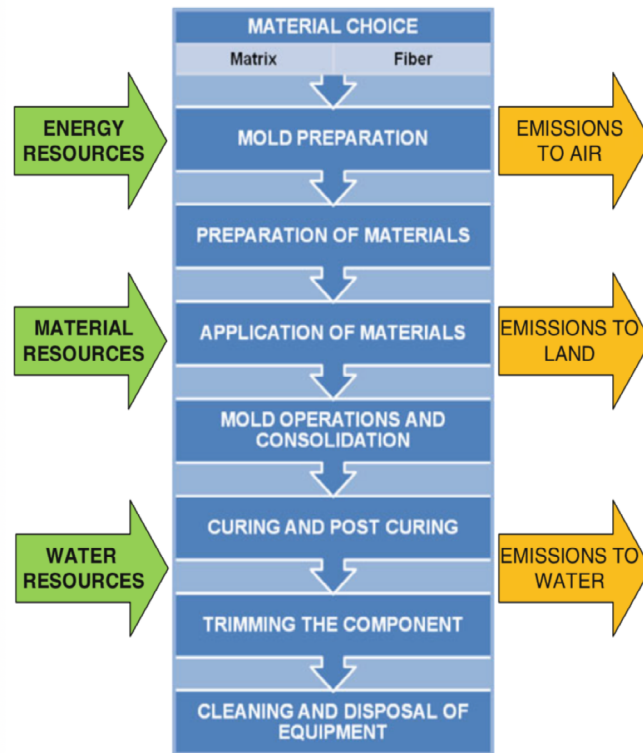


Figure 3.1 Environmental Impact of Composite manufacturing processes [31].

2.3 A Nuanced Picture

The life-cycle assessment of FRP leads to draw a nuanced picture. FRP still has to surmount substantial challenges if it is to meet its full potential for sustainability. Such tensions between the reality of the present and the potential of the future is not a shortcoming of the material. Rather, it is an invitation to capitalize on the material's favorable properties and investigate the exhibited deficiencies.

To evaluate the sustainability of the case-study, attention will be brought to the different phases of construction. Through deriving structural form that optimally use material's properties, the generated geometries will capitalize on the known advantages of FRP. Generally, it will be more lightweight and thus more energy efficient. The generated structure will be a free-form design. Molding preparation becomes particularly important. Furthermore, it is thus important to complement the sustainability of the particular construction with the overall site design strategies.

3. Durability of FRP

The durability of a material is its ability to retain its original properties under loading and with time. It is often associated with the resistance to environmental-based degradation. Specific to environmental conditions, durability in composite material is defined as the material's ability to resist cracking, oxidation, chemical degradation, delamination, wear, and effects of impact under load conditions over a period of time [4], [23], [33], [35].

The following describes the current status of durability of FRP, focusing on mechanical and in-service properties of the material. While FRP still undergoes degradation in certain properties over its service life, it presents significant advantages over conventional materials such as concrete or steel in structural applications.

3.1 Mechanical Mechanism Failure of FRP

Failure mechanisms in FRP is often a sequential process with one failure mechanism leading to another failure mechanism. Damage is thus either tied to the composite nature of the material (inter/intra laminar failure mechanisms) or result from the in-service properties of the material (fatigue and creep).

i. Intralaminar and interlaminar failure mechanisms

Damage is generally categorized in two main modes: (1) intralaminar and (2) interlaminar failures.

- **Intralaminar failure** is the failure inside of a single laminae due to the stresses and strains in each corresponding ply of the laminate; fiber cracks often occur in the plane perpendicular to the axis of the fiber direction and can extend across the entire width of the ply. One common form of fiber failure is the fiber buckling. Similarly, to other material, fibers can buckle under compressive loads in the fiber direction. The fiber buckling induces bending stresses, reduces the compressive stiffness of the lamina, and can ultimately lead to the failure of the fibers. Ply buckling can lead to delamination damage. Buckling can be addressed by using a more rigid material or increasing resistance of the structure through smaller unsupported lengths. Intralaminar failure criteria are closely examined in Chapter 3.

- **Interlaminar failure** is the failure between two different adjacent laminae such as delamination, matrix cracking, or fiber-matrix debonding [19]. Fractures in a composite material result from the formation of a crack in either the fiber or the polymeric matrix. Cracks are far more likely to occur in the matrix as the level of stresses required to cause crack growth are much smaller for the matrix. They generally appear in the plane parallel to the fiber direction. Harder to approximate by the classical lamination theory, the interlaminar stresses in a composite element can cause the following interlaminar failures:

- Matrix cracks occur in the polymeric matrix, often at a distance from the fiber-matrix interface.
- Fiber-matrix debonding results from a crack around the periphery of a fiber (the interphase region): the load can no longer get transferred from the matrix to the fiber [19].
- Splitting cracks run parallel to the fibers in the matrix, through the whole thickness dimension of one or more fibers. They often result from in-plane bending or a sheet of laminate are particularly vulnerable. Splitting is often avoided by stacking plies with different orientation.
- Despite resembling splitting, **delamination** is a crack that occurs between two plies in the plane of the laminate. Under loading, different angle-ply layers present a mismatch in Poisson's ratio or in the shear coupling coefficient inducing transverse stresses (also referred to as free-edge stresses) in order to satisfy the deformation compatibility. Near the free edges, the transverse stresses require the development of interlaminar shear stresses. The shear stresses near the edges lead to a bending moment, then balanced by interlaminar normal stresses. With no reinforcement between two ply layers, the high shear stresses lead to delamination; the most vulnerable place is the edge of a sheet. Providing additional layers or avoiding a mismatch in stiffness of layers are possible steps to avoid the manufacturing process.

ii. Fatigue

When composite structures are subjected to oscillating loads, fatigue can take place and can lead to significant damage. Fatigue cracks can appear in laminates, spread in multiple directions, and even join to form larger cracks. Fatigue can also occur in combination with other failure mechanism; its effects are further exacerbated when the structures are subject to corrosion.

Fatigue in composite structure leads to degradation, extensive damage, or complex failure mechanisms of the mechanical properties of fiber-matrix plies. Fatigue can lead to the loss of stiffness of composite materials, creep in case of constant fatigue loads (tensile or compressive stress), or even stress relaxation (due to external pre-tensioning or constant displacement) [4].

This is not an indication that FRP performs worse under fatigue conditions. To the contrary, specific measures can allow composite structure of handling much heavier fatigue loads [4]. Fatigue resistance is increased by adapting materials and fiber orientation to the loads: loading is optimized or stresses are decreased by adding more layers.

Four basic failure mechanisms of polymeric composites under fatigue loading can be identified:

- Fiber cracking interface debonding;
- Matrix cracking;
- Interface shear failure with fiber pull-out; and
- Brittle failure.

The most pronounced growth area in FRP has been to rehabilitate structural members using externally bonded composites. In particular, their strengthening capacities as well as fatigue resistance has led this extensive use of FRP.

iii. Creep

FRP can undergo creep and possibly creep-rupture if subjected to long-term permanent loading. Undesired, the creep process can lead to the degradation of the composite material mechanical properties reducing its stiffness as well as its strength. It can ultimately lead to the material's failure and as such is often the determining factor of the service life of FRP.

Under a constant load over an extended period of time, the matrix component of a composite material assumes a visco-elastic behavior and the fibers an elastic one. This difference of behavior causes the transfer of resin stress to the stress in the fibers, increasing the strains and deformation in the FRP laminate. Indeed, fibers have a stabilizing effect on the composite structure under creep loading due to their very low creep values. Creep will consequently also depend on the fiber volume fraction and orientation of the fibers in respect to the applied loads.

Beyond being time-dependent, creep characteristics also depend on the external or environmental factors, such as temperature, humidity (moisture content), or presence of corrosive aggressive chemicals.

Material related factors
<ul style="list-style-type: none">- the type of resin- the type of reinforcement- the quality of the interface between the resin and fibers- the volume fraction of the fibers- the orientation of fibers in regards to the applied loads
Environmental-related factors
<ul style="list-style-type: none">- Type and duration of loading- Temperature- Humidity (moisture content)- Presence of corrosive or aggressive chemicals

Table 3.1 Summary of creep determining factors.

3.2 Environmental Degradation of FRP

While all materials undergo degradation due to environmental conditions, composite structures do offer particularly durable properties over conventional materials. Their long-term properties have been the center of ongoing research; the significant challenge remains the length of time it takes to verify such a behavior [9], [33]. The durability of composite material is thus a direct function of the environment in which it is placed. The following section offers an overview of FRP's resistance to each of the major environmental causes.

i. Moisture

Moisture is easily absorbed in organic polymers in FRP. This absorption of the moisture exacerbates the microcracks and surfaced defects in fiber, reducing the tensile strength of fibers. Other mechanisms such as swelling, plasticization, saponification, and hydrolysis can also take place modifying the composite's chemical and mechanical properties and creating reversible or irreversible damage.

Different strategies have been applied to reduce the diffusion of water in composite materials [4].

- Applying additives can be the matrix at the time of manufacturing can prove to be an efficient and successful method to decrease diffusion in composite materials: silanes (organofunctional trialkoxysslanes) or organotitanates are used as a barrier against moisture ingress.
- Applying a high-degree of cross-linking has leads to a decrease in the permeability of the matrix. This, in turn, leads to a decrease to the diffusion process.

ii. Corrosion

Corrosion is an important degradation problem of structures in severe environments, particularly in bridges and marine structures. Resistance of polymers to chemical attacks highly depends on their chemical compositions, particularly the bonding of their monomers. This degradation can either be chemical or physical. **Chemical degradation** refers to the bonds of the polymer being broken due to a chemical reaction with the environment. On the other hand, physical degradation refers to the alteration of a composite material's properties due to an interaction with the environment but without any chemical reaction.

Unlike metals, composite materials do not rust, making them an ideal material where corrosion is a concern. Composite materials have consequently been used in lieu of materials that incur high maintenance costs because of corrosion. Important applications where composites' resistance to corrosion is used are: reinforcement bars or grids in concrete, cable stays, pipelines, cladding, and structural element exposed to harsh environments.

iii. Thermal effects (temperature and UV-radiation)

The properties and performance of a composite materials will change with temperature variation. For that reason, the behavior of FRP materials is often defined over a range of temperatures. Indeed, temperature's influence on polymers is thus classified in two categories: short-term and long-term effect.

While short-term effects are often only physical and reversible when the temperatures return to its original state, long-term effect are irreversible, more durable, and often include a chemical change. This long-term effect is identified as the aging of the material.

Four effects of temperature are identified in the following:

- The glass transition temperature T_G and melting point T_M ;
- The coefficient of thermal expansion CTE;
- The thermal conductivity; and
- The effect of ultraviolet radiation (even though it is not strictly a temperature property).

Measures to limit their effect on the degradation of polymers are available for designers. They are discussed in more detail in appendix B1.

iv. Fire

The fire safety of a structure refers to a structure's ability to withstand in a reliable and economic manner the actions and influence during execution and use. The fire resistance of a structure is expressed in minutes referring to the time before a structure collapses.

In fact, the polymer component of composite materials used in civil engineering applications is an organic material; composed of carbon, hydrogen, and nitrogen, composite materials are thus considered highly flammable. At temperatures above T_g , the matrix is in a "rubbery" state. At higher temperatures, both thermosetting and thermoplastic polymers burn, destroying the bonding between the fibers. This ultimately leads to failure, especially in structures with predominantly compression stress.

However, the major hazard of polymer components becomes the toxic combustion products resulting from the burning of the material. The produced smoke can be very hazardous and toxic with a wide array of products from combustible gases, vapors, and particulates. The degree of toxicity depends on material factors (component system used), the phase of burning (flaming combustion or fully developed combustion), and thermal inertia of the boundary conditions (ventilation). As smoke inhalation is the prominent reason of death in case of fire, smoke production and smoke toxicity are very important to control.

As such, measures at multiple levels have been developed to reduce the hazards and risk of combustible FRP. Standards measures can be applied to all structures to ensure fire safety: sprinkler systems, smoke alarms, ventilation systems, and escape routes. Beyond such measures, modification at the material level can also be brought. It is important to incorporate these lessons in any case-study in order to reach an integrated design.

- The introduction of additives in the resin. The process of incorporation additives can improve the fire resistance of FRP but also can introduce impurities to the composite material, compromising some mechanical or in-service properties.
 - Introducing nano-composite particles, for example, prove to be more efficient but remains far too complex and expensive for civil engineering applications [20], [36], [37] .
 - Introducing aluminum trihydrite (ATH) can have a fire-retarding effect. It changes the reaction into an endothermic reaction: it withdraws heat from the environment and produced water as a byproduct.
 - Introducing halogens such as chlorine or bromine increases the flashpoint of a resin. However, such compounds are generally not environmentally friendly: the released gases are very toxic.
- The application of a fire-resistant coating to the surface. Applying passive fire protection strategy, the manufactured composites are covered with an intumescent coating layer that will char and release gases at a designed temperature.
- The application of thick laminates. Thick laminates can delay the structural deterioration of elements due to their low thermal conductivity coefficients, yielding only superficial fire damage.

4. Conclusion

This chapter answers the following sub-questions

- What is the environmental challenge facing structural engineers?
- What is a proper framework to study sustainability?
- What is the definition of durability?
- What are the mechanical failure mechanisms of FRP?
- What environmental conditions cause degradation of FRP?

This chapter first highlights the sustainability challenge facing the construction industry today to emphasize the urgency of the situation. It then traces the solutions adopted by structural engineers for the short long-term to address the global impact of the industry's practices. This positions this research within the larger context of these efforts.

FRP's sustainability is assessed through the framework of a life-cycle assessment: from material selection to mold preparation, the structural performance of FRP components to their disposal or re-use. The life-cycle assessment reveals a nuanced picture. The sustainability promise of FRP must be assessed in a case-by-case basis, revealing how much a specific design embodies the principles of sustainability.

FRP's durability is also assessed in this chapter. Mechanical damage distinguishes between damage due to the composite nature of FRP (intra and interlaminar failures) and damage that results from FRP's in-service properties (creep and fatigue). Environmental degradation is also addressed, lending a closer look at moisture, corrosion, thermal effects, and fire. The discussion around environmental degradation is centered around possible measures to apply in order to limit and even avoid such damage.

The next and final chapter of the literature review traces the development of form-finding methods, from physical models to optimization algorithms. Focusing on structural optimization in FRP in particular, this chapter lays down the required knowledge to then develop the tool for formal exploration in FRP.

CHAPTER 4:

FROM FORM-FINDING TO STRUCTURAL OPTIMIZATION

Since the end of the twentieth century, fiber-reinforced polymers have witnessed an increased interest in civil engineering applications. However, their use has been primarily in strengthening and rehabilitations of old structure. In new structures, the use of FRP composites has remained limited to a few typologies, principally bridge structures. These limitations are seen as the consequence of a widespread design approach that doesn't exploit the material's most advantageous properties and render it not cost competitive with traditional construction materials.

The following chapter contains a brief overview of the generic form-finding methods, from physical model to structural optimization. The inherent limitations of these techniques are then discussed in order to broaden the scope of structural shape optimization. An overview of the optimization landscape in FRP as well as an overview of the available design tools are then described in order to uncover this thesis' main focus, formal exploration in FRP.

The chapter aims to tackle the following sub-questions:

- What physical methods of form-finding are available for engineers?
- What are their limitations?
- What is structural optimization and how can it solve those limitations?
- What specific strategies can be applied for design in FRP?
- What available tools do designers have access to implement such strategies?

1. Form-finding, from physical to numerical methods

Form-resistant structures have captivated the imagination of architects and engineers alike. This section displays an overview of the methods engineers have developed and relied on since the advent of the past century.

1.1 Physical Methods

In the pre-computer age, architects and engineers developed multiple experimental approaches to derive shape-resistant structures; these approaches are form-finding methods. As the resulting structure defied two-dimensional representation in conventional drawings, physical models took a central role in the development and representation of these shape-resistant structures. Relying mostly on physical models, three main experimental methods are identified: hanging models, tension models, and pneumatic models.

- **Hanging models** are usually derived for structures meant to work in pure-compression, such as arches and vaults. With certain constraints, this method's final stage represents an equilibrium state for flexible materials in pure tension under their self-weight (and sometimes an additional applied load). Once turned upside down, a state of pure compression is realized. Heinz Isler famously applied this approach of hanging models to derive the shape of his concrete structures [38] [39] as shown in figure 4.1.
- **Tension models** are structural systems in a state of self-stress, with as their name indicates, stresses in pure tension. The stiffness of the resulting tensile structures results from a system of internal stresses in static equilibrium. Often made of soap film or gauze, tension models derive equilibrium shapes with minimal material surface. Frei Otto pioneered in the development of tensile structures in order to achieve maximal efficiency of structures and materials. In his pursuit of "the architecture of the minimal," Otto's experiments in simulation the actual stress was highly significant to the development of tent and cable structures [40] as shown in figure 4.2.
- **Pneumatic models** achieve a state-of-equilibrium of flexible materials under air pressure with stress states in pure tension. With a set of applied constraint conditions, pneumatic models achieve minimal structures *par excellence* as just air pressure is required to support them without requiring cables or mats as tension models would. With pre-set boundaries, soap films or other membrane piece can be blown in place. Isler adopted this method for his concrete shells, most notably the COOP Storage and Distribution Centre in Wangen, Switzerland [41]. Otto formulated pneumatic models' first coherent theory and developed an impressive number of structures both realized and never-built, ranging from water towers to grain silos. Most remarkable is his work on the never-realized 2km dome *the Artic City* in the Arctic circle [40] shown in figure 4.3.

1.2 Modern form-finding

There is a clear and fundamental distinction between the aforementioned methods of form-finding and modern form-finding [38]. The methods employed by Gaudi, Isler, and Otto, otherwise known as classical form-finding, are based on a definition of form as structural shape. "Form follows force" is their guiding principle. Their tools and methods were limited to the above physical models such as hanging chains, tension models, and soap films.

The Information Age brought a paradigm shift to what and how architects and engineers design [42]. Today most, if not all, of architecture's practices rely on computational and digital methods. However, since the 1990s, a branch of architecture – digital architecture- has recast itself as the branch of experimentation of forms and topologies, "a generative, kinematic sculpting of space" [43] Digital architecture thus refers to the computational tools used for form generation. As Kolaveric argues in his paper, such concepts of digital architecture have since multiplied: topological architecture, isomorphic surfaces, animate architecture, keyshape animation, and genetic algorithms [42]. However, in keeping with the frame of our research, our discourse around digital architecture is limited to modern methods of form-finding used by architects and engineers. Unlike classical form-finding, they do not follow a singular principle, such as "form follow force." Modern form-finding includes a plethora of tools, processes, and algorithms to generate form such as NURB surface generation, structural optimization tools, and parametric design [38].

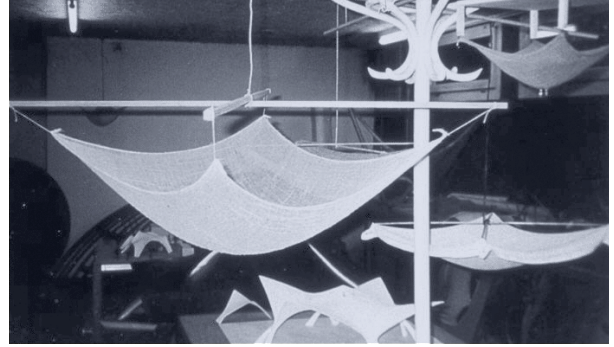


Figure 4.1 (left) The construction of Isler shells in Norwich Sports Park, Norwich England, 1991.
(right) Physical model made by Isler.

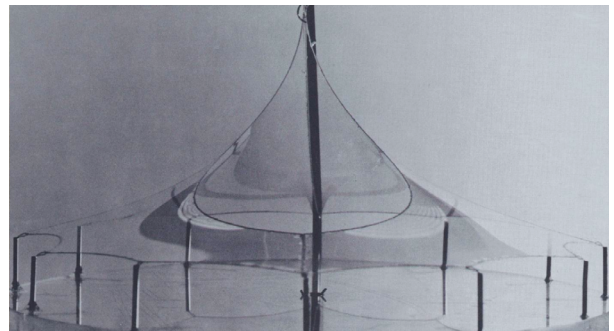
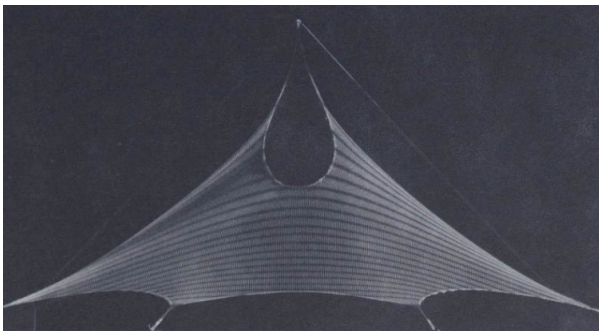


Figure 4.2 Study models completed by Frei Otto for the German Pavilion, Montreal, 1967.

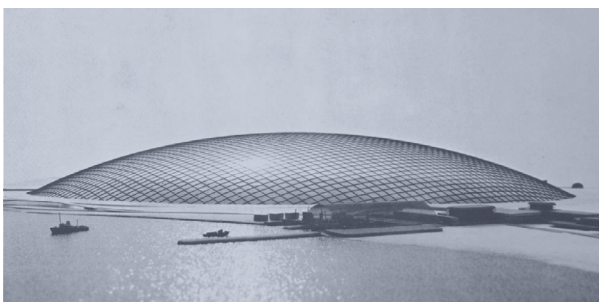


Figure 4.3 (left) Study models by Frei Otto for agricultural use, project 1959.
(right) COOP Storage and Distribution Centre by Heinz Isler in Wangen, Switzerland.

1.3 Form-finding numerical methods and their limitations

The development of computational techniques saw form-finding processes translated from physical model into mathematical ones. Such numerical methods have become the primary tool in generating force-active structural systems. In their book *Shell Structures for Architecture: Form Finding and Optimization* [44], Veenendaal and Block identify three families of computational methods corresponding to the aforementioned form-finding physical methods: (1) stiffness matrix methods, (2) geometric stiffness methods, and (3) dynamic equilibrium methods. Each family consists of multiple numerical method. A more extensive overview of the numerous available method can be found in their book. However, beyond the significant prevalence acquired in recent years, the numerous computational methods inherited the limitations of the physical methods they sought to simulate. Limitations include isotropic material, uniform stresses, and constant material properties during the form-finding process [35]. Such restrictions to the numerical methods do not allow exploring some competitive material properties (such as fiber-reinforced polymers).

2. Structural optimization

The advent of structural optimization techniques however has allowed to account for rising complexity in the engineering field. Numerical optimization methods allow to account for additional constraints brought by new materials: anisotropy, non-uniform stresses, and variable material properties [7], [8]. Structural optimization is defined as the process in which parameters are optimized in order to find the geometry of a structure such that an objective function or fitness criterion is minimized or maximized [45]. Computational methods of solving have thus risen to prominence in recent years to improve the performance of structures or optimize their behavior defined by one or multiple performance objectives. In the following, a quick introduction to such computational methods is provided.

2.1 Optimization Types

Structural optimization can be classified in three distinct categories [45], [46]:

- **Size-optimization** deals with the cross-sectional areas of the elements to find the optimal solution.
- **Shape optimization** shifts the boundary of the structural design to find the optimal solution.
- **Topology optimization** adds and subtracts elements and notes of the geometry to find the optimal solution.

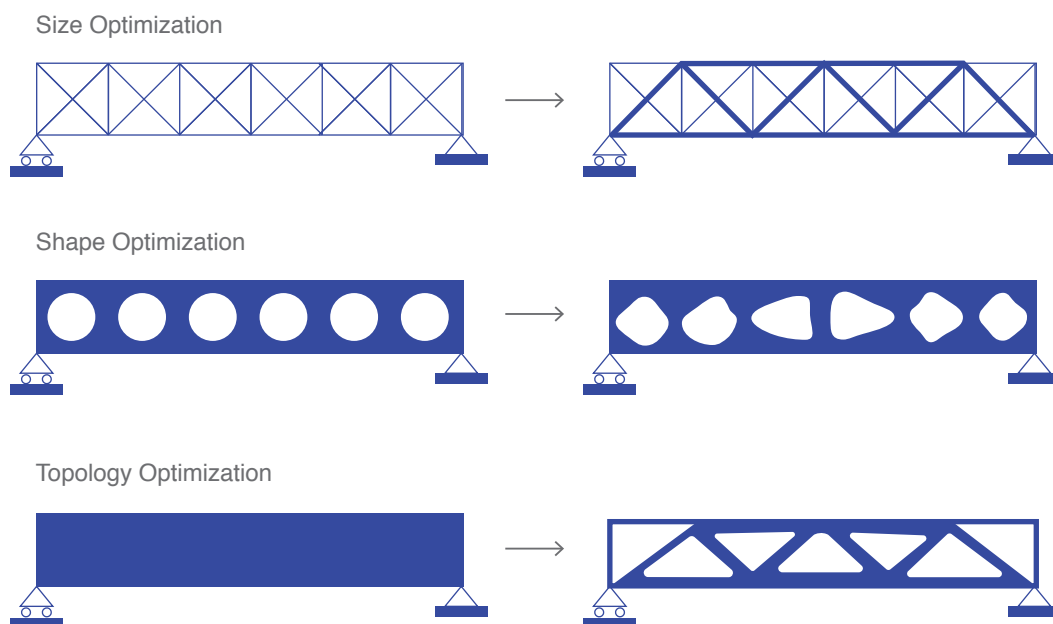


Figure 4.4 (left) Different optimization categories [43], [44].

While the taxonomy of optimization algorithms is difficult to provide, the discussion hereinafter is limited to a classification of optimization techniques available to engineers. Many single and multi-objective optimization techniques have been developed; each has specific applications, advantages, and disadvantages. The main types of optimization are distinguished in the following [38], [47], [48], [49]:

- **Discrete *versus* continuous optimization**

Discrete optimization refers to models whose variable can only take on values from a discrete set whereas continuous optimization refers to models whose variable can take any real value within a defined interval. Continuous optimization problems are generally easier to solve than discrete optimization problems. The smoothness of the functions allows to approximate the objective function at a point and its neighborhood.

- **Global *versus* local optimization methods**

Global optimization refers to finding the optimal solution (global minima or maxima) for a given objective function(s) among all the possible solutions of the search space. Differently, local optimization finds an optimal value (local minimum or maximum) within the subset of the search space without any guarantee that it will correspond to the global optimal value. In local optimization, the defined initial state significantly affects the found local optimum.

- **Deterministic *versus* stochastic optimization methods**

Deterministic optimization assumes that data can be known accurately. As such, the output of the model fully depends on the parameter values and preset conditions. However, the data cannot be accurately determined as the data often relates information about the future. Stochastic programming models are thus based on the fact that the probability distribution governing data can be estimated. As such, stochastic algorithms possess some inherent randomness. They take in consideration the inherent uncertainty of any problem.

- **Direct *versus* gradient optimization methods**

Direct optimization problem is a method that does not use the gradient or higher derivatives of the objective function. Diversely, gradient based algorithms are employed with continuously differentiable objective functions; they can be faster than direct search algorithms.

The formulation of an optimization problem is perhaps the single most important step of the optimization process; it is of paramount importance in obtaining the optimal solution. In other words, can a solution be considered optimal if it answers the wrong solution? As such, rather than attempting to summarize the breadth and depth of the literature available on each of the topic mentioned hereafter – an ambitious if not impossible task, the following section limited to what is deemed relevant to formulate the thesis' own optimization method. A preliminary look at the key aspects of single and multi-objective optimization is deemed necessary to better understand this thesis' developed framework.

2.2 Single-Objective Optimization

A general single-objective optimization problem is defined as the maximization or minimization of a certain scalar function. It is defined within constraints, in relation to parameters, and with respect to one or multiple objective. Optimization can lead to a collection of feasible structures, referred to as the design space.

- The **constraints** allow to limit the design space. They include performance criteria such as maximum stresses, deformation, buckling factors etc.
- The **parameters** refer to the design variables of the geometry to be optimized. They can either be discrete or continuous, depending on the definition of the problem. They often relate to the geometry or material properties of the structure in consideration.
- The **objective function** is defined in relation to the design parameters. An optimization process can contain one or multiple objective function. In a multi-objective optimization, the objective can include non-structural ones. Subject to constraints, objective functions evaluate the “efficiency” of a structure in order to improve its structural properties. The defined objectives are either load dependent properties such as stress, strain energy, and deflection or load-independent properties such as weight, area, or volume.

The single-objective optimization problem is mathematically formulated as:

$$\begin{aligned}
 &\text{Objective:} && \text{Minimize (or maximize)} \\
 & && f(x) \\
 &\text{Subject to:} && \begin{cases} g_i(x) \geq 0 & i = 1 \text{ to } m \\ h_j(x) = 0 & j = 1 \text{ to } p \\ X^L \leq x \leq X^U \end{cases} \\
 & && f(x) \quad \text{Objective Function} \\
 & && x \quad \text{Design variable vector} \\
 & && X^L \quad \text{Lower bound of the design variable} \\
 & && X^U \quad \text{Upper bound of the design variable} \\
 & && g(x), h(x) \quad \text{Inequality and equality constraints}
 \end{aligned}$$

2.3 Multi-objective Optimization

A multi-objective optimization problem refers to problems where the goal is to simultaneously optimize multiple objective. A multi-objective problem consists of objectives function. Linear or non-linear, continuous or discrete, the multiple functions form a vector function . A general multi-optimization problem is thus defined by the maximization or minimization of the objective function set , subject to equality and inequality constraint, that must be fulfilled while satisfying evaluation of It is mathematically formulated as:

$$\begin{aligned}
 & && F(x) = \begin{bmatrix} f_1(x) \\ f_2(x) \\ \vdots \\ f_k(x) \end{bmatrix} \\
 &\text{Objective:} && \text{Minimize (or maximize) } F(x) \\
 &\text{Subject to:} && \begin{cases} g_i(x) \geq 0 & i = 1 \text{ to } m \\ h_j(x) = 0 & j = 1 \text{ to } p \\ X^L \leq x \leq X^U \end{cases} \\
 & && f(x) \quad \text{Objective Functions} \\
 & && x \quad \text{Design variable vector} \\
 & && X^L \quad \text{Lower bound of the design variable} \\
 & && X^U \quad \text{Upper bound of the design variable} \\
 & && g(x), h(x) \quad \text{Inequality and equality constraints}
 \end{aligned}$$

Unlike single-objective optimization problems that result in a unique optimal solution, multi-objective optimization problems result in multiple solutions. No longer unique, the optimum in multi-objective optimization problems is seen as a trade-off or compromise between the different objective function. The most commonly adopted notion of optimum is known as the Pareto optimality, first introduced by Francis. Y. Edgeworth in 1881 and generalized by Vilfredo Pareto in 1906 [47]. Notions of Pareto optimality are elaborated in more detail in appendix D1.

Plotting all Pareto-solutions reveals a Pareto-front. The Pareto-front must maintain a certain diversity in the objective and design space to allow the decision maker to make a value judgment. Difficult to be determined analytically, the Pareto front is computed through the generation of as many points in the design space as possible. Multi-objective optimizations thus reveal a vicious circularity: the number of iterations is increased to clearly define the Pareto-front, which in turn results in too many solutions to choose from. Determining of a single solution for multi-objective thus requires a significant effort for post-processing. Many procedures and approaches to narrow the solution set of a multi-objective optimization have been/are the topic of ongoing research. The efforts include partition clustering, pseudo-ranking or hierarchical algorithms, weighted sum methods, etc. This additional level of post-processing allows the designer to narrow the solution set and select a solution representative of the set priorities [50], [51], [52], [53].

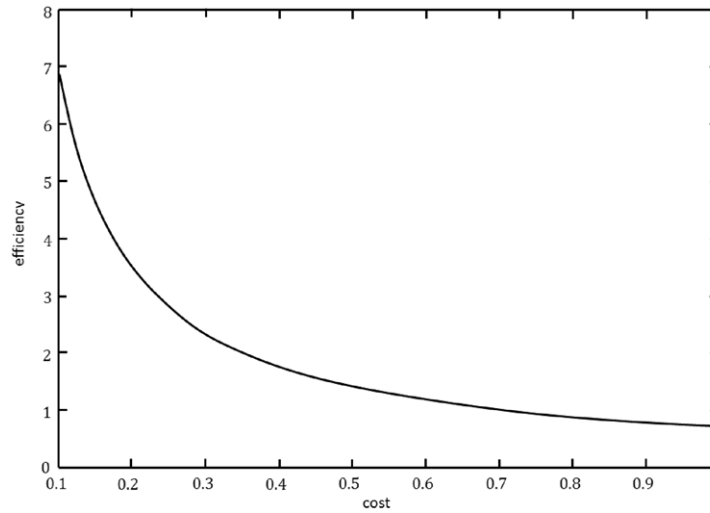


Figure 4.5 Example of a Pareto-front with two objective function: cost and efficiency [45].

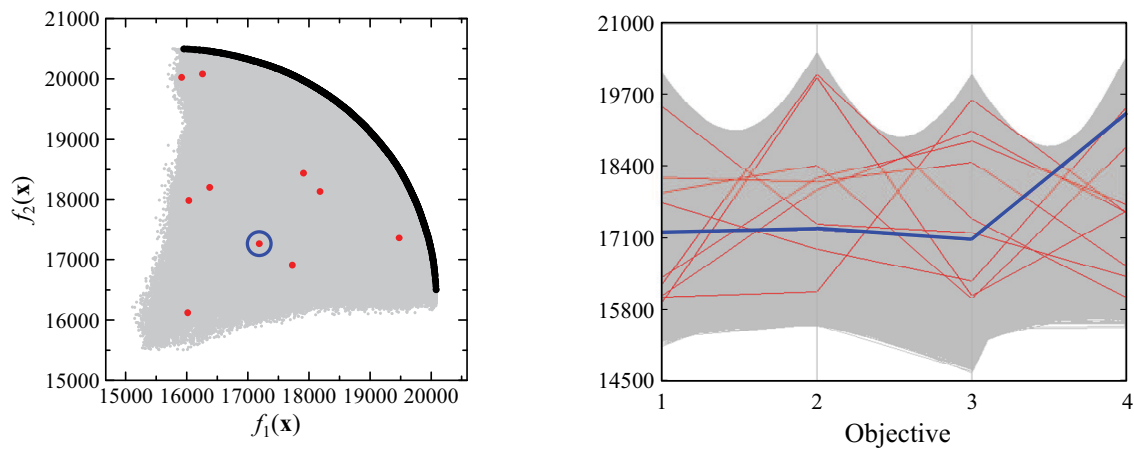


Figure 4.6 (right) Selection methods for a small number of non-dominated solutions from the objective subspace **(left)** and the corresponding parallel coordinate [52], [53].

3. Structural Optimization in FRP

3.1 Parameters and objectives

The maturity of materials and development of methods of analysis often leads to the emergence of new concepts and systems of design [54]. This claim motivates this thesis' research in new optimization of FRP form finding. As already established, form-finding numerical methods inherited the limitations of their corresponding physical experiments. Computational structural optimization techniques have become paramount for dealing with the constraints brought by FRP's anisotropic behavior.

An efficient and optimal FRP design often combines an optimization of the structure's geometry with an optimization of the material at the laminate level (mesoscale). The large number of design variables, both discrete and continuous, and large number of design functions make the optimization problems in FRP highly non-linear and non-convex.

According to the literature review of FRP optimization, the most recurrent parameters are:

- the three-dimensional free-form shape of a structure;
- the number of laminae;
- their respective angle orientation;
- their respective thickness; and
- the stacking sequence of laminae within the laminate layer.

Similarly, the most recurrent objectives:

- Optimizing stiffness of the structure (minimizing the compliance);
- Optimizing the weight of the structures (minimizing the weight); and
- Optimizing for maximal buckling factor.

The literature review reveals however a significant advancement in the optimization methods at the mesoscale, focusing on ply thicknesses, orientation, and stacking sequence. Seeking to achieve structural performance and minimum cost, optimization techniques and algorithms have become numerous, ranging from gradient-based methods, direct search methods, or genetic and evolutionary algorithms. This section does not attempt to summarize all the numerous algorithms available to designers to design optimal structure in composite layups, more extensive literature reviews and discussions can be found in [6], [11], [w55], and [56]. However, perhaps more important than discussing the findings of these papers is examining what is absent from them. Indeed, a closer look at the available optimization techniques reveals more research devoted to optimization at the mesoscale. This is a result of FRP being a material more extensively used in the aerospace applications. In the aerospace industry, research is focused on minimizing weight and costs and is less interested in formal explorations of FRP.

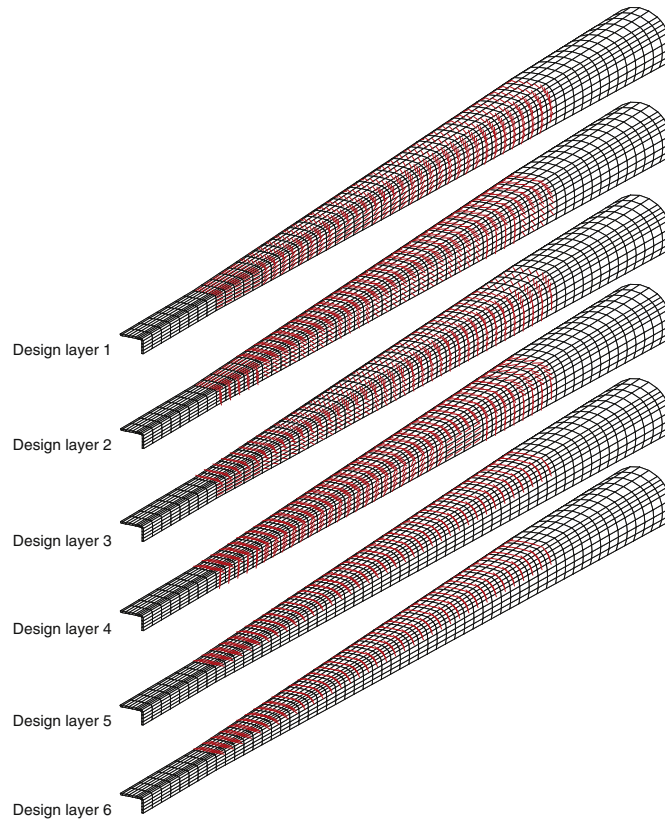


Figure 4.7 Fiber angle results from nonlinear buckling optimization for half of the generic wind turbine main spar [57].

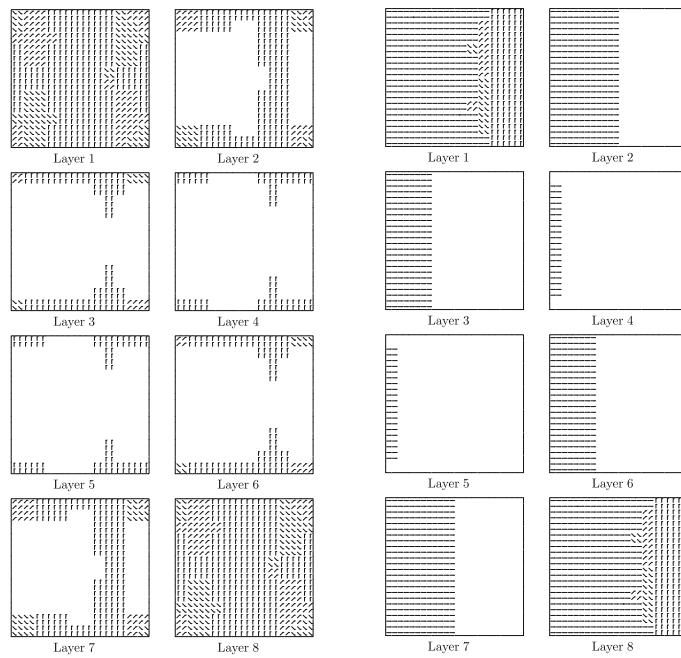


Figure 4.8 Optimized material directions (fiber angles) for maximum buckling load factor design of an eight-layer plate: layer 1 is the bottom layer and layer 8 is the top layer [58].

3.2 Evaluating the landscape

An optimal composite shape must consider the design space defined by the continuous geometric parameters as well as material properties (thickness of laminates, orientation, stacking sequence). A first approach at this non-linear and complex problem is proposed by Miki and Sugiyama and Fukunaga and Vanderplaats, both in 1991 [59], [60]. They suggested a two-tier structural shape optimization that maximizes the stiffness of the structure while the weight of the structure is limited.

- the first level generates the optimal geometric shape using lamination parameters (appendix E1) to maximize the stiffness of the structure.
- the second level finds the optimum lamination parameters and then the corresponding stacking sequence using genetic algorithms.

It bases heavily on the simplification of the optimization problem brought by the use of lamination parameters. More recently, Burgeño and Wu applied the two-tier integrated approach to free-form bridge systems and shells [7], [8]. Seeking formal exploration in FRP, they modernize Miki and Sugiyama's approach with innovative numerical algorithms that verify the validity of this two-tier strategy.

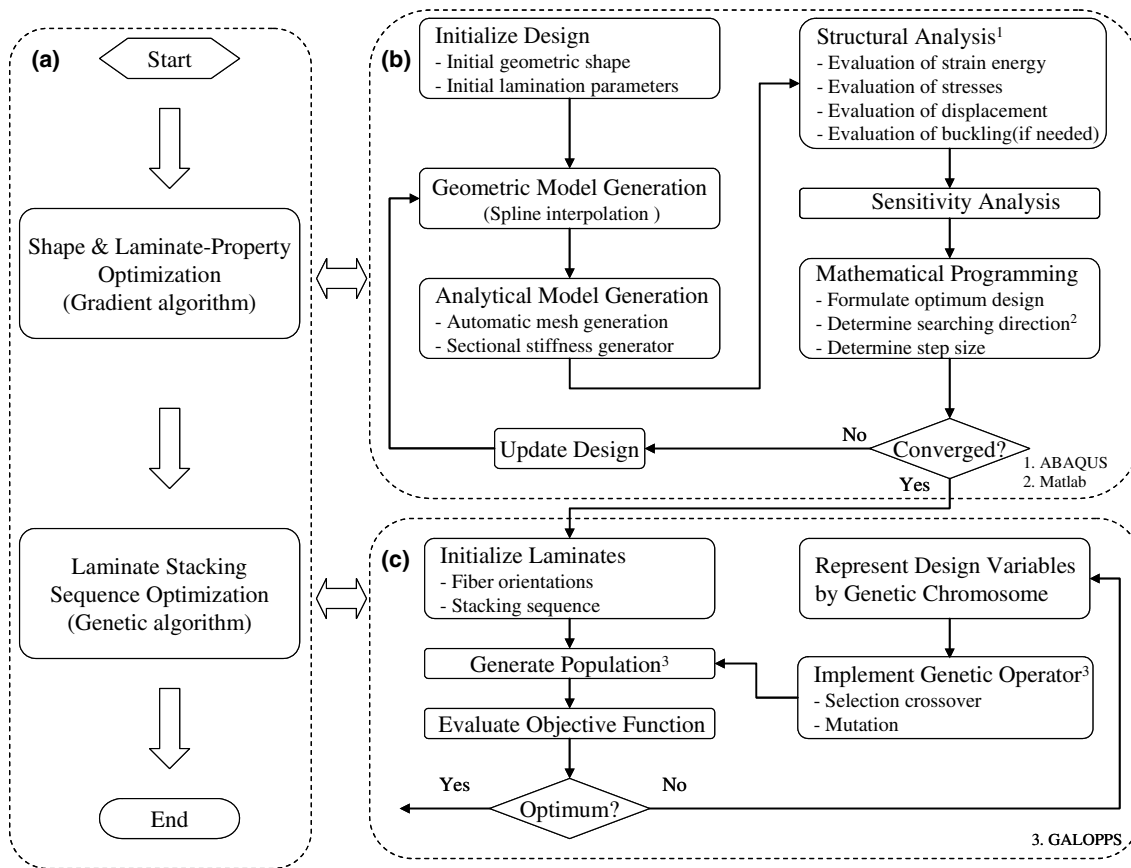


Figure 4.9 Two-level approach of shape and laminate stacking sequence optimization and its implementation as developed in Burgeño and Wu's research [7], [8].

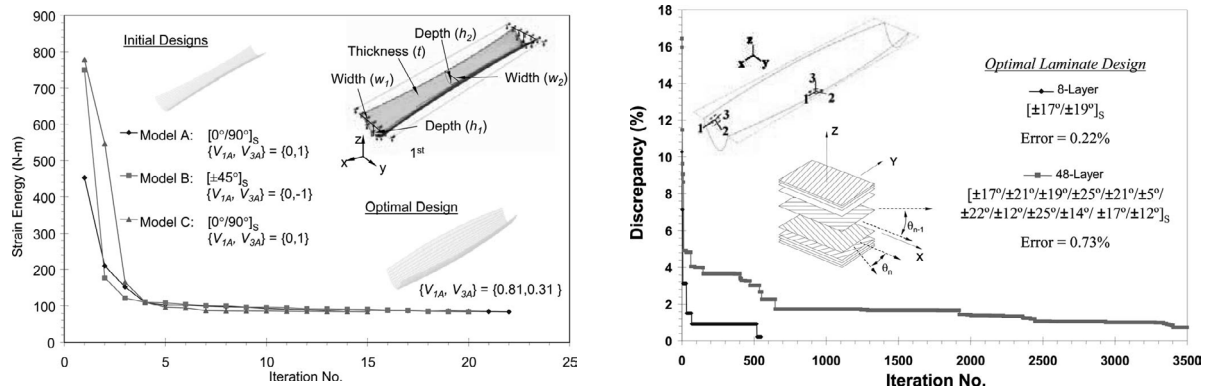


Figure 4.10 (right) First-level optimization of the shape and laminate property optimization **(left)** and second-level optimization of the stacking sequence optimization for CMB bridges as developed in Burgeño and Wu's research [7] .

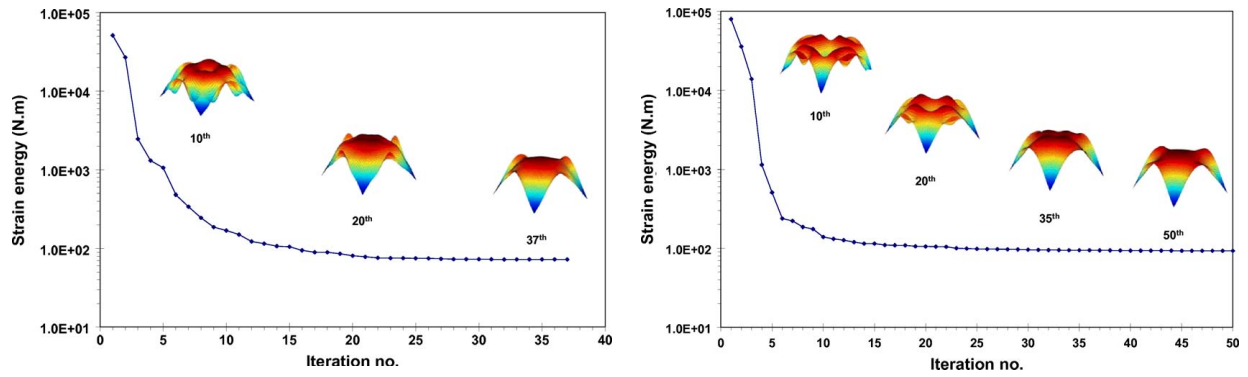


Figure 4.11 (right) Shape optimization process of $[45^\circ/-45^\circ/-45^\circ/45^\circ]_{6S}$ laminated FRP shell and **(left)** shape optimization process of $[0^\circ/90^\circ/90^\circ/0^\circ]$ laminated FRP shell as developed in Burgeño and Wu's research [8].

It is however paramount to mention that the generated structures in these research remain simple with a small number of geometric continuous parameters [7], [8], [59] and [60]. More complex free-form architecture requires then to alter the two-tier approach. Furthermore, the optimal stacking sequences generated in the second-tier optimization include lamina orientation beyond the standard and widely available angles such as 0° , 30° , 45° , 60° , and 90° . While such sequences result in lighter and thus more “optimal” structures, the adopted approach seem to disregard any practical considerations within the civil engineering industry. They are not in line with the manufacturing of large free-form structures which often include production methods such as hand layup and vacuum infusion. Therefore, this research's suggested optimization must adapt the methodology developed by Miki and Sugiyama and extended by Burgeño and Wu. It should extend its core principles to fit more complex geometries exhibiting shell-like behavior as well as more realistic production methods of such free-form structures. An example of formal exploration found in typology optimization framework is found in the research of Smits, Gkaidatzis, Blok, and Teuffel [61].

4. Formal Exploration in FRP

Every optimization problem presents unique challenges and must be treated as such. The nature of this design problem depends on the design variables, constraints, criteria, and objectives. With each optimization technique having its advantages and disadvantages, choosing a structural optimization method becomes a compromise between the different aspects of the problem. Formulating the optimization problem is arguably the most important step in finding optimal solutions. Simply put, obtaining the right answers depends on asking the right questions to begin with. This requires a proper formulation of the challenge to answer (parameters, constraints, and objectives) as well as the availability of tools in the market.

4.1 Framework Ambitions

As described in the introduction of this research, this research's proposed tool aims to catalyze formal exploration in FRP. Considering the advantageous FRP properties in durability and sustainability, it aims to encourage structural designers to view FRP as a viable option to design with. As summarized in the first chapters, FRP's leading qualities are its inherent in-plane stiffness and strength and its main liability is its weakness through the thickness direction. Using modern form-finding tools, shape resistant structures in composites that transfer their loads dominantly through in-plane forces can be derived. Formal exploration in FRP will capitalize on the material's strength (in-plane stiffness) with minimal and efficient use of the materials (weight).

To underscore geometric exploration, the proposed optimization tool must be easy to use and implement to different geometries. To facilitate geometry generation of structure exhibiting shell-like behavior, the 3D modeler Rhinoceros is used with the parametric algorithm. This allows for quick generations of FRP geometries and their consequent assessment. The next section of this chapter focuses on the search spaces defined in such geometric exploratory problems before addressing algorithms fit to search the size and complexity of those search spaces.

4.2 Complex Search Spaces

This research's suggested framework focuses primarily on geometry generation for structure exhibiting shell-behavior. The design boundaries of the considered structure must be first set. The geometric parameters of the cross-sections (width, depth, slenderness, etc.) as well as material parameters (thickness, laminate layup, etc.) are the parameters defining a certain design. The design's performance (fitness) is then evaluated according to a single or multiple objectives. Such geometric explorations for structures result in large and complex search spaces because of the numerous continuous parameters. Detecting local or global optima becomes challenging. Using brute force algorithm, iterating between all available solutions of the design space, is unrealistic in terms of required time.

The increasing complexity of problems has fueled interest in nature inspired algorithms to find global optimum [62]. Nature inspired algorithms refer to optimization algorithm emulating biological phenomenon. Various stochastic optimization techniques exist under the umbrella of nature-inspired algorithms. In particular, metaheuristics techniques refer to a family of stochastic tools that aim to efficiently explore a search space. Considered as "higher level frameworks" [62], they are more efficient than direct algorithms in finding a global optimum solution. These algorithms include both nature-inspired techniques such as Evolutionary Algorithms (EA), Particle Swarm Optimization (PSO), Simulated Annealing (SA), Ant Colony Optimization (ACO), etc.

In his dissertation [63], Brownlee identifies six main categories of nature-inspired algorithms:

1. Stochastic algorithms, introducing randomness into heuristic methods;
2. Evolutionary algorithms, emulating the process of natural selection;
3. Physical algorithms, imitating physical and social systems;
4. Particle Swarm algorithms, inspired by the “collective intelligence” of agents (flocks of bird, colonies of ants, schools of fish);
5. Immune algorithms, reproducing the adaptive mechanism of the immune system; and
6. Neural algorithms, copying the plasticity and adaptive nature of the nervous system.

Each type of algorithm has expansive literature that discusses its applications, advantages, as well as its limitations. When discussing the suitability of an optimization algorithm for a certain problem, it is worth introducing the no free lunch theorem (NFLT) developed by Wolpert and Macready. The no free lunch theorem underscores that the performance of any optimization algorithm depends on the formulation of the problem [64]. Differently said, the theorem states that there is no global optimization algorithm that can be applied to all problems to find the optimal solution. However, there are algorithm types that are more fitting for the defined search spaces.

4.3 Evolutionary Algorithms

This research focuses on evolutionary algorithms among Brownlee’s six nature inspired algorithm categories. The evolutionary algorithms are considered most appropriate to use with complex and large design spaces to find global designs. While significantly more time-consuming than others, evolutionary algorithms retain “a sufficiently large populations of designs covering more effectively the complete design space and increasing the likelihood of detecting different local optima” [65]. Emulating Darwinian principle of “survival of the fittest,” evolutionary algorithms are defined as population-based algorithms. They generate solutions or individuals: the variable defining a solution are encoded in its genome (as genes) and its performance is evaluated by a fitness function. The algorithm will then evolve towards the fittest solution through crossover (crossing genetic material), random mutation (the descendent individuals to increase diversity), and natural selection.

In particular, genetic algorithms are optimization methods inspired by the process of natural selection and belong to the larger family of evolutionary algorithms. They are initially introduced by John Holland in the 1960s and extended by his student David. E. Goldberg in 1989 [38]. Today, they constitute an important field of research encompassing many sectors: biomedical, aeronautical, architectural, and structural design to name a few.

In table 4.1, a comprehensive picture of the advantages and disadvantages of GA are summarized.

Advantages of GA	Disadvantages of GA
<ul style="list-style-type: none"> - In principle, GA allow to find global optimum. - GA are flexible and can be applied to a wide range of problems. - GA have a progressive run-time with intermediate solutions that can be harvested at any point of the process. - GA are transparent. They uniquely allow for interaction with the users and a high degree of specificity for each problem. - GA can be used with both single or multi-objective optimization. 	<ul style="list-style-type: none"> - Characteristically, GA are slower than other optimization tools. - GA require users to define the convergence of the problem in terms of run-time or generation in order to effectively reach a solution. - GA might require a significant amount of testing and repetition in order to ensure that the global optimum has been obtained and avoid pre-mature convergence.

Table 4.1 Advantages and disadvantages of Genetic Algorithms (GA) [66], [67], [68]

Recalling the no free lunch theorem, other optimization algorithms can also be deemed fit for searching large and complex search spaces. Specifically, Particle Swarm Optimization algorithms are powerful in finding a global optimum [63]. However, the wide availability of GA plug-ins I (both single and multi-objective algorithms) and the general popularity of GA has lead this research to focus specifically on GA [62].

4.4 Available Plug-ins

In order to be easily implemented by engineers at the preliminary stage, the developed framework must be based on an empirical exploration of the available tools for designers at the conception phase [66]. As such, the considered tools are limited to the plug-ins used in Grasshopper 3D to facilitate implementation. Genetic solvers in are Galapagos, Octopus, Wallacei.

- **Galapagos** is one of the first evolutionary solver plug-ins implemented for Grasshopper 3D. The tool provides two metaheuristic algorithms: a genetic algorithm (GA) and a simulated annealing (SA) [69].
- **Octopus** is an evolutionary solver introduced for multi-objective evolutionary algorithms, producing multiple optimal solutions that define the Pareto-front. Octopus employs SPEA-2 and HypE algorithms from ETH Zurich [70], [71].
- **Wallacei** is a newly introduced evolutionary solver allowing to run multi-objective optimization in Grasshopper, also generating a Pareto-front. Wallacei employs NSGA-2 algorithm as well as multiple comprehensive selection methods including algorithm clustering to better understand the results at the Pareto-front. The tool is special in providing the user with many tools to reconstruct and analyze solutions after any optimization [72], [73].

Choosing a specific plug-in requires the comparison of the different aspects of the tools. Besides converging on the global optimum in a reasonable amount of time, it is fundamentally important for the structure to be easy to use and implement to new geometries. Beyond the limitation of the adopted algorithm, the advantages and disadvantages of the three genetic solvers are summarized in table 5.2.



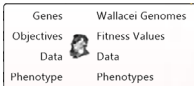
Galapagos 	Single objective optimization: Genetic Algorithm (GA) + Simulated Annealing (SA)	Advantages: <ul style="list-style-type: none"> - Implementing the tool is straightforward and simple. - Visualization of results is possible in separate tab. Disadvantages: <ul style="list-style-type: none"> - Additional attention must be brought to export data.
Octopus 	Multi-objective optimization: SPEA-2 + HypE	Advantages: <ul style="list-style-type: none"> - Implementing the tool is straightforward and simple. - Visualization of results is possible in separate tab. Disadvantages: <ul style="list-style-type: none"> - Additional attention must be brought to export data. - Significant post-processing is required to cluster and/or rank the solutions at the Pareto-front.
Wallacei 	Multi-objective optimization: NSGA-2	Advantages: <ul style="list-style-type: none"> - Implementing the tool is straightforward and simple. - Visualization of results is possible in separate tab. - Accessing the solutions is possible whether it is selecting, reconstructing, and analyzing solutions in post-optimization. Disadvantages: <ul style="list-style-type: none"> - As a new tool, some experimentation is still required to accrue popularity.

Table 4.2 Advantages and disadvantages of the different EA plug-ins available in Grasshopper 3D [69], [70], [71], [72], [73].

5. Conclusion

This chapter answers the following sub-questions:

- What physical methods of form-finding are available for engineers? What are their limitations?
- What is structural optimization and how can it solve those limitations?
- What specific strategies can be applied for design in FRP?
- What available tools do designers have access to implement such strategies?

The chapter introduces the physical methods structural designers have developed over the past century to derive form-resistant structures. These methods include hanging, tension, or pneumatic models used by Gaudi, Isler, and Otto. The advent of the computational age has expanded classical form-finding methods beyond their guiding principle of “form follows force.” In fact, they allowed structural designers to overcome some of the limitations of physical methods such as isotropy, uniform stresses, and constant material properties.

Computational methods include many structural optimization tools and algorithms. Structural optimization in particular includes three main categories: size, shape and topology; each has its specific applications. This chapter does not offer a full taxonomy of optimization methods available for the engineer; it however distinguishes between the main types of optimization: discrete versus continuous, global versus local, deterministic versus stochastic optimization methods, direct versus gradient based optimization. Most importantly, the chapter contrasts single-objective and multi-objective optimization. Unlike single-objective optimization that result in a unique optimal solution, multi-objective optimization results in multiple solutions, known as Pareto solutions requiring significant post-processing to select the most-optimal.

Lastly, this chapter evaluates the landscape of optimization in FRP in order to define the most common parameters and objectives. It identifies pivotal studies for FRP form-finding and extrapolate the knowledge to define a new framework that encourages formal exploration specifically in FRP. The proposed framework favoring geometric exploration entails numerous parameters resulting in large and complex search spaces. Nature-inspired algorithms are briefly investigated as tools proper to deal with the size and complexity of those search spaces. In specific, the wide availability of GA tools and their overall popularity in structural design have made the choice of algorithm for this research. The various plug-ins available in Grasshopper 3D are then laid out, each with their advantages and limitations.

The next chapter of the research establishes the context of the chosen case-study. It traces the development of the suggested tool, before implementing it on the chosen case-study.

CHAPTER 5:

CASE-STUDY CONTEXT AND OPTIMIZATION FRAMEWORK

This thesis aims to develop a framework for structural form-finding of FRP shells. To clearly explain the suggested framework, the Wilhelminaberg Viewpoint designed by Ney & Partners is chosen as the case-study. The Wilhelminaberg Viewpoint has the potential to become the manifesto project of FRP. It capitalizes on the advantages that render FRP a promising construction material as well as the aspects that have limited its proliferation. The conditions of the site as well as the vision of the Parkstad Limburg further extend the structure's ambitions.

The following chapter elicits the vision of the IBA initiative in Parkstad Limburg in general and the Wilhelminaberg Viewpoint in particular. The context of the project is central to the structure's ambitions. After describing the context of the case-study, this chapter traces back the development of the optimization framework. It defines the important aspects of the optimization: geometry generation, finite-element analysis, parameters, design criteria, and used algorithms/plugin-ins. Specifically, each aspect is illustrated with the example of the Wilhelminaberg Viewpoint. With the cornerstone of the optimization tool laid out, the limitations of the suggested framework are finally discussed.

The chapter aims to answer the following sub questions:

- What is the context of the chosen case-study? Why was it adopted?
- What were the steps in the development of this tool?
- What are the objectives, design criteria, constraints of this optimization?
- What are the limitations and restrictions of the suggested framework?

1. Case-Study

1.1 The IBA Context

The Wilhelminaberg Viewpoint is part of the first International Building Exposition IBA in the Netherlands, set in the Parkstad Limburg region. The *Internationale Bauausstellungen* (IBA) was initiated in 1901 in Germany as a celebration of modern construction and a demonstration of the state of the art in architecture [74]. Since its inception, the IBA has continuously redefined its mission and expanded its reach. From celebrating technological innovation in the early 20th century, the IBA's objective is to restore the social and political relevance of architecture and urban development. Each IBA iteration is created in a specific region and answers a specific geographic, historic, economic, and social context. The involved stakeholders identify the needs of a certain region. Programs and projects are then proposed to enact the structural change required to revitalize the region. In the newest formulation of its mission, the IBA experiments with broadening its reach to create projects that have a strong halo effect on their surrounding areas.



Figure 5.1 Different IBA iterations in different cities from different phases.

(top) 1957 IBA Berlin. **(middle)** 1989-1999 IBA Emscher Park. **(bottom)** 2006-2013 IBA Hamburg.

1.2 The IBA Parkstad

The Parkstad region in Limburg is the first formulation of the IBA in the Netherlands. Comprised of eight municipalities with a shared history, the Parkstad has undergone important social and economic change since the closure of its mining industry in 1969. With a high unemployment and human capital flight, even the government's effort *van zwart naar groen* (from black to green) were insufficient to revitalize the area. Since 2013, the Parkstad IBA initiative has been focusing on reviving the former mining region, inviting urban renewal, and stimulating the economy. Through a series of innovative and creative projects, it is focused on celebrating the green and sustainable version of the entire region.



Figure 5.2. (left) Bicycle bridge in Onderbanken. (right) Center Court in Kerkrade to Gravenrode [74].

1.3 The Wilhelminaberg Viewpoint

Extending the longest staircase in the Netherlands, the Wilhelminaberg Viewpoint is a proposal to mark both physically and metaphorically the orientation of the area recovering from its industrial past as shown in figure 5.3 and 5.4. The Wilhelminaberg Viewpoint, by Ney & Partners, is an iconic landmark proposal, to celebrate innovation of form and technology. The viewpoint takes the shape of an oloid, a three-dimensional structure consisting of two intersecting circles (first discovered by Swiss sculptor and mathematician Paul Schatz [75]).

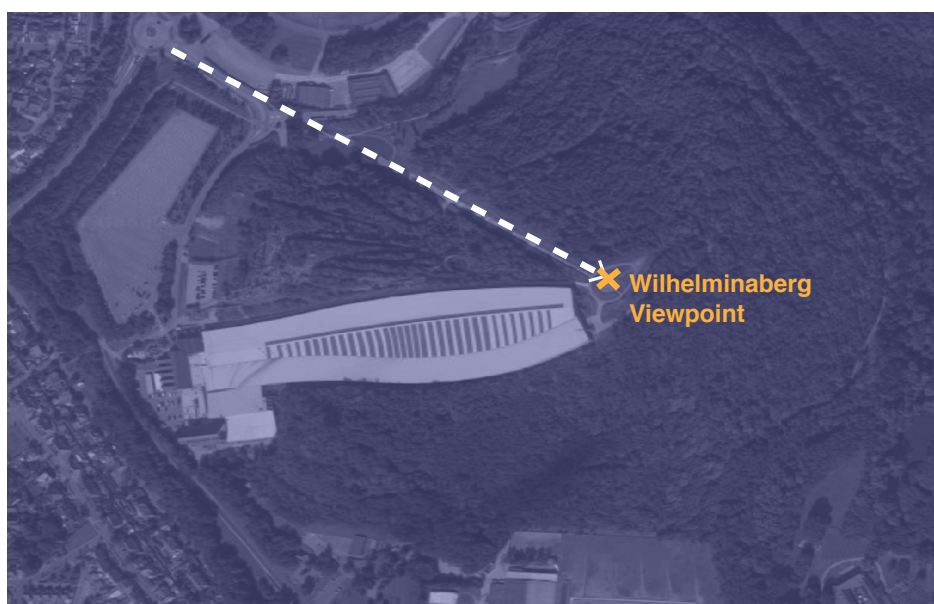


Figure 5.3 Location of the Wilhelminaberg Viewpoint in Landgraaf using Google Maps [75] .

1.4 Wilhelminaberg Viewpoint Renders



Figure 5.4 The Wilhelminaberg Viewpoint renders by Ney & Partners [76].

1.5 An FRP Manifesto?

Ney & Partners designed a steel structure in order to prove the construction's viability. Two intersecting rings connected with steel cables, topped with a cladding mesh surface as shown in figure 5.5. This steel design fits traditional means of construction and is innovative in its application of steel. However, the used material leads to a heavy design. In light of the site's limited accessibility, the poor soil condition in the heavily mined area, and the seismic nature of the area, it becomes interesting to study alternative material options.

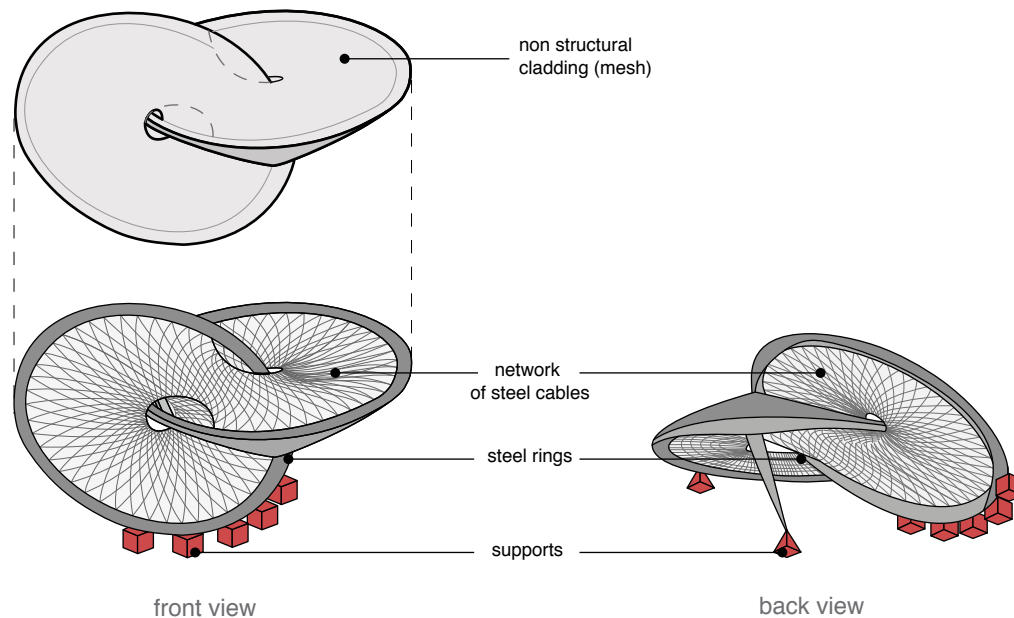


Figure 5.5 Structural system of the Wilhelminaberg Viewpoint (steel proposal).

For those same reasons, an FRP design is particularly interesting. Furthermore, the vision of IBA Parkstad 2020 extends further the aspiration to design a light, durable, and sustainable structure. As part of a project that celebrates innovation, technology, and sustainability, the Wilhelminaberg Viewpoint can become a manifesto project for composite structures. It capitalizes on the advantages that render FRP a promising construction material such as long-durability properties, tailorable mechanical properties, customizable production for free-form design, and a light weight design. The case-study will also allow to highlight the aspects that have limited its proliferation such as the need for advanced computational methods, non-competitive methods for repetitive production processes, and the limited knowledge in some of its long-term durability properties.

The framework to be developed is intended as an exploration tool used in the preliminary design stage. It generates structures that utilize the properties of FRP. In the post-optimality structure, the research allows to assess the difference between the potential of FRP and the realities of what's buildable in FRP. The remaining of this chapter will first describe the development of the framework before describing the different aspects of the optimization (objectives, parameters, constraints, etc.)

2. Tool Development

Retroactively explaining the development of the framework is an ambitious task. The process of developing the optimization tool was not a linear but rather circular requiring constant fine-tuning and iterating. Implementing structural optimization techniques to shell-like materials is an interesting topic of research. Different techniques have been applied to optimize the size, shape, and topology of shells. The research develops a framework for optimization of FRP shells, revisiting where the Miki/Sugiyama or Burgeño/Wu studies had left off [7], [8]. The process has to be significantly modified to account for more complex geometries in structural engineering. Beyond extending the already developed frameworks in the literature review, the development of this thesis's framework requires testing of the different design strategies and tools available for structural designers.

2.1 Optimization Objectives

Clearly defining the objective of an optimization is a difficult, but central task, of developing an optimization framework. As mentioned in the previous chapter, obtaining the right solutions depends on asking the right questions to begin with. Through the literature review, FRP's inherent in-plane stiffness and strength constitutes the material's main strength. Its main liability is its weakness through the thickness direction. With modern form-finding, shape resistant structures in composites that transfer their loads dominantly through in-plane forces can be derived. These correspond to structure exhibiting shell-like behavior. As such, formal exploration in FRP will capitalize on the material's strength (in-plane stiffness) with minimal and efficient use of the materials (weight). This optimization framework first limits the form-finding to two main objectives: maximizing the structural stiffness to generate shape resistant structure and minimizing the weight of the geometry for efficient material use.

i. Stiffness Maximization

Maximizing the global stiffness of a structure, an objective of the suggested framework, is equivalent to minimizing its compliance. Defined as the sum of the strain energy of all its elements, the compliance of a structure is a measure of its overall flexibility or stiffness [8], [78] .

The total strain energy is defined in terms of the initial strains and stresses:

$$U = \frac{1}{2} \int_V \{\epsilon\}^T E \{\epsilon\} dV = \frac{1}{2} \{D\}^T \{K\} \{D\} \quad (1)$$

with

$$D = [K]^{-1} \{R\} \quad (2)$$

Equation (2) is substituted in equation (1). Strain energy is then evaluated as:

$$U = \frac{1}{2} \{R\}^T \{K\}^{-1} \{R\} \quad (3)$$

Equation (3) reveals that the total strain energy U decreases as the structural stiffness $[K]$ increases for a given equivalent load $\{R\}$.

ii. Weight Minimization

Minimizing the weight of the generated geometry is the objective of the second level optimization. A lighter structure generally translates in less energy expended during transportation and installation.

2.2 From a Multi-Objective to a Single-Objective Design

A first approach consists in combining the two objectives of minimizing weight with maximizing stiffness in a multi-objective optimization. Combining these objectives leads to light structures that exhibit an optimal performance of the composite material FRP. The initial multi-objective optimization framework is tested for a simplified geometry of the case-study. The simplified design case considers a straight non-curved design with a span of 106m, equal to the rolled-open span of the considered segment of the Wilhelminaberg Viewpoint. Using table 4.2, the multi-objective optimization uses Octopus rather than Wallacei. While straightforward and simple, implementing the tool

in Wallacei requires additional attention when compared to Octopus. The results of the multi-optimization approach are discussed in depth in appendix F1.

As discussed in chapter 4 of the literature review, each optimization scenario in a multi-objective framework results in numerous “optimal solutions” rather than a singular solution as shown in figure 5.6. This renders the post-optimality analysis quite laborious and unproductive: extensive post-processing is required to organize and rank the solutions (figure 5.7). The post-optimality analysis required for a multi-objective optimization is a significant weakness of this approach. This significant amount of post-processing is antithetical to the research’s main objective, to encourage formal exploration in FRP.

Formal exploration at the conception phase entails running multiple structural optimization for various geometric scenarios. If one solution requires substantial post-processing, a multi-objective optimization is counter-productive. Furthermore, once a structure verifies all the design criteria, obtaining the stiffest design is not necessarily advantageous. Minimizing the weight of the structure becomes a more relevant objective. In the next section, the proposed framework is explained.

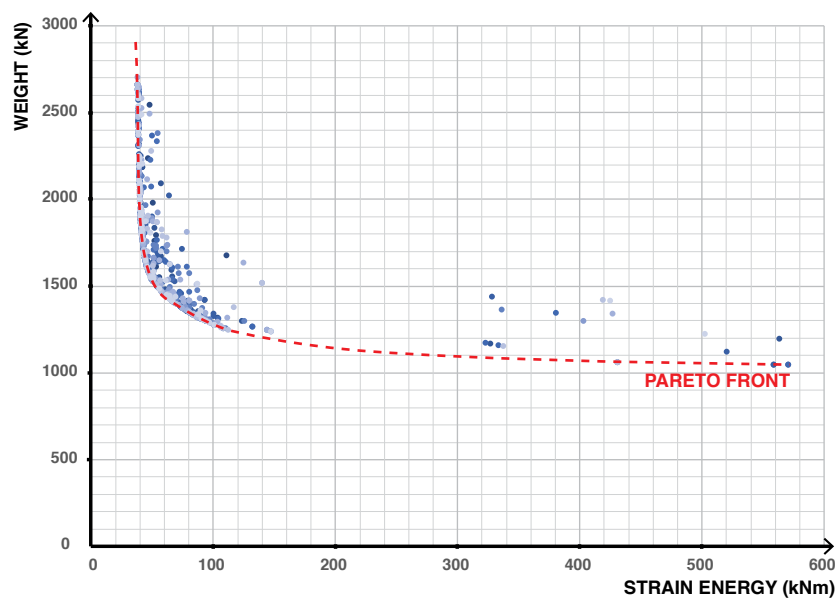


Figure 5.6 Pareto-front generated in the multi-objective optimization of the straight quadrilateral beam.

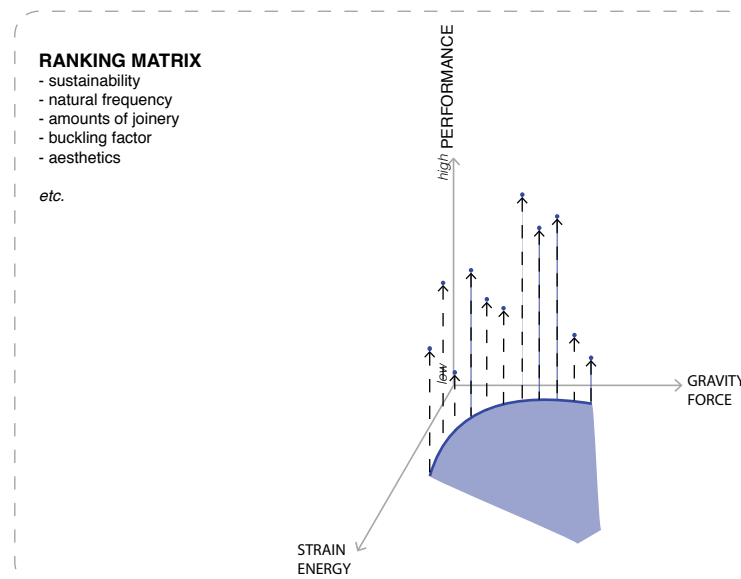


Figure 5.7 Significant post-processing required to rank the “optimal” solutions on the Pareto Front.

2.3 Multi-Step Single Objective Optimization

A new optimization framework is configured. Moving away from a multiobjective optimization, combining both material and geometric variables in one-step renders any search space too large and complex. Rather, the new framework uses multiple steps of single-objective optimization. The suggested tool verifies the objective of the research: it prioritizes exploration of form and geometries while utilizing FRP's advantageous properties. The resultant of the suggested multiple step framework is a single optimal structure. This allows to implement the tool on different geometric scenarios and explore the design space.

Based on the available literature study and an empirical exploration of the available tools, the proposed design space is organized in two-levels:

- **Level 1:** using brute force algorithm (a deterministic and direct algorithm), the first level finds the laminate layup that maximizes the stiffness of the structure, using material properties as parameters.
- **Level 2:** using a genetic algorithm (stochastic and direct algorithm), the second level generates the optimal cross sections using geometric parameters defining the section of the structure and its thickness.

This succession of the two levels (maximizing stiffness first and then minimizing weight) allows the optimization process to explore the largest part of the solution space. For a specific geometry, the maximization of the stiffness of the structure requires finding the optimal material properties. Differently stated, for a certain shape or design boundaries, the stiffness of a structure will always be greatest for the same material parameters regardless of its geometric parameters. This is based on empirical exploration of the available tools. In order to make the proposed framework most efficient, the first level optimization finds the material properties for a certain design boundary that maximize the stiffness. As such, the second level optimization becomes more efficient by only considering geometries with the stiffest material properties.

3. The Proposed Framework

- **The first level** of the optimization maximizes the stiffness through iterating through the optimal material properties. This step allows to capitalize on an important advantage of the FRP: its alterable material properties over a single structure. The total structure can be divided into multiple sub-spans to allow material properties to change for each sub-span.
- **The second level** optimizes the weight through a genetic algorithm that considers geometric parameters.

Shown in figure 5.8, the framework is organized as follows:

1. Geometric and material parameters are defined. The geometry is generated in Rhinoceros using a parametric model coded in Grasshopper 3D. A mesh is generated.
2. Support conditions, load-cases, and load areas are specified. A structural analysis of the generated mesh is completed in Karamba 3D, a finite element plug-in of Grasshopper 3D.
3. Design constraints are defined.
For each design boundary,
 4. step 1 of the optimization is run once. The employed brute force algorithm iterates through the different material properties to maximize the stiffness of the structure. The material properties correspond to the different laminate layups.
For each different scenario,
 5. step 2 of the optimization is run. The defined fitness function (weight of the structures) evaluates the quality of the solution; a penalty is defined if the design constraints are not verified. The lightest structure is found using a genetic algorithm. The chosen genetic algorithm is not scripted by the author but is a plug-in (Galapagos) to Grasshopper 3D taken from the available algorithms as described in table 4.2.

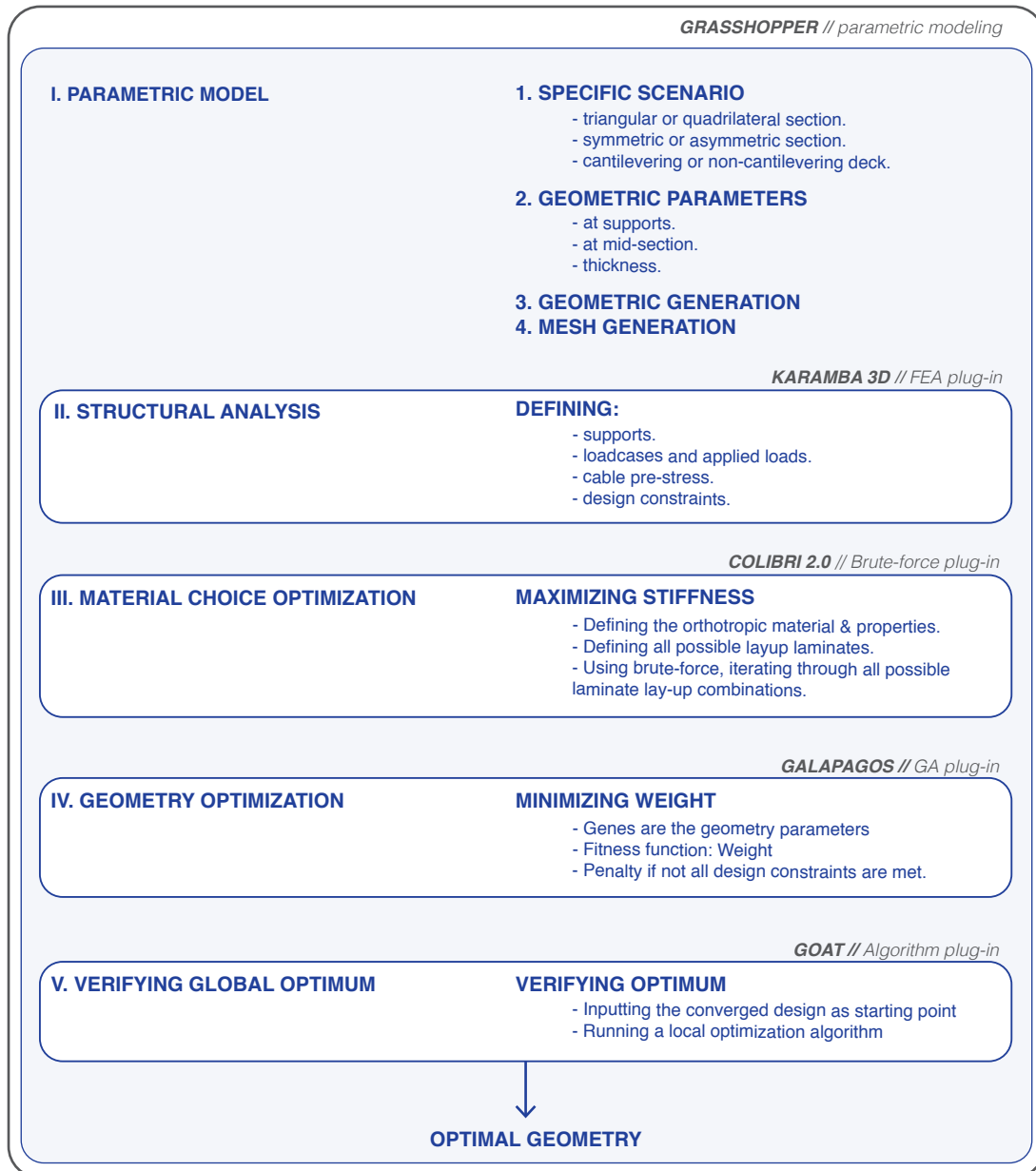


Figure 5.8 Proposed Optimization Framework.

To better understand the developed structural optimization framework, the next section defines the important aspects of the proposed tool. Each notion is illustrated using the case-study, the Wilhelminaberg Viewpoint.

First, in order to implement the framework to any structure, the user must define the following:

1. Design boundary
2. Geometric parameters
3. Material parameters
4. Load-cases and applied loads
5. Support conditions
6. Design constraints

Then, the user must run the two-levels of the optimization:

7. Stiffness optimization
8. Weight optimization

3.1 Design Boundary

The proposed framework requires first defining a general design boundary of the geometry. The design boundary refers to the bounding box of a specific design. The different scenarios to be explored must be defined next.

Case-Study: The Wilhelminaberg Viewpoint

The initial geometry is taken from Ney and Partners. Focusing on the most critical part of the structure allows to restrict the scope of the project. The most critical part of the structure is defined as the longest unsupported span of the structure. It consists of the slanted ring of 106m and excludes the columns for now.

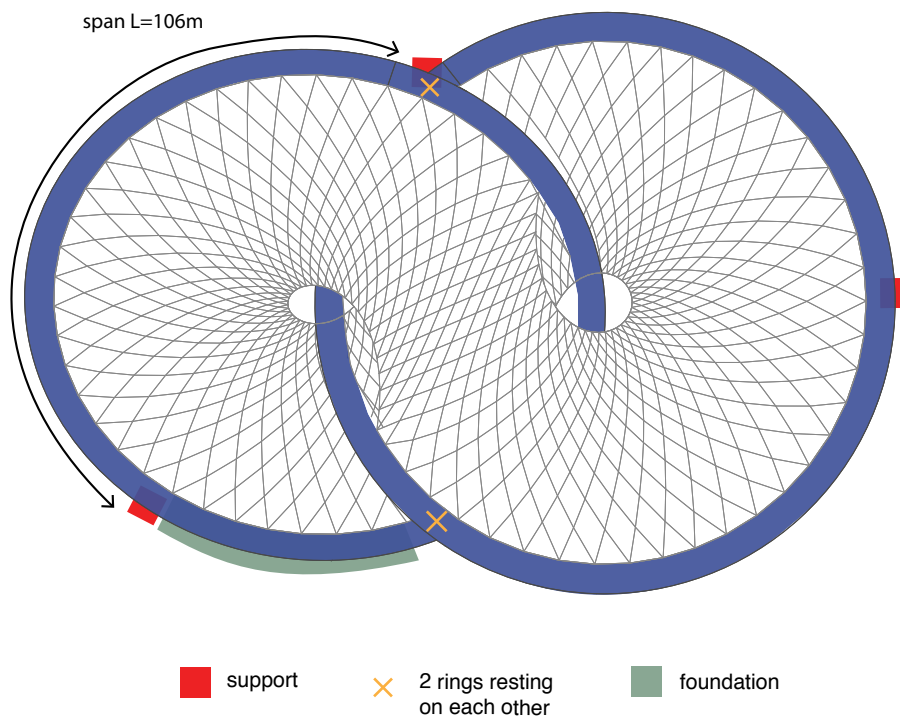


Figure 5.9 Diagram of the Wilhelminaberg Viewpoint with hinged supports at the considered span.

3.2 Geometric Parameters

Within the suggested framework, the geometry of a structure is set up in Rhinoceros 3D, a Computer Aided Design (CAD) software [79]. A generative algorithm is defined in Grasshopper: the structure is set up parametrically [80]. A model made of shell-like elements is generated in Grasshopper 3D with the defined geometric parameters of each scenario. The model is then connected to a finite element analysis that will allow to define the materials to be used, the load cases and corresponding applied loads, the design criteria, and evaluate the structural performance of the model. Karamba 3D, a plug-in for Grasshopper 3D, is used for structural analysis. At a preliminary stage of the design process, it is fully embedded in the parametric environment of Grasshopper 3D. In turn, other plug-ins can be utilized for the optimization process keeping all the components in a singular interface.

The design variables concerning the geometry or shape of the structure are the continuous geometric parameters defining the shape. These can be the coordinates, key geometric points, width at critical sections and height. They are chosen from the initial geometry of the structure and are controlled by implementing an upper and lower constraints. The developed framework is intended to be used as a preliminary tool to explore different geometries for a structure in FRP. As such, choosing the parameters is an important task in achieving the goal of the optimization. Different geometric scenarios, each with their own set of parameters, are defined to encourage formal exploration in the preliminary stage. Once the parameters of a scenario are decided, determining the upper and lower constraint of each variable are important to make sure the search space of the optimization framework is defined correctly.

Case-Study: The Wilhelminaberg Viewpoint

Different scenarios are envisioned in order to explore different geometric forms for the case-study. These scenarios are defined relating to three aspects: the cross-section typology, the symmetry of the cross-section and span, and the cross section's top flange (holding the deck). The combination of these three aspects result in eight different scenarios for this design problem, summarized in table 5.1. Each scenario's design space is different resulting from each scenario's different parameters and their different corresponding constraints. Thus, the proposed optimization framework, steps 1 through 5, will run eight times. Once all the optimization iterations are run, eight optimal structures will be generated. Post-optimality analysis will evaluate the generated geometries in terms of their structural, computational, and production performance. Each scenario yields advantages in certain fields and disadvantages in others. For example, a symmetric design might lead to a significantly smaller computational energy and easier manufacturing. However, the structure's weight might be considerably higher. An asymmetric cantilevering design might be lighter than a symmetric fixed-width deck design. However, its manufacturing and detailing might be considerably more complex. Exploring multiple scenarios is thus essential in order to not limit the design possibility at the preliminary stage. Designers ultimately advise if any of the FRP structure should be studied further than a preliminary design.

i. Defined Scenarios

	Triangular Section	Quadrilateral Section	Symmetric Section	Asymmetric Section	Fixed Deck	Cantilevering Deck
TSF	x		x		x	
TSC	x		x			x
TAF	x			x	x	
TAC	x			x		x
QSF		x	x		x	
QSC		x	x			x
QAF		x		x	x	
QAC		x		x		x

Table 5.1 Summary of the eight generated scenarios, each scenario is given a three-letter acronym.

Each scenario is identified by a three letter acronym, relating to each of the three aspects.

- **The cross-section type** distinguishes between triangular sections (T) or quadrilateral sections (Q), as shown in figure 5.10.

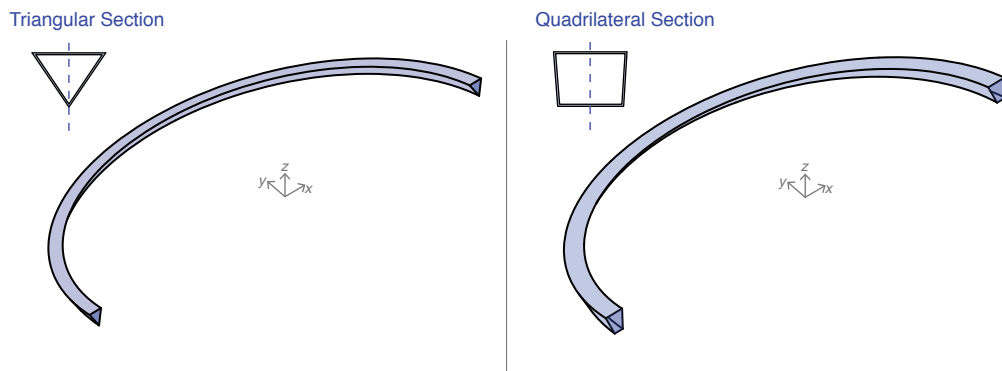


Figure 5.10 Triangular versus Quadrilateral Sections.

- **The symmetry of the cross-section and span** distinguished between the symmetrical geometries (S) or asymmetrical geometries (A), both at the cross-section level as well as at the overall span as shown in figures 5.11 and 5.12;

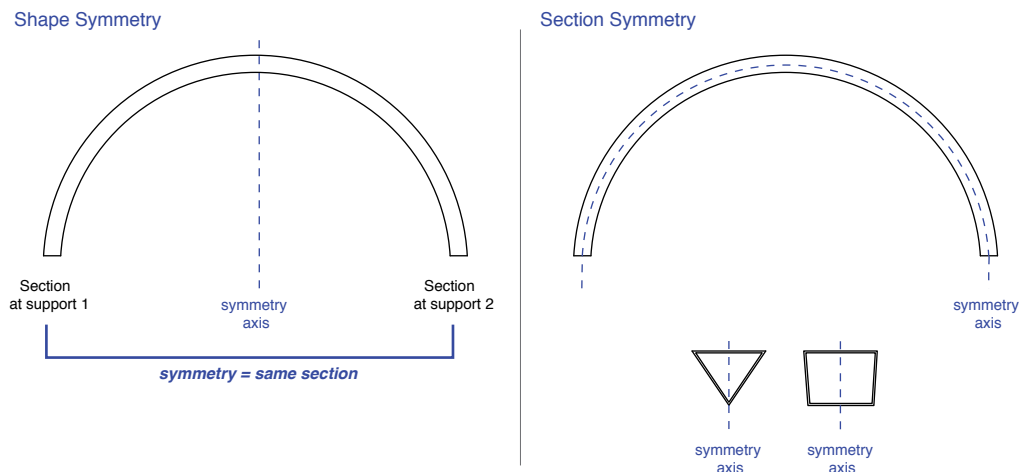
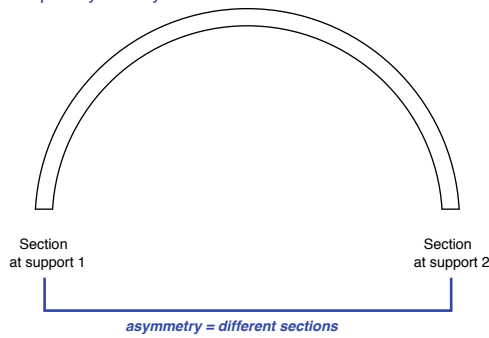


Figure 5.11 Symmetry in the shape and section of the structure.

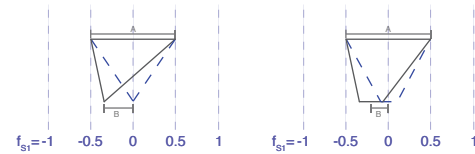
Shape Asymmetry



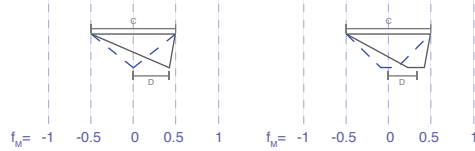
Section Asymmetry

At the given section, an asymmetric section is produced by shifting the bottom corner for a triangular section or the mid-point for a quadrilateral section by a factor f .

At the support S1, $f_{S1} = B/A$



At mid-span M, $f_M = D/C$



At the support S2, $f_{S2} = E/F$

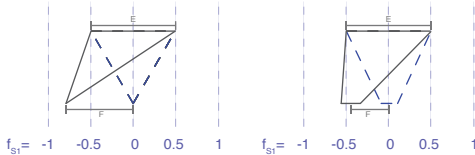
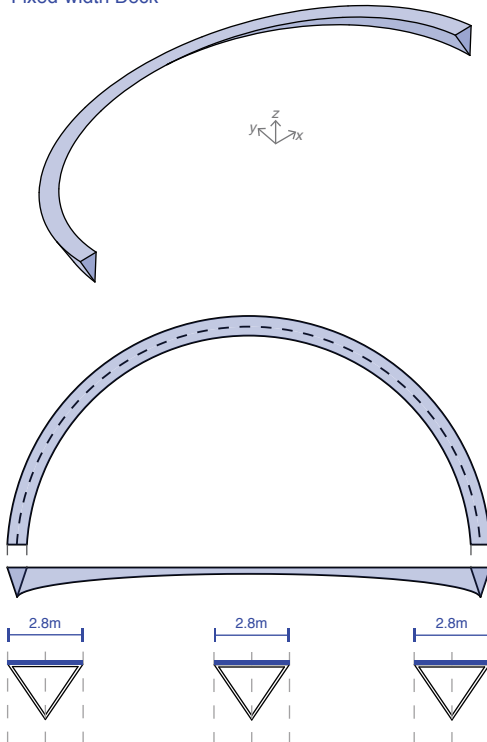


Figure 5.12 Asymmetry in the section of the structure.

- **The cross-section top flange** distinguished between the cross sections with fixed-width deck (F) equal to 2.8m (value taken from the original design 2.8m) and cross sections that can present a cantilevering deck sections (C) as shown in figure 5.13.

Fixed-width Deck



Cantilever Deck

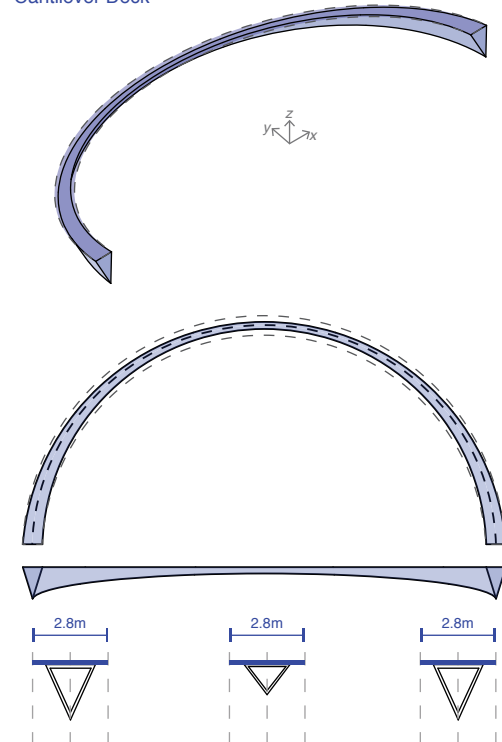


Figure 5.13 Fixed-width deck (2.8m) versus Cantilevering Sections.

ii. Geometry Generation

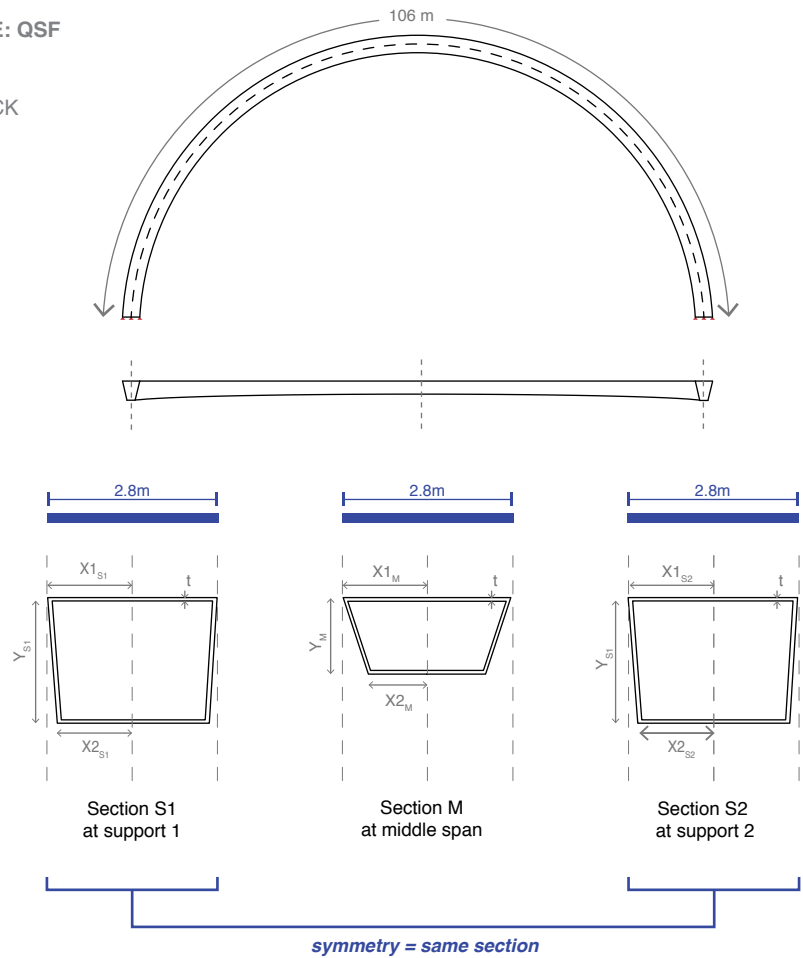
In the Wilhelminaberg viewpoint, the geometry for each scenario is generated using parameters defining the sections at the supports and middle section of the span. A continuous and smooth surface is generated using the loft function in Grasshopper 3D. The process is visualized in figure 5.14. The parameters of scenario QSF are shown in figure 5.14. The parameters for the rest of the scenarios are shown in appendices G1 through G8. Once the variables of the optimization are decided, determining the upper and lower constraint of the variables is equally important. These bounds define the search space of the optimization framework.

- For the height of the sections, the upper limit of the interval is derived from the original design of the Wilhelminaberg Viewpoint. The lower limits are set to 0. This creates large search spaces. It is however considered appropriate to make sure the algorithm explores all possible solutions within the design space. Increasing the lower limit might otherwise disregard viable and “fitter” solutions.
- For the fixed deck options, a deck width is fixed at 2.8m, similarly to the original design.
- The cantilevering deck option is an added design iteration. The width of the deck was limited by manufacturing possibilities. To avoid technical problems in the production of the beam, the minimum width of the cross-section is to be equal to at least one-third of the entire 2.8m deck allowing for a realistic connection between the 2.8m wide cantilevering deck and the beam.
- The thickness of the cross-section is an important parameter. Its interval is defined between 5.0 and 10.0cm. The lower limit is empirically defined to avoid local buckling. The upper limit is defined at 10.0cm to avoid thick shell behavior. Below a thickness of $t=10.0\text{cm}$, material properties of FRP calculated with the classical lamination theory (CLT) are still valid. The thickness is constant for all walls of the cross-section and through the entire span.
- The search space for each parameter consists of all values with one decimal between the upper and lower limit.

1. SCENARIO & PARAMETER DEFINITION

Depending on the chosen scenario, define the parameters of the sections at the supports and mid-section.

i. SCENARIO CHOICE: QSF
QUADRILATERAL
SYMMETRIC
FIXED-WIDTH DECK



2. PARAMETERS

$X1_s$	Top width at sections S1 & S2	1.4	(m)
$X2_s$	Bottom width at sections S1 & S2	[0.1 - 1.4]	(m)
Y_s	Depth at sections S1 & S2	[0.1 - 8.0]	(m)
$X1_M$	Top width at section M	1.4	(m)
$X2_M$	Bottom width at section M	[0.1 - 1.4]	(m)
Y_M	Depth at section M	[0.1 - 4.0]	(m)
t	Constant thickness of the sections	[5.0 - 10.0]	(cm)

2. GEOMETRY GENERATION

Loft the sections and generate geometry.

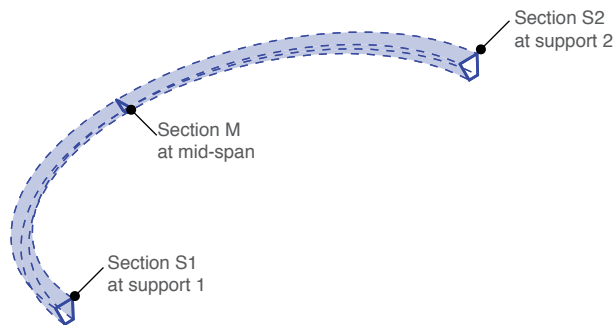


Figure 5.14 Geometry and mesh generation framework.

3.3 Material Parameters

Designing in FRP requires to consider certain parameters proper for FRP in particular. These are thickness of laminates, orientation, and stacking sequence. In order to not turn into a complex and non-linear problem, the framework proposes a simplified approach more fit for structural engineering applications as well as form exploration at the preliminary stage. Instead of iterating between all possible lamina orientation and stacking sequence (as in the Miki/Sugiyama and Burgeño/Wu studies), the suggested framework iterates in its first step between a series of established stacking sequences that utilize widely available angles such as 0° , $\pm 45^\circ$, and 90° (figure 5.15). As such, the adopted approach is more in line with the manufacturing of large free-form structures as well as level of required detailing at the laminate level. Once the composite material is chosen, the properties of different laminate layups are derived using the classical lamination theory as well as the rules of thumbs mentioned in chapter 2 of the literature review.

Case-Study: The Wilhelminaberg Viewpoint

i. Material Selection

The material for a specific laminate will be chosen for either low, medium, or high performance. Value for E_{11} , E_{22} , G_{12} , G_{13} , G_{23} , and ν_{12} are specified. Material options are the high performing carbon/epoxy options shown in table 5.2.

	AS4	IM6	IM7
Longitudinal Modulus (E_1, GPa)	142	172	156
Transverse Modulus (E_2, GPa)	10.3	10.0	10.8
Shear Modulus (G_{12}, GPa)	7.2	6.2	6.0
Poisson's Ratio (ν_{12})	0.27	0.29	0.30
Longitudinal Tensile Strength (X_t, MPa)	2280	2760	2860
Longitudinal Compressive Strength (X_c, MPa)	1440	1540	1875
Transverse Tensile Strength (Y_t, MPa)	57	50	49
Transverse Compressive Strength (Y_c, MPa)	228	152	246
Shear Strength (S, MPa)	71	124	83

Table 5.2 Composite Materials and their corresponding properties. Tabulated material properties for the materials options to conduct this research. AS4/APC2: carbon-PEEL; IM6/3501-6: carbon-epoxy; IM7/8552: carbon-epoxy [81], [82].

ii. Laminate Selection

IM6 is chosen: it has a $V_f = 60\%$, appropriate for vacuum infusion production. Using this material, different laminate layup combinations are generated: their properties are determined using CLT. As long as the thickness of the shell-like element is limited to 10.0cm, the properties remain true. For thick shells, the assumptions behind CLT no longer hold. This research uses an online available, based on CLT, to generate the properties of the different laminate layups [83] (figure 5.17); these properties can also be calculated manually using matrices of CLT. In this case-study, the considered laminate layup combinations are summarized in table 5.3 and the laminate layup sections are visualized in figure 5.16. The percentage of each lamina in any specific direction is at least 12.5% for manufacturing constraints. The calculation verifying the results are shown in appendices H1 and H2.

	Laminate Layup Combinations	E_1 (GPa)	E_2 (GPa)	G_{12} (GPa)	ν_{12}	σ_1 (MPa)	σ_2 (MPa)	τ_{12} (MPa)
C1	$0^\circ/62.5\%; 45^\circ/12.5\%; 90^\circ/12.5\%; -45^\circ/12.5\%$	118.7	40	15.6	0.3	1425	480	250
C2	$0^\circ/12.5\%; 45^\circ/12.5\%; 90^\circ/62.5\%; -45^\circ/12.5\%$	40	118.7	15.6	0.1	480	1425	250
C3	$0^\circ/12.5\%; 45^\circ/37.5\%; 90^\circ/12.5\%; -45^\circ/37.5\%$	47.7	47.7	35	0.5	572	572	560
C4	$0^\circ/25\%; 45^\circ/25\%; 90^\circ/25\%; -45^\circ/25\%$	65.9	65.9	25	0.3	791	791	400
C5	$0^\circ/50.0\%; 45^\circ/12.5\%; 90^\circ/25.0\%; -45^\circ/12.5\%$	100	60.4	15.6	0.2	1200	724	250
C6	$0^\circ/25.0\%; 45^\circ/12.5\%; 90^\circ/50.0\%; -45^\circ/12.5\%$	60.4	100	15.6	0.12	724	1200	250
C7	$0^\circ/37.5\%; 45^\circ/12.5\%; 90^\circ/37.5\%; -45^\circ/12.5\%$	80	80	15.6	0.15	960	960	250

Table 5.3 Properties of the different laminate layup combinations.

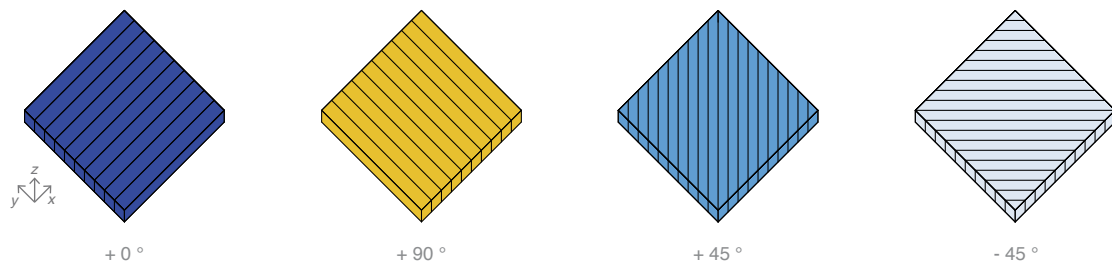


Figure 5.15 The considered laminate layups (0° , $\pm 45^\circ$, and 90°), widely available in structural applications.

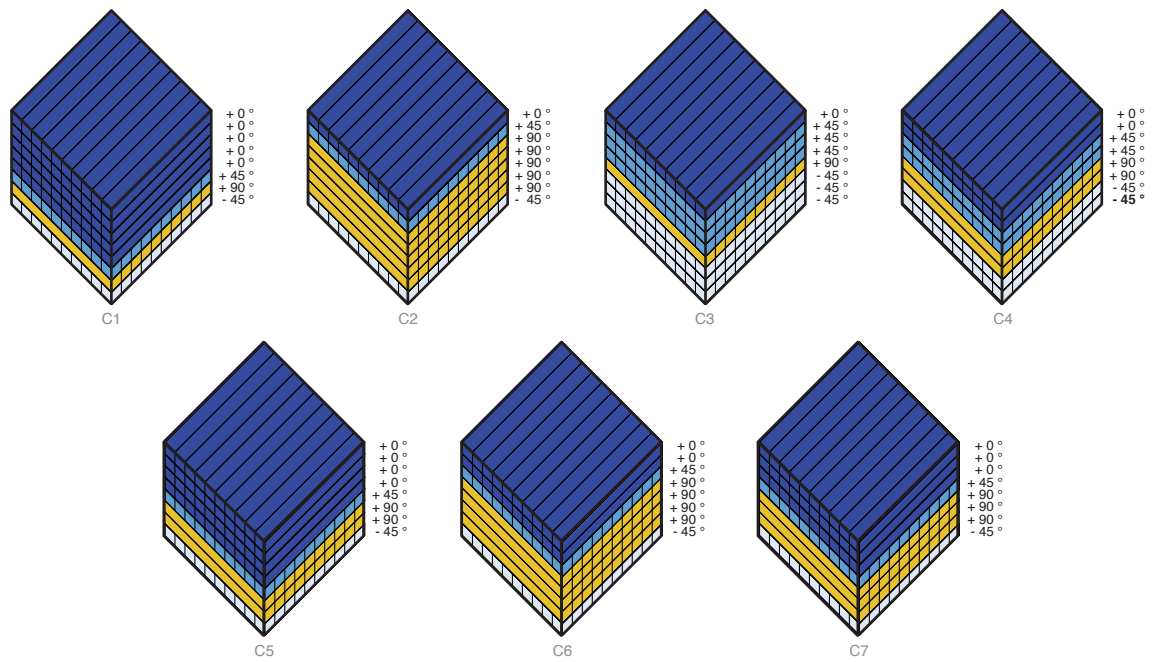


Figure 5.16 Sections of the different considered laminate layup combinations.

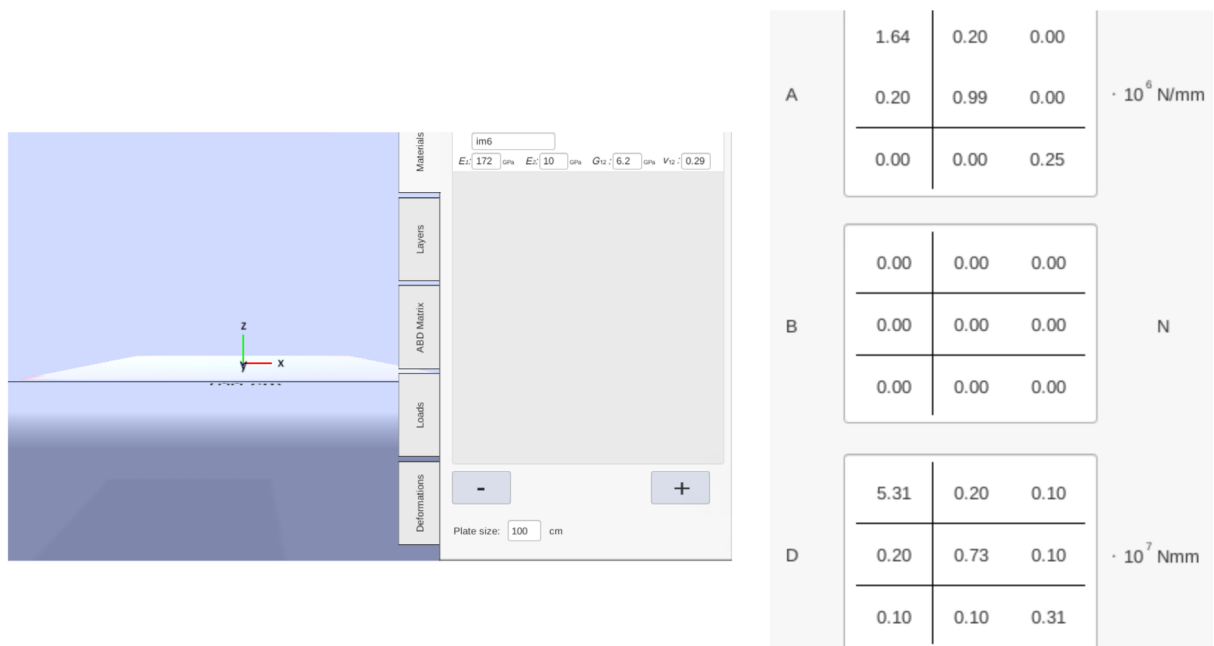


Figure 5.17 Screenshot from the online tool generating the [A], [B], [D] matrices for a laminate using CLT [83].

3.4 Load-cases and Applied Loads

Choosing the appropriate load-cases and corresponding applied loads is an important step in any structural design. For certain structures, wind or earthquake loads might be critical load-cases and corresponding load-areas for their structural optimization. For other structures, applying the loads asymmetrically might be more critical. Obtaining an optimal design directly depends on the ability to formulate the most critical load cases and corresponding loads area. The optimization process however can be easily modified to include as many load cases as necessary such as wind or earthquake loads.

Case-Study: The Wilhelminaberg Viewpoint

i. Load-Cases

For the preliminary design stage of the Wilhelminaberg Viewpoint, two load cases are taken into account during the optimization of the structure. They correspond to the ultimate limit state and serviceability limit state, deemed most critical for the structure. the two considered load cases are defined in table 5.4. They correspond to the loads classified as a class consequence CC3 structure. With DL referring to the dead load and LL to live load, the loads are taken similarly to the values adopted by Ney & partners to allow for a fair comparison in the post-processing of the results.

ULS Load-case	1.3DL + 1.65LL
SLS Load-case	1.0DL+1.0LL

Table 5.4 The chosen load-cases.

- The live load on the rings is taken as $LL = 2.5 \text{ kN/m}^2$
- The dead load takes in consideration the weight of the FRP structure and the dead load of the deck. The weight of the structure in FRP is taken with a 15% contingency for connections and additional work. The calculation behind the dead weight is shown in table 5.5.

Construction	Material		Weight kN/m^2
Finishing Steps (t=10cm)	Ultra-high strength concrete	2500 kg/m^3	2.75 (10% contingency)
Finishing Coat (t=8mm)	Polyurethane resin with infused carbon granules	2300 kg/m^3	0.184
Added Surface	Net filing	0.4 kN/m^2	0.4
Deck Dead Weight			3.334
Handrail			0.5 kN/m

Table 5.5 Dead weight of the deck.

ii. Applied Load-Areas

Defining the corresponding load areas is equally important. A study of all possible load-area combinations was conducted in order to find the most critical situation (figure 5.18). The most critical load-area was found for the load over the entire structure (appendix I1).

The Grasshopper 3D plug-in Karamba 3D is utilized to evaluate the structural performance during the optimization process through first and second order analysis. It allows to introduce loads and evaluate stresses, deflections, buckling load factors, and natural frequency [80], [84].

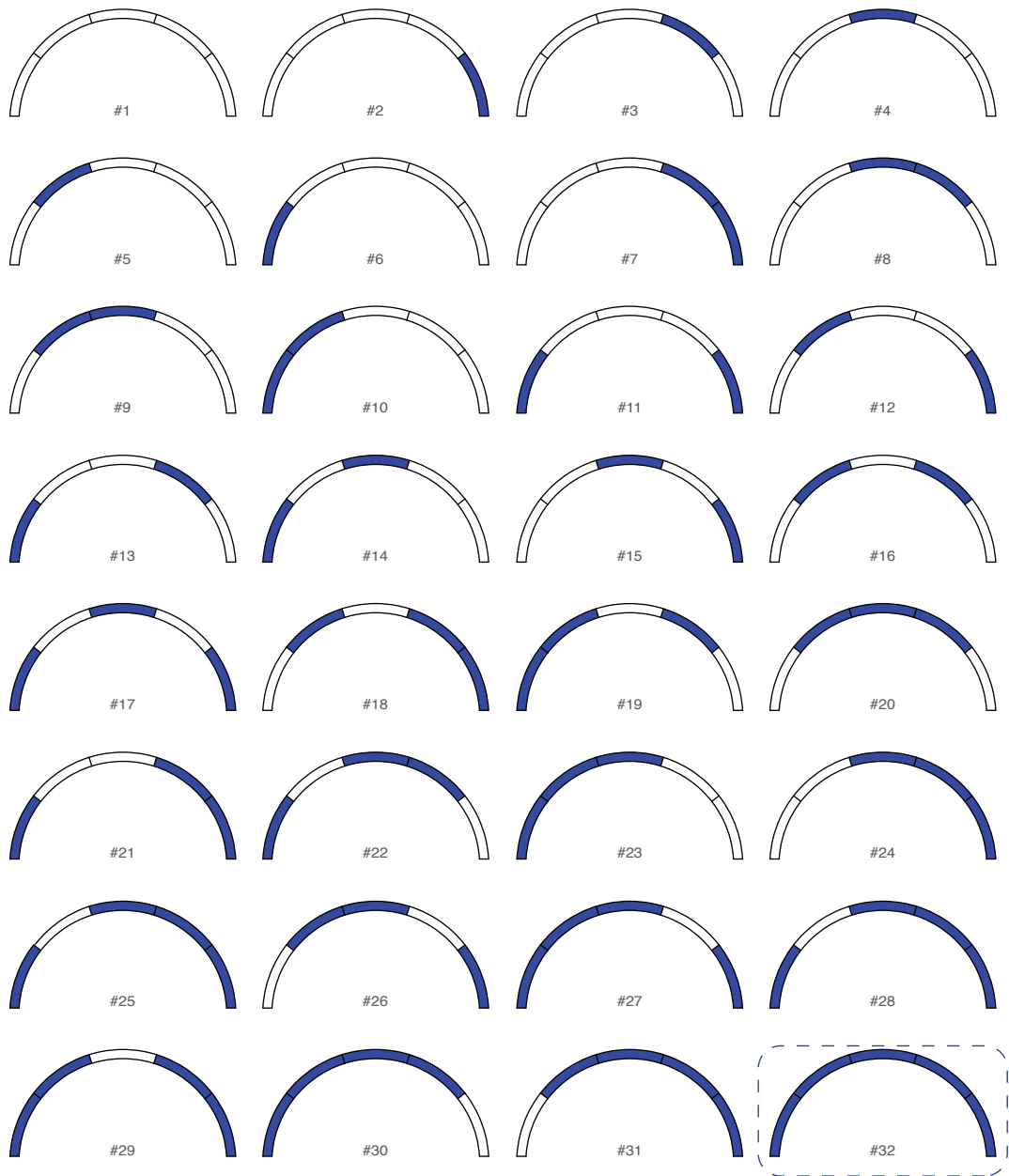


Figure 5.18 The different load-areas tested to find the most critical load-area.

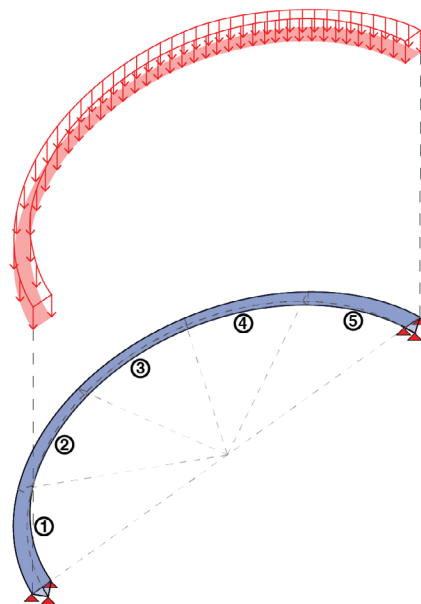


Figure 5.19 The dead load applied on the structure.

iii. Pre-Stressed Cables

The Wilhelminaberg Viewpoint presents a complex-structural system combining the rings (originally designed in steel) and pre-stressed cables (figure 5.5). The effect of the cables must be incorporated in the structural analysis. The cables contribute to the global stability of the structure. They must be modeled as such and cannot be simplified as simple forces. The considered span has about 46 cables (figure 5.20).

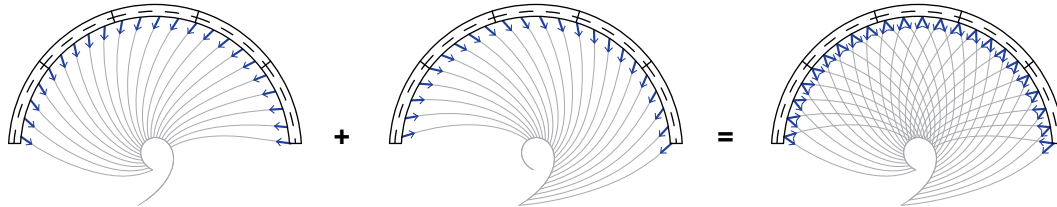


Figure 5.20 The arrangement of the cables of the considered span.

In order to accelerate the structural analysis of any particular solution and render any optimization more time-efficient, it was sought to simplify the effect of the cables into a smaller amount of cables. Significant experimentation took place in order to model the effect of the cables as close as possible to reality. The experimentation proved first the effect of the cables on the stability of a structure. A Grasshopper 3D code was developed to simplify the many cables over the considered span into a smaller number of cables with equivalent pre-stress loads. The smaller number of cables must be equivalent to the more complex situation of the Wilhelminaberg Viewpoint. Systems of forces are considered equivalent if they have the same magnitude and direction and produce the same moment about any point O.

In Grasshopper 3D, the stress in each cable is input manually, then the cables are divided in 7 groups and for each group a cable with an equivalent force and moment are generated (figure 5.21). This is done twice for both the ULS and SLS load cases. While this approximation saves time, it leads to some discrepancy between the real situation and the equivalent one. The division in 7 groups is not arbitrary. Grouping the cables in 7 cables was found to accurately model the effect of the cables over the considered span: an error less than 10% is found in both ULS and SLS. This allows to expedite the modeling process significantly (appendix I2).

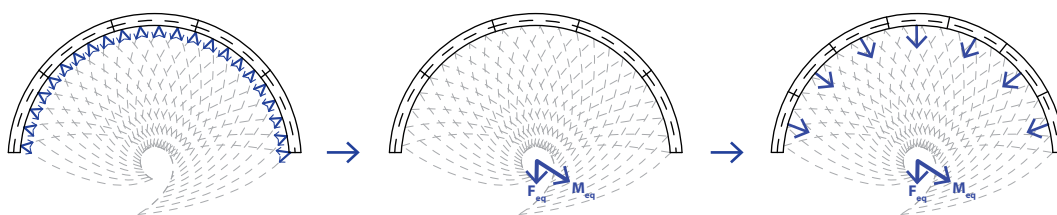


Figure 5.21 Simplification of the cables into 7 cables, in which an equivalent force and moment are generated.

3.5 Design Constraints

Multiple design criteria can be defined to verify the structural performance and structural safety of the generated geometry. These allow to limit the design space. They include performance criteria such as maximum stresses, deformation, buckling factors.

Case-Study: The Wilhelminaberg Viewpoint

For the chosen case-study, the following are the adopted design criteria:

- 1.FRP stress criterion for laminae and laminate
- 2.Deflection
- 3.Buckling load-factor

i. FRP stress criterion for laminae and laminate

Positioned as the new icon of the area and symbol of the region's green efforts, the Wilhelminaberg Viewpoint is conceived as a structure that celebrates technology and innovation. It is classified as a class consequence CC3 structure. With this status in mind, insuring the safety of the structure over its service life is of paramount importance. Referring to chapter 3 (sections 3.2 and 3.3), the first-ply failure criterion will be adopted as a conservative approach that safeguards the structure's safety.

The failure of a laminate according to this criterion follows the procedure [12], [85] based on the laid-out knowledge of in chapter 2:

- Determine the mechanical properties E_{11} , E_{22} , G_{12} , ν_{12} and ν_{23} of each lamina.
- Calculate the stiffness matrix for each lamina in the local coordinate system according to equations (1, 2a, 2b, 2c). Transform the stiffness matrix of each lamina from the local to the global coordinate system according to equations (3, 4a, 4b).
- Calculate the stiffness matrix of the laminate according to (6a, 6b) and (7a, 7b, 7c).
- Calculate the stress state of each lamina under a specific load. Or note the stress state from a finite element program.
- Check the stress state against a selected failure criterion (the Tsai-Wu failure or maximum stress criterion) to see if any ply has reached the failure criterion.
- The laminate is then evaluated whether it reached failure according to the defined first-ply criterion.

In this free-form design, the steps 1 through 4 allow to obtain the stress state of the laminate structure are accounted for the finite-element analysis. It is important however to check for the appropriate failure criterion for a lamina and laminate as done in steps 6 and 7.

• The Tsai-Wu Failure Criterion

Referring to the discussion in chapter 3 (section 3.2), the Tsai-Wu criterion is adopted as it considers the interaction through a single equation that defines the failure state. It is formulated as follows:

$$\sigma_1 \left(\frac{1}{f_{1t}} - \frac{1}{f_{1c}} \right) + \sigma_2 \left(\frac{1}{f_{2t}} - \frac{1}{f_{2c}} \right) + \frac{\sigma_1^2}{f_{1t}f_{1c}} + \frac{\sigma_2^2}{f_{2t}f_{2c}} + \frac{\tau_{12}}{f_{12}^2} - \frac{\sigma_1 \sigma_2}{\sqrt{f_{1t}f_{1c}f_{2t}f_{2c}}} = 1 \quad (4)$$

• The Maximum-Stress Failure Criterion

In addition to the Tsai-Wu criterion, the maximum-stress failure criterion is also considered. The maximum stress criterion can be written as follows:

$$\sigma_1 = \begin{cases} f_{1t} & \text{for } \sigma_1 > 0 \\ -f_{1c} & \text{for } \sigma_1 < 0 \end{cases} \quad (5)$$

$$\sigma_2 = \begin{cases} f_{2t} & \text{for } \sigma_2 > 0 \\ -f_{2c} & \text{for } \sigma_2 < 0 \end{cases} \quad (6)$$

$$|\tau_{12}| = F_{12} \quad (7)$$

ii. Deflection

Deflection of the generated structure is limited to $< L/350$ where L is the span of L=106m, similarly to the criterion adopted by Ney & Partners.

iii. Buckling Load Factor

The FEA plug-in, Karamba 3D, calculates the critical load factor at which buckling occurs. To account for any imperfection in the shell, the critical load must be multiplied by a knockdown factor. The results must be larger than 1. If the critical load factors F_b are larger than 6, the structure can be considered safe for buckling [86].

3.6 Stiffness Optimization

The first level of the optimization maximizes the stiffness through iterating through the optimal material parameters. As stated, this steps allows to capitalize on an important advantage of the FRP: its alterable material properties over a single span. The total structure can be divided into sub-spans to allow material properties to change for each sub-span. Modifying the laminate layup allows to increase the torsional and bending stiffness.

Dividing the structure in n number of spans increases substantially the number of possible laminate layup combination. For the first level optimization, each of the n sub-span can adopt one of the k laminate layups. This results in k^n possible laminate layup combinations. The first level optimization is run once for each design boundary (bounding box of the structure) iterating through all k^n laminate options for a geometry is thus reasonable. Each laminate lay-up is defined by their derived mechanical properties as shown in table 5.3. All the different combinations of laminate layup must then be defined using parametric tools in Grasshopper. A brute-force algorithm plug-in, Colibri, is used to iteration through all the possible combinations [87]. Brute force is chosen over a genetic algorithm. Simple measures can be defined to limit the search space, rendering brute force algorithm possible and more efficient than genetic algorithms. Genetic algorithms are not beneficial to employ to find the optimal structure especially considering some of the disadvantages of genetic algorithm such as its slowness to converge and the required testing and repetition to avoid pre-mature convergence as shown in table 4.1.

In iterating through the k^n laminate options, the data must be recorded and the analyzed to choose the combination of laminate layup that results in the stiffest structure, as shown in figure 5.22.

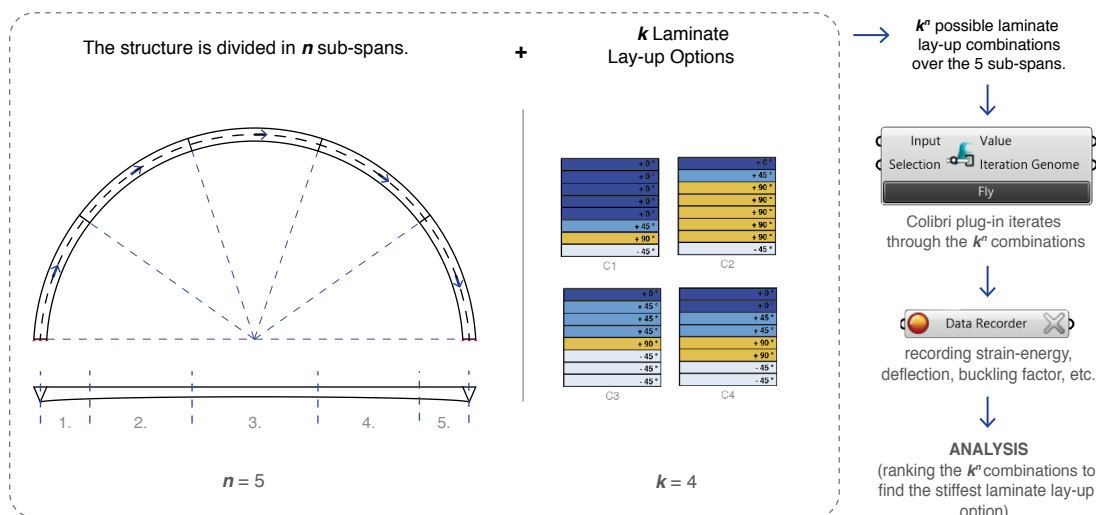


Figure 5.22 Schematic representation of the level 1 stiffness optimization.

Limiting k^n from become too large of a number, both components k and n should be constrained:

- Since the proposed framework is interested in formal exploration in the conception phase, the number of divisions n of sub spans can be restricted in the early stages. At later stages of the design when a specific scenario is chosen to focus on, the structure can then be divided in multiple sub-spans.
- As mentioned in material parameters, numerous laminate layup combination can be considered. It is worthwhile limiting the number of laminate layup options to the ones that provide extreme values for E_1 , E_2 and G_{12} should be considered.

Special attention should be given to modeling orthotropic material. In Grasshopper 3D, modeling an orthotropic material requires defining the longitudinal (x) and through-thickness direction (z). This is particularly important in curved structures in which the longitudinal direction is constantly changing. Realistically, the laminate fiber angle cannot continuously change over a specific span; the coordinate system needs to be simplified to take in consideration manufacturing constraints.

Case-Study: The Wilhelminaberg Viewpoint

i. Modeling the Orthotropic Material in Grasshopper 3D and Karamba 3D

In order to highlight the alterable properties of FRP, it is advisable to divide the structure into multiple sub-spans. The structure is divided in a series of smaller spans. In this case, the 106m structure is divide into $n=5$ parts of approximately 20 meters, the maximum span that fits in a transportation truck. In the case of the Wilhelminaberg Viewpoint, 5 is deemed as an appropriate simplification. Increasing the number of division will significantly increase the number of required iterations to find the stiffest structure by brute force. Investigations at a later stage can take in consideration manufacturing and productions constraints in dictating the size of each sub-span.

The orthotropic material is defined in Grasshopper 3D and Karamba 3D. This required defining the local axis of the material and inputting the correct properties. For each sub-span, the direction of the fibre is simplified for the entire sub-span as the direction of the center point as shown in figure 5.23.

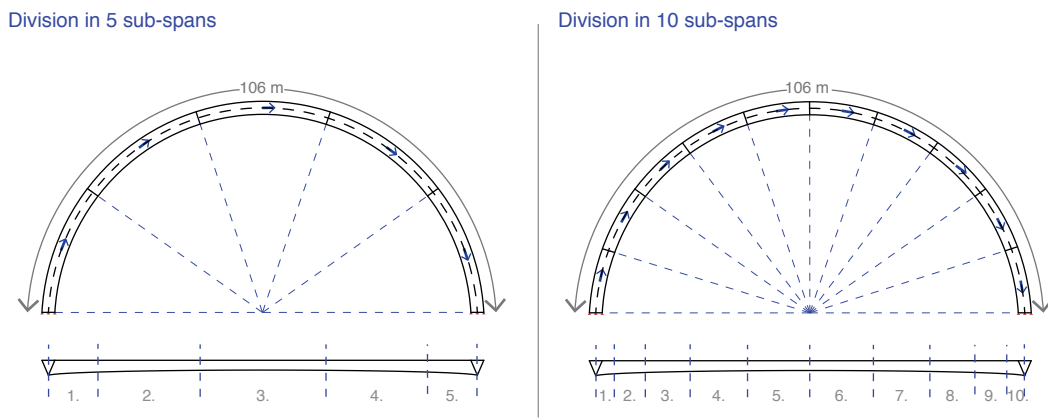


Figure 5.23 (left) Division of the 106m span into 5 sub-spans (right) Division of the 106m in 10 sub-spans for future improvement in the design.

In order to limit the number of possible laminate layup combinations, the number of laminate layups for each span (k) is limited: the laminate layup options that provide extreme values for E_1 , E_2 and G_{12} are considered. The chosen options are summarized in table 5.6.

	Laminate Layup Combinations	E_1 (GPa)	E_2 (GPa)	G_{12} (GPa)	ν_{12}	σ_1 (MPa)	σ_2 (MPa)	τ_{12} (MPa)
C1	0°/62.5°;45°/12.5°; 90°/12.5°; -45°/12.5°	118.7	40	15.6	0.3	1425	480	250
C2	0°/12.5°; 45°/12.5°; 90°/62.5°; -45°/12.5°	40	118.7	15.6	0.1	480	1425	250
C3	0°/12.5°; 45°/37.5°; 90°/12.5°; -45°/37.5°	47.7	47.7	35	0.5	572	572	560
C4	0°/25°; 45°/25°; 90°/25°; -45°/25°	65.9	65.9	25	0.3	791	791	400

Table 5.6 Properties of the chosen laminate layup combinations with the extreme values for E_1 , E_2 and G_{12} .

For the first level optimization, each sub-span can adopt 1 of 4 layups. The structure is divided in 5 sub-spans, this lends to $4^5=1024$ possible combinations. Finding the optimal layup combination is done through brute-force, iterating through all of the possible combinations. After iterating through the k^{th} laminate options, the data is analyzed to choose combination of laminate option that results in the stiffest structure (minimal strain energy and minimal deflection). For a certain design boundary, the stiffness of the structure is always maximal with the same laminate layup combination over the five sub-spans. This was an empirical observation of the suggested framework.

3.7. Weight Optimization

Following the stiffness optimization, the stiffest laminate option that results. For each design boundary, the laminate layup combination that results in the stiffest structure is set. The designer can start the weight optimization. This consists of finding the lightest structure using a genetic algorithm plugin: a lighter structure generally translates in less energy expended during transportation and installation.

I. Fitness Function and Penalty

The fitness computation step is the interface between the genetic algorithm and the optimization process [68]. It is however a fundamental step in an evolutionary design: a fitness function measures the quality, or “fitness” in the solution space. As such, the fitness function is simple or complex depending on the optimization problem at hand. Most approaches aim to minimize or maximize a certain criterion. The fitness function in this proposed framework is the weight of the resultant structure.

One must however account for the applied constraints of any optimization process. These reduce significantly the solution space of a structure. Constraints make any optimization problem harder to solve: they modify fitness landscapes and can lead to unstable typologies (figure 5.24). Such constraint can be incorporated in the genetic algorithms through different strategies: constrain functions, death penalty, penalty functions, repair approaches, or decoder functions. A more detailed discussion of each method can be found in Kramer’s *Genetic Algorithm Essentials* (chapter 5) [68]. This research focuses on penalty functions. Among the different strategies to handle constraint, penalty functions are the easiest to implement and to control. They decrease the fitness of unfeasible solutions. A choice of the penalty function depends on the specific problem.

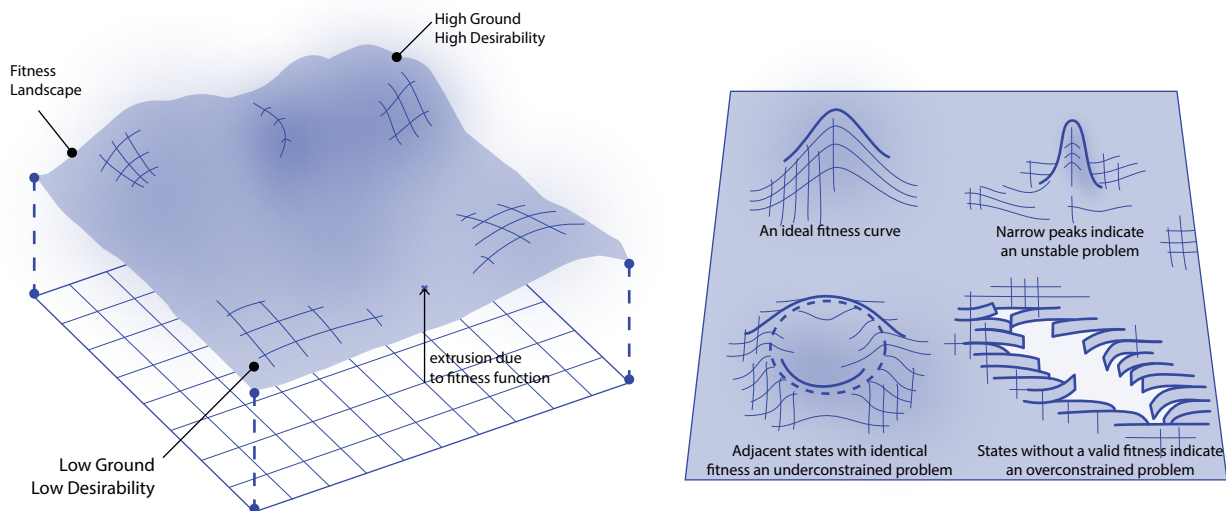


Figure 5.24 (left) Phase space and their corresponding fitness landscapes.
(right) Common fitness landscapes. [88]

A typical penalty function penalizes the fitness value of a solution through a penalty factor whose magnitude is proportional to the constraint violation. In the proposed framework, a structure is generated and analyzed in the finite element plug-in (Karamba 3D). With the fitness value being the weight of the structure, If the structure doesn't verify all of the design constraints, its structural performance is unsatisfactory. A penalty must thus be included in the outputted objective to be optimized, here the weight of the structure. However, the proposed framework presents a binary situation: a structure can either verify all the constraints or not. In other words, it is unimportant if a structural almost verifies the constraint. As such, a penalty of 5000 kN is given for the weight of structures that do not verify all constraints. In the post-processing of the results, the solutions with the 5000 kN penalty can be disregarded. It is worth mentioning that the penalty can be altered easily by the user to reflect a different set of priorities and pre-requisites.

Objective:	Minimizing weight
Subject to the following design constraints:	$\left\{ \begin{array}{l} \text{Stress criteria (Tsai – Wu and maximum)} \\ \delta \leq L/350 \\ F_b \geq 6 \end{array} \right.$
$f(x)$	Fitness Function
If all the design constraints are verified,	$f(x) = \text{weight of the generated geometry}$
If any of the design constraints is not verified,	$f(x) = 5000 \text{ kN}$

ii. GA Algorithm: Galapagos

In order to run the second level optimization and find the lightest geometry, a genetic algorithm is run using a Grasshopper 3D plug-in: Galapagos. The choice of the plug-in is motivated by the comparison laid out in table 4.2. In the following, Galapagos' settings are discussed.

The geometry of the structure is generated through a parametric code in Grasshopper 3D. This research's framework uses a genetic algorithm to optimize the geometry. Multiple Grasshopper 3D plug-ins are available for designers to choose from: Galapagos, Octopus, and Wallacei. Factors affecting the choice of a genetic algorithm plug-in are primarily (1) whether it is a single or multiple objectives optimization and (2) whether the framework is intended to find a global or local optima.

The developed framework employs Galapagos evolutionary solver. The Grasshopper 3D plug-in is deemed fit for a single-objective optimization searching for a global optimum. As shown in figure 5.25, the required inputs for Galapagos are:

- **Genes** defining the geometry generated. In this framework, the genes are the geometric parameters defining the sections.
- **The fitness value** evaluating the quality of the generated geometry.

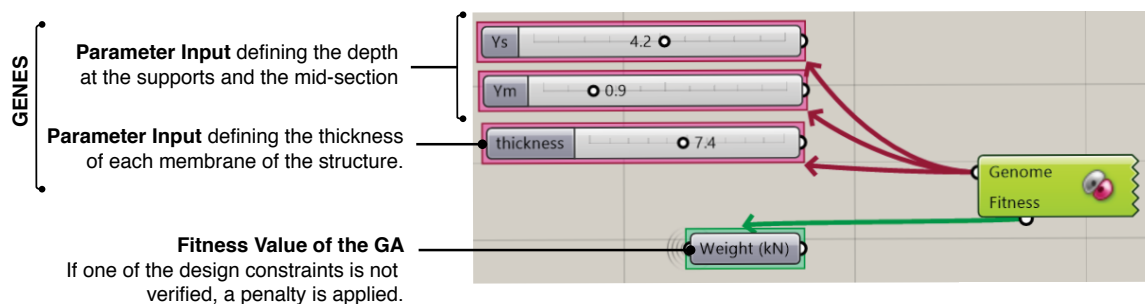


Figure 5.25 Screenshot of the Grasshopper 3D code showing the GA algorithm, Galapagos. The genome is the set of variables defining the geometry. The fitness value is the weight of the corresponding structure (with penalty if required).

Further information must be provided for the interface before the genetic algorithm can run (figure 5.26). These include:

- Generic information:
 - Minimizing or maximizing the fitness value.
 - Enabling or not run-time limitations and a corresponding maximum duration.
- Evolutionary information set-up:
 - Population: the number of individual that form a population.
 - The initial boost: the multiplication factor of the first generation.
 - The maximum stagnant limit: the required number of consecutive generations without finding an improved solution before which the genetic solver terminates. The maximum stagnant limit is the stopping criteria of the genetic algorithm.

- The maintain percentage: percentage of solutions of a generation that can be transferred to the next generation).
- The inbreeding percentage: a value of -100% is used for fully zoophilic and the value of 100% for fully incestuous.

The default values of these input settings according to the Galapagos developers are summarized in figure 5.26. The input settings used in this research's framework are also shown in figure 5.26.

Setting	Default (Left)	Modified (Right)
Generic		
Fitness	Maximize	Minimize
Threshold		
Runtime Limit	Enable	Enable
Max. Duration	01 Hours, 30 Minutes	01 Hours, 30 Minutes
Evolutionary Solver		
Max. Stagnant	00050	00030
Population	00050	00100
Initial Boost	00002	00002
Maintain	005%	005%
Inbreeding	+075%	+075%
Annealing Solver		
Temperature	100%	100%
Cooling	0.9500	0.9500
Drift Rate	0.25%	0.25%

Figure 5.26 (left) Default Galapagos Settings. (right) Modified Default Settings.

They correspond in most cases to the default setting with two differences: the population size was set to 100 and the maximum stagnant limit to 30 generations. These changes allow the genetic algorithm to cover a larger part of the solution space. They were dictated by an empirical testing of the tool.

- A generation size of 100 individuals is driven by the need to increase population size to better capture the solution space. With many unfeasible solutions, a significant fraction of the solutions of a generation have a penalty.
- The maximum stagnant limit was decreased from 50 to 30. In testing the genetic algorithm in this framework, the largest interval of consecutive generations before an improved solution is generated is 21. Additionally, the number of solutions in one generation was doubled, from 50 to 100. A value of 30 was thus deemed conservative enough for the maximum stagnant limit.

If this proposed framework is to be adopted for another problem (different general shape), the input settings of Galapagos can and should be modified accordingly. Consequently, this requires some initial testing of the tool. Otherwise, using the default settings (or more conservative) settings is considered appropriate.

4. Limitations

4.1 Genetic Algorithm Limitations

As elaborated in chapter 4, genetic algorithms have limitations and disadvantages. Genetic algorithms are characteristically slower than other optimization tools. This is true for Galapagos, and especially in our framework where the search space is very large and complex. There is theoretically not a guarantee that the reached design is a global optimum. There are multiple approaches to deal with this drawback of genetic algorithms.

- **A first approach** is to repeat the genetic algorithm multiple times, without limiting the run-time of each GA.
- **A second approach** is to use the GA for a global optimum. A local optimization can then be implemented with the reached solution as a starting point. This approach allows to conclude whether the optimum of the GA can be confidently considered the fittest possible solution [89].

In our developed framework, a significant amount of testing was run to verify that the converged design corresponds to a global optimum. The first approach was implemented in the early stages of tool development. The same second level optimization was run for the TSF scenario from 5 different starting points. Repeatedly, the GA converged on the same optimal geometry (figure 5.27).

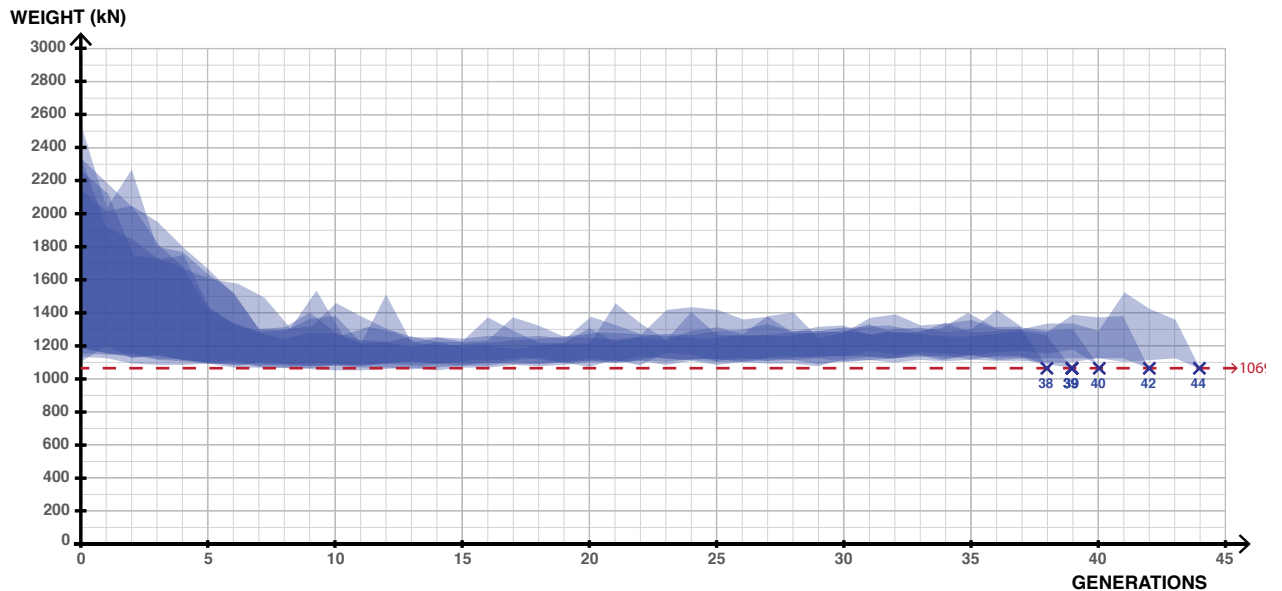


Figure 5.27 Convergence of GA on the same optimal solution, initiated from 5 different starting points.

The second approach was also implemented. The plug-in GOAT was used as a second level local optimization. In all cases, the solution found in the GA was confirmed to be the fittest possible solutions [90].

Furthermore, the converged design can be confidently considered the fittest possible solution as the stopping condition in the GA was not defined in-term of run-time but population convergence. However, it is worth repeating that concluding that a solution is a global optimum can only be guaranteed or verified by brute force algorithms. In the complex and very large spaces defined by geometric parameters, brute force algorithms would be very time consuming. For example, the smallest search space defined for the Wilhelminaberg Viewpoint would require about 352 years of constant computing to go through all possible solutions using brute force algorithms with only 30 seconds for each solution.

4.2 Generative Modeling

i. On Mesh Size

Mesh size is an important aspect of finite element analysis. Defining the mesh density of an analysis is thus a compromise between accuracy of results and computational time. Bigger mesh elements lead to results with large errors while smaller elements increase significantly the computational time. Furthermore, it is hard to predict where exactly a chosen mesh size is on that scale but it can be estimated. Running a mesh density analysis is thus central to determine the mesh size and obtain accurate enough results with an acceptable computational time [86], [91] . A mesh density analysis requires to perform a chosen analysis multiple times for different mesh sizes. The data of each should be recorded: number of elements, number of nodes, the computation time, the outcome (deflection, buckling factor, etc.) of the model. A similar mesh analysis, as related in appendix K1, was run to determine the mesh size of this framework. A size of 0.5m was chosen.

ii. On Mesh Type

There exists two different type of 2D meshes: triangular and quadrilateral, each with benefits and limitations. Triangular elements (either TRI3 or TRI6) may behave too rigidly due to the fact that they are triangles with TRI6 behaving better than TRI3 meshes. Quadrilateral elements (either QUAD4 or QUAD8) are decent but can become computationally heavy, especially with QUAD6 [86] [92].

The FEA plug-in used in Karamba 3D is TRI3. This is a limitation to the proposed optimization framework. The framework however remains valid. It can be easily modified using other Grasshopper 3D plug-ins or other FEA processors. Furthermore, the limitation is accepted as the research pertains to preliminary design and will need to be verified with multiple FEA software in its next advanced stages.

5. Conclusion

The chapter aims to answer the following sub questions:

- What is the context of the chosen case-study? Why was it adopted?
- What were the steps in the development of this tool?
- What are the objectives, design criteria, constraints of this optimization?
- What are the limitations and restrictions of the suggested framework?

This chapter provides an in-depth description of the case-study, the Wilhelminaberg Viewpoint, and its general context, as part of the IBA Parkstad initiative. Launched in 2013, the IBA Parkstad sets out to transform the former mining region and stimulate its economy. Since the mines' closure in 1969, the area has suffered significantly with high unemployment and human capital flight despite the government's *van zwart naar groen* efforts (from black to green) to revitalize the area. Among the proposed projects, the Wilhelminaberg Viewpoint is a landmark to mark, both physically and metaphorically, the orientation of the area recovering from its industrial past. Ney and Partners create an iconic landmark atop the mountain, one that celebrates innovation of form and technology. The case-study will allow to critically assess the characteristics that render FRP a promising construction material: long-durability properties, tailorable mechanical properties, customizable production for free-form design, and a light weight design.

Extending the literature review established in previous chapters, a new framework is established for FRP optimization. The developed framework encourages exploration of forms at the preliminary stage of the design process. This chapter examines the important steps of this framework's development, highlighting the important choice of the objectives. A critical step in the development of the suggested framework is simplifying a multiobjective optimization to a multiple-step single objective optimization. This allows the user to get one optimal solution for each optimization rather than multiple Pareto-optimal solutions with the multi-objective optimization.

The chapter then defines the important aspects of the optimization framework: geometry generation, finite-element analysis, geometric parameters, material parameters, design criteria, load-cases, applied loads, and used plug-ins. After implementing the proposed framework to the case-study, the chapter concludes with a discussion on the limitations of the framework, and how they were addressed.

The following chapter presents the results of the optimization. After running the optimization for the eight proposed scenarios, a post-optimality discussion is elaborated to evaluate the different generated structures.

III. RESULTS AND POST-OPTIMALITY ANALYSIS

CHAPTER 6

RESULTS AND POST-OPTIMALITY ANALYSIS

Chapter 5 introduced in detail the case-study of this research (the Wilhelminaberg Viewpoint) and its general context. The development steps of the proposed optimization framework are then laid out and applied to the case-study. Different scenarios are suggested to encourage formal exploration at the preliminary stage.

This chapter presents the results of the optimization study and evaluates their performance in the post-optimality study.

1. Results

The eight different geometries generated for the eight different proposed scenarios of the case-study are presented. These geometries are the lightest structures generated within their corresponding parameters.

2. Post-Optimality Study

The post-optimality study evaluates the generated geometries from different perspectives: computational efficiency, material efficiency, and production efficiency. This allows to discuss the structures according to different criteria to eventually decide on an optimal design.

The chapter concludes on a single structure, considered the best at meeting the ideals of an integrated design [65]. It also concludes on the feasibility of such a structure and the line of work that must follow this research.

1. Results

1.1 Level 1 of the Optimization: Maximizing Stiffness

With the parametric model set up in Grasshopper 3D and the structural analysis set-up in Karamba-3D, the first step of the optimization is run. In order to highlight the alterable properties of FRP, the structure is divided in 5 sub-spans as shown in figure 6.1. The first step of the optimization consists in finding the optimal laminate layup for each sub-span. In other words, the first step of the optimization finds the combination of optimal laminate layups for the sub-spans, in order to maximize the stiffness of the overall structure.

The four considered laminate layups are presented in figure 6.2; this leads to $4^5=1024$ possible combinations over the 5 sub-spans of each geometry. As discussed in the chapter 5, initial exploration of the available tools revealed that for a specific overall shape (boundaries of the design), the stiffness of the structure is always greatest for the same combination of laminate layups. Otherwise stated, no matter the considered cross-section, the stiffness of the structure is always maximal with the same laminate layup combination. This was an empirical observation of the suggested framework.

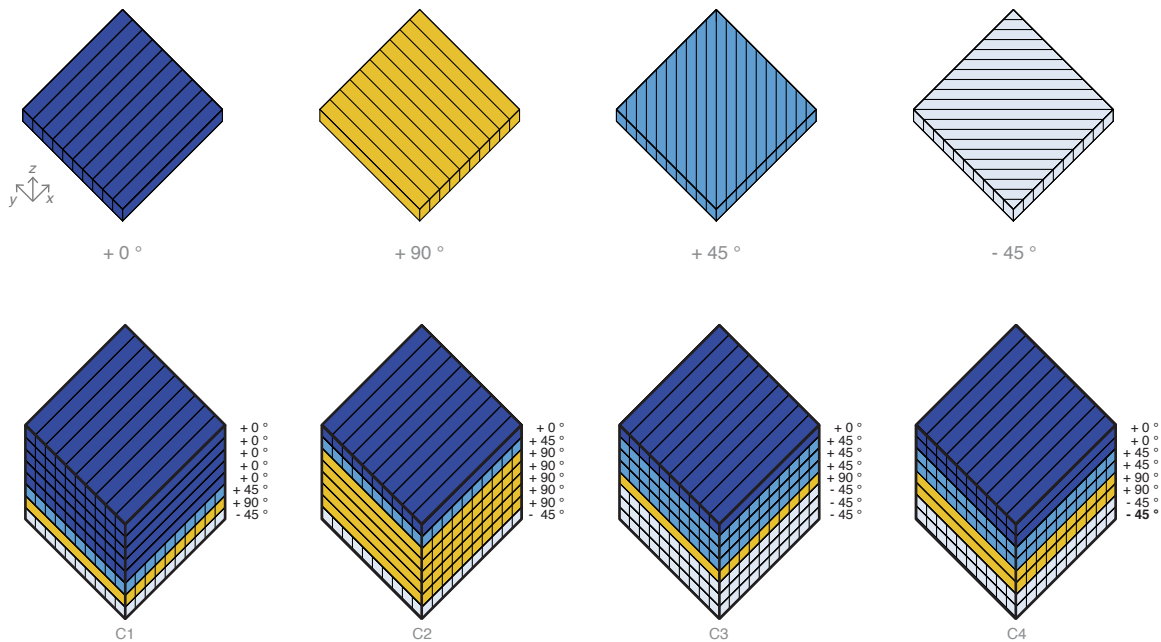


Figure 6.1 Division of the structure in 5 sub-spans.

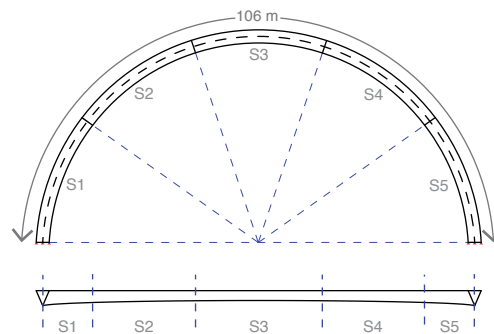


Figure 6.2 (top) The four considerate laminate. (bottom) The four considered laminate layup combination in this structural optimization framework.

Numerous geometries were generated at random. Then, through prescribing properties to each of the sub spans, the 1024 combination of layup-laminations were tested for each geometry. For each combination, the strain energy value is recorded to allow for comparison of structure's stiffness. This test was run more than 25 times with more than 25,000 generated geometries. The different layup combinations are ranked according to their strain energy allowing to evaluate their stiffness.

The following observation can be made across geometries:

- The order of laminate layup combinations from highest stiffness to lowest stiffness is consistently similar across all generated geometries. While there are always variations in the exact ranking order of the laminate layup combination. In comparing the 100 stiffest laminate layup combination for each geometry, 90 of the 100 laminate layup combinations reappear for each generated geometry.
- In ranking the 1024 possible laminate layup combination. The top three performing laminate layup combinations are repeatedly the same, as shown in figure 6.3.
- The stiffest solution is significantly stiffer than the worst performing structure (in terms of strain energy and deflection). As shown in figure 6.4, the strain energy of the stiffest layup combination is, on average, 1.2 smaller than the strain energy of the least stiff combination or a relative decrease of 23%. Similarly, the deflection of the stiffest layup combination is, on average, about 2.1 smaller than the deflection of the least stiff combination or a relative decrease of 69%.

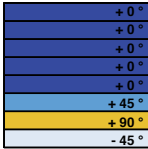
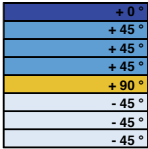
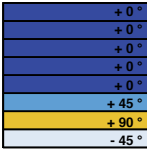
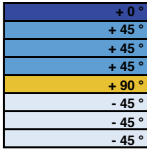
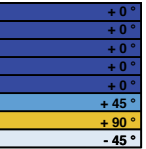
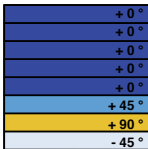
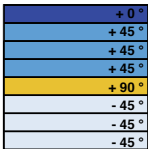
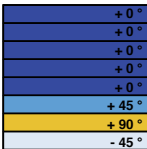
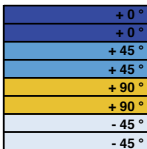
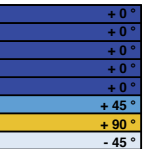
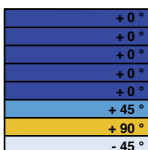
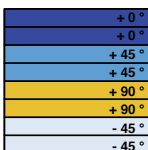
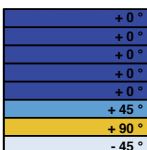
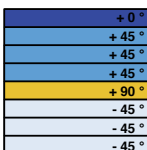
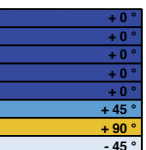
	S1	S2	S3	S4	S5
Rank 1 Stiffest Laminate Lay-up	 C1	 C3	 C1	 C3	 C1
Rank 2 2 nd Stiffest Laminate Lay-up	 C1	 C3	 C1	 C4	 C1
Rank 3 3 rd Stiffest Laminate Lay-up	 C1	 C4	 C1	 C3	 C1

Figure 6.3 The three laminate layup combination generating consistently the stiffest structures.

	S1	S2	S3	S4	S5
Rank 1 Stiffest Laminate Lay-up	<div> <div>+0°</div> <div>+0°</div> <div>+0°</div> <div>+0°</div> <div>+0°</div> <div>+45°</div> <div>+90°</div> <div>-45°</div> </div> C1	<div> <div>+0°</div> <div>+45°</div> <div>+45°</div> <div>+45°</div> <div>+90°</div> <div>-45°</div> <div>-45°</div> </div> C3	<div> <div>+0°</div> <div>+0°</div> <div>+0°</div> <div>+0°</div> <div>+0°</div> <div>+45°</div> <div>+90°</div> <div>-45°</div> </div> C1	<div> <div>+0°</div> <div>+45°</div> <div>+45°</div> <div>+45°</div> <div>+90°</div> <div>-45°</div> <div>-45°</div> </div> C3	<div> <div>+0°</div> <div>+0°</div> <div>+0°</div> <div>+0°</div> <div>+45°</div> <div>+90°</div> <div>-45°</div> </div> C1
Rank 1024 Least Stiff Laminate Lay-up	<div> <div>+0°</div> <div>+0°</div> <div>+45°</div> <div>+45°</div> <div>+90°</div> <div>+90°</div> <div>-45°</div> <div>-45°</div> </div> C4	<div> <div>+0°</div> <div>+0°</div> <div>+45°</div> <div>+45°</div> <div>+90°</div> <div>+90°</div> <div>-45°</div> <div>-45°</div> </div> C4	<div> <div>+0°</div> <div>+0°</div> <div>+45°</div> <div>+45°</div> <div>+90°</div> <div>+90°</div> <div>-45°</div> <div>-45°</div> </div> C4	<div> <div>+0°</div> <div>+0°</div> <div>+45°</div> <div>+45°</div> <div>+90°</div> <div>+90°</div> <div>-45°</div> <div>-45°</div> </div> C4	<div> <div>+0°</div> <div>+0°</div> <div>+45°</div> <div>+45°</div> <div>+90°</div> <div>+90°</div> <div>-45°</div> <div>-45°</div> </div> C4

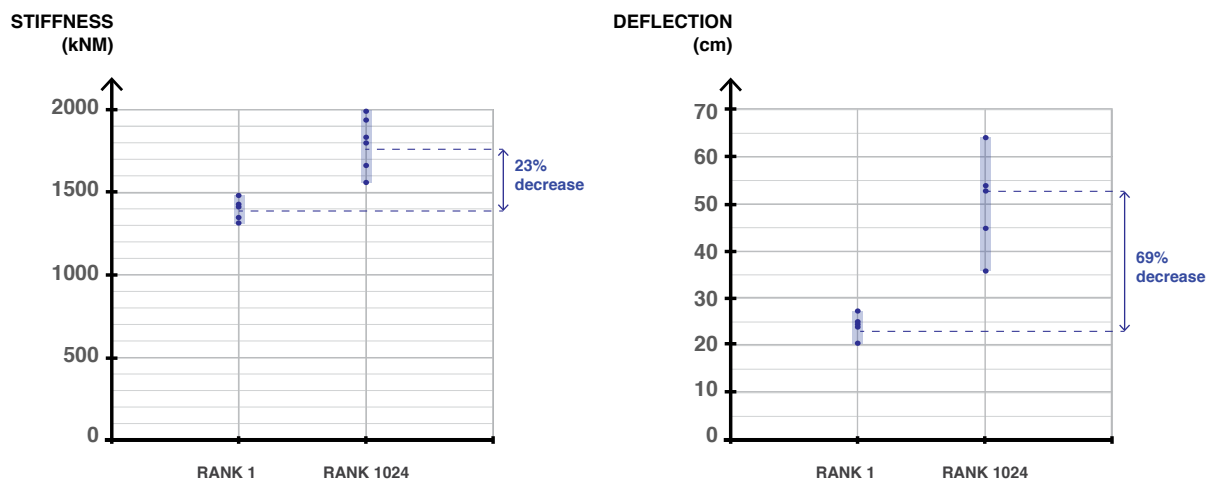


Figure 6.4 Comparison of the strain energy and deflection of the best performing (stiffest) and worst performing (least stiff) laminate layout. Each dot is for a different geometry.

In step 2 of the optimization, the structure is given the layup combination with the stiffest properties (rank 1), as shown in figure 6.5. Laminate layup combinations with high percentages of 0° laminates are located in sub-spans 1, 3, and 5 where bending stiffness is required. Laminate layup combinations with a high percentage of $\pm 45^\circ$ are located in sub-spans 2 and 4 where torsional stiffness is required.

	S1	S2	S3	S4	S5
Rank 1 Stiffest Laminate Lay-up	<div> <div>+0°</div> <div>+0°</div> <div>+0°</div> <div>+0°</div> <div>+0°</div> <div>+45°</div> <div>+90°</div> <div>-45°</div> </div> C1	<div> <div>+0°</div> <div>+45°</div> <div>+45°</div> <div>+45°</div> <div>+90°</div> <div>-45°</div> <div>-45°</div> </div> C3	<div> <div>+0°</div> <div>+0°</div> <div>+0°</div> <div>+0°</div> <div>+0°</div> <div>+45°</div> <div>+90°</div> <div>-45°</div> </div> C1	<div> <div>+0°</div> <div>+45°</div> <div>+45°</div> <div>+45°</div> <div>+90°</div> <div>-45°</div> <div>-45°</div> </div> C3	<div> <div>+0°</div> <div>+0°</div> <div>+0°</div> <div>+0°</div> <div>+45°</div> <div>+90°</div> <div>-45°</div> </div> C1

Figure 6.5 The laminate layup combination used in step 2 of the optimization framework.

1.2 Level 2 of the Optimization: Minimizing Weight

Once the material properties of the structure are determined, the second step of the optimization framework is run: minimizing the weight.

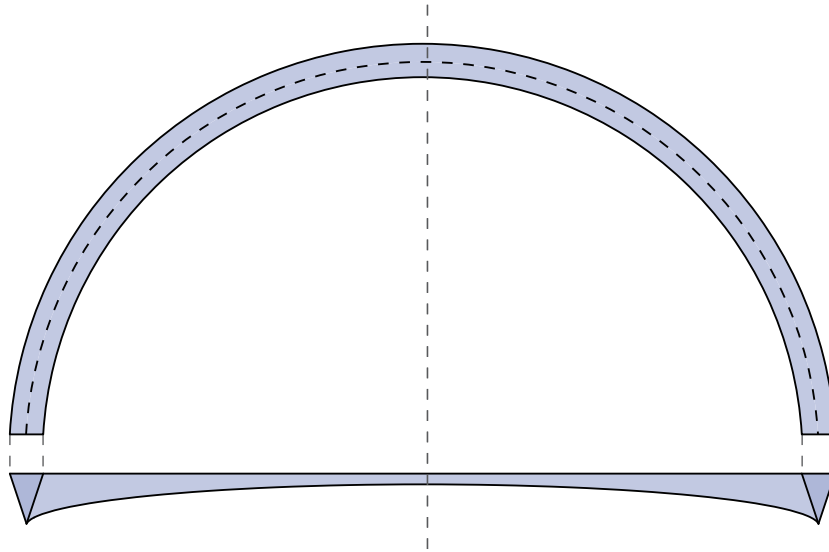
For each scenario, a genetic algorithm is run to optimize the weight of the structure. The recorded data is then processed to remove non-viable solutions (with a penalty) as they do not verify the design constraints. The clean data is transferred to spreadsheets using the Google drive plug-in Leafcutter. The processed data is then analyzed to visualize the genetic algorithm. For each scenario, the following graphs are produced:

- **A graph of the fitness function convergence in function of generations:** for each generation, the average, minimum value, maximum value, and standard deviation of the fitness function values are computed. This graph allows to visualize the convergence of the genetic algorithm on the fittest solution through all the generations of solutions.
- **A graph of the fitness function convergence in function of individual solutions:** only viable solutions (with no penalty) are considered. This graph allows to visualize the convergence of the genetic algorithm on the fittest solution through all the generated (viable) solutions.
- **A parallel coordinate plot of the genomes for the top 10 lightest generated geometries.**

For the eight scenarios discussed in chapter 5, the generated geometries in step 2 of the optimization are verified to be the fittest possible with the local optimization plug-in GOAT. The generated geometries and the three graphs are presented in the next pages hereinafter.

i. Triangular Symmetric Fixed-width Deck (TSF)

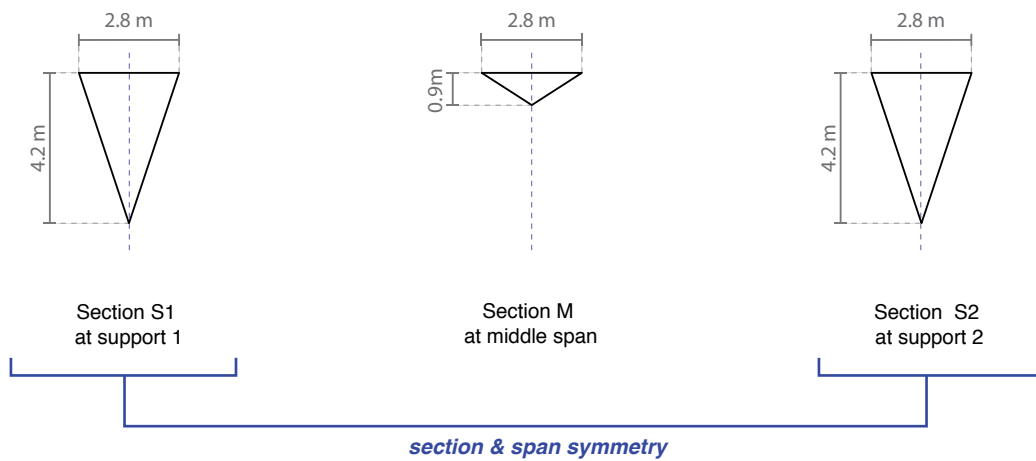
PLAN VIEW



SIDE VIEW



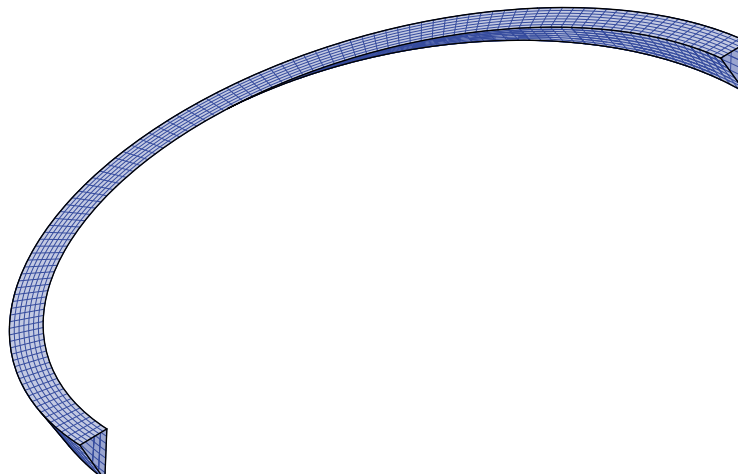
SECTIONS



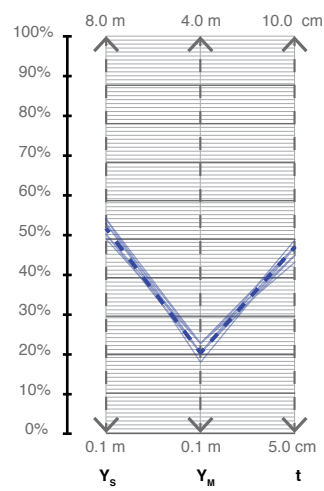
VARIABLES

$$X_{S1} = X_{S2} = X_M = 2.8 \text{ m} ; Y_S = Y_{S2} = 4.2 \text{ m} ; Y_M = 0.9 \text{ m} ; t = 7.4 \text{ cm}$$

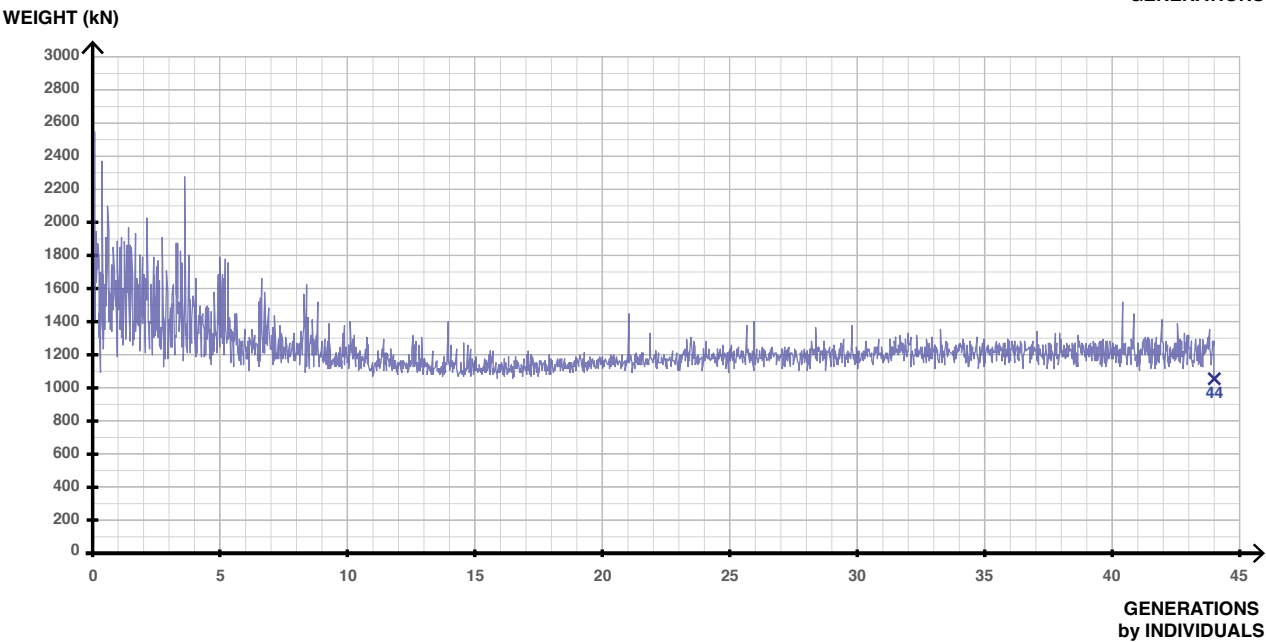
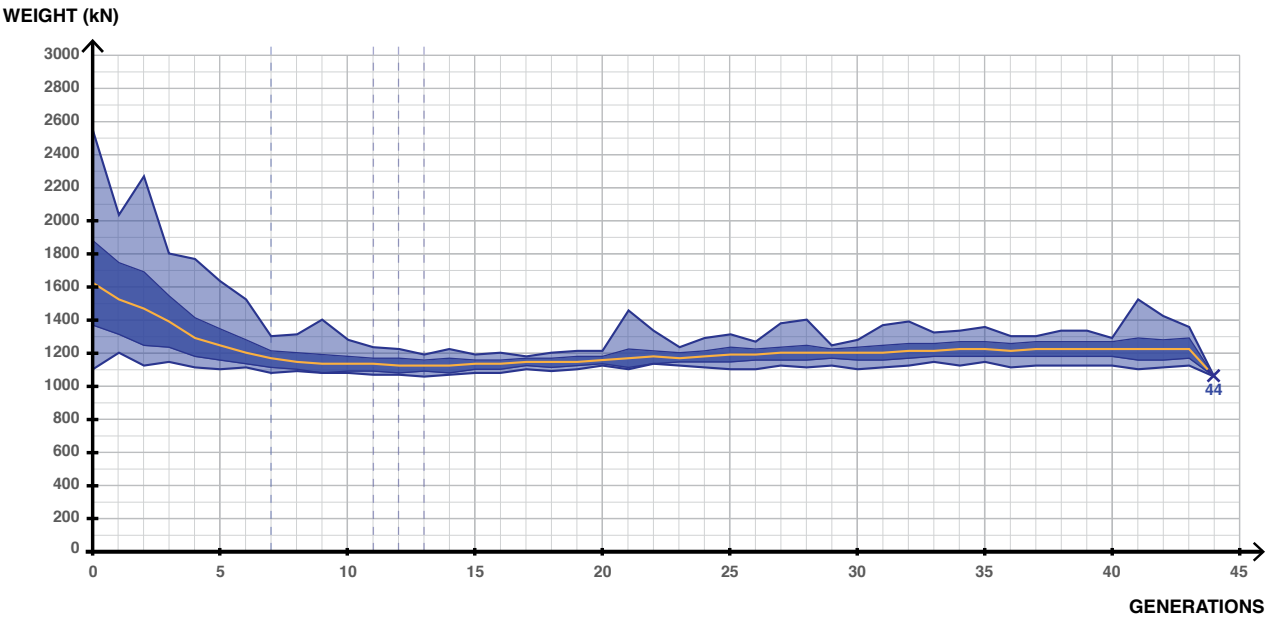
3D IMPRESSION



PARALLEL COORDINATE PLOT: TOP PERFORMING GENOMES

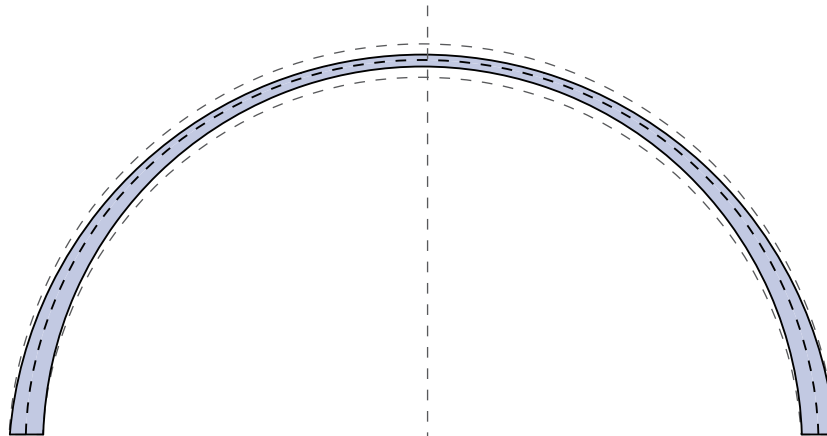


WEIGHT CONVERGENCE GRAPHS



ii. Triangular Symmetric Cantilevering Deck (TSC)

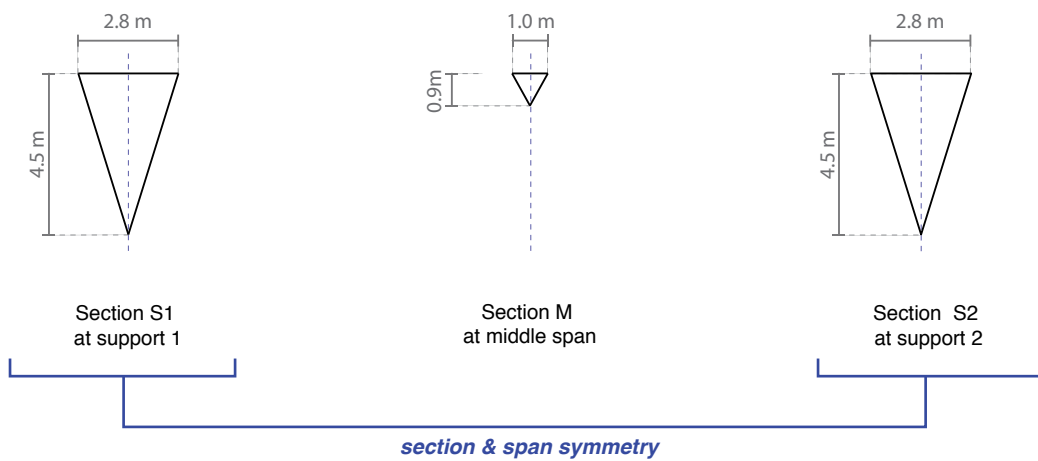
PLAN VIEW



SIDE VIEW



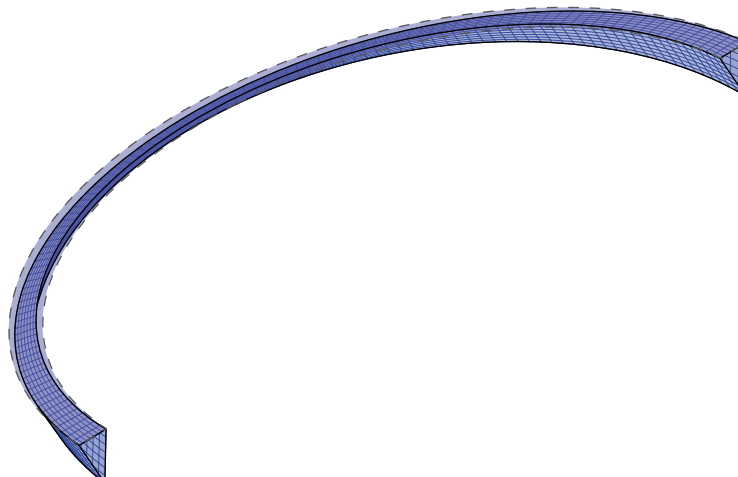
SECTIONS



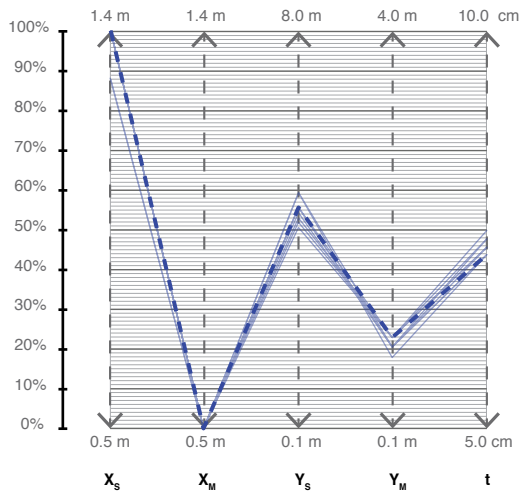
VARIABLES

$$X_{S1} = X_{S2} = 2.8 \text{ m} ; Y_S = Y_{S2} = 4.5 \text{ m} ; X_M = 1.0 \text{ m} ; Y_M = 0.9 \text{ m} ; t = 7.2 \text{ cm}$$

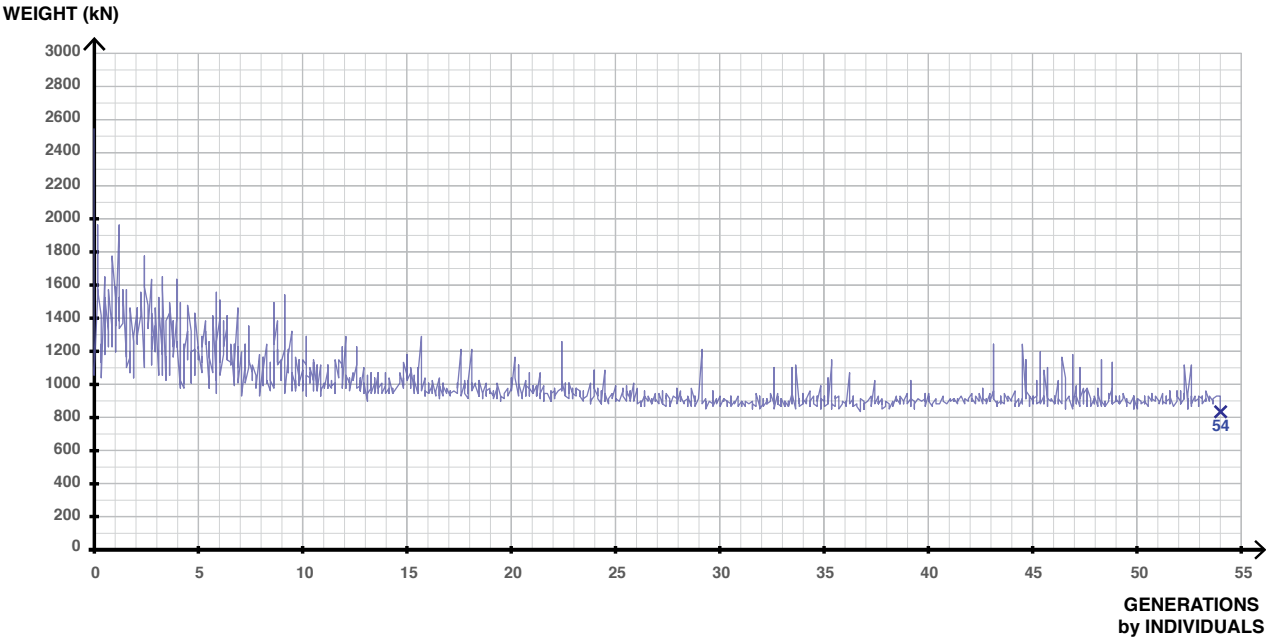
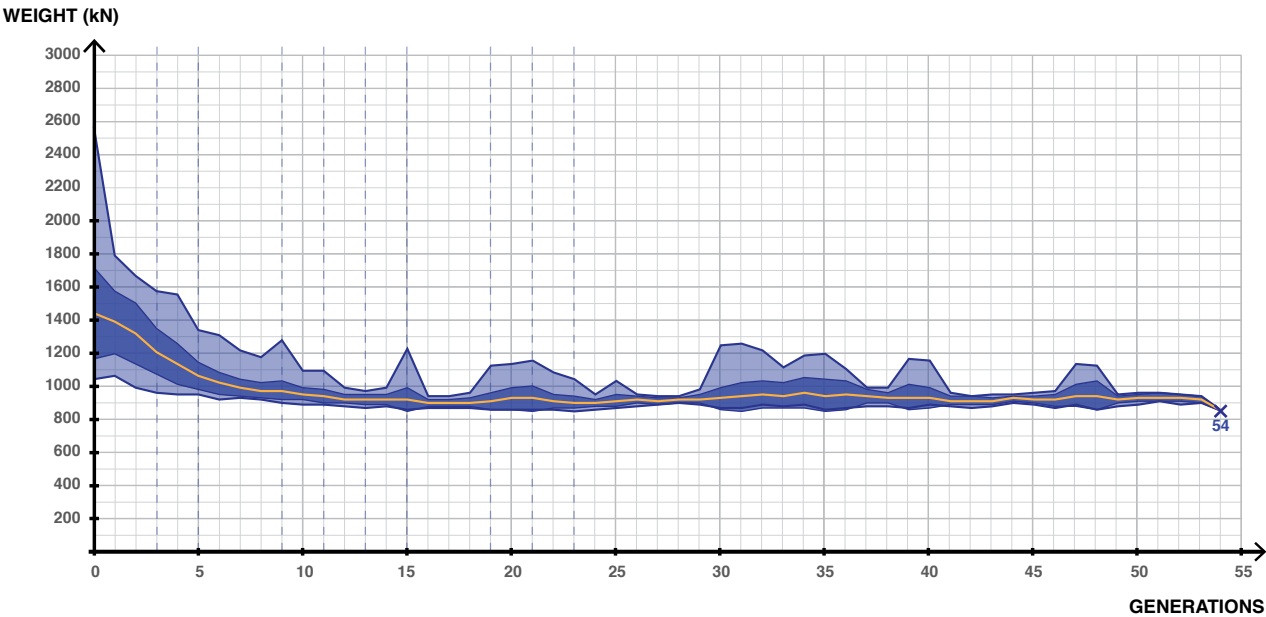
3D IMPRESSION



PARALLEL COORDINATE PLOT: TOP PERFORMING GENOMES

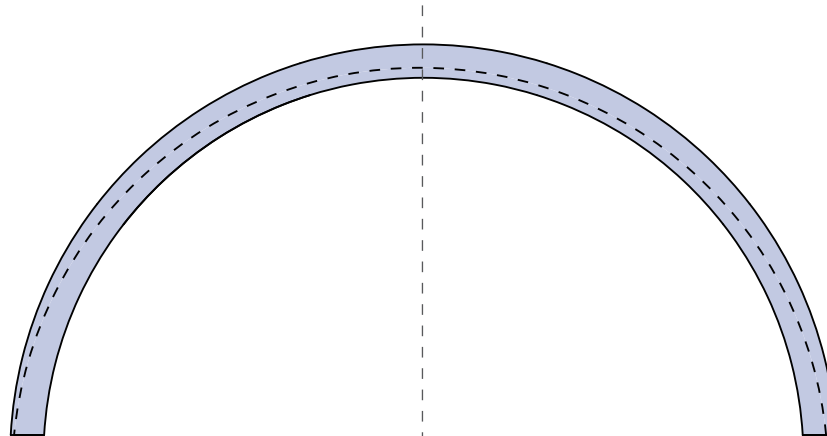


WEIGHT CONVERGENCE GRAPHS



iii. Triangular Asymmetric Fixed-width Deck (TAF)

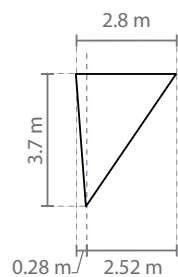
PLAN VIEW



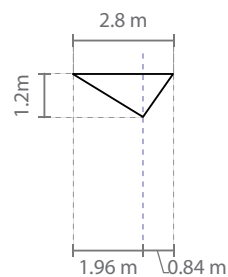
SIDE VIEW



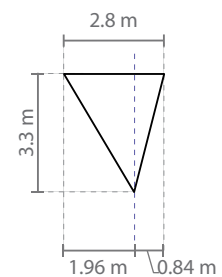
SECTIONS



Section S1
at support 1



Section M
at middle span



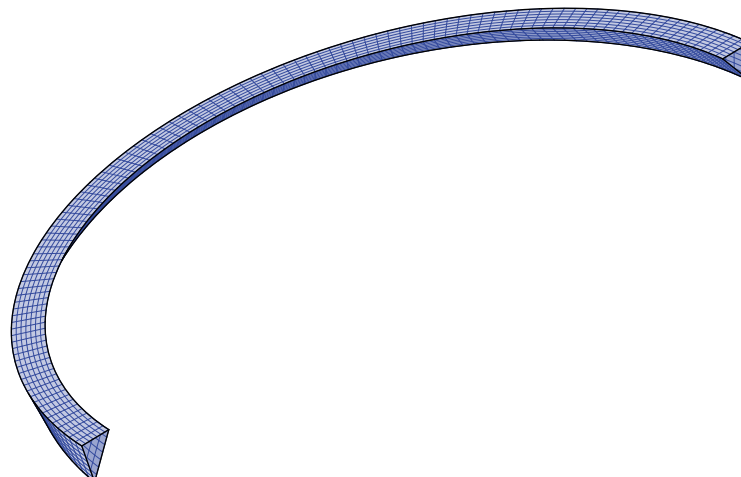
Section S2
at support 2

VARIABLES

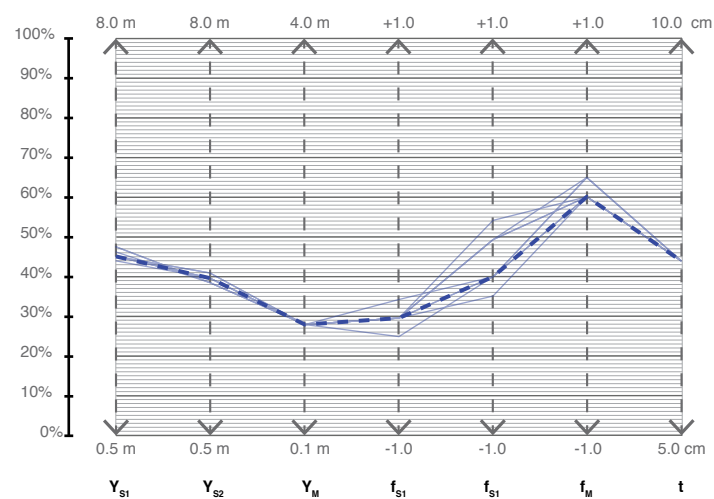
$$X_{S1} = X_{S2} = X_M = 2.8 \text{ m} ; Y_S = 3.7 \text{ m} ; Y_{S2} = 3.3 \text{ m} ; Y_M = 1.2 \text{ m} ; t = 7.2 \text{ cm}$$

$$f_{S1} = -0.4 ; f_M = 0.2 ; f_{S2} = -0.2$$

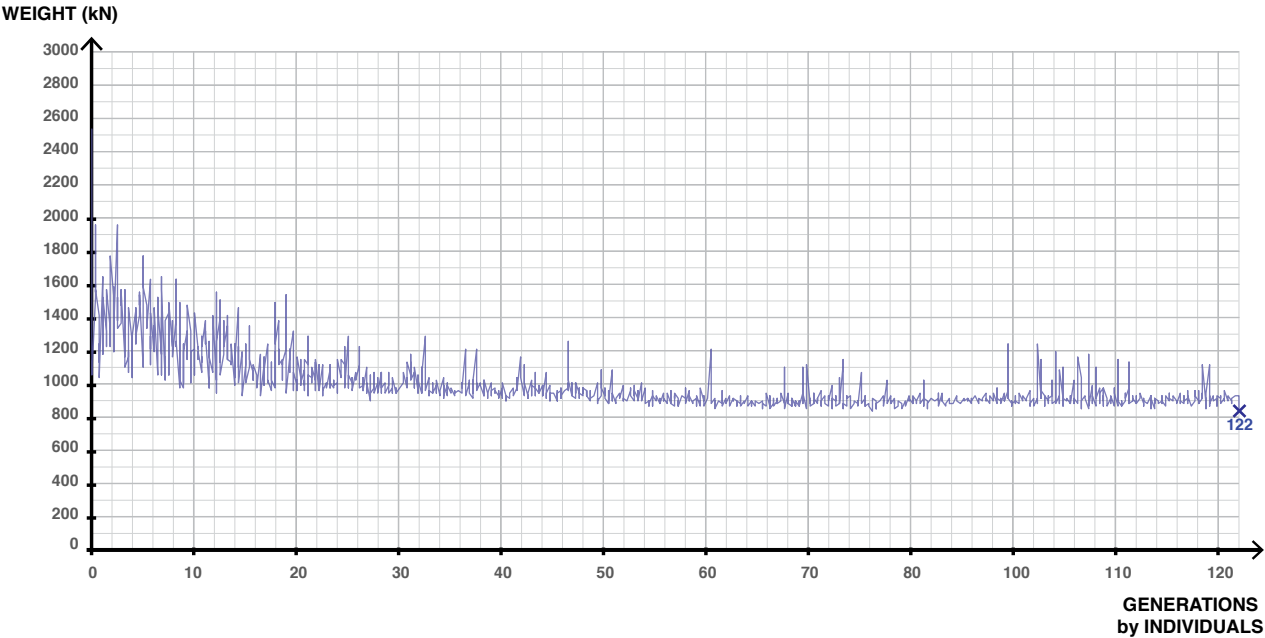
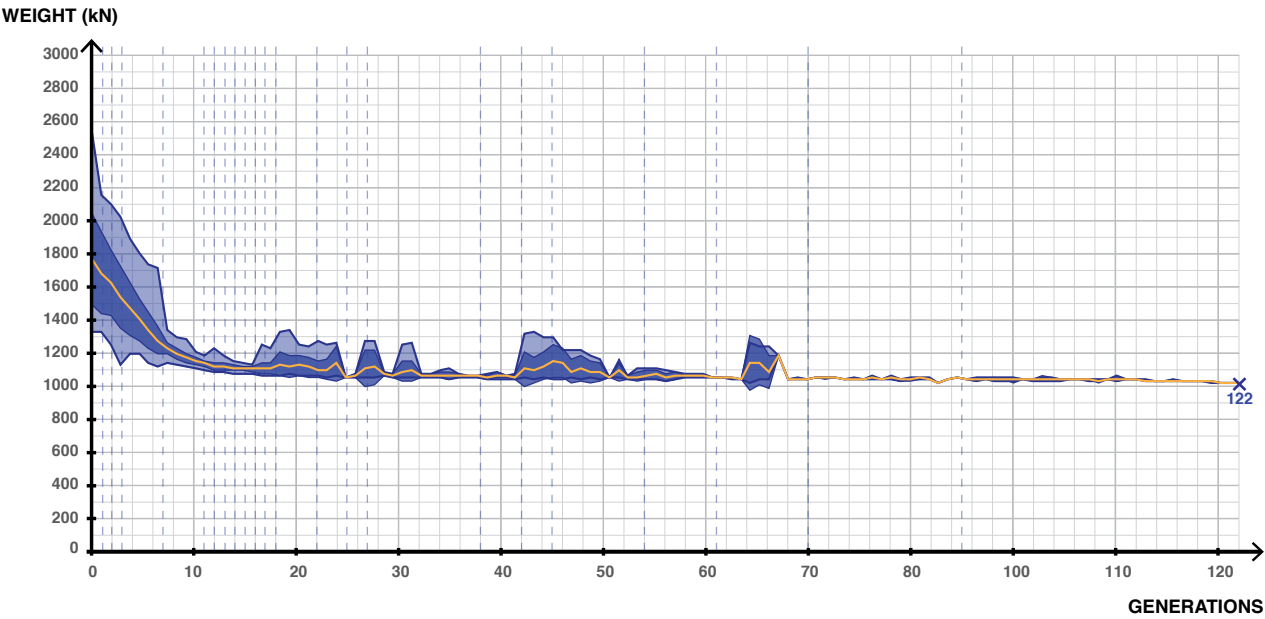
3D IMPRESSION



PARALLEL COORDINATE PLOT: TOP PERFORMING GENOMES

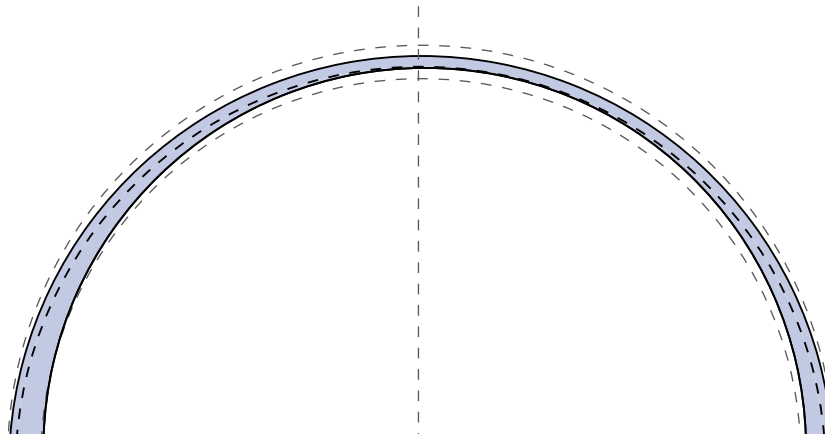


WEIGHT CONVERGENCE GRAPHS

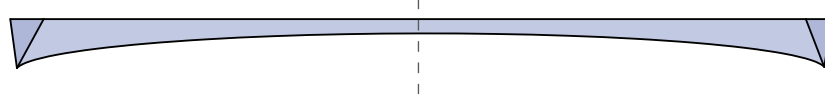


iv. Triangular Asymmetric Cantilevering Deck (TAC)

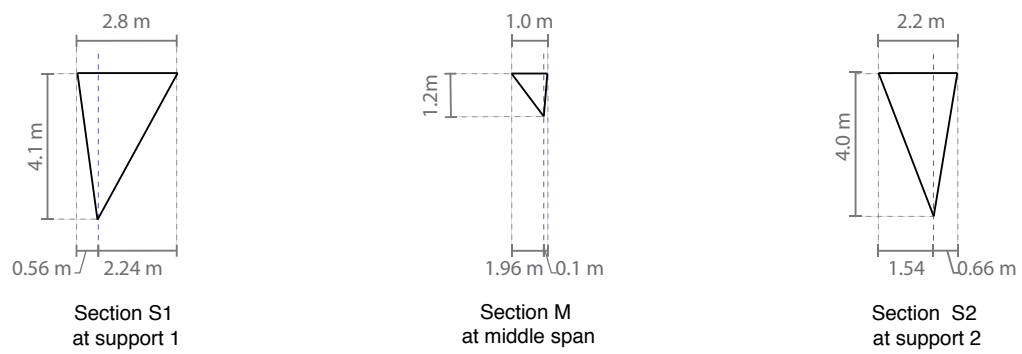
PLAN VIEW



SIDE VIEW



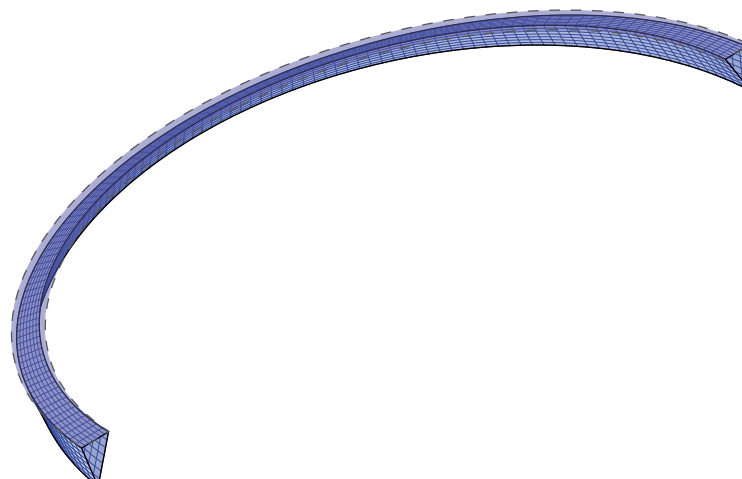
SECTIONS



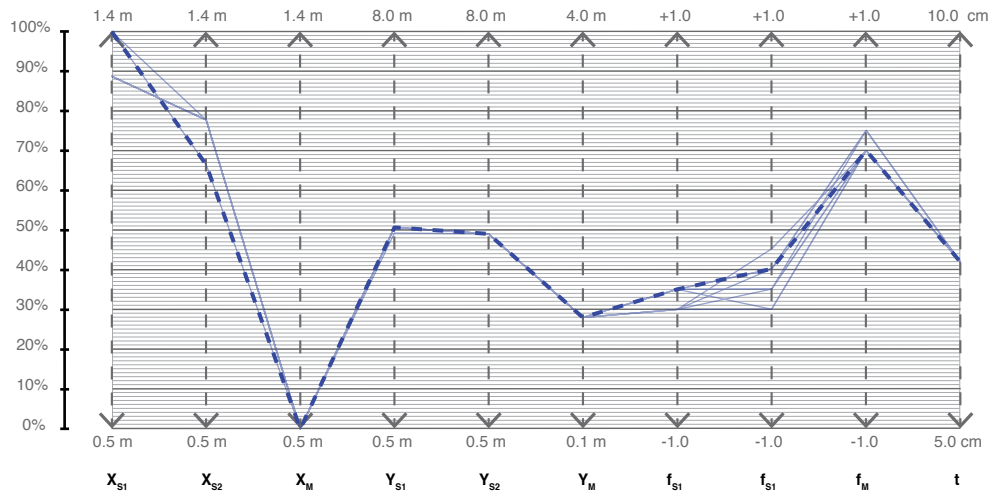
VARIABLES

$$\frac{X_{S1} = 2.8 \text{ m} ; X_{S2} = 2.2 \text{ m} ; Y_{S1} = 4.1 \text{ m} ; Y_{S2} = 4.0 \text{ m} ; X_M = 1.0 \text{ m} ; Y_M = 1.2 \text{ m} ; t = 7.1 \text{ cm}}{f_{S1} = -0.3 ; f_M = 0.4 ; f_{S2} = -0.2}$$

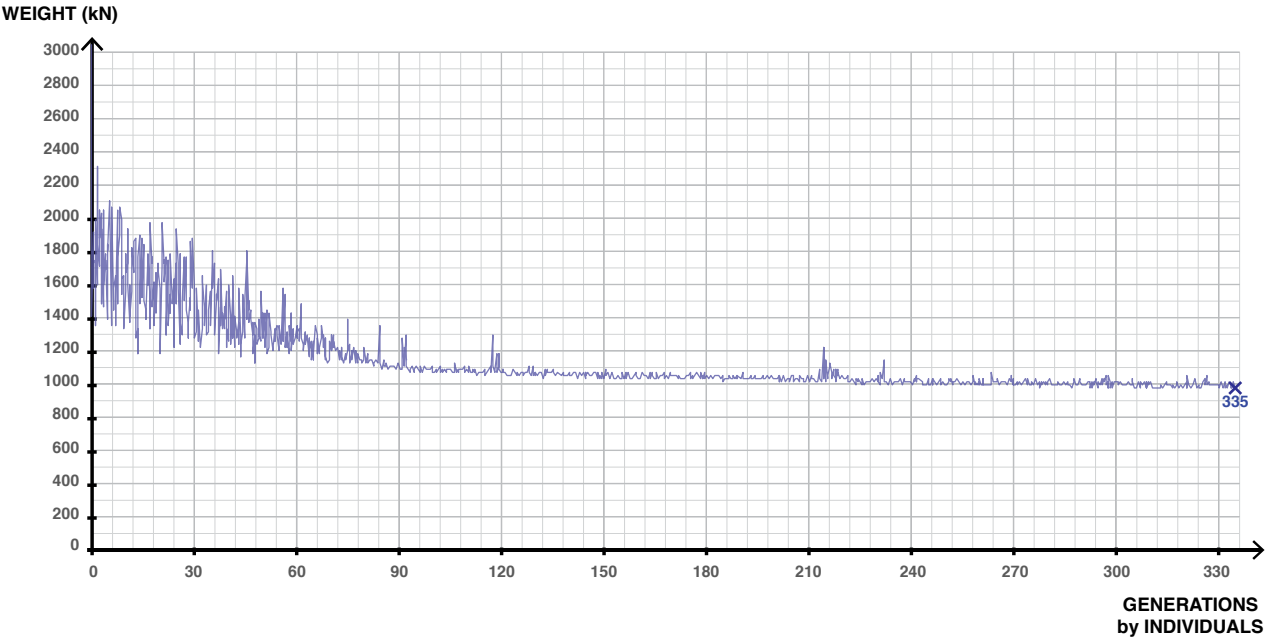
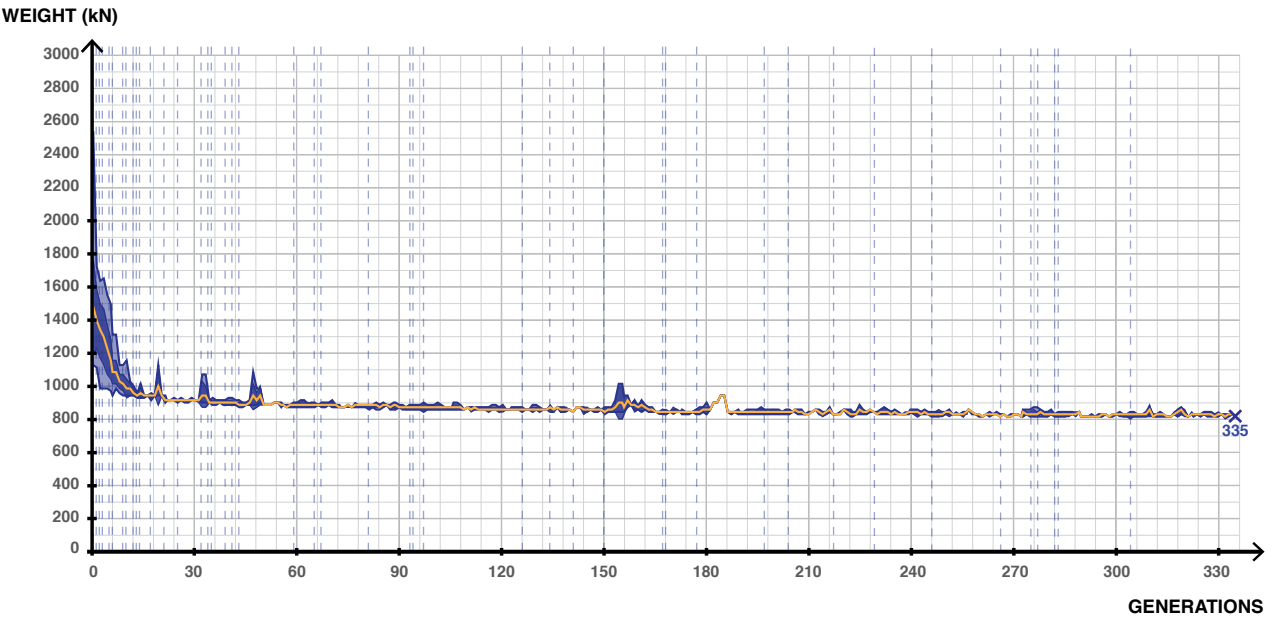
3D IMPRESSION



PARALLEL COORDINATE PLOT: TOP PERFORMING GENOMES

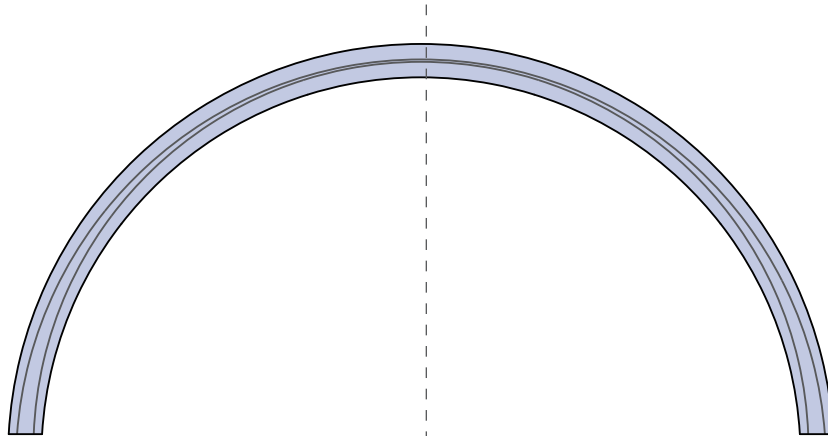


WEIGHT CONVERGENCE GRAPHS

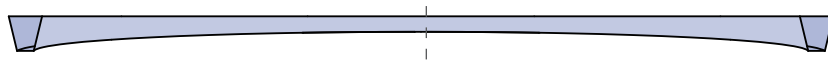


v. Quadrilateral Symmetric Fixed-width Deck (QSF)

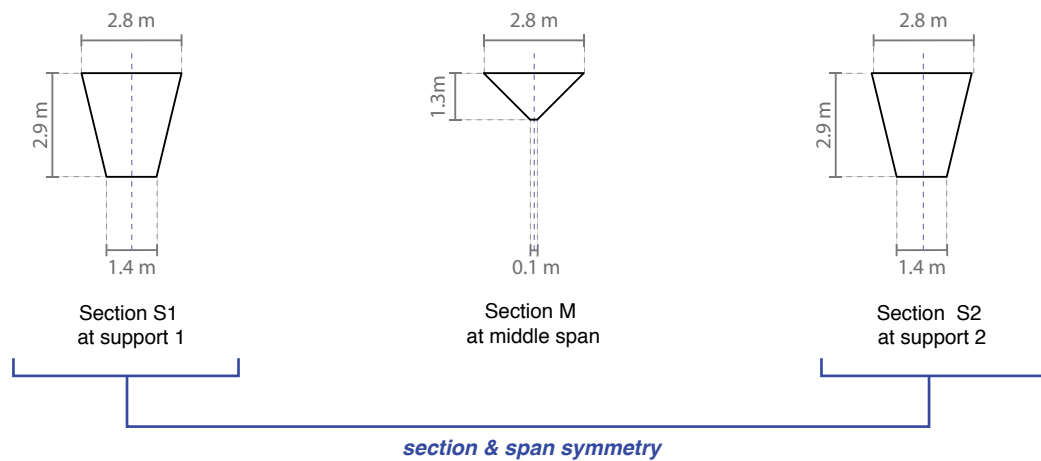
PLAN VIEW



SIDE VIEW



SECTIONS

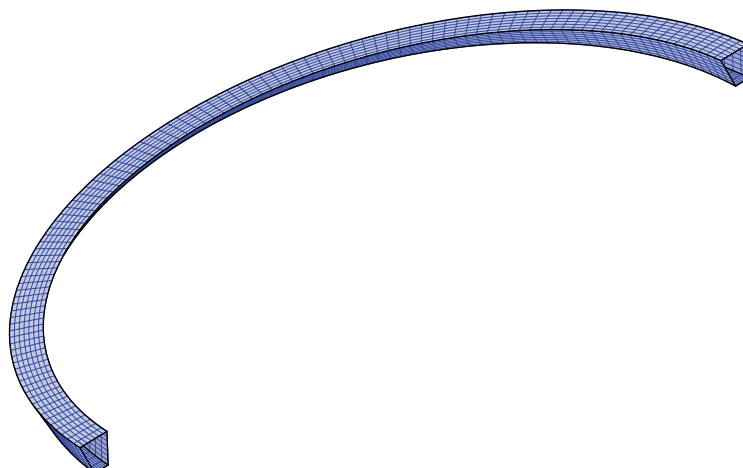


VARIABLES

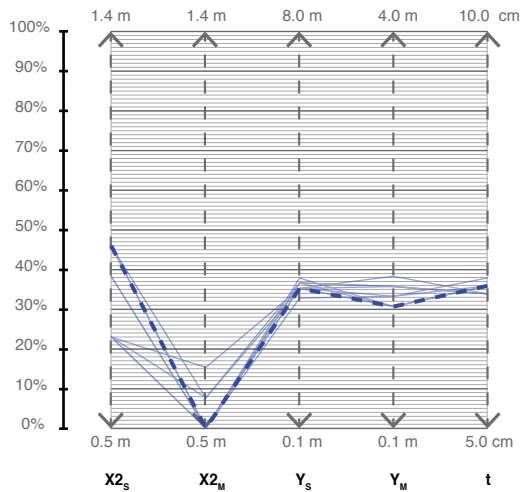
$$X1_{S1} = X1_{S2} = 2.8 \text{ m} ; X2_{S1} = X2_{S2} = 1.4 \text{ m} ; Y_S = Y_{S2} = 2.9 \text{ m} ; X1_M = 2.8 \text{ m} ;$$

$$Y_M = 1.3 \text{ m} ; t = 6.8 \text{ cm}$$

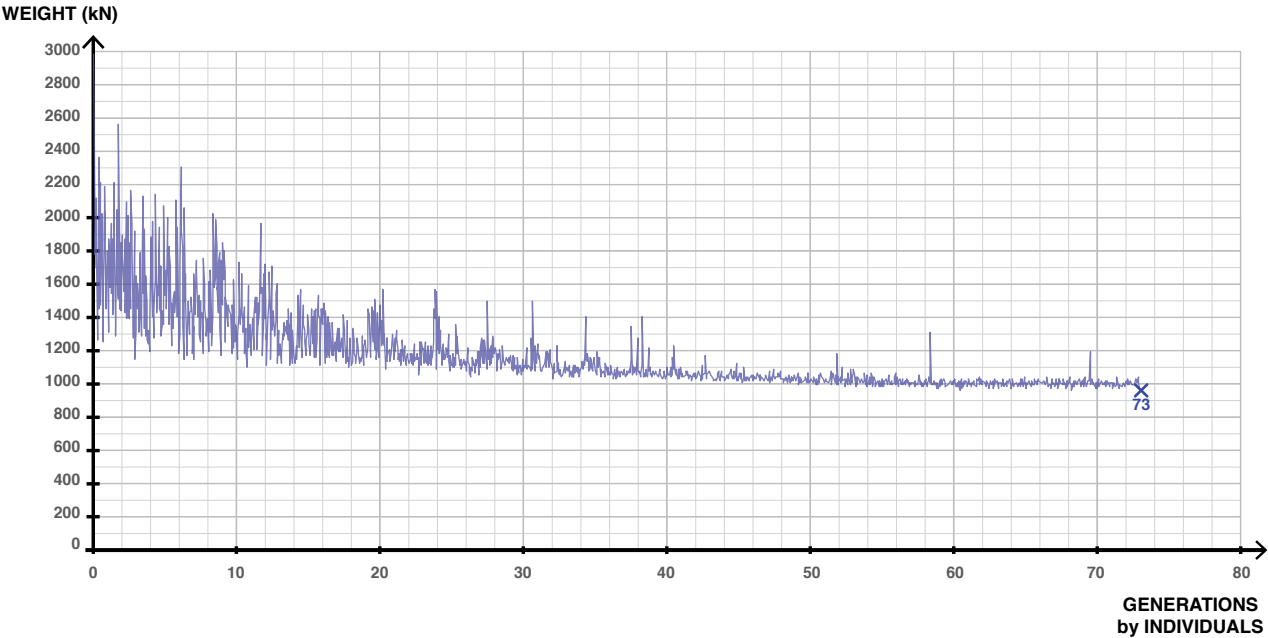
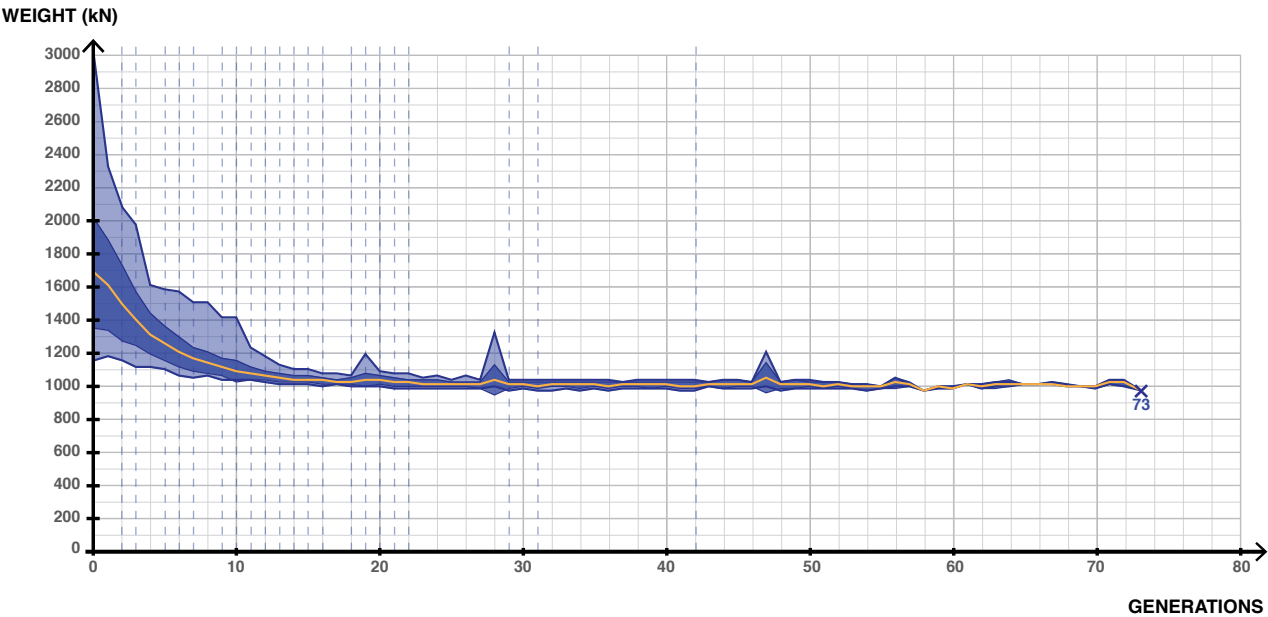
3D IMPRESSION



PARALLEL COORDINATE PLOT: TOP PERFORMING GENOMES

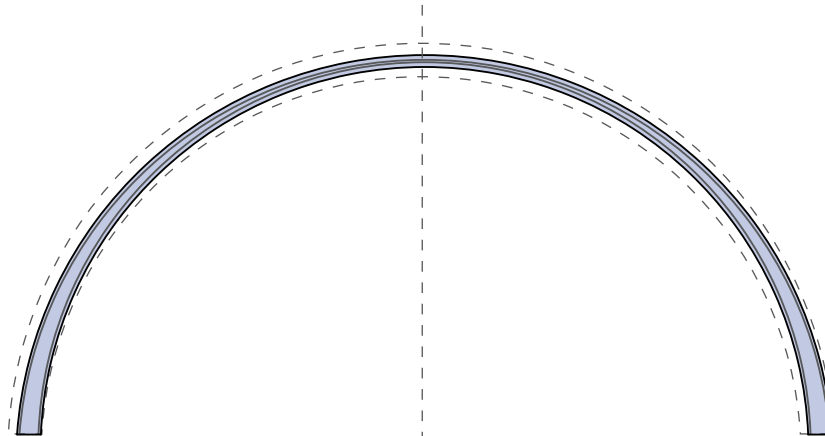


WEIGHT CONVERGENCE GRAPHS

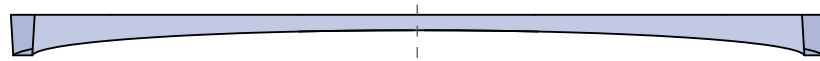


vi. Quadrilateral Symmetric Cantilevering Deck (QSC)

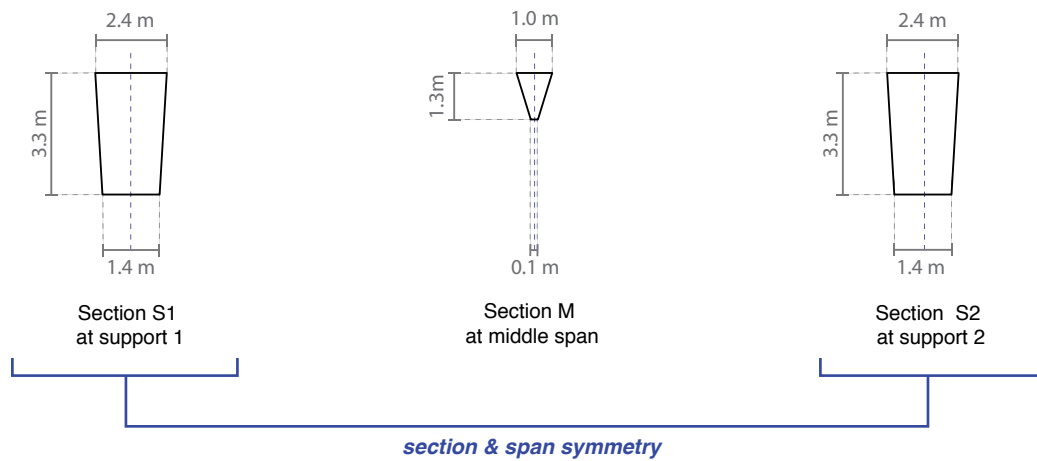
PLAN VIEW



SIDE VIEW



SECTIONS

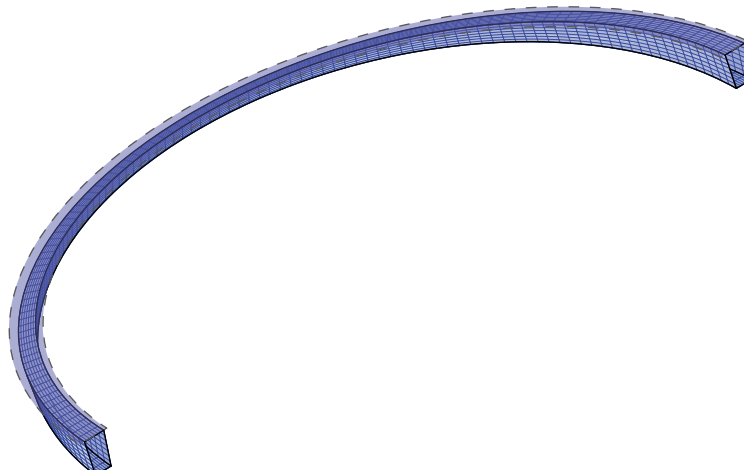


VARIABLES

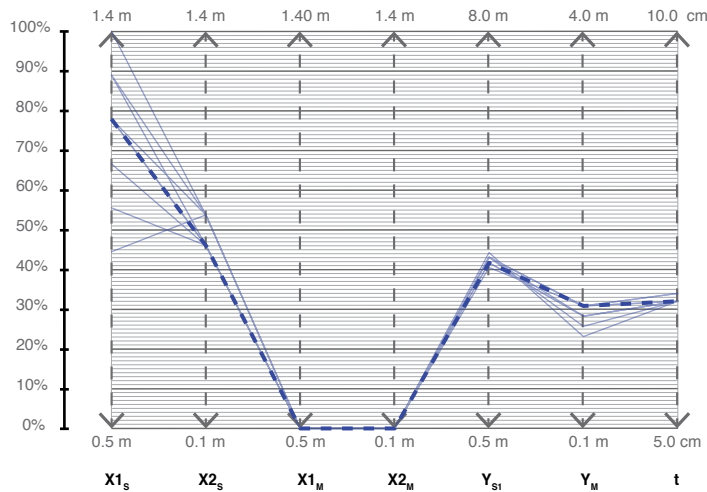
$$X1_{S1} = X1_{S2} = 2.4 \text{ m} ; X2_{S1} = X2_{S2} = 1.4 \text{ m} ; Y_S = Y_{S2} = 3.3 \text{ m} ; X1_M = 1.0 \text{ m} ;$$

$$Y_M = 1.3 \text{ m} ; t = 6.6 \text{ cm}$$

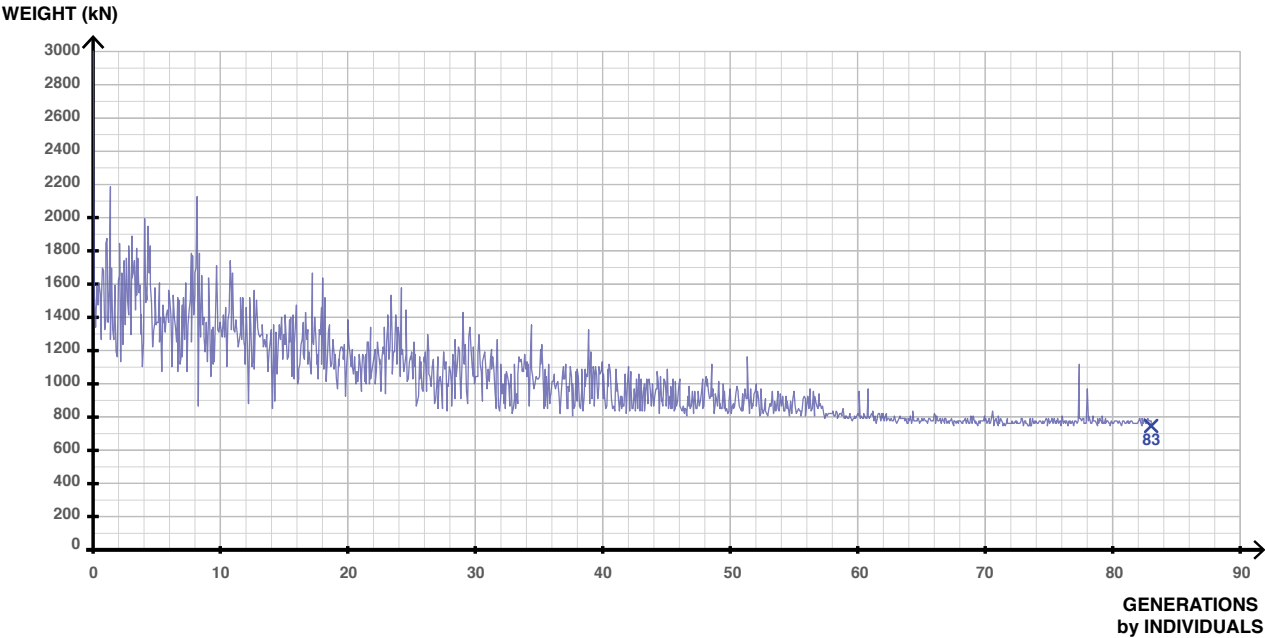
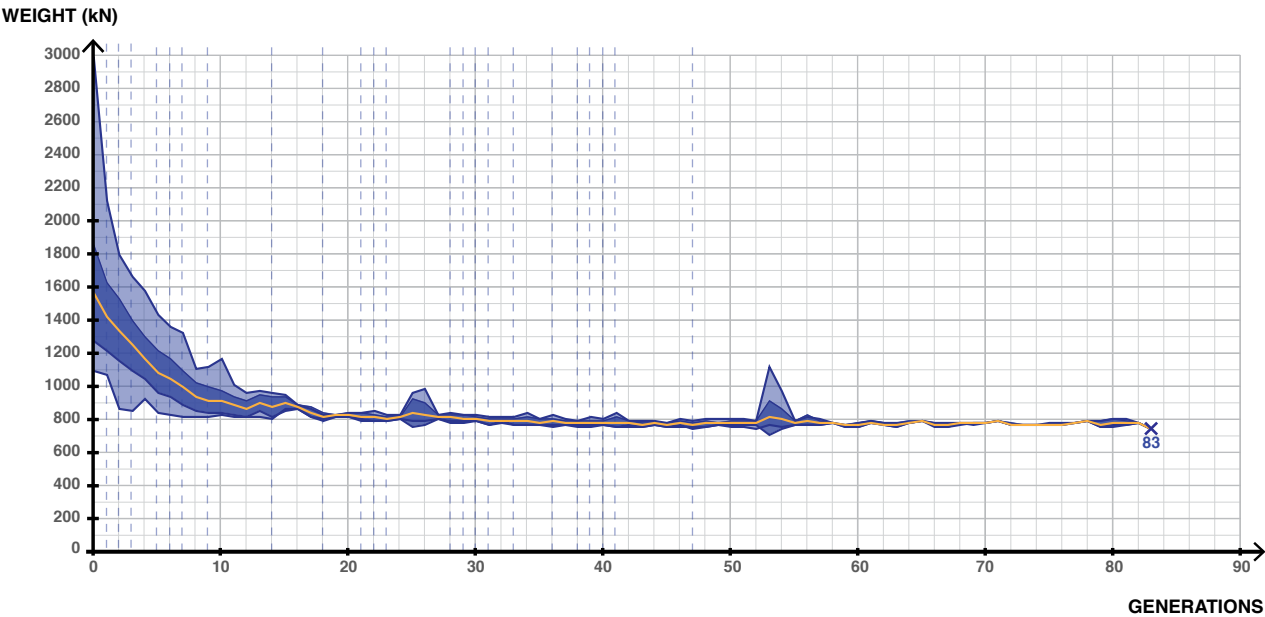
3D IMPRESSION



PARALLEL COORDINATE PLOT: TOP PERFORMING GENOMES

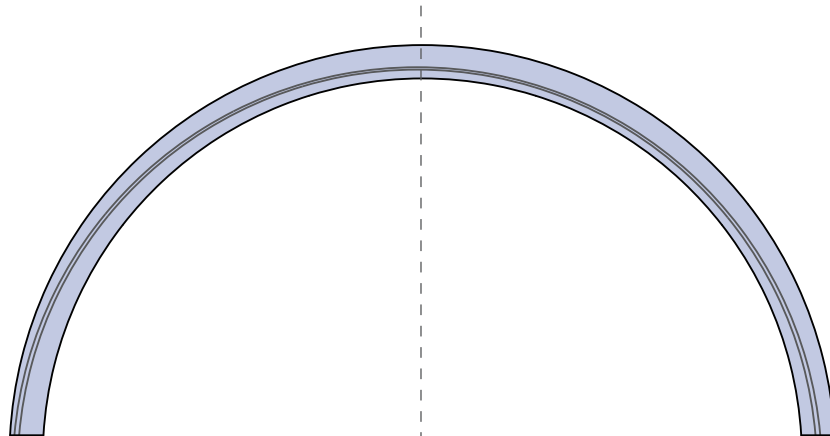


WEIGHT CONVERGENCE GRAPHS

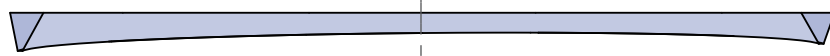


vii Quadrilateral Asymmetric Fixed-width Deck (QAF)

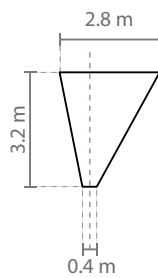
PLAN VIEW



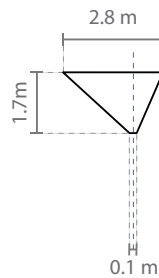
SIDE VIEW



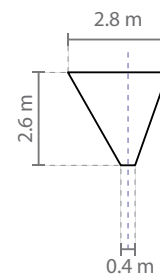
SECTIONS



Section S1
at support 1



Section M
at middle span



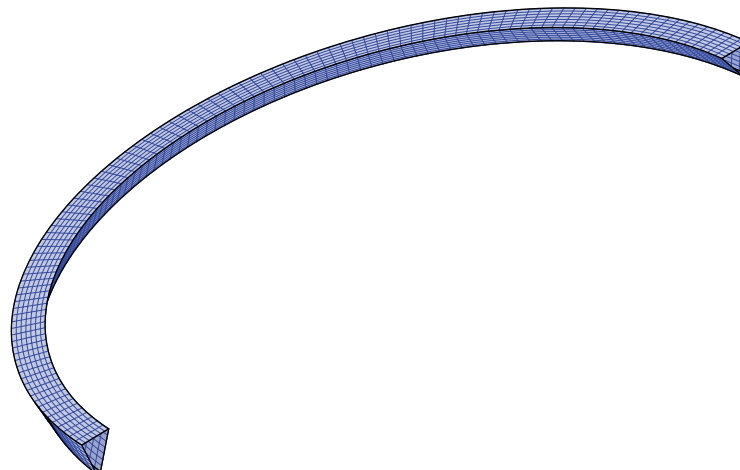
Section S2
at support 2

VARIABLES

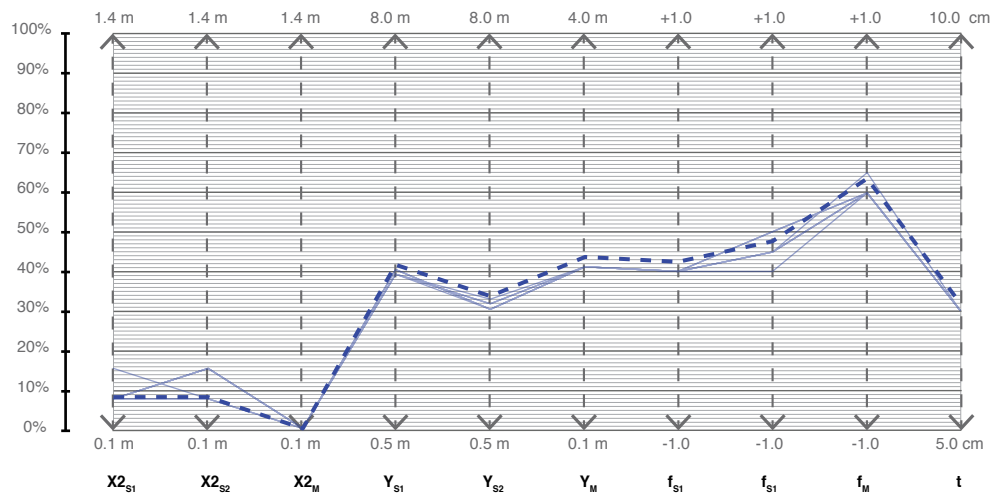
$$X_{S1} = X_{S2} = X_M = 2.8 \text{ m} ; Y_S = 3.2 \text{ m} ; Y_{S2} = 2.6 \text{ m} ; Y_M = 1.7 \text{ m} ; t = 6.5 \text{ cm}$$

$$f_{S1} = -0.2 ; f_M = 0.2 ; f_{S2} = -0.1$$

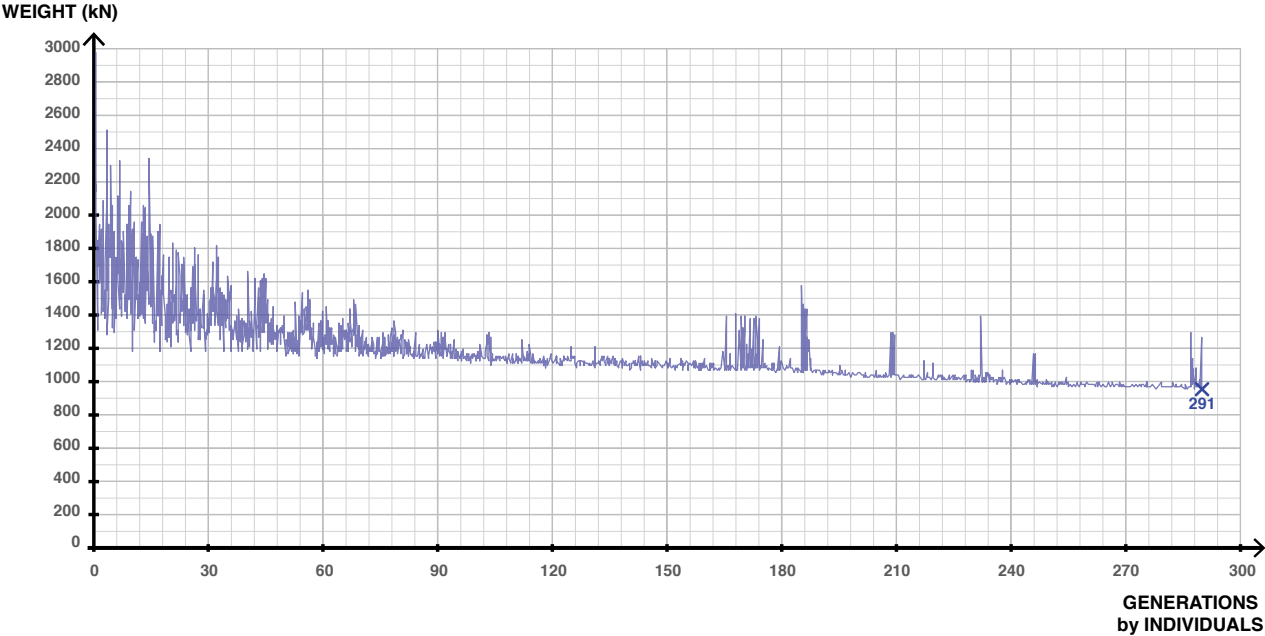
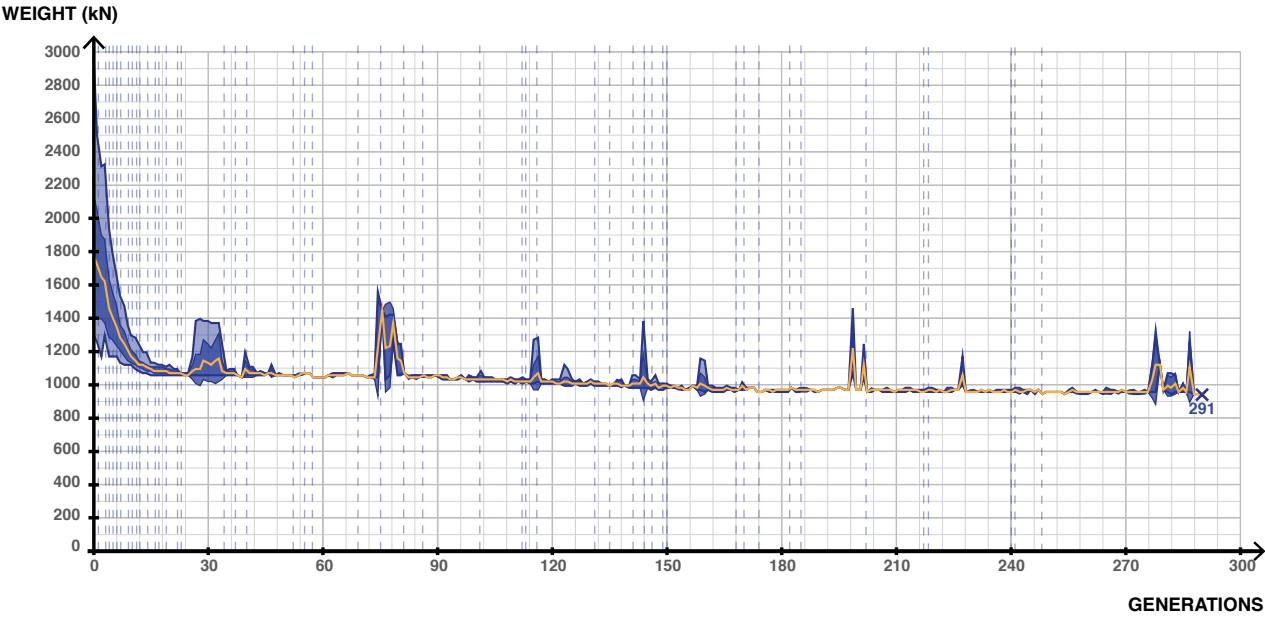
3D IMPRESSION



PARALLEL COORDINATE PLOT: TOP PERFORMING GENOMES

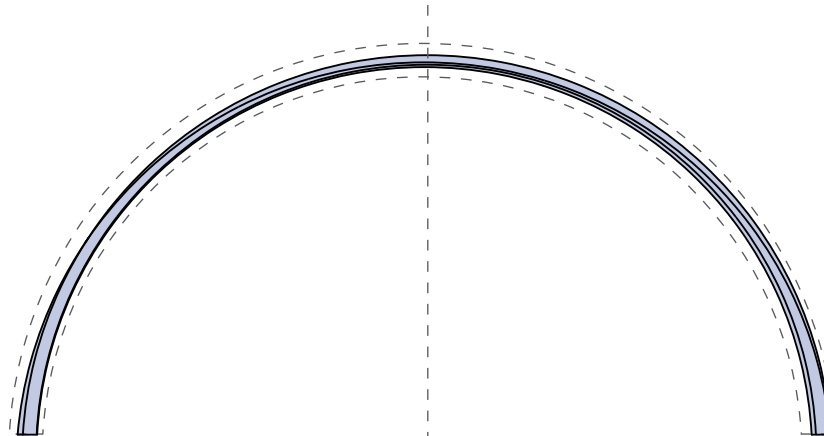


WEIGHT CONVERGENCE GRAPHS

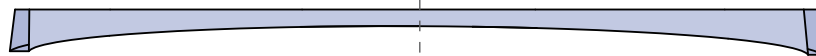


viii. Quadrilateral Asymmetric Cantilevering Deck (QAC)

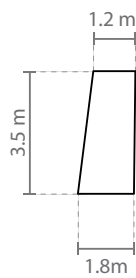
PLAN VIEW



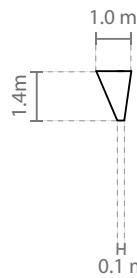
SIDE VIEW



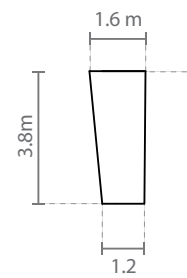
SECTIONS



Section S1
at support 1



Section M
at middle span

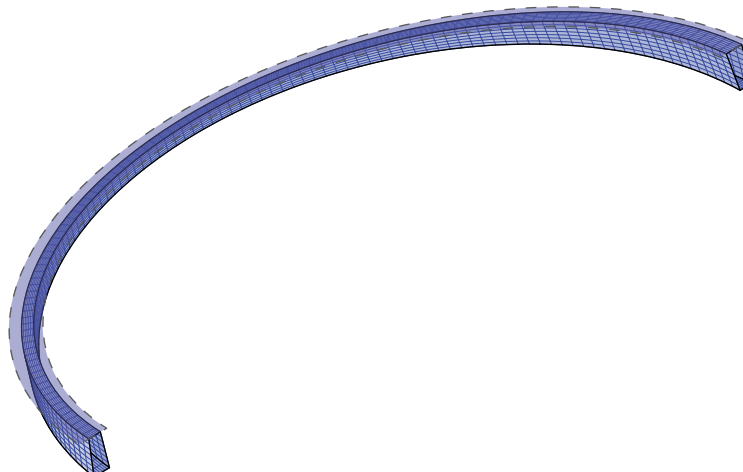


Section S2
at support 2

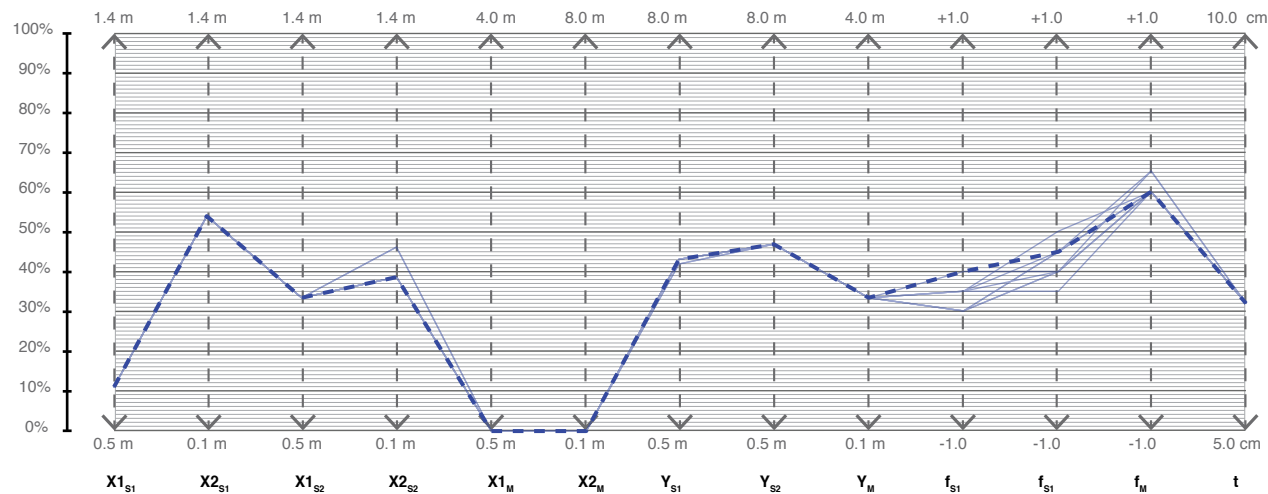
VARIABLES

$$\begin{aligned} X_{S1} = X_{S2} = X_M = 2.8 \text{ m} ; Y_S = 3.2 \text{ m} ; Y_{S2} = 2.6 \text{ m} ; Y_M = 1.7 \text{ m} ; t = 6.6 \text{ cm} \\ f_{S1} = -0.2 ; f_M = 0.2 ; f_{S2} = -0.1 \end{aligned}$$

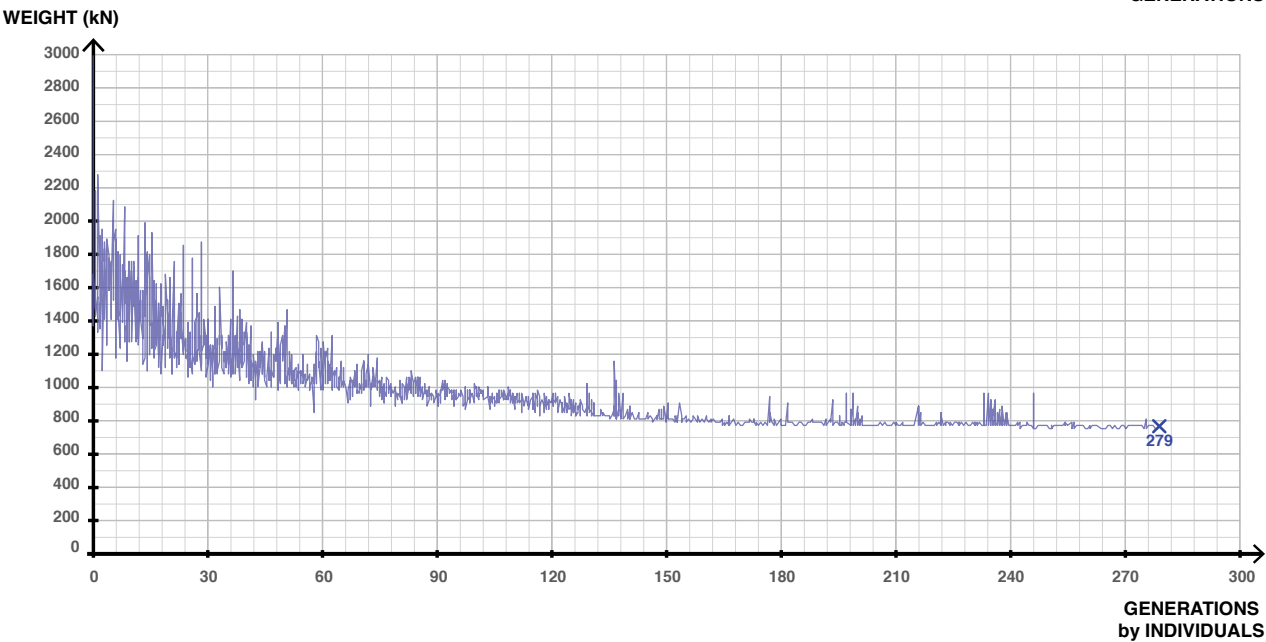
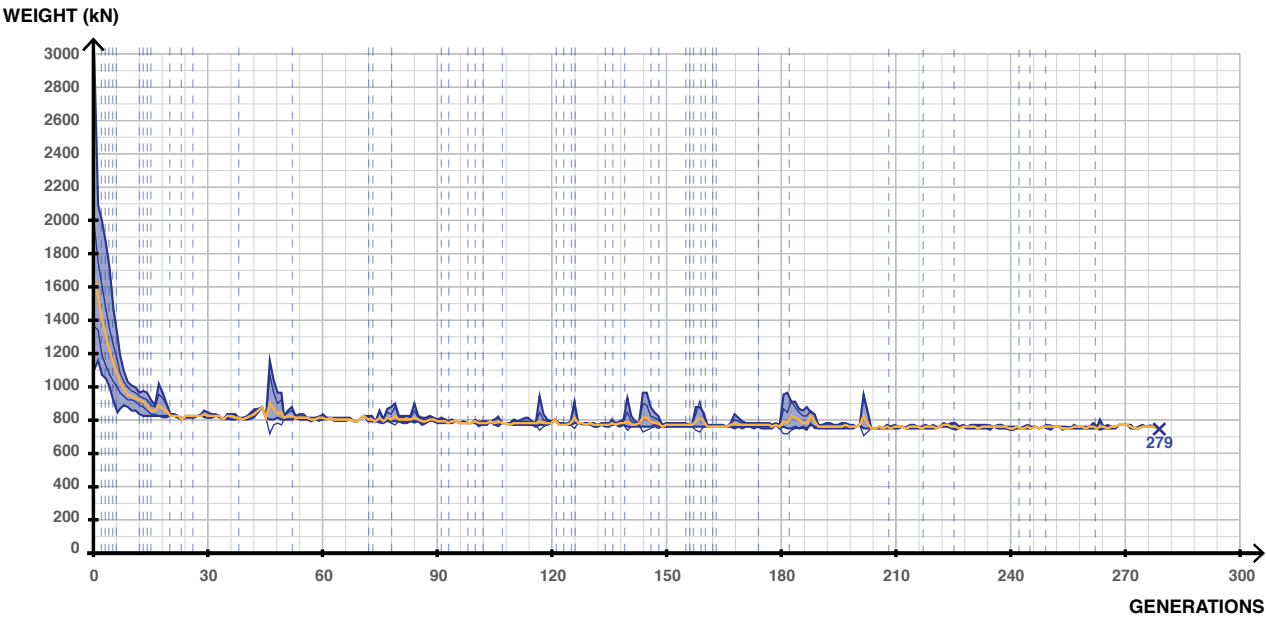
3D IMPRESSION



PARALLEL COORDINATE PLOT: TOP PERFORMING GENOMES



WEIGHT CONVERGENCE GRAPHS



2. Post-optimality Study

Two main objectives motivated the start of this research:

- Encouraging formal exploration in FRP through a framework that capitalizes on the possibilities and ambitions of FRP.
- Drawing a contrast between what is structurally feasible and realistically buildable.

Developing the optimization framework achieved the first objective. The comparative framework must thus address the feasibility of the generated FRP structures. In the next section, we propose multiple frameworks to evaluate the different generated geometries. Developing comparative criteria is by no means an easy task. Quantifying the performance of a structure is a challenging task especially when it comes to themes like efficiency, manufacturing, or aesthetics. Developing each criterion can be the topic of a research of its own.

In *The Tower and the Bridge*, Billington popularized the term “structural art” as the integration of efficiency, economy, and elegance in any construction [93]. Today, the terms “structural art” invites to be reinterpreted to reflect contemporary challenges. As addressed in the introduction to this research, the urgent and eminent challenge for the world, in general, and the construction industry in particular, is sustainability. If the gravity of this threat is truly understood, the framework of assessing structures must be modified to reflect these new incentives. Efficiency can no longer only mean minimal materials and economy can no longer mean minimal costs. Sustainability must become an important pillar of evaluating any design. As such, three main avenues of comparisons are identified to evaluate the sustainability of a design. In no particular order of importance or impact, the three criteria are: (1) computational efficiency, (2) material efficiency, and (3) production efficiency. In fact, the three criteria are defined in relation to the phases of a construction: efficient geometry generation (criteria 1), minimal resource use for a structurally sound performance (criteria 2), and low environmental impact through its manufacturing and execution.

In the following, the framework and results of each comparative criterion are elaborated before making a value and holistic judgment on a single efficient solution.

2.1 Computational Efficiency

i. Framework

Computational efficiency refers to the minimum computational power or energy required to run an analysis. It is an interesting criterion to compare as it allows to minimize the energy costs and running time associated with long computational algorithms. Even though the computational energy has already been spent running these genetic algorithms, the form exploration is not complete. As a design in the preliminary phase is constantly changing, it is considered productive to focus down on specific scenarios. In deciding which scenarios should be explored further, an important criterion becomes the running time associated with the corresponding GA.

Computational efficiency can be evaluated by comparing the convergence rates for genetic algorithms. In fact, the convergence rate of genetic algorithms depends on multiple factors: parameter properties such as the number of genes and their corresponding search space, or genetic algorithm settings such as the crossover rate, the mutation rate, or selection rate. Additionally, there is always an inherent randomness in every genetic algorithm that contributes to its convergence rate.

ii. Results

For each scenario, the number of genes, total search space, and convergence rate are recorded. The design optimization used a computer with an Intel Xeon processor with a CPU E5-1620 v3 with 3.50 GHz. The calculations of the search spaces and their corresponding convergence rates are shown in appendix L1. The convergence rates are visualized in figure 6.6. The results are summarized in table 6.1 and ranked in table 6.2 from quickest convergence to slowest convergence. Examining the results of tables 6.2 and 6.3 contributes to the following observations:

The larger the size of the search space the longer the GA takes to converge. There is an exception among the generated results: the search space for the TAC case is smaller than those of QAF and QAC, but the genetic algorithm takes longer to converge. Considering the eight scenarios have the same GA settings, this inconsistency must be to the randomness inherent to any genetic algorithm.

According to the suggested definition of computational efficiency, scenario TSF is most efficient with the smallest number of genes, the smallest search space, and the quickest convergence rate.

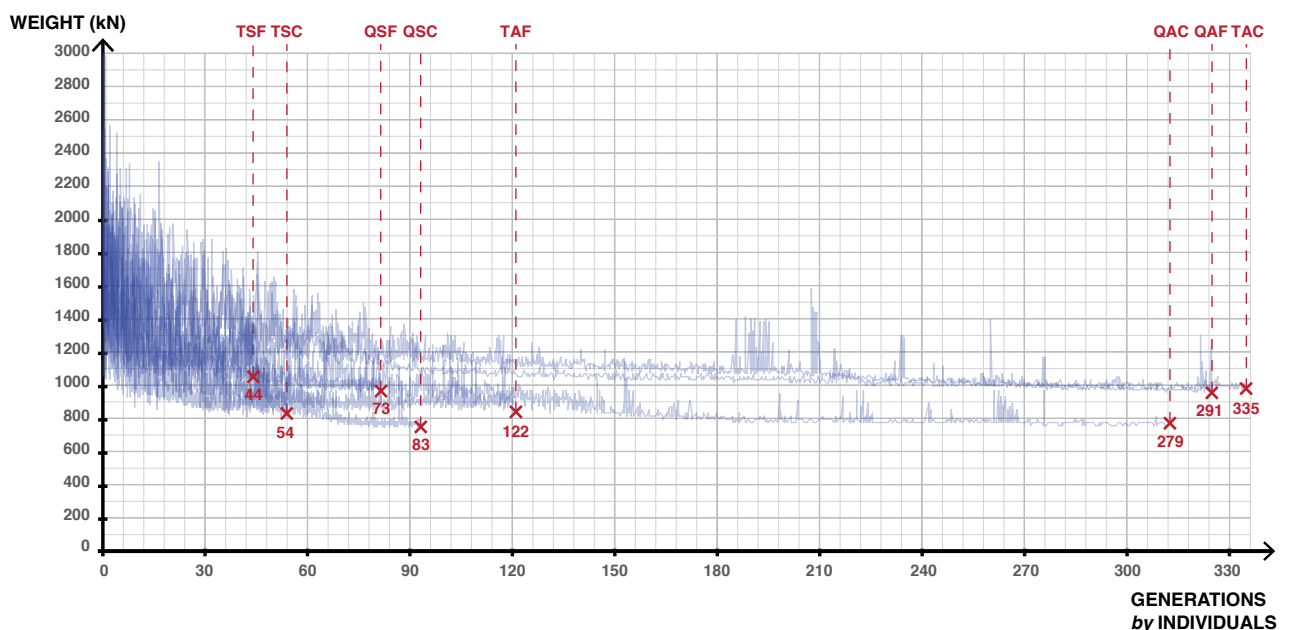


Figure 6.6 Convergence of the genetic algorithms for the eight generated geometries (appendix L2).

	Number of Genes	Search Space	Number of generations before convergence
TSF	3	1.54E+05	44
TSC	5	2.60E+07	54
TAF	7	9.74E+10	122
TAC	10	7.10E+13	335
QSF	5	2.60E+07	73
QSC	7	2.11E+09	83
QAF	10	2.14E+14	291
QAC	13	1.56E+17	279

Table 6.1 Variables to evaluate the computational efficiency of the generated geometries.

	Number of Genes	Search Space	Number of generations before convergence
TSF	3	1.54E+05	44
TSC	5	2.60E+07	54
QSF	5	2.60E+07	73
QSC	7	2.11E+09	83
TAF	7	9.74E+10	122
QAF	10	2.14E+14	291
QAC	13	1.56E+17	279
TAC	10	7.10E+13	335

Table 6.2 Ranked geometries from quickest to longest convergence (in terms of number of generations before convergence).

iii. Discussion

Limiting the number of parameters or their corresponding search space is a successful method at limiting the computational energy and time required for a genetic algorithm. However, such measures limit the formal exploration at the preliminary stage. Therefore, the opportunity cost of decreasing the search space size must be measured against its benefits. If the structural designer and architect have a clearly delineated form (shape and section) of the geometry in mind and are looking only for the optimal dimensions, then limiting the parameters is not necessarily restrictive. However, if the architect-engineer team is still not decided on a particular form in the early stages of a design, the conception stage is considered essential for formal exploration. The opportunity cost of limiting the search space would then be significant in such a case.

In light of this discussion, the most computationally efficient structure is not necessarily the best design. Other perspectives must be compared. One of those perspective, material efficiency, is studied next.

2.2 Material Efficiency

i. Framework

Material efficiency is the closest to the notion of efficiency as used by Billington. It refers to the minimum material use. Generally speaking, lighter structures translate in less energy expended during production, transportation, and installation. Furthermore, it can be complemented by structural performances deemed important in assessing a design. In this research, natural frequency is considered an important structural criterion. However, as shown in appendix L3, no solution presents a significant advantage over the others when it comes to natural frequency. It will thus not be discussed hereinafter.

ii. Results

The weights of the eight structures are summarized in table 6.3, ranked from lightest to heaviest. A factor f is calculated to quantify how much a structure is lighter than the worst (of the best) performing structure.

$$f = \frac{\text{weight of the considered structure}}{\text{weight of the heaviest structure}}$$

	Force of Gravity (kN)	Weight (tons)	Relative Difference	
QAC	750.2	76.5	35.13	0.70
QSC	753.1	76.8	34.75	0.70
TAC	812.0	82.8	27.40	0.76
TSC	831.4	84.8	25.08	0.78
QAF	954.0	97.3	11.45	0.89
QSF	968.6	98.8	9.94	0.91
TAF	1025.4	104.6	4.24	0.96
TSF	1069.9	109.1	0.00	1.00

Table 6.3 Ranked geometries from heaviest to lightest structure.

	Force of Gravity (kN)	Weight (tons)
QAC	750.2	76.5
QSC	753.1	76.8
QAF	954.0	97.3
QSF	968.6	98.8

Table 6.4 Ranked geometries with quadrilateral sections from heaviest to lightest structure.

	Force of Gravity (kN)	Weight (tons)
TAC	812.0	82.8
TSC	831.4	84.8
TAF	1025.4	104.6
TSF	1069.9	109.1

Table 6.5 Ranked geometries with triangular sections from heaviest to lightest structure.

Examining the results of table 6.4 through 6.6 contributes to the following observations summarized in figure 6.7.

- Scenario QAC generates the lightest structures with 76.5 tons in weight, closely followed by the geometry of scenario QSC with a 76.8 tons in weight.
- For symmetric or asymmetric sections, both cantilevering and fixed width-deck, the quadrilateral scenario is consistently lighter than its triangular equivalent. This means that the quadrilateral scenario is able to verify the design constraint more efficiently than the equivalent triangular section (in material use).

$$W_{QAC} < W_{TAC}; W_{QSC} < W_{TSC}; W_{QAF} < W_{TAF}; W_{QSF} < W_{TSF};$$

- For both triangular and quadrilateral sections, the cantilevering geometries (QAC and QSC for triangular sections, TAC and TSC for quadrilateral sections) are lighter than the geometries with the fixed width-deck of 2.8m (QAF and QSF for triangular sections, TAF and TSF for quadrilateral sections).

$$W_{QAC} < W_{QAF}; W_{QSC} < W_{QSF}; W_{TAC} < W_{TAF}; W_{TSC} < W_{TSF};$$

- For both triangular and quadrilateral sections, the asymmetric geometries (QAC and QAF for triangular sections, TAC and TAF for quadrilateral sections) are always lighter than its corresponding symmetric geometries (QSC and QSF for triangular sections, TSC and TSF for quadrilateral sections).

$$W_{QAC} < W_{QSC}; W_{QAF} < W_{QSF}; W_{TAC} < W_{TSC}; W_{TAF} < W_{TSF};$$

iii. Discussion

The eight generated geometries are part of efforts of formal exploration at the preliminary stage of the design. These scenarios combine different cross-sections (quadrilateral or triangular), symmetry or asymmetry of the cross-sections, symmetry or asymmetry of the span, and finally cantilevering decks above the generated section or fixed-width decks. Looking at minimal resource use, scenarios QAC and QSC become most efficient. However, these designs are 0.7 lighter than the heaviest solution (design QSF). Stated differently, the relative difference between the lightest and the heaviest designs is of only 35%. This 35% improvement can become significant because of the expensive nature of the chosen material. In appendix L4, the material costs of each geometry are estimated based only on the carbon-fiber use(reinforcement). This comparison reveals the significant impact of a 35% of material saving between the lightest and heaviest geometry of the eight scenarios. Such costs will only increase when labor, manufacturing, transportation, and assembly costs are considered. As such, these structures designed with carbon-fiber are not cost-competitive yet [94], [95]. Cost-effective production methods and form-resistant structures are some methods that render the material more efficient and competitive when compared to the traditional counterparts.

As discussed, the weights of these structure and their corresponding costs are not enough to comprehensively decide on the most efficient or integrated design. There are two sides to compare. First, the weight of FRP must be compared to the steel counterpart in order to understand the complete picture. Second, the benefits of lightness and material efficiency of such solutions can be counterweighed by the manufacturing constraints of free-form design in FRP.

iv. Comparison with steel

In order to compare FRP to steel, the same scenarios are run again in the optimization framework, this time using steel S355. The choice to run the optimization again in steel is considered more appropriate than to compare the FRP geometries to the geometry of Ney & Partners, generated within a different framework (different optimization, more load-cases, etc.). The proposed framework in FRP can be easily simplified to become a form-finding tool in steel. Without material parameters (laminated layups), the optimization framework for steel form-finding becomes a single-step optimization. The optimization framework for steel form-finding is run for the eight scenarios with the same parameters and their corresponding boundaries. The obtained weights of the steel geometries are shown in figure 6.8. FRP geometries present a weight reduction between 72% and 78% when compared to the corresponding

steel structure; the average weight decrease is of 74%. Although generated within a different framework, the steel structure designed by Ney & Partners presents a weight in the same order of amplitude of the steel geometries generated with this tool. This significant decrease in weight between steel and FRP is thus noteworthy when discussing energy and costs savings. However, it is worth highlighting that the weight savings of the FRP structures might be reduced due to the significant amount of connections required. 2.3

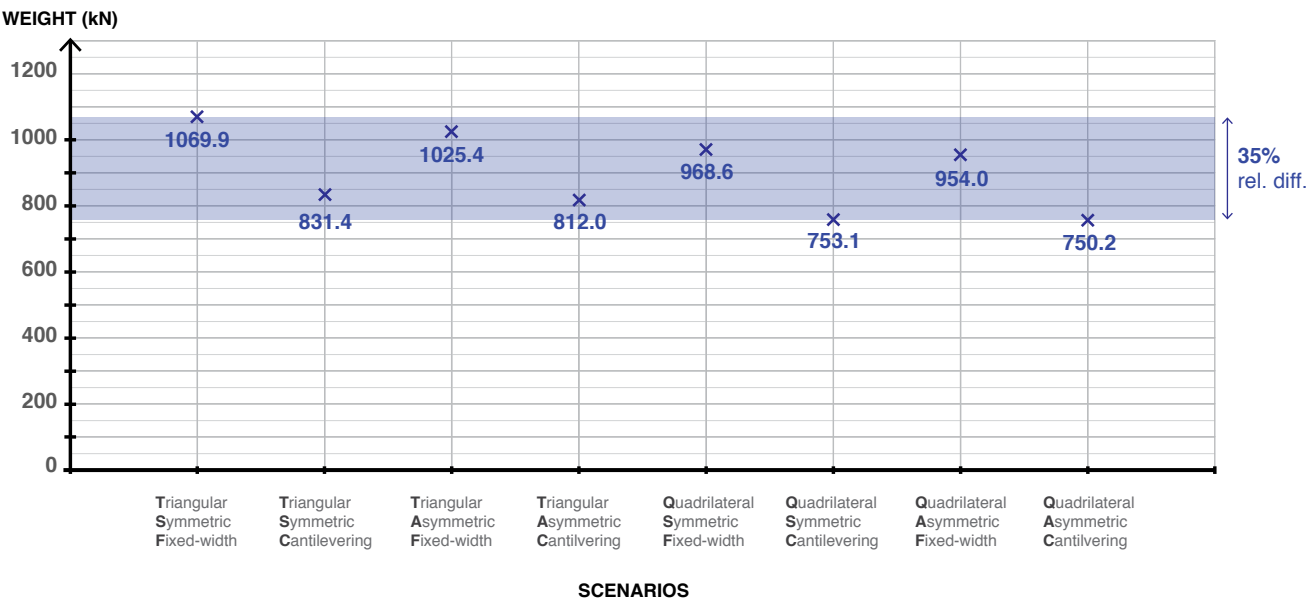


Figure 6.7 Graph of the weights of the generated geometries in FRP.

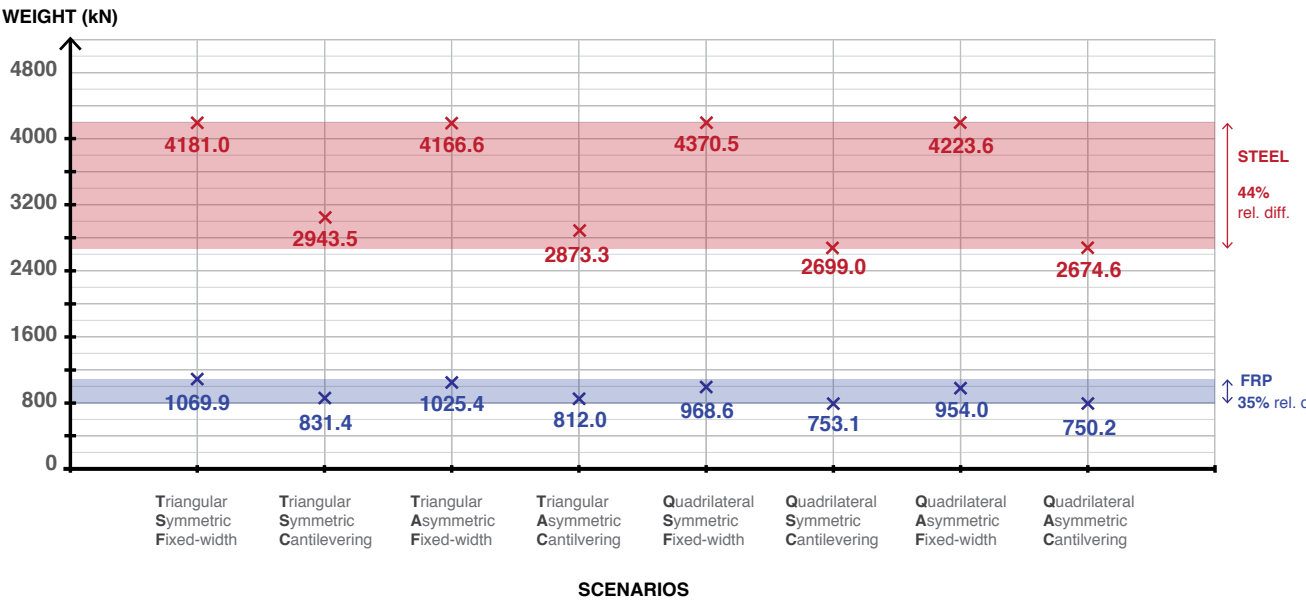


Figure 6.8 Graph comparing the weights of the steel structures to the weights of the FRP structures.

2.3 Production Efficiency

i. Construction

In order to assess the production efficiency of the generated geometries, a construction proposal for building a structure like the Wilhelminaberg Viewpoint in FRP must be addressed. This depends on many factors such as transportation, site accessibility, budget constraints, etc. The following section constitutes thus only one construction proposal. Different construction proposal can be inferred depending on the different set of factors.

As discussed in the first chapter of the literature review, vacuum infusion will be used for the production of the generated geometries because of the free-form design. Because of the land-locked nature of the site in Landgraaf, the structure can either be transported by air (helicopter) or land (vehicle). The maximum weight one helicopter can transport is around 20 tons [96]. With the weight of the eight generated geometries significantly higher than 20 tons, it is clear that this structure cannot be manufactured and transported to site in one piece by helicopter, as the Pont y Draig Bridge in the UK or the Pontresina bridge in Switzerland. Dividing the structure in five sub-spans as implemented for this case-study in chapter 5 (section 3.6.i) does not render each sub-span transportable by helicopter either. Table 6.6 shows the weight of each of the sub-spans shown in figure 6.9. In every generated geometry, at least two sub-spans exhibit weights higher than 20 tons.

As such, the structure must be transported by land. As discussed in chapter 1 (section 3), acceptable dimensions for vehicle transportation are equal to a width of 3.0m, a height of 4.0, and a length of 22.0m; the maximum mass is of 50 tons. Exceeding those dimensions is not impossible. However, it requires additional attentions such as permits. In contrast, exceeding the weight conditions is more critical as it can cause damage to roads. A Grasshopper 3D code is developed to fit each sub-span in a box with minimal dimensions. Table 6.7 described the dimensions of these boxes fitting each sub-span. The dimensions of the generated boxes slightly exceed, in some instances, the acceptable dimensions of vehicle transportation in the Netherlands. However, none of the sub-spans' weights exceed the maximum weight, the more critical criterion. The transportation by vehicle is thus not impossible but requires additional attention. There are means to render this transportation even more efficient; one example is to locate the manufacturing warehouse close to the construction site.

Considering the scale and dimensions of the generated geometry, the closed-sections cannot be manufactured in a singular piece. Rather, each sub-span of the generated geometries is built from FRP curved walls that exhibit shell-like behavior, an essential characteristic for the generated geometries to exhibit their intended optimal behavior. To manufacture these curved walls efficiently, lessons can be learned from the boat production process. The connections of the FRP walls of each sub-span is of paramount importance to ensure they act as one closed section. Furthermore, special attention should be brought to the connection between each of the five sub-spans to ensure they are acting as one singular structure. A temporary structure must be built in order to place and connect the sub-spans on site. With the construction logic explained, next section introduces two units to measure the production efficiency of the generated geometries

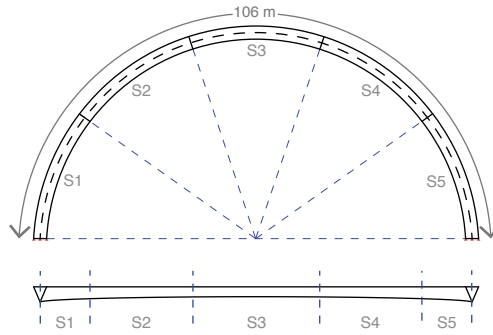


Figure 6.9 Division of the generated geometries in 5 sub-spans.

	TSF	TSC	TAF	TAC	QSF	QSC	QAF	QAC
S1 (ton)	26.8	24.9	23.3	21.7	22.6	20.5	19.9	20.8
S2 (ton)	19.3	13.2	18.8	12.8	18.3	12.9	18.0	13.5
S3 (ton)	17.0	8.7	17.6	10.1	17.0	9.9	17.8	10.4
S4 (ton)	19.3	13.2	19.5	14.2	18.3	12.9	19.2	12.5
S5 (ton)	26.8	24.9	25.4	24.1	22.6	20.5	22.4	19.5
Total (ton)	109.1	84.8	104.6	82.8	98.8	76.8	97.3	76.5

Table 6.6 Weight of each sub-span of the generated geometries.

		TSF	TSC	TAF	TAC	QSF	QSC	QAF	QAC
S1	h (m)	4.2	3.7	3.3	3.2	2.9	3.3	2.6	2.9
	w (m)	4.2	4.5	4.2	4.0	4.2	3.4	4.2	3.8
	d (m)	20.7	20.3	20.7	20.3	20.7	20.3	20.7	20.2
S2	h (m)	2.5	2.4	2.0	2.3	2.0	2.1	2.0	2.4
	w (m)	4.3	3.2	4.3	2.8	4.3	2.8	4.3	2.6
	d (m)	20.7	20.4	20.7	20.3	20.7	20.3	20.7	20.2
S3	h (m)	1.1	1.1	1.4	1.3	1.4	1.4	1.8	1.6
	w (m)	4.3	2.6	4.3	2.6	4.3	2.5	4.3	2.5
	d (m)	20.7	20.4	20.9	20.3	20.7	20.3	20.7	20.2
S4	h (m)	2.2	2.4	2.3	2.4	2.0	2.1	2.4	2.2
	w (m)	4.3	3.2	4.3	3.3	4.2	2.8	4.3	2.5
	d (m)	20.7	20.4	20.7	20.3	20.7	20.3	20.7	20.2
S5	h (m)	4.2	4.1	3.7	4.1	2.9	3.3	3.2	2.8
	w (m)	4.3	4.5	4.3	4.1	4.2	3.4	4.2	3.5
	d (m)	20.7	20.4	20.7	20.3	20.7	20.3	20.7	20.3

Table 6.7 Dimension of the smallest box fitting each sub-span of the generated geometries.

ii. Production efficiency

Unlike computational and material efficiency that can be easily quantified, production efficiency is more challenging to estimate. As such, production efficiency is defined as the limitation of waste of energy in the manufacturing of a design. In this framework, production efficiency is defined in terms of (1) opportunities for repetitions in the manufacturing process (molding/ formwork) as well as (2) the amount of connection between the different parts of the structure. More efficient productions will most likely contribute to sustainability as well as costs reduction due to time and labor savings. A general ranking of production costs and for the generated solutions can thus be inferred from the ranking of production efficiency. However, the following section does not attempt at estimating the production costs as they depend on too many variables, unknown at the preliminary stage of a design. Estimating costs is thus certainly productive and useful; however, it falls beyond the scope of this research.

iii. Manufacturing

As discussed, the closed-section of each sub-span is built-up from curved FRP walls presenting shell-like behavior. According to each scenario, different levels of efficiency can be achieved in the production process. More efficient structure will present more opportunities for repetitions in the manufacturing process. With the current landscape of FRP production, an estimate of the number of molding required for each scenario is made. Figures 6.10 and 6.11 show the opportunities for repetition in each scenario for both the triangular and quadrilateral geometries, thus increasing manufacturing efficiency. The following observations are made:

- The triangular cross-section geometry requires three FRP walls to make a closed triangular section. With five sub-spans, the total number of FRP walls for the entire generated geometry is 15. Similarly, quadrilateral cross-section geometries will require 20 FRP walls to build-up the entire generated geometry. As such, triangular sections require significant less energy in production as the total number of FRP walls to be produced is less than the number of FRP walls required for the quadrilateral sections.
- Among the symmetric and asymmetric geometries, structures with the uniform width deck of 2.8m (TSF, TAF, QSF, QAF) allow for a higher level of repetition as the top wall of the cross-section, uniform across the structure of the deck. In contrast, geometries with the cantilevering deck (TSC, TAC, QSC, QAC) offer limited opportunities for repetition in the production of the top wall of the cross section
- Geometries with symmetry (TSF, TSC, QSF, QSC) across their span and their sections offer opportunities for repeated formwork in their mold. Their production can be considered more efficient. It allows at least to utilize the formwork defining the curvature of the FRP walls. In contrast, Geometries without any symmetry (TAF, TAC, QAF, QAC) across their span and their section offer limited opportunities for repetition in their production.

SCENARIO	top piece 	side piece 1 	side piece 2 	total number of molds
Triangular Symmetric Fixed-width deck	 1 mold	 3 molds	 3 molds	7 molds
Triangular Symmetric Cantilevering deck	 3 molds	 3 molds	 3 molds	9 molds
Triangular Asymmetric Fixed-width deck	 1 mold	 5 molds	 5 molds	11 molds
Triangular Asymmetric Cantilevering deck	 5 molds	 5 molds	 5 molds	15 molds

Figure 6.10 Number of molding/framework required for the production of the triangular geometries.

For each scenario, a different color indicates a singular mold.

SCENARIO	top piece 	side piece 1 	side piece 2 	bottom piece 	total number of molds
Quadrilateral Symmetric Fixed-width deck	 1 mold	 3 molds	 3 molds	 3 molds	10 molds
Quadrilateral Symmetric Cantilevering deck	 3 molds	 3 molds	 3 molds	 3 molds	12 molds
Quadrilateral Asymmetric Fixed-width deck	 1 mold	 5 molds	 5 molds	 5 molds	16 molds
Quadrilateral Asymmetric Cantilevering deck	 5 molds	 5 molds	 5 molds	 5 molds	20 molds

Figure 6.11 Number of molding/framework required for the production of the quadrilateral geometries.

For each scenario, a different color indicates a singular mold.

The summary of the assumption and the estimates of number of molding for each scenario can be summarized in table 6.8. In contrast with the “.” that refers to a neutral situation, the “+” sign refers to an advantageous situation with opportunities for repletion and efficient production.

	Triangular vs. Quadrilateral Section	Symmetry vs. Asymmetry	Fixed-Width Deck vs. Cantilevering Deck	Production
TSF	+	+	+	+++
TSC	+	+	.	++
TAF	+	.	+	++
TAC	+	.	.	+
QSF	.	+	+	++
QSC	.	+	.	+
QAF	.	.	+	+
QAC

Table 6.8 Opportunities for efficient production according to the different design categories.

iv. Connections

As discussed earlier, the structure will be made of 5 sub-spans; each sub-span is built-up from curved FRP walls. There are then two types of connections important for the generated structures, shown in figure 6.12. First, it is of paramount importance to correctly connect the FRP walls of each sub-span to ensure they act as a single closed-section (figure 6.12, left). Second, special attention must be brought to connecting the five sub-spans to ensure they act as one single structure (figure 6.12, right).

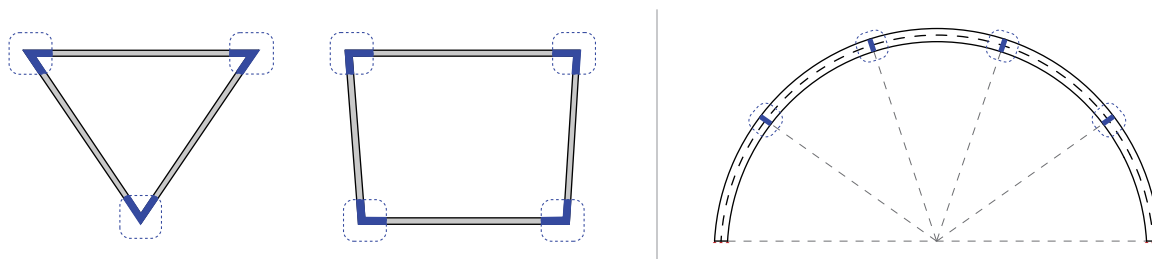
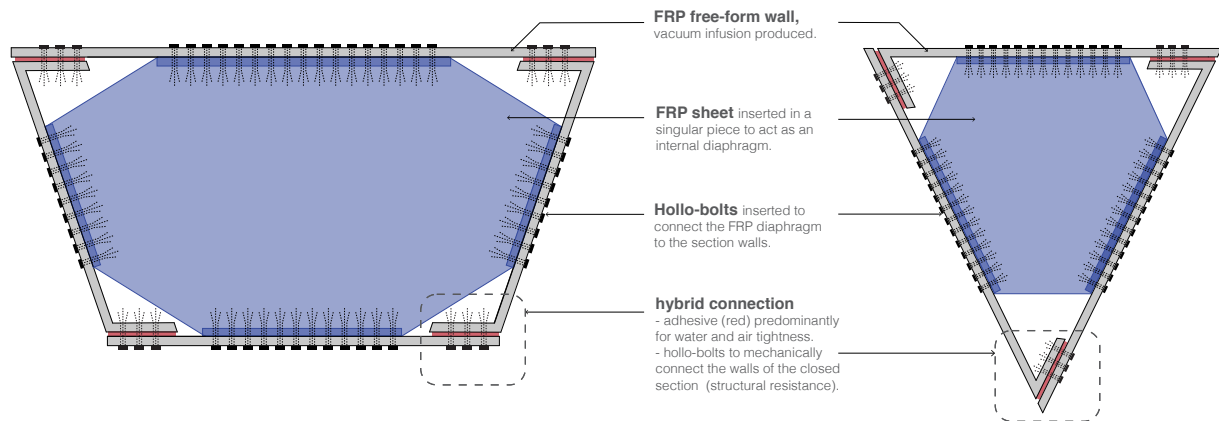


Figure 6.12 Two types of connections important for the suggested design. **(left)** Connection between the walls of the closed section. **(right)** Connection between the sub-spans of the structure.

Estimating the amount of energy for each requires detailing of each connection. The proposed preliminary details are hybrid connections, mixing both adhesive and mechanical joints.

1. The connection between the walls of a cross-section (connection type A) can be made off-site in a controlled environment. The sub-span is then transported to site as discussed in section 3.1. As shown in figure 6.13, the connection of the FRP walls of the section exhibit a hybrid connection. The adhesive contributes to the structural stiffness of the cross-section but its main function is to ensure water and air tightness of the cross-sections. Hollow bolts allow to mechanically connect the cross-section at their corner. Furthermore, to ensure the walls of the cross-section form a closed section, diaphragm FRP walls are added to the design. These diaphragm walls will contribute in additional weight; they are placed in a singular piece and repeated every x distance. They are mechanically connected using holo-bolts [97].

2. The connection between the sub-spans (connection type B) requires intricate detailing. As shown in figure 6.14, the two sub-spans are interlocked: this allows to connect the sub-spans at the corners. FRP connecting plates are introduced to connect the two walls of the sections. They are mechanically connected to the structure.



SYSTEM 1

hybrid connections are used to connect the walls of the section at the corners, using adhesive for water and air tightness and hollo-bolts for ease of assembly.

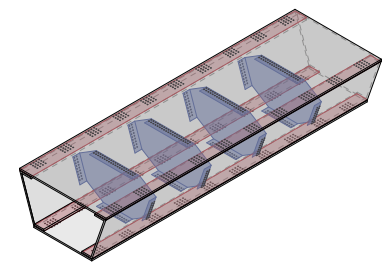
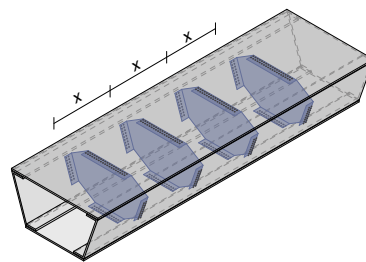
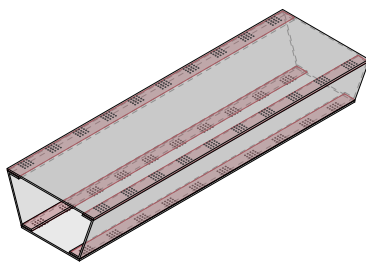
SYSTEM 2

an FRP wall is inserted every x distance to enforce the four walls of the cross-sections are acting as one closed section. The inserted FRP walls act as internal diaphragms.

COMBINED SYSTEM

provides a manufacturable solution to produce the generated geometries, ensuring that the walls act as a single closed section.

TSF, TSC, TAF, TAC



QSF, QSC, QAF, QAC

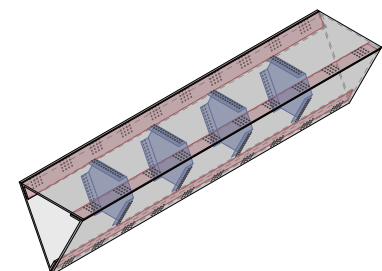
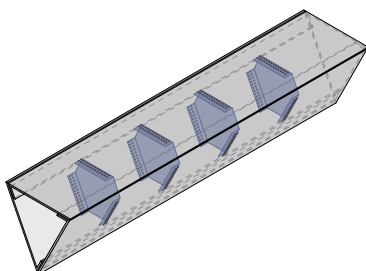
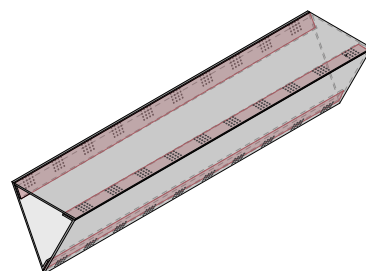
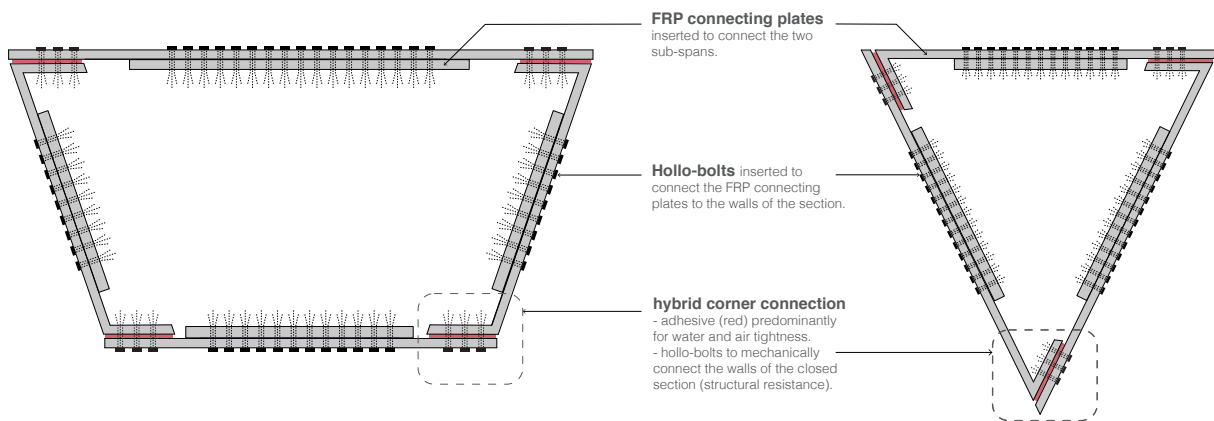
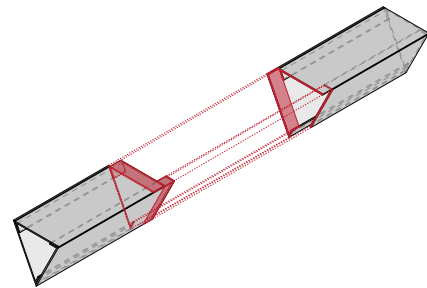
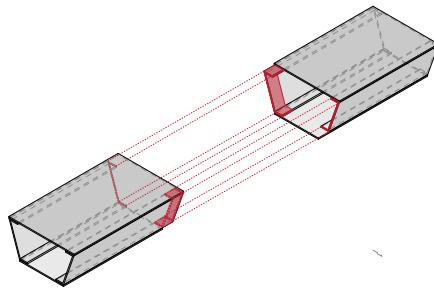


Figure 6.13 Schematic drawing of the connection type A, between the walls of the closed section. This highlights the systems of the connection and not the sequence of assembly.



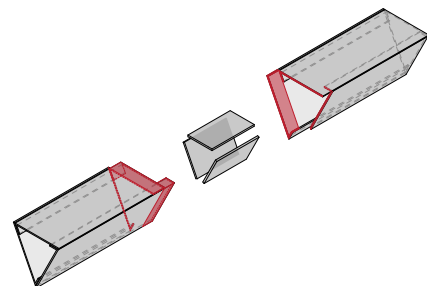
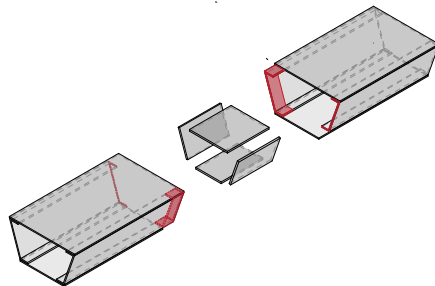
SYSTEM 1

The edges of the two sub-spans are designed to overlap at the corners when they are connected. The overlapping surfaces at the corners are indicated in red; they exhibit the same hybrid connection (adhesive for water/air-tightness and hollo-bolts for ease of accessibility).



SYSTEM 2

FRP connecting plates are introduced in order to connect the two sub-spans over the entirety of the cross section and not just the corners. They will be mechanically connected to the structure. Special attention should be brought to the number bolts and bolt-holes used in these connections.



SEQUENCE

- FRP connecting plates are first connected to one sub-span using hollo-bolts. This can be done in a controlled setting, allowing bolt-holes to be determined in advance.
- The FRP connecting plate will then project outside the span and can then be connected to the second sub-span.
- Special attention should be brought to connecting the second sub-span: this will be done on site and will require the bolt-holes to include placement tolerance.

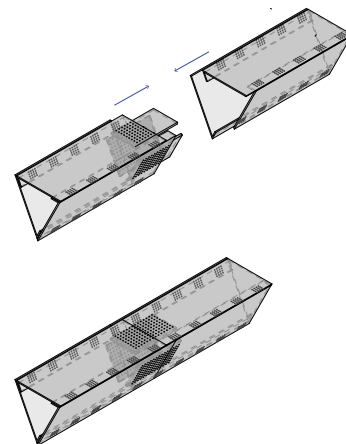
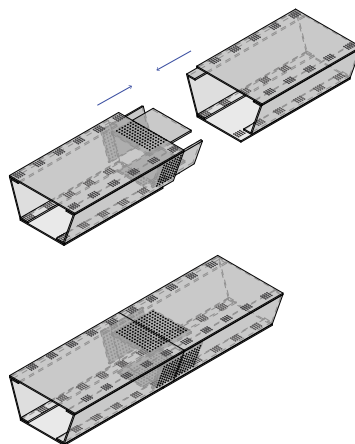


Figure 6.14 Schematic drawing of the connection type B, between the sub-spans of the generated geometries.

Correctly detailing the connections of these geometries will require significant research as well as collaboration with contractors. One way to estimate the amount of work required for such details is to measure the length of the corresponding connections. A preliminary estimate of the length of each connection allows to compare which designs will require more detailing. The corresponding lengths of the connections between the walls of a section (connection type A) and the length of the connection between the sub-span (connection type B) are shown in table 6.9. They take in consideration knowledge shown in appendix L6.

	Length for the connection A between the walls of a section (m)	Length for the connection B between the sub-spans (m)	Total (m)
TSF	302	29	331
TSC	302	21	323
TAF	302	29	331
TAC	302	21	323
QSF	403	29	432
QSC	403	22	425
QAF	402	31	433
QAC	403	22	424

Table 6.9 Length estimates of the different connection types for the different generated designs.

The following observations can be made:

- Triangular sections are more efficient than quadrilateral sections (connection type A). This is inherent to the nature of the section: the quadrilateral closed sections are built-up of four FRP walls instead of three walls to build up the triangular section.
- For both triangular and quadrilateral sections, geometries with a cantilevering deck (TSC, TAC, QSC, QAC) are more efficient than the geometries with fixed-width deck of 2.8m (TSF, TAF, QSF, QAF) for connection type B.
- Combining the estimates of detailing for both connections (A&B), the ranking of efficiency in production is visualized in table 6.10. The biggest distinction is between triangular and quadrilateral cross-section, the improved performance of cantilevering deck when compared to fixed-width deck is only marginal.

	Combined length of connections (m)
TSC	323
TAC	323
TSF	331
TAF	331
QAC	424
QSC	425
QSF	432
QAF	433

Table 6.10 Total lengths of connections for the different generated designs.

3. Integrated design

3.1 Towards an Integrated Design

Integration of different facets of a design is a central discussion in the construction industry. Today, new computational tools such as BIM (Building Information Modeling) among many have streamlined the generation, construction, and management aspect of new structures in an effort to create comprehensive and integrated designs. With the concept of integration becoming mainstream in the building field, definitions of the term have multiplied. In his essay “Structural Honesty”, Arup interprets the notion of structural integration and defines it on two separate levels:

- “-The integration of the architectural and structural idea, achieved by intimate collaboration between architect and engineer.
- The integration of the structural idea and the method of construction, achieved by pooling the knowledge of the economics of contracting and manufacturing processes. This can best be achieved by an early collaboration in the design stage with a nominated contractor. [98]”

Arup’s notion of structural integration borrows from his original notion of “total architecture” [98], a philosophical set of principles for engineers and architects as well as all involved parties in a construction project [99]. Seeking “artistic wholeness or excellence,” integrated design is a northern star that “can never – or only very rarely- be fully realized in practice” [98]. This discussion of integration preoccupied Arup over his long career. Arup made sure not to oversimplify the industry landscape; he is aware of the increasing complexities and multiplication of inputs in a design process. In another lecture, Arup acknowledges the manifest schism between design and construction, one that plagues the construction industry “unparalleled [to] any other industry.” He refers even to the building industry as “a battleground for sectional interests than a meeting place for a combined effort to find the best solution” [98]. In the framework of structural integration, any design decision calls for the different facets of a design to be evaluated and weighted against each other. The following section applies the context of integrated design to the Wilhelminaberg Viewpoint. The efficiency criteria evaluated in the previous section are weighed against each other. This will motivate the decision behind a singular optimal design.

In the previous section, in an attempt to evaluate the generated structures, three main criteria of efficiencies are identified to evaluate the design’s sustainability: (1) computational efficiency, (2) structural or material efficiency, and (3) production efficiency. These three criteria are defined in relation to the phases of a construction, from conception through production. Each criteria reveals a specific ranking. However, the difference in the geometries’ performances is lost. Comparing the overall performances of the eight structures thus requires to weight the influence of each criteria and sub-criteria [100] and make a value judgment motivated by the project’s ambitions and vision.

Indeed, the results of the three criteria are summarized in figure 6.15. Appendix M1 presents the same graph separately for each scenario. However, figure 6.15 does not allow to understand the level of improvement within each criteria. An improvement factor f is calculated again for each criterion to understand how the eight geometries compare to the worst performing one in each specific criterion. Figure 6.16 visualizes the improvements of a certain geometry when compared to the worst performing structure in the considered criteria. A more efficient structure translates in closer factors f to zero. Appendix M2 presents the same graph separately for each design.

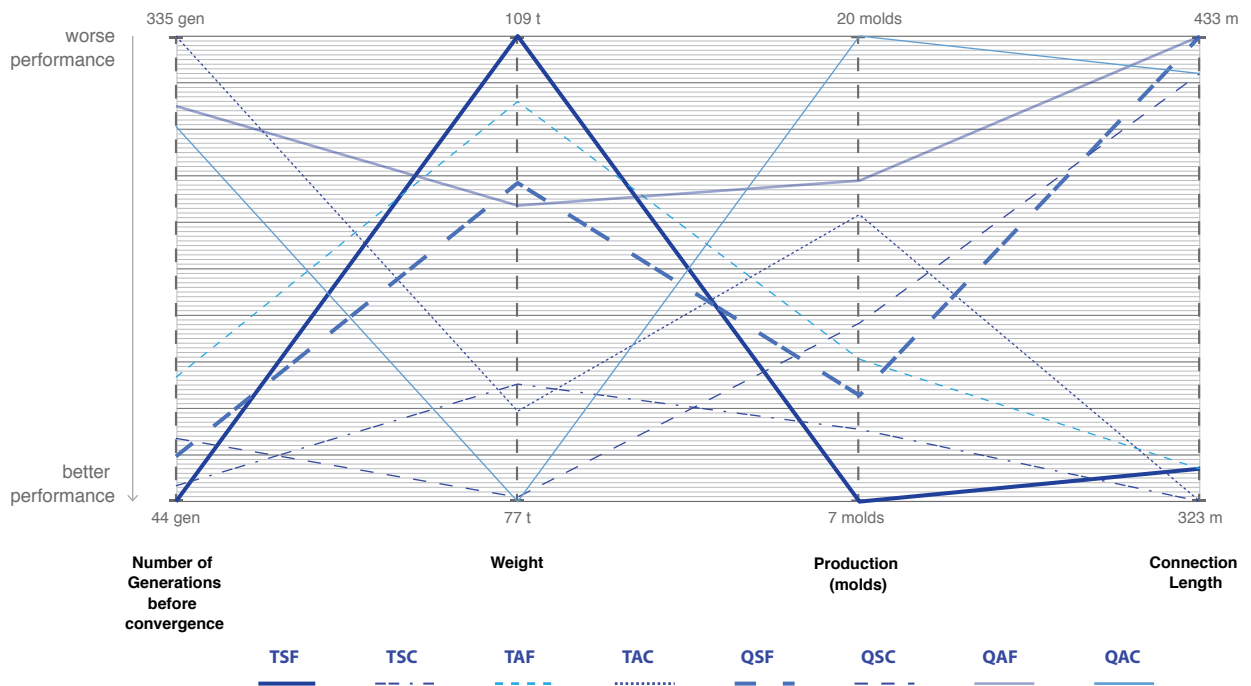


Figure 6.15 Graph summarizing the performance of the eight generated geometries for the 3 criteria.

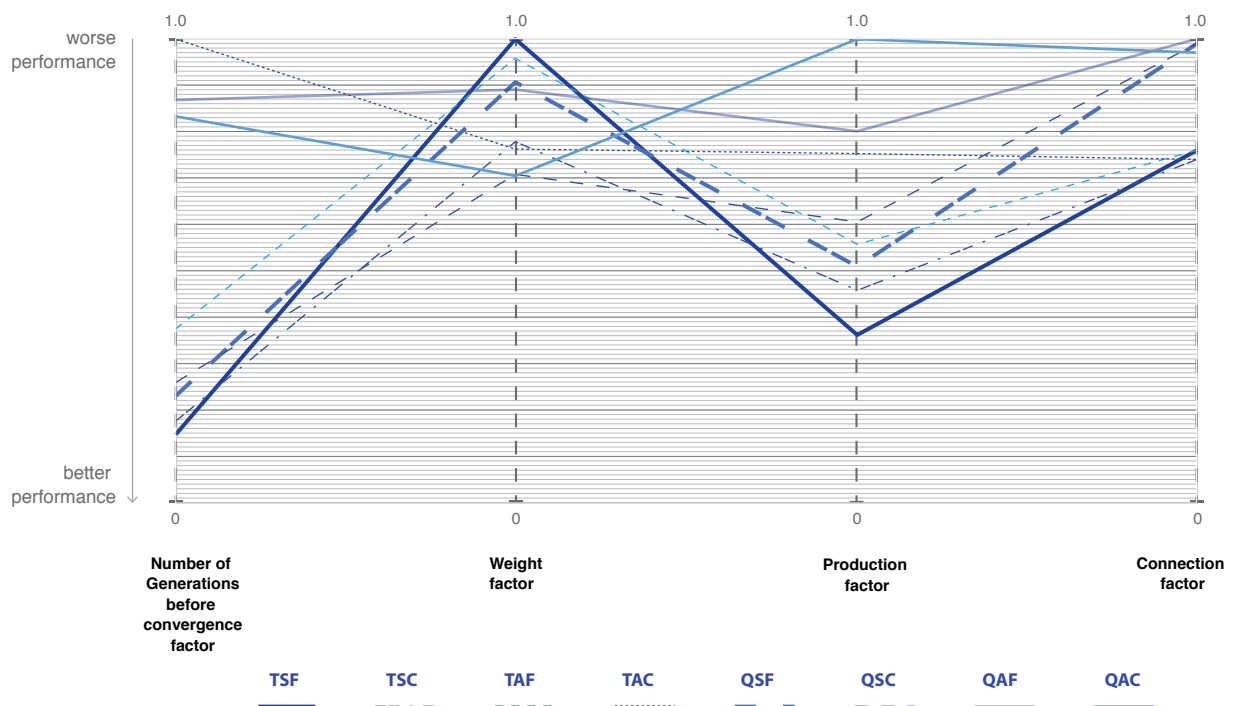


Figure 6.16 Graph summarizing the performance of the eight generated geometries for the 3 criteria, using the improvement factor f .

3.2 Post-Optimality Assessment

Depending on the weight given to each criteria, a different ranking of the structures can be achieved. A structure can then be chosen as most integrated design. Numerous cases can be considered to reflect different priorities for the involved parties (architect, engineer, or contractor). Experimenting with the criteria and their corresponding weights is thus an interesting approach to illustrate the many factors influencing the design and construction of a structure. However, no framework can reflect all the forces at play. The full picture is constantly evolving and changing. Any chosen framework and the resulting structure reflects a compromise of certain driving forces, reconciling the objectives of the parties involved. In collaboration with the architect or contractor, the designer must assess what are the important factors and decide on the best method to estimate or quantify such a performance.

Defining those cases and the corresponding weights is arguably hard to complete at such an early stage of the design. However, doing so will provide insight into the factors influencing the performance of a design and how to achieve integration. In light of the three types of efficiencies, figure 6.17 considers three distinct cases

- **Case 1:** all criteria are given the same weight of importance.
- **Case2:** material efficiency is more important than the other two criteria, reflecting the high price of carbon-fiber.
- **Case 3:** production efficiencies are more paramount than the other two criteria, reflecting the high price of producing such a structure.

Across the three defined cases shown in figure 6.17, the most integrated designs are TSF (Triangular Symmetric Fixed-width deck) and TSC (Triangular Symmetric Cantilevering deck). The best performing structures are visualized in figure 6.18.

- TSF (Triangular Symmetric Fixed-width deck) is most computationally efficient. With the smallest number of parameters and the smallest corresponding search space, geometry TSF was fastest to converge. This property of computational efficiency is particularly important for further exploration in the steps past the preliminary stage. This includes geometry exploration for different aesthetics or incorporating different structural concerns such as additional load-cases and design constraints. TSF is also most efficient in production (manufacturing and connections) because of its fixed-width deck as well as its symmetry of its section and span. Production efficiency could translate in significant energy savings.
- TSC is second best performing geometry in both computational and production efficiency. Furthermore, it presents significant savings in weight: 25% weight savings when compared to TSF. This can translate in significant material costs savings. However, the cantilevering aspect of the design introduces additional production issues that will require significant attention in detailing the deck attached to the FRP.

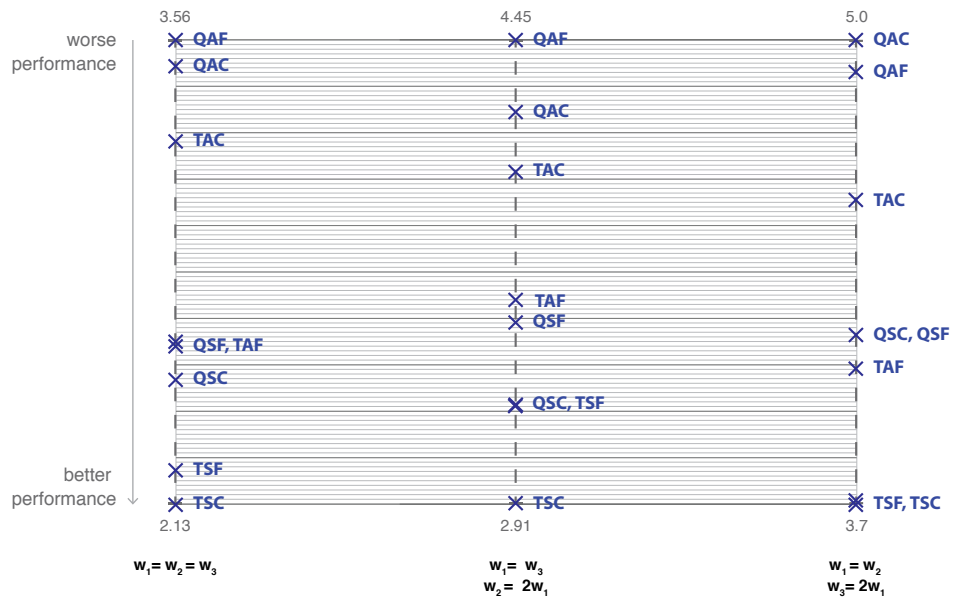


Figure 6.17 Multiple cases generated with different weights to assess the overall efficiency of the geometries.
 w_1, w_2, w_3 are the weights for computational, material, and production efficiency respectively.

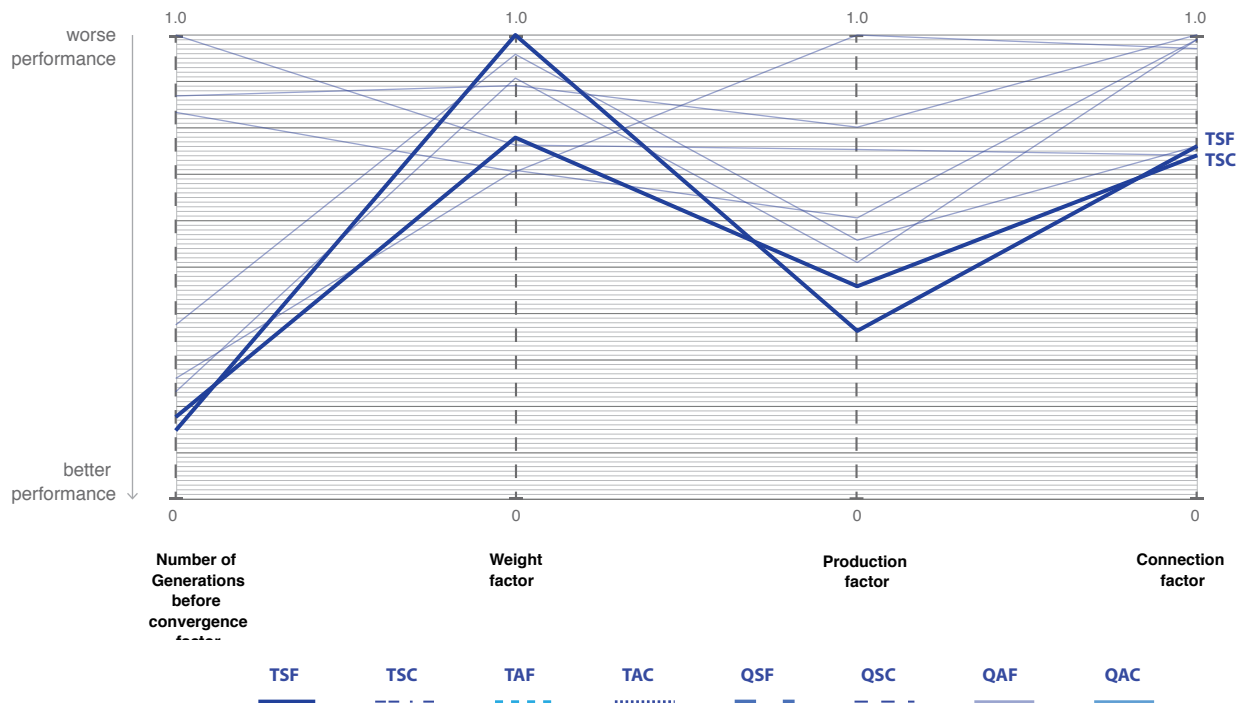


Figure 6.18 Graph highlighting the top performing structure among the eight generated geometries.

4. Conclusion

This chapter implements the proposed optimization framework in chapter 5 with the Wilhelminaberg Viewpoint case-study. The framework is run for eight different scenarios, generating eight different geometries.

The first-level of the optimization finds the optimal laminate layup combination over the 5 sub-spans of the structure. When compare to the least stiff design, the stiffest combination reduces the strain energy by a factor of 1.2 or a relative decrease of 23% and the deflection by a factor of 2.2 or a relative decrease of 69%. Laminate layup combinations with high percentages of 0° laminates are located in sub-spans where bending stiffness is required. Similarly, laminate layup combinations with a high percentage of $\pm 45^\circ$ are located in sub-spans where torsional stiffness is required.

The laminate layup combination generating the stiffest structure is chosen and the second-level optimization is run for the eight scenarios. In post-optimality, the eight generated geometries are analyzed in terms of their computational efficiency, material efficiency, and their production efficiency. A framework to assess each of these criteria is developed in this chapter highlighting a few of the factors at play in evaluating a structure.

- **Computational efficiency** is evaluated in the convergence rate of the genetic algorithm. Scenarios with the least number of parameters and smallest search spaces converge the quickest.
- **Material efficiency** is evaluated by the lightness of the generated geometry. In fact, in the Wilhelminaberg Viewpoint, the relative decrease between the lightest and the heaviest designs is of 35%. However, when compared to the same designs run in steel, the weight reduction increases to 74% in weight reduction.
- **Production efficiency** is evaluated in terms of manufacturing and connection efficiency. Assessing the production efficiency requires determining the construction logic of the considered structure. In the Wilhelminaberg Viewpoint case-study, the manufacturing of the cross-section is assessed in terms of the number of molding required to producing the structure. Similarly, details of the connections are suggested for connecting the walls of a closed-section as well as the 5 sub-spans; they are quantified in terms of the respective lengths.

The chapter concludes with a framework to evaluate the integration aspect of the generated geometries. The integration of the design is assessed with weights given to each criterion. While any framework will fail to reflect all the forces at play with weights, experimenting with the criteria and their corresponding weights provides insight into the factors assessing the performance of a design.

The next and final chapter of the thesis starts with answering the research question. Then, discussions and reflections relating to the research's main topics are elaborated. The final chapter concludes with recommendations and potential future research directions.

1. Answer to the research question

Numerous challenges face the construction industry today. However, the environmental challenge is undoubtedly a priority for the profession. Efforts to address the environmental impact of the construction industry will require a wide-scope re-evaluation of the principles and practices of the profession. This research situates itself as part of the broad efforts interrogating the industry's limits. In particular, the research examines the untapped potential of FRP, an alternative material that has permeated the construction field in recent decade because of its advantageous in-service properties (durability and sustainability). This thesis intended to answer the following research question:

What strategies capitalize on FRP's favorable mechanical properties in order to promote formal exploration with the material in the preliminary phase of a design considering its durable and sustainable potential?

The previous chapters of the thesis elaborated a tool for structural form-finding in FRP. Organized in a multi-step optimization framework, the developed tool reflects the specificity of the material's behavior, primarily its orthotropic nature and alterable laminate layup. Furthermore, it capitalizes on the advantageous mechanical of FRP, such as its stiffness and lightness. The tool defines an optimization process for FRP allowing the designer to explore forms and geometries in FRP. The research then proposes a post-optimality framework to evaluate the efficiency and integration of their designs. Multiple criteria are defined to assess each geometry: computational efficiency, material efficiency, and production efficiency. This provides designers and engineers insight on the factors affecting the overall performance of a structure. It also allows them to gage the feasibility of their structures in the preliminary stages of the design process.

The optimization framework and post-optimality assessment are implemented with a case-study: the Wilhelminaberg Viewpoint, a structure designed by Ney & Partners. General lessons about efficient structural forms in FRP, conclusions on the landscape of construction in FRP, and reflections on parametric design and modern form-finding are drawn from the case-study. These topics are discussed in the next section.

2. Critical Reflections

Following the literature review, this research establishes the framework for the geometric optimization. Chapter 5 elaborates the steps involved in the development of the structure: it defines the parameters, scenarios, design constraints, and objective function of the optimization as well as tracing the steps of the framework's development. Chapter 6 first presents the results of the framework implemented with the adopted case-study, the Wilhelminaberg Viewpoint case-study; before it expands a post-optimality framework to compare the performance of the different generated geometries.

This research allows the pursuit of additional avenues of questioning. Primarily, the thesis allows to reflect on seeking integration in construction, the computational tools that have become prevalent in modern-day structural design, and the feasibility of "free-form" design in FRP in particular. The next section expands on relevant discussions relating to the developed tool, the case-study, as well as larger themes that are adjacent to the research.

2.1 On the developed Framework and its Limitations

This research traces back the development and rise of FRP as an alternative material in infrastructure applications, in general, and rehabilitating existing structures in particular. With the challenge of climate change weighing on engineers, this alternative material has gained further momentum for its sustainable and durable properties. Despite this interest, there remains a split between the material's studied behavior in the laboratory and its use in the construction industry. As such, this research was motivated by the aspiration to encourage exploration in FRP and better understand the material's limitation.

The research is set to develop an optimization framework fit for structural designers. This framework allows to utilize FRP's mechanical properties at both, the mesoscale and macroscale. Devised as a multiple-step framework, the developed tool encourages formal exploration at the preliminary stage. Special structures in general and free-form structures exhibiting shell-like behavior in particular would benefit most from implementing the proposed framework. The framework is developed and tested around a specific case-study, but can be easily implemented to new projects. Adopters of the frame must thus first determine the general boundaries of a design (the overall shape) that exhibits shell-like behavior. Then, the parameters within that geometry must be determined. The design variables can be coordinates, key geometric points, width and height at critical sections, thickness, etc. For a specific project, it is worth defining multiple scenarios of different sets of parameters. This encourages formal exploration at the preliminary stage.

This thesis' proposed framework employs technical concepts and notions familiar to structural engineers. While this research motivates the decision behind the tool's development, possessing technical knowledge is important for running the optimization. Implementing the tool requires clearly defining the structural constraints, load cases, and support conditions before running the optimization. In processing the framework's results, the tool user must critically assess the structural performance of the generated geometries. The tool can also be used by architects working in close collaboration with structural designers: the technical aspects must be defined and verified by a structural engineer, then an architect with some structural skill can also use this tool.

The tool is defined in one interface Rhinoceros 3D alongside Grasshopper's parametric modeling. Multiple plug-ins are employed in Grasshopper 3D such as Karamba 3D, Galapagos, and GOAT. All the used programs and plug-ins are widely available on the market; however, structural engineers must be familiar with parametric modeling in order to implement this framework to new projects. Fundamentally, structural designers must be familiar with Rhinoceros and Grasshopper 3D. This is central to define the parametric geometry generating code (first and essential phase of the framework). It is advantageous if the structural designers are familiar with the various plug-ins used in this framework; it is not disqualifying if they are not. Coded within the Grasshopper 3D environment and using Grasshopper's language, these plug-ins are easy to learn and code with. Furthermore, the important settings of Karamba 3D, Colibri, Galapagos, Leafcutter, and GOAT are laid out in this research to provide guidance in implementing the framework, in addition to the existing manuals and tutorials.

The developed framework utilizes both brute force and genetic algorithm to generate optimal solutions. This renders the process quite time-consuming. This is certainly a limitation in the overall process; nonetheless, there are ways to avoid these shortcomings. Structural designers can utilize more powerful computers or even multiple computers to expedite the process. This might be costly in terms of required Rhinoceros, Grasshopper 3D, and Karamba 3D licenses. In testing the framework with the chosen case-study, eight scenarios were defined. Up to four scenarios were run at the same time. In a few days, eight optimal geometries were generated; more than 120,000 solutions are generated. The richness of solutions produced with this optimization is thus a double-edged sword. Favorably, the framework allows for significant exploration of the search space; Unfavorably, it requires significant running-time and post-processing of the collected data.

2.2 On Integration in Structural Design

Recounting Arup's essay "Structural Honesty", there are two types of integration: between structural engineer and architect, and between structural engineer and contractor [98]. The proposed tool is intended for preliminary design exploration, specifically with FRP. As such, the developed tool helps achieve Arup's first level of integration. The formal expression of the chosen project must extend the architectural vision. This can only result from a collaboration between engineer and architect in the preliminary stages of a design. In fact, special structures often display an intrinsically close relation between architecture and structure; the two becoming indistinguishable in works of "structural art" [93].

The proposed tool does not directly incorporate aspects relating to construction. The tool does not directly fulfill Arup's second type of integration. It is only in post-optimality analysis that the research addresses construction concerns. In post-optimality, efficiency criteria for evaluating the performance and buildability of the generated geometries are suggested. These criteria rely in part on the knowledge exposed in the literature review. Even though they expose the main concerns and possibilities of designing in FRP, these criteria are not all encompassing. As will be discussed in reflections on parametric modeling and free-form design, computational tools are very powerful but should only provide "a sense of structure. [98]" They can never reflect all the forces at play in a design. To best assess the buildability of a structure in FRP, further investigation might be necessary. A close collaboration with a specialized contractor from the early stages can prove to be beneficial: it allows to incorporate manufacturing constraints in the optimization process, rather than only in the post-optimality analysis. It will allow to increase the cost-efficiency and cost-competitiveness of the generated geometry. This will ultimately yield geometries that get closer to both ideals of structural integration.

2.3 On Parametric Modeling

The advent of the Information Age has fundamentally changed how architects and engineers approach the design and construction of the built environment. It has even led some theorists to proclaim a revolution, "the end of a cycle of around 5000 years of architecture, stretching from the age of the cavemen to the Postmodern" [101]. Revolution or not, today's architecture practices rely heavily on computational and digital methods throughout all phases of a design. This thesis is no exception. In fact, this research's ambitions are to encourage formal explorations with alternative materials such as FRP. The research highlights the potential of computational tools, in general, and digital form-finding, in particular, to exploit the advantageous and sustainable properties of alternative materials. However, to offer a nuanced and critical picture of these new tools available for designers, it is worth elaborating on their potential shortcomings.

Notably, the most important limitations of parametric modeling are designers relinquishing their decision making process in favor of a series of computerized procedures. A way to mitigate this potential shortcoming is for designers to critically question the results of computational methods. Rejecting the tyranny of the results, the designer can develop an intuition, "a sense of structure." Arup famously stated that engineering problems are "under-defined" with many possible solutions, both good and bad; arriving to a specific solution becomes a creative process that

involves “imagination, intuition, and deliberate choice” [98]. These statement remain true with the advent of new computational methods. The designer using such tools must not lose sight that they are the means to an end and not the end in itself.

2.4 On Free-Form Architecture in FRP

This research focuses on developing a tool of form-finding in FRP, in the aim to catalyze formal exploration with this alternative material. As discussed in reflections on integration, the proposed tool does not consider manufacturing constraints in its formulation; rather, such restrictions are included in the post-optimality analysis. In doing so, the research is able evaluate the divide that exists between the potential of FRP and its manufacturing limitations.

The tool allows to generate free-form structures that optimally utilize the material's property. Furthermore, minimizing the weight of the generated geometries translate in less energy consumed during production, transportation, and installation. At face value, the tool generates sustainable designs. However, the post-optimality analysis reveals a much more nuanced picture. Free-form architecture still has a ways to go to prove its sustainable ambitions. While the generated designs are light and stiff, their production presents many challenges that question its sustainability aspirations. As explained in chapter 6, quantifying manufacturing efficiency is challenging and estimating costs even more so. Assessing the sustainability performance of FRP, in design and production, becomes more complex. FRP is thus best suited for recurring free-form design, a design that includes repetitive geometries that can be constructed from the same mold.

Possible avenues to remedy this limitation of FRP include research in production methods for FRP. Such efforts are being undertaken in steel with 3D printing efforts and concrete with 3D printing efforts and flexible mold preparation. In FRP, these efforts can lean in two distinct directions. Already underway, the first class of efforts moves towards standardization and mass-customization of FRP panels. Such efforts freeze architectural imagination and move away from free-form structures: “The tailor-made job tends to be replaced by the ready-to-wear article” [98]. The second class of efforts develop more efficient production methods (i.e. flexible molds and 3D printing), allowing to efficiently build free-forms in FRP [102]. It will take a concerted effort on all fronts for FRP to become cost-competitive with traditional building materials and proliferate further in the construction industry.

2.5 On the Case-Study

As one of the projects of the first Dutch IBA iteration at Parkstad, - The Wilhelminaberg Viewpoint proves to be a very valuable case-study. Its complex geometry and overall vision makes it an ideal candidate to capitalize on the properties that make FRP a promising material: sustainable and durable properties, customizable free-form production, and tailorable mechanical properties. Through this case study, the research evaluates the landscape to conclude in what type of projects FRP is most cost-competitive with traditional material.

For this case-study, multiple scenarios are generated; each scenario yields advantages in certain fields and disadvantages in others. This is an important step to define in any case-study to explore the different formal opportunities. The eight generated geometries are then evaluated in post-optimality analysis according to different efficiency criteria. The post-optimality analysis allows to determine the most efficient and buildable structure as well as assess its construction feasibility. From the eight generated geometry, the symmetric triangular sections with the fixed-width deck (TSF) or cantilevering deck (TSC) are found to be the most integrated designs. While the TSF geometry is not the lightest of the eight geometries, it is most efficient in computational and production efficiency, rendering it more competitive than the other geometries. TSC exhibits significant weight reduction due to the cantilevering deck aspect of the design. The weight reduction in combination with the geometry's good performance in computational and production efficiency render TSC an integrated design.

Between ambition...

The Wilhelminaberg viewpoint is introduced in this research as a possible manifesto project for FRP. In concluding, the research verifies the promise of the material in terms of strength, stiffness, and weight reduction. The FRP designs are significantly lighter than their steel counterparts. This research was completed in light of the climate change challenge facing structural engineers today. In light of this imminent threat, it is important to investigate all avenues of action. With the material's potential for durability, sustainability, and lightness, building a structure of this scale in FRP will push the boundaries of the material, expanding the scope of what is feasible and possible to build in FRP. Furthermore, using FRP for this structure echoes the ambition of the wider IBA project that celebrates innovation and technology. Despite some of the issues still to be resolved, such a project can become the precursor and catalyzer for the much needed research in alternative materials. The amplitude of the challenge of climate change requires bold, large-scale, and ambitious projects.

... and limitations.

In order to provide a nuanced and comprehensive picture of the landscape, important limitations for an FRP design are discussed hereinafter. First, it is undeniable that FRP has never been used at this scale with such large cross-sections; Further research and investigations will be needed to realize such a structure, particularly for correctly connecting the walls of the section and the sub-spans. Additionally, carbon-fiber, an expensive material, is used to generate the geometries of this research. The cost of this project will also increase because of the required amount of mold preparation. Multiple strategies can be investigated to increase the cost-competitiveness of FRP structures. This research minimizes weight thus optimizing material costs. Additional steps include reducing the costs of labor associated with the production and assembly. As discussed in reflections on free-form design in FRP, it will take both intensive research and investment in the field to make FRP production methods more energy efficient whether through standardization, mass-customization, or development of flexible molds. In general, projects could benefit from increasing the repetition in the geometry; designing the entire Wilhelminaberg Viewpoint as two identical circles where the half-circle spans are repeated is a beneficial route to investigate.

3. Conclusions

3.1 On the Proposed Framework

Regarding the developed framework, the following general conclusions can be made:

- The developed tool is not restricted to a specific shape but can be applied to any structure with shell-like behavior. The boundaries of the design must be determined and the geometry to be optimized must be defined in terms of geometric parameters.
- The structural designer, in close collaboration with the architect, can define the design constraints, load cases, and material properties.
- With the entire framework integrated in one interface (Grasshopper), the developed tool encourages formal exploration at the preliminary stage. The user can test out multiple scenarios for one structure. With the developed tool, designers can generate structures that optimally use FPR properties, maximized stiffness and minimized weight.
- The developed framework allows for integration of architecture and structural concerns. In post-optimality, integration related to construction can be incorporated. The designer must identify the most important forces at play for a project. The post-optimality analysis defines three levels of efficiency and weighs them against each other: computational, material, and production efficiency. In collaboration with a contractor, the structural engineer can weigh the efficiencies against each other.
 - **Computational efficiency** is achieved when the search space of an iteration is limited, allowing the GA to converge rather rapidly. There is thus a benefit to limiting the parameters of a design, and its corresponding search space. The opportunity cost of limiting the search space is less formal exploration in the conception phase.
 - **Material efficiency** refers to the minimal material use. This translates in a lighter structure which in turn reduces expended energy during transportation and installation.
 - **Production efficiency** refers to limiting waste of energy in manufacturing and assembly of a design; it is hard to quantify without early involvement of a contractor.
- Through the post-optimality analysis, the structural designer is able compare the different generated geometries and compare their performance. Further analysis focuses on a single specific scenario and the corresponding geometry. Following the preliminary phase of the design, the structural engineer can assess the feasibility of the design by investigating details, connections, and production methods.

3.2 On the Case-Study

i. Qualitative Conclusions

- Eight different geometries are generated for the structure in FRP. Each geometries presents its advantages and limitations. Quadrilateral sections verify the design constraints more efficiently than the triangular sections. However, in both triangular and quadrilateral sections, the asymmetric sections are lighter than their symmetric counterparts and the cantilevering decks are lighter than the fixed-width deck designs. The asymmetry and cantilevering-deck aspects allow for more specificity in the designs, removing weight where not needed.
- The post-optimality analysis allows to compare the efficiency of the structures beyond their material efficiency (lightness). It is quantified in terms of number of required molds as well as the length of the connection needed for the structure.
 - Triangle cross-sections reduce the number of required formwork for the production. They also require a significantly smaller amount for connection, especially between the different walls of the closed-section.
 - Symmetry in the section and span of the geometries render the structure more efficient in manufacturing: it introduces opportunities for repetition in the formwork of the structure.

- Production efficiency (manufacturing and connection) is highest for this triangular symmetric fixed-width and cantilevering decks.
- The chosen case-study highlight the potential of FRP in terms of structural performance but also the limits in terms of production constraints:
 - In generating possible geometries in FRP, this case-study highlights the potential of FRP. Despite its many complexities, this alternative material presents important and valuable properties. Its durable and sustainable properties, its adjustable mechanical properties, and its lightness offers considerable benefits and opportunities. In a world fighting climate change, the construction industry must change its incentive structure to reflect these new priorities.
 - As shown in appendix L4, the material cost of carbon-fibers is significantly high and will only increase when additional costs relating to labor, manufacturing, transportation, and assembly are considered. This renders FRP structures less cost-efficient than other building material [94], [95] in the current framework of construction. However, changing the incentive structure to include life-cycle costs is important to reframe the discussion and consider FRP structures as a viable and efficient material.
- As outlined in the introduction to the thesis, significant research is required to propel FRP and heal the divide between the myth of laboratories and the realities of the construction field.

ii. Quantitative Conclusions

The framework is implemented with the Wilhelminaberg Viewpoint case-study. This allows to quantify some of the behavior of FRP.

- The first level of the optimization finds the laminate layup combination that maximizes the stiffness of the structure. Using a brute force algorithm, the first level iterates through all the possible laminate layup combinations to find the one generating the stiffest structure.
 - The stiffest laminate layup combination reduces the strain energy by a factor of 1.2 or a relative decrease of 23% when compared to the least stiff laminate combination.
 - Similarly, the stiffest laminate combination reduces the deflection by a factor of 2.2 or a relative decrease of 69% when compared to the least stiff laminate combination.
 - Laminate lay-up combinations with high percentages of 0° laminates are located in sub-spans where bending stiffness is required. Similarly, laminate lay-up combinations with a high percentage of $\pm 45^\circ$ are located in sub-spans where torsional stiffness is required.

The second level of the optimization finds the lightest geometries using a genetic algorithm.

- Defining multiple scenarios for the second level optimization is important for formal exploration in FRP, especially when comparing the different efficiencies of the structure. In comparing the eight generated geometries, the relative decrease between the lightest and the heaviest designs is of 35%. This weight reduction could become important because of significant material costs savings associated with carbon-fiber.
- However, when compared to the same designs run with steel, the weight reduction increases to a 74% weight reduction. However, it is worth noting that this significant decrease in weight due to the FRP design might be reduced to the connections required for such a structure.

4. Recommendations

Following the research, recommendations can be made to structural designers and builders in the construction industry and research and educator at academic institutions.

4.1 Structural Designers, Architects, and Contractors

It is recommended that structural engineers and designers:

- **consider** implementing the proposed framework in the early stages of a design for geometries who exhibit shell-like behaviors. The tool is meant for formal explorations; structural designers should consider defining multiple scenarios with different parameters.
- **cooperate** closely with architects to reach the ideals of integrated design. First, they must inspire the clients by informing them about the formal opportunities and benefits of this alternative material. They must also cooperate in the conception phase to define the different scenarios of geometry generation.
- **consider** running multiple iteration simultaneously in order to increase computational efficiency. Another option to reduce running time is using a more powerful computer or even running the iterations on multiple computers.
- **use** the default settings of the genetic algorithm if they are not familiar with the suggested plug-ins. Otherwise, structural engineers should test and verify the validity of any modified settings. Specifically, they must make sure there is no pre-mature convergence in the genetic algorithm.
- **assess** the results of the proposed tool. Beyond the suggested post-optimality analysis, designers must apply common sense laws to the generated geometries.
- **work** closely with FRP contractor to assess the feasibility of a certain design in FRP. This can be from the early stages of the design conception or at latest at the level of post-optimality analysis. In turn, contractors of FRP must start a dialogue with the aviation and boat building industries. There is significant knowledge to learn in efficient FRP manufacturing.
- **incorporate** repetition in order to generate more efficient geometries in FRP.

4.2 Researchers and Educators

- It is recommended that educators introduce students to alternative materials, in general, and FRP, in particular. In highlighting the benefits and opportunities of the material, students will be encouraged to explore with this new material.

It is recommended that researchers:

- **Investigate** FRP manufacturing methods. With standardization and mass-customization methods already underway, efforts to make free-form architecture in FPR more efficient are paramount. This can become particularly important to make FRP competitive with traditional building material on all fronts.
- **Investigate** the durability and sustainability properties of FRP, in order to increase its life-cycle performance as well as in-service properties. This includes research in organic applications in FRP.

4.3 The construction Industry

All involved parties in the construction industry must cooperate together to address the threat of climate change: governments, educational institutions, designers, researchers, and contractors. The incentive structure of the industry must be modified to reflect the priorities and challenges of the 21st century. It is no longer about efficiency and cost-reduction during construction but the overall life-cycle costs of materials.

5. Further Investigations

Multiple steps will be required to further improve the framework as well as the resulting design. These efforts include:

- **Fine-tuning the framework to better account for lamination layup variations.** In determining the laminate layup combination that generates the stiffest structure (level 1 of the optimization), the proposed framework considers that all the walls of one sub-span section have the same laminate layup combination. An improvement of the first level optimization can include allowing the walls of a sub-span to have different laminate properties. This renders the material use more efficient and might increase the weight savings of a structure.
- **Fine-tuning the framework to better account for geometric exploration.** In the second-level optimization, a genetic algorithm is run to find the lightest geometry for each scenario. As defined now, the defined framework limits the number of geometric parameters and uses a constant thickness over the entire structure. The geometric optimization can be expanded with introducing more geometric parameters and making the thickness a variable parameter design instead of constant over the cross-section. This can lead to lighter and thus more “optimal” structures.
- **Fine-tuning the framework for better finite-element modeling.** The framework can also be improved by plugging-in another FEA software to address some of the limitations of Karamba 3D. The logic and reasoning of the tool can be easily applied.
- **Further investigation in optimization tools.** The research of optimization tool can be expanded beyond only evolutionary algorithm plug-ins. This allows to compare more of Brownlee’s nature-inspired algorithms (discussed in chapter 4, section 4.3).
- **Further development of the post-optimality framework to better account for laminate properties.** Significant investigations must be run in order to verify the correct behavior of laminate properties, such as: verifying laminate specific behavior (inter and intra-laminate failure, debonding), determining the stacking sequence of the laminate layups, and solving the progression or blending of the different laminate layup from one sub-span to the next. These do not necessarily need to be included in the optimization framework but must be addressed past the preliminary phase of the design.

1. Main Report Bibliography

- [1] B. Obama, "Obama's Speech on Climate Change," 22 September 2002. [Online]. Available: <https://www.nytimes.com/2009/09/23/us/politics/23obama.text.html>. [Accessed 01 August 2019].
- [2] Global Alliance for Buildings and Construction (GlobalABC), "2018 Global Status Report: Towards a zero-emission, efficient and resilient buildings and construction sector," 2018. [Online]. Available: https://wedocs.unep.org/bitstream/handle/20.500.11822/27140/Global_Status_2018.pdf?sequence=1&isAllowed=y. [Accessed 1st August 2019].
- [3] J. A. Ochsendorf, "Sustainable Engineering: The Future of Structural Design," *Structures Congress 2005: Metropolis and Beyond*, 20-24 April 2005.
- [4] L. Nijssen, *Composite Materials an introduction*, 1st ed., 2015.
- [5] V. M. Karbhari, "Durability of FRP Composites for Civil Infrastructure – Myth, Mystery or Reality," *Advances in Structural Engineering*, vol. 6, no. 3, 2003.
- [6] L. C. Hollaway, "Chapter 58: Applications of fibre-reinforced polymer composite materials," *ICE Manual of Construction Materials*, pp. 675-699, 2009.
- [7] R. Burgueño and J. Wu, "Membrane-Based Forms for Innovative FRP Bridge Systems through Structural Optimization," *ASCE Journal of Composites for Construction*, vol. 10, pp. 453- 461, 2006.
- [8] R. Burgueño and J. Wu, "An integrated approach to shape and laminate stacking sequence optimization of free-form FRP shells," *Computer Methods in Applied Mechanics Engineering*, vol. 195, p. 4106–4123, 2006.
- [9] L. C. Hollaway, "Chapter 50: Polymer fibre composites: an introduction," *ICE Manual of Construction Materials*, pp. 599-601, 2009.
- [10] M. Pavlovic and F. Csillag, *CIE5128 Reader - FRP Structures*, TU Delft, 2018.
- [11] F. Campbell, *Structural Composite Material*, ASM International, 2010.
- [12] L. C. Hollaway, "Chapter 51: Characterization of fibre and matrix materials used in construction," *ICE Manual of Construction Materials*, pp. 603-617, 2009.
- [13] K. D. L. H. Ghiasi, "Optimum stacking sequence design of composite materials Part II: Variable stiffness design," *Composite Structures*, vol. 93, pp. 1-13, 2010.
- [14] R. McCallion, "Composite materials: enter the dragon," 13 March 2017. [Online]. Available: <https://www.themanufacturer.com/articles/composite-materials-enter-the-dragon/>. [Accessed 1st August 2019].

- [15] Rijkdsdienst Wegverkeer, [Online]. Available: <https://www.rdw.nl/>.
- [16] C. C. C. Laboratory, "Pontresina bridge," [Online]. Available: <https://www.epfl.ch/labs/cclab/projects/pontresina/>. [Accessed 1st August 2019].
- [17] F. v. d. Meer, Materials and Failure Analysis (of FRP), TU Delft, 2016.
- [18] L. C. Hollaway, "Chapter 54: Mechanical properties of FRP composites," *ICE Manual of Construction Materials*, pp. 641-7, 2009.
- [19] T. M. E., "7. Predicting Failure of a Multiangle Composite Laminate," *Structural Analysis of Polymeric Composite Materials*, 2004.
- [20] J. G. T. a. J. F. C. T. Yu, "Chapter 55: Failure criteria for FRP composites," *ICE Manual of Construction Materials*, vol. 2009, pp. 649-54.
- [21] R. Cuntze and A. Freund, "The predictive capability of failure mode concept-based strength criteria for multidirectional laminates," *Composites Science and Technology*, vol. 64, p. 343–377, 2004.
- [22] H. Hahn and S. Tsai, "A General Theory of Strength for Anisotropic Materials," *Journal Composite Materials*, vol. 5, pp. 58-80, 1971.
- [23] a. R. J. L. Lee, "The Role of FRP Composite in a Sustainable World," *Clean Technologies and Environmental Policy*, pp. 247-9, 2009.
- [24] The Energy and Resources Institute (TERI), "Sustainable Development Timeline," 2016. [Online]. Available: https://www.teriin.org/library/files/SD_timeline.pdf. [Accessed 2019 August 2019].
- [25] G. Brundtland, "Our Common Future," *World Commission on Environment and Development*, 1987.
- [26] B. J. van Ruijvena, D. P. van Vuurenb, W. Boskaljonb, M. L. Neelis, D. Sayginc and M. K. Patel, "Long-term model-based projections of energy use and CO2 emissions from the global steel and cement industries," *Resources, Conservation and Recycling*, vol. 112 , p. 15–36, 2016.
- [27] M. Chrimes, Civil Engineering 1839-1889, Sutton Publishing Ltd. , 1991, p. 24.
- [28] Institution of Civil Engineers, Agenda for the Future, London, 2003.
- [29] American Society of Civil Engineers (ASCE), "The Vision for Civil Engineering in 2025," in *The Summit on the Future of Civil Engineering—2025*, 2006.
- [30] Circle-Economy; Dutch Green Building Council (DGBC); Metabolic; SGS Search; Redevco Foundation, "A Framework for Circular Buidings," August 2018. [Online]. Available: <https://www.circle-economy.com/wp-content/uploads/2018/10/A-Framework-For-Circular-Buildings-BREEAM-report-20181007-1.pdf>. [Accessed 1st August 2019].

- [31] The Ministry of Infrastructure and the Environment and the Ministry of Economic Affairs, "A Circular Economy in the Netherlands by 2050," September 2016. [Online]. Available: <https://www.government.nl/a-circular-economy-in-the-netherlands-by-2050>. [Accessed 1st August 2019].
- [32] T. Nguyen, T. Shehab and Z. Gao2, "Evaluating Sustainability of Architectural Designs Using Building Information Modeling," *The Open Construction and Building Technology Journal*, vol. 4, pp. 1-8, 2010.
- [33] R. J. L. S. a. C. R. L. Lee, "Chapter 1: An Introduction," *Strategies for Sustainability*, pp. 1-21, 2012.
- [34] S. Halliwell., "Chapter 59: Recycling of FRP materials in construction," *ICE Manual of Construction Materials*, pp. 695-705., 2009.
- [35] L. C. Hollaway., "Chapter 52: Advanced polymer composites," *ICE Manual of Construction Materials*, pp. 619-632, 2009.
- [36] R. C. a. A. Freund, "The predictive capability of failure mode concept-based strength criteria for multidirectional laminates," *Composites Science and Technology*, vol. 64, pp. 58-80, 2004.
- [37] H. H. a. S.W.Tsai, "A General Theory of Strength for Anisotropic Materials," *Journal Composite Materials*, vol. 5, no. vol. 5, 1971, pp. 58-80., pp. 58-80.
- [38] J. Coenders, Reader for the course CT5251: Structural Design - Special Structures, Delft University of Technology , 2008.
- [39] J. Chilton, The Engineer's Contribution to Contemporary Architecture: Heinz Isler, London: Thomas Telford Books, 2000.
- [40] L. Glaeser, The Work of Frei Otto, Greenwich, Connecticut: The Museum of Modern Art , 1972.
- [41] Q. Li, Y. Su, Y. Wu, A. Borgart and J. G. Rots, "Form-finding of shell structures generated from physical models," *International Journal of Space Structures* , vol. 32, pp. 11-13, 2017.
- [42] B. Kolarevic, "Digital Architectures," *Eternity, Infinity and Virtuality in Architecture [Proceedings of the 22nd Annual Conference of the Association for Computer-Aided Design in Architecture]*, October 2000.
- [43] P. Zellner, Hybrid Space: Generative Form and Digital Architecture, Rizzoli International Publications, 1999.
- [44] P. D. V. a. C. W. S. Adriaenssens, Shell Structures for Architecture: Form Finding and Optimization, Routledge, Ed., 2014.
- [45] M. Bendsøe and O. Sigmund, Topology Optimization. Theory, Methods, and Applications., Springer, Ed., 2003.
- [46] Q.Q.Liang, Performance-based Optimization of Structures. Theory and Applications., Spon Press, 2005.

- [47] M. C. S. F. F. V. G. Chiandussi, "Comparison of multi-objective optimization methodologies for engineering applications," *Computers and Mathematics with Applications*, vol. 63, p. 912–942, 2012.
- [48] "neos Optimization Guide," [Online]. Available: <https://neos-guide.org/optimization-tree>.
- [49] Mathworks, "What Is Direct Search?," [Online]. Available: <https://www.mathworks.com/help/gads/what-is-direct-search.html>.
- [50] M. Cheikh, B. Jarboui, T. Loukil and P. Siarry, "A Method for Selecting Pareto Optimal Solutions in Multiobjective Optimization," *Journal of Informatics and Mathematical Sciences*, vol. 2, pp. 51-62, 2010.
- [51] M. Ehrgott, *Multicriteria Optimization*, Berlin: Springer, 2000.
- [52] H. Ishibuchi, H. Masuda and Y. Nojima, "Selecting a small number of non-dominated solutions to be presented to the decision make," in *2014 IEEE International Conference on Systems, Man, and Cybernetics (SMC)*, San Diego, 2014.
- [53] V. Veerappa and E. Letier, "Understanding clusters of optimal solutions in multi-objective decision problems," in *2011 IEEE 19th International Requirements Engineering Conference*, Toronto.
- [54] T. Robbin, *Engineering a new architecture*, New Haven, Conn.: Yale University Press, 1996.
- [55] Z. K. Awad, T. Aravinthan, Y. Zhuge and F. Gonzalez., "A review of optimization techniques used in the design of fibre composite structures for civil engineering applications," *Materials and Design*, vol. 33, p. 534–544, 2012.
- [56] M. S. a. J. S. K. Ikeya, "Multi-objective free-form optimization for shape and thickness of shell structures with composite materials," vol. 135, p. 262–275, 2016.
- [57] E. Lindgaard and E. Lund, "Nonlinear buckling optimization of composite structures," *Computer Methods in Applied Mechanics and Engineering*, vol. 199 , p. 2319–2330, 2010.
- [58] E. Lund, "Buckling topology optimization of laminated multi-material composite shell structures," *Composite Structures*, vol. 91, p. 158–167, 2009.
- [59] M. Miki and Y. Sugiyama, "Optimum Design of Laminated Composite Plates Using Lamination Parameters," *AIAA Journal*, vol. 31, no. 5, pp. 921-922, 1993.
- [60] H. Fukunaga and G. N. Vanderplaats, "Stiffness Optimization of Orthotropic Laminated Composites Using Lamination Parameters," *AIAA Journal*, vol. 29, no. 4, pp. 641-646, 1991.
- [61] J. Smits, R. Gkaidatzis, R. Blok and P. Teuffel, "Bio-Based Composite Pedestrian Bridge—Part 1: Design and Optimization," *Proceedings of the IASS Annual Symposium 2016 "Spatial Structures in the 21st Century"*, September 2016.
- [62] R. Chiong, *Nature-Inspired Algorithms for Optimisation*, Springer, 2009.

- [63] J. Brownlee, *Clever Algorithms: Nature-Inspired Programming Recipes*, Melbourne: Swinburne University , 2011.
- [64] D. Wolpert and W. Macready, "No free lunch theorems for optimization," *IEEE Transactions on Evolutionary Computation*, vol. 1, no. 1, pp. 67 - 82, April 1997.
- [65] A. Rothwell, *Optimization Methods in Structural Design*, vol. 242, Springer.
- [66] J. Arora, *Introduction to optimum design*, 3rd ed., Elsevier, 2012.
- [67] D. Rutten, "Evolutionary Principles applied to Problem Solving," Grasshopper 3D, 25 September 2010. [Online]. Available: <https://www.grasshopper3d.com/profiles/blogs/evolutionary-principles>. [Accessed 1st August 2019].
- [68] O. Kramer, *Genetic Algorithm Essentials*, Cham, Switzerland: Springer, 2017.
- [69] C. Cubukcuoglu, B. Ekici, M. F. Tasgetiren and S. Sariyildiz, "OPTIMUS: Self-Adaptive Differential Evolution with Ensemble of Mutation Strategies for Grasshopper Algorithmic Modeling," *MDPI*, vol. 12, no. 151, 12 July 2019.
- [70] R. Vierlinger, "Octopus," [Online]. Available: <https://www.food4rhino.com/app/octopus>. [Accessed 1st August 2019].
- [71] "PISA, A Platform and Programming Language Independent Interface for Search Algorithms," [Online]. Available: <https://sop.tik.ee.ethz.ch/pisa/>. [Accessed 1st August 2019].
- [72] "WALLACEI (by Wallacei)," [Online]. Available: <https://www.food4rhino.com/app/wallacei-0>. [Accessed 1st August 2019].
- [73] "Wallacei," [Online]. Available: <https://www.wallacei.com/about>. [Accessed 1st August 2019].
- [74] Internationale Bauausstellung (IBA) , "Four Stages: The Development of International Building Exhibitions," [Online]. Available: <https://www.open-iba.de/en/geschichte/>. [Accessed 1st August 2019].
- [75] P. Schatz, *Berichte Aus Der Arbeit*, 1987.
- [76] [Online]. [Accessed 1st August 2019].
- [77] N. & Partners, "Ney & Partners," [Online]. Available: <https://www.ney.partners/project/viewpoint-wilhelminaberg.html>. [Accessed 1st August 2019].
- [78] M. Stolpe and K. Svanberg, "An Alternative Interpolation Scheme for Minimum Compliance Optimization," *Structural and Multidisciplinary Optimization*, vol. 22, p. 116–124, 2001.
- [79] Robert McNeel & Associates, "Rhinoceros 3D," 2014. [Online]. Available: <https://www.rhino3d.com/>. [Accessed 1st August 2019].

- [80] Robert McNeel & Associates, "Grasshopper," 2014. [Online]. Available: <https://www.grasshopper3d.com/>. [Accessed 1st August 2019].
- [81] L. A. Carlsson, D. F. Adams and R. B. Pipes, *Experimental Characterization of Advanced Composite Materials*, Taylor & Francis Group, 2014.
- [82] S. T. IJsselmuiden, *Optimal Design of Variable Stiffness Composite Structures Using Lamination Parameters*, TU Delft, 2011.
- [83] W. van Tol, "Fibre Reinforced Polymer Tool," [Online]. Available: <http://wijnandvantol.com/projects/#29>. [Accessed 1st August 2019].
- [84] Clemens Preisinger, "Parametric Structural Modeling. Karamba User Manual 1.2.2," 2016. [Online]. Available: <https://www.karamba3d.com/>. [Accessed 1st August 2019].
- [85] L. C. Hollaway, "Chapter 54: Mechanical properties of FRP composites," *ICE Manual of Construction Materials*, vol. 2009, pp. 641-7.
- [86] P. Hoogenboom, *Reader for the course CIE4143: Shell Analysis, Theory and Application*, Delft University of Technology, 2019.
- [87] Core Studio, Thornton Tomasetti, "Colibri Release," 2017 January 2017. [Online]. Available: <http://core.thorntontomasetti.com/colibri-release/>. [Accessed 1st August 2019].
- [88] D. Rutten, "Galapagos: On the Logic and Limitations of Generic Solvers," *Architectural Design. Special Issue: Computation Works: The Building of Algorithmic Thought*, vol. 83, no. 2, pp. 132-135, April/May 2013.
- [89] S. Schoina, *Performance-based form-finding and material distribution of free form roof structures: Implementation in the Post Rotterdam Case Study (Master Thesis)*, TU Delft, 2016.
- [90] S. Flöry, "GOAT," [Online]. Available: <https://www.grasshopper3d.com/group/goat>. [Accessed 1st August 2018].
- [91] L. Skotny, "Correct mesh size – a quick guide!," [Online]. Available: <https://enterfea.com/correct-mesh-size-quick-guide/>. [Accessed 1st August 2019].
- [92] Ł. Skotny, "What are the Types of Elements Used in FEA?," Enterfea Blog, [Online]. Available: <https://enterfea.com/what-are-the-types-of-elements-used-in-fea/>. [Accessed 1st August 1 2019].
- [93] D. P. Billington, *The Tower and the Bridge: The New Art of Structural Engineering*, Princeton, New Jersey: Princeton University Press, 1985.
- [94] S. N. Rao, T. Simha, R. K.P and R. Kumar, "Carbon Composites are Becoming Competitive and Cost effective," *InfoSys - External document*, 2018.
- [95] "Cheaper carbon fibre will slash auto making costs-manufacturer," 24 March 2014. [Online]. Available: <https://www.reuters.com/article/sgl-fibres/cheaper-carbon-fibre-will-slash-auto-making-costs-manufacturer-idUSL5N0MP2RP20140328>. [Accessed 1st August 2019].

- [96] "Helikoptertypen," [Online]. Available: <https://www.lasten-flug.de/helikoptertypen.html>. [Accessed 1st August 2019].
- [97] Lindapter International, "Hollo-Bolt by Lindapter," [Online]. [Accessed 1st August 2019].
- [98] O. Arup, *Philosophy of Design: Essays 1942-1981*, Munich: Prestel, 2012.
- [99] M. S. Uihlein, "Ove Arup's total design, integrated project delivery, and the role of the engineer," *Architectural Science Review*, vol. 59, no. 2, pp. 102-113, 2016.
- [100] K. van Hee and K. van Overveld, "New criteria for assessing a technological design," April 2012. [Online]. Available: https://www.4tu.nl/sai/en/testimonials/2012-12-10_2012_April_NewCriteriaSAI.pdf. [Accessed 1st August 2019].
- [101] B. Zevi, "After 5000 Years: The Revolution," *Lotus: New Structures and the Informal*, vol. 104, March 2000.
- [102] Royal HaskoningDHV, "Royal HaskoningDHV, Cead and DSM Design First Lightweight 3D Printed Bridge Using FRP," 3 September 2019. [Online]. Available: <https://www.royalhaskoningdhv.com/en-gb/news-room/news/royal-haskoningdhv-cead-and-dsm-design-first-lightweight-3d-printed-bridge-using-frp/10008>. [Accessed 5 September 2019].
- [103] European Committee for Standardization, "Part 2: Traffic Loads on Bridges," 2003.

2. Appendices Bibliography

- [1] M. Pavlovic and F. Csillag, CIE5128 Reader - FRP Structures, TU Delft, 2018.
- [2] L. C. Hollaway, "Chapter 51: Characterization of fibre and matrix materials used in construction," *ICE Manual of Construction Materials*, pp. 603-617, 2009.
- [3] L. Nijssen, Composite Materials an introduction, 1st ed., 2015.
- [4] R. J. L. S. a. C. R. L. Lee, "Chapter 1: An Introduction," *Strategies for Sustainability*, pp. 1-21, 2012.
- [5] M. C. S. F. F. V. G. Chiandussi, "Comparison of multi-objective optimization methodologies for engineering applications," *Computers and Mathematics with Applications*, vol. 63, p. 912–942, 2012.
- [6] K. D. L. H. Ghiasi, "Optimum stacking sequence design of composite materials Part II: Variable stiffness design," *Composite Structures*, vol. 93, pp. 1-13, 2010.
- [7] H. Hahn and S. Tsai, "A General Theory of Strength for Anisotropic Materials," *Journal Composite Materials*, vol. 5, pp. 58-80, 1971.
- [8] R. Burgueño and J. Wu, "An integrated approach to shape and laminate stacking sequence optimization of free-form FRP shells," *Computer Methods in Applied Mechanics Engineering*, vol. 195, p. 4106–4123, 2006.
- [9] L. A. Carlsson, D. F. Adams and R. B. Pipes, Experimental Characterization of Advanced Composite Materials, Taylor & Francis Group, 2014.
- [10] S. T. IJsselmuiden, Optimal Design of Variable Stiffness Composite Structures Using Lamination Parameters, TU Delft, 2011.
- [11] W. van Tol, "Fibre Reinforced Polymer Tool," [Online]. Available: <http://wijnandvantol.com/projects/#29>. [Accessed 1st August 2019].
- [12] P. Hoogenboom, Reader for the course CIE4143: Shell Analysis, Theory and Application, Delft University of Technology, 2019.
- [13] L. Skotny, "Correct mesh size – a quick guide!," [Online]. Available: <https://enterfea.com/correct-mesh-size-quick-guide/>. [Accessed 1st August 2019].
- [14] European Committee for Standardization, "Part 2: Traffic Loads on Bridges," 2003.
- [15] S. N. Rao, T. Simha, R. K.P and R. Kumar, "Carbon Composites are Becoming Competitive and Cost effective," *InfoSys - External document*, 2018.
- [16] "Cheaper carbon fibre will slash auto making costs-manufacturer," 24 March 2014. [Online]. Available: <https://www.reuters.com/article/sgl-fibres/cheaper-carbon-fibre-will-slash-auto-making-costs-manufacturer-idUSL5N0MP2RP20140328>. [Accessed 1st August 2019].

<u>Appendix A.</u>	138
A1. Thermoset Polymers	138
A2. Fibers Types	139
A3. Manufacturing Processes	141
<u>Appendix B.</u>	142
B1. Thermal Effects on FRP	142
B2. Sustainability of Constituent Materials	143
<u>Appendix C.</u>	144
C1. Micro-Mechanics of a Lamina	144
<u>Appendix D</u>	145
D1. Pareto Optimality	145
<u>Appendix E</u>	146
E1. Lamination Parameters	146
<u>Appendix F</u>	148
F1. Tool Development: Multi-objective Optimization	148
<u>Appendix G</u>	150
G1. Parameters of Scenario 1: Triangular Symmetric Fixed-width Deck	150
G2. Parameters of Scenario 2: Triangular Symmetric Cantilevering Deck	151
G3. Parameters of Scenario 3: Triangular Asymmetric Fixed-width Deck	152
G4. Parameters of Scenario 1: Triangular Asymmetric Cantilevering Deck	153
G5. Parameters of Scenario 1: Quadrilateral Symmetric Fixed-width Deck	154
G6. Parameters of Scenario 1: Quadrilateral Symmetric Cantilevering Deck	155
G7. Parameters of Scenario 1: Quadrilateral Asymmetric Fixed-width Deck	156
G8. Parameters of Scenario 1: Quadrilateral Asymmetric Cantilevering Deck	157
<u>Appendix H</u>	158
H1. Material Properties: Summary	158
H2. Material Properties: Derivation	160
<u>Appendix I</u>	164
I1. Determining Load-Areas	164
I2. Approximating Cable-effect in the case study	168
<u>Appendix K</u>	170
K1. Determining Mesh Size	170
<u>Appendix L</u>	174
L1. Search Spaces for the 8 Scenarios	174
L2. Convergence of Graphs	177
L3. Natural Frequency of the 8 structures.	178
L4. Cost Estimates	178
L5. Production Methods	179
L6. Joint Design	180
<u>Appendix M</u>	182
M1. Performance Graphs	182
M2. Performance Graphs, using improvement factor	184

Appendix A

A1. Thermoset Polymers

The most important distinction between thermoset and thermoplastic is made in Chapter 1. With thermoset polymers mostly used in structural application. Closer attention is brought to the most widely used thermosets hereinafter.

1. Polyester resins are commonly used in commercial applications such as yacht building or automobile manufacturing. They consist often of 3 ingredients: a polyester, a cross-linking agent, and an imitator. An important advantage is the processing versatility with curing possible either at room or elevated temperatures. However, their curing process is also marked by a high rate of shrinkage, a clear disadvantage. While displaying easy workability and lower cost than epoxies, polyester resins exhibit lower mechanical properties, lower temperature capabilities, and an inferior environmental resistance.

2. Vinyl ester resins are commonly used in applications that require a higher chemical resistance than polyester. They are very similar to polyesters in their molecular configuration but with reactive groups at the end of the molecular chains. Exhibiting lower crosslinks densities, vinyl ester resins are tougher than their polyester counterparts: they are more resistant to degradation from water and moisture. While vinyl esters' mechanical properties outperform polyesters', they remain lower than those of epoxy resins [1].

3. Epoxy resins remain the most common matrix material for high-performance composites (i.e: wind turbines blades) and adhesives due to their advantageous properties. Their properties combine strength, adhesion, low shrinkage, processing versatility, and high fatigue strength. These commercial epoxy matrices can be as simple as a single epoxy and a single curing agent. Many matrices however combine a major epoxy, multiple minor epoxies and curing agents. The minor epoxies are added in many cases to improve properties, mainly: a lower moisture absorption, higher elevated temperature properties, as well as an upgraded toughness. Such enhanced properties combined with the matrix's price competitiveness have allowed epoxy resins to out-perform other resins.

4. Phenolic resins are often used in circuit boards or interior components of trains and aircrafts. This is mostly due to their good fire and smoke resistance properties: they do not burn, melt, or lose their properties at elevated temperatures. Their weak mechanical properties, brittleness, and release of water and volatile substance s in the curing process are among factors limiting their use.

A2. Fibers Types

The most frequently used fiber types in structural application are discussed hereinafter. They may be used separately or as a hybrid of two or even three different types. Hybrid systems are used when fiber type are combined to reach certain properties of strength and stiffness.

1. Glass Fibers are extensively used in commercial composite applications. With a basis in silica (SiO_2), glass fibers are generally low in cost with advantageous properties, mainly: a high tensile strength paired with a high impact and environmental resistance. Although many types of glass fiber manufactured, three main types of glass fibers used are most broadly used: E-glass, S-glass and Quartz. Other types include C-glass (chemically resistant), D-glass (low dielectric).

E-glass is the most common and least expensive option. E-glass is characterized by a good combination of tensile strength (3.5 GPa) and elastic modulus (70GPa).

S-glass is also extensively used but slightly more expensive than E-glass. Typically stiffer and 40% stronger than E-glass at room temperature, S-glass has a tensile strength of 4.5 GPa and an elastic modulus of 87 GPa. Additionally, it retains its properties at high temperature and exhibits good corrosion resistance. This higher performance renders it more expensive [2].

Quartz is the most expensive of the three options due to the ultrapure silica glass that it uses. It is frequently used in electrical applications.

2. Carbon and Graphite Fibers are extensively used in high-performance composite structure. Producing with a wide range of properties, they generally exhibit both superior compressive and tensile strength, a high moduli of elasticity, as well as excellent fatigue and creep resistance. Carbon and graphite fibers display a strong resistance to corrosion and environmental impacts. If the optimal material is defined as combining high strength, stiffness, and toughness with a low weight, then carbon fibers meet such criteria more than any other material.

Despite their near-ideal behavior, carbon and graphite fiber still present some disadvantages. Extremely anisotropic, the transverse strength and modulus of the fibers are significantly smaller than the longitudinal values. Furthermore, significant disadvantages worth mentioning are its low impact resistance, low strain-to-failure, a brittle behavior, lower compression strength than tensile strength, and its higher cost than glass fibers [1].

3. Aramid Fibers are organic fibers with properties intermediate to those of glass and carbon fibers, in terms of stiffness, strength, and costs.

Its advantages include its light weight, high tensile strength and modulus, and superior toughness. Their abilities to undergo plastic deformation in compression or to defibrillate during tensile fracture are also main benefits of aramid fibers [41]. They can absorb large amounts of energy during fracturing due to their high strain-to-failure. Their extreme toughness and wear resistance have rendered them ideal for applications such as stay-cables or ballistic protection. Contrary to glass and carbon fibers, aramid fibers exhibit a structure that allows for a ductile, non-brittle, failure. Furthermore, its aromatic structure (aromatic rings) contribute to its excellent thermal stability and flame resistance; its durability is also underlined with the resistance of the tensile strength is resistant to effect of moisture.

Some limitations of the material are its sensitivity to short-term creep even at room temperature, despite performing better than glass fibers for long-term creep. Furthermore, its lack of adhesion to the matrix results in a poor longitudinal compression, transverse tension, and inter-laminar shear strengths. Unlike their glass, carbon, or graphite counterparts, no surface treatment has been developed for aramid fibers. Aramid fibers can be processed in relatively most textile because of their flexibility and non-brittleness [3].

4. Textile

Fibers and fiber bundles are often processed to form a textile.

4.1 Woven Fabrics

Unlike other types of fiber, woven products are two-dimensional with different fiber orientation usually at 0° and 90° , but $\pm 45^\circ$ can also be achieved. Woven fabrics often combine different fibers such as carbon or glass. They are tailored to obtain specific properties whether exploiting aramid's toughness by mixing it with carbon or reduce costs by mixing glass with carbon fibers.

Weaves are often classified by the pattern of interlacing; the two most used ones in high-performance composites are the plain and the satin weaves.

The plain weave is the simplest pattern. With more interlaces per unit area than any other type of weave, plain weaves are considered as the tightest basic fabric design and the most resistance to in-plane shear movement. Its disadvantages lie in its difficulty to wet-out during impregnation or its "waviness" that can reduce the strength and stiffness of the composite [3].

Satin weaves have a minimum of interlacing. This results in reducing less resistance to in-plane shear movement and have the best drapability.

4.2 Reinforced Mats

Reinforced mats are made of either chopped strands or continuous strands organized in a swirl pattern. They are often used for medium-strength parts having uniform cross sections, such surfacing mats or veils available in various weights and dimensions.

4.3 Chopped Fibers

Often used to reinforced thermoplastic parts, chopped fibers exhibit higher strength in compression and in-injection molded parts. Their availability ranges from 3.2 to 50mm and are often blended with resins and other additives to prepare compression molding compounds or injection molding.

4.4 Prepeg Manufacturing

Prepeg refers to "pre-impregnated" composite fibers, either unidirectional or woven clothes, with a controlled amount of resin. The resin in the prepeg is either staged or advanced (B-stage) to the point where it becomes a semisolid layer at room temperature. It is the most prevalent product form used in advanced composite manufacturing. During curing, the B-stage advanced resin remelt from its semisolid state and flows.

A3. Manufacturing Processes

1. Spray-up or hand lay-up

Generally applied for large projects or as coating for marine or civil construction, spray up is a low-tooling cost and low-technology process. It is carried using a spray pistol to apply a mixture of short fibers and a low-viscosity liquid resin onto a mold with little attention to fiber direction.

Similarly, to spray-up, hand lay-up is also straightforward with little equipment requirement. Also referred as wet lay-up, they are often used to make very large parts with minimal associated tooling costs.

It is carried out by manually applying the loose plies for reinforcement onto the mold and then applying liquid resin with a roller or brush. The labor-intensive of the process needed to prevent the plies from shifting is an important limitation of the project. Another constraint is due to the impregnation by hand of the process that can result in resin-starved or resin-starved areas.

2. Filament Winding

Filament winding is an application-specific process used to fabricate any body of revolution: cylinders, cones, spheres, or shafts. In use since the mid-1940s, it is a highly repetitive technique ideal for controlling the local thickness of structures as well as reach an excellent fiber density. It is a continuous process consisting of two concurrent steps: positioning the fibers and applying the resin. It applies continuous rovings around a rotating mandrel in order to form large and thick-walled structures; there exist multiple filament winding patterns: helical, polar, or hoop. Such filament winding processes control the angle of winding to obtain the optimal circumferential stiffness and strength [1].

3. Pultrusion

Applied since the 1950s, pultrusion is a technique capable of making a wide variety of structural shapes. The term “pultrusion” is the combination of the verb “to pull” and noun “extrusion” [3]. Extrusion is used with materials such as steel or aluminum to create profile. The shape of the profile is generated through compressing the material in the mold. As composite materials cannot be pushed through a mold, reinforcement is pulled from bundles and brought together gradually in a resin bath. The reinforcement is thus impregnated with liquid resin and transferred through the mold. Relying on simple machinery and advanced degree of automation, this repetitive and continuous process yields low production costs. While it is possible, in principle, to produce infinitely long profiles, the process becomes semi-continuous with profiles sawn to length.

Other limitations, however, also stem from its repetitive and automated nature. The process is restricted by rather long and labor intensive setting up and the production is limited by a narrow selection of cross-sections. Furthermore, the reinforcement oriented primarily in the longitudinal direction is a limitation for the stiffness and strength.

Appendix B

B1. Thermal Effects on FRP

While short-term effects are often only physical and reversible when the temperatures return to its original state, long-term effect are irreversible, more durable, and often include a chemical change. This long-term effect is identified as the aging of the material.

1. Glass transitions T_g and melting point T_m

The glass transition temperature refers to the temperature below which the physical properties of an amorphous or amorphous/crystalline polymer vary in a similar manner to a solid phase (brittle or glassy state) and above which it behaves in a “rubbery” state.

The physical properties of thermoset polymers are intrinsically linked to the intermolecular cross-links for their strength. Below T_g , polymers are rigid and have both stiffness and strength. As temperature nears the T_g value, the matrix will soften yielding soft or viscous state polymers, that don't have any stiffness and strength above T_g .

2. Coefficient of thermal expansion

The coefficient of thermal expansion refers to the change in unit rise in temperature. The CTE of polymer materials are of the order 100×10^{-6} , an order higher than traditional civil engineering materials. This property is particularly important when connecting a polymer composite to a different material. The CTE of thermosetting polymers is primarily influenced by the degree of cross-linking of the molecules of polymer and the overall stiffness of the units between those cross-linkages.

3. Thermal conductivity

The thermal conductivity is a measure of the ease with which temperature is transmitted through a material. The thermal conductivity of all polymers is low making them good heat insulators. This property is particularly relevant for structure exposed to direct sunlight.

Steps can be taken to influence the thermal conductivity of a polymer. While using the material in its foam form can reduce the thermal conductivity, metallic filler can be added to the resin at the time of polymerization to increase the thermal conductivity value.

4. Ultraviolet radiation

Ultraviolet radiation from the sun-radiation is strong enough to split up covalent bonds in an organic material such as composite polymers. This leads to a degradation of the composite material, yielding weakening, embrittlement, and yellowing of the structure. A surface layer containing an additive to the composite matrix can be added to FRP structures in harsh environment or long weather exposure. Such UV stabilizers include adding pigmented gel coat or a UV inhibitor; the composite material is then protected from degradation through impeding UV infiltration. It is important to note that designers must seek the manufacturer's input regarding the UV-resistance of an intended construction.

B2. Sustainability of Constituent Materials

Following the established life-cycle assessment, a closer look at the resource use of composite materials, evaluating the environmental impact of the different types of the matrix-fiber constituents.

		Strengths	Weaknesses
Matrix	Epoxy	<ul style="list-style-type: none"> + high mechanical strength + low viscosity + low shrinkage rates + overall environmental durability 	<ul style="list-style-type: none"> - Relatively expensive in comparison to other polymers. - Irreversible curing process (impossibility to recycle)
	Polyester	<ul style="list-style-type: none"> + low cost + high corrosion resistance + uncomplicated processing 	<ul style="list-style-type: none"> - Low temperature tolerance - Shrinkage from cross-linking - Potential health problems
	Vinylester	<ul style="list-style-type: none"> + fast and simple cross-linking of unsaturated polyester + corrosion resistance + durability in alkaline environments 	<ul style="list-style-type: none"> - Fewer crosslinks of unsaturated polyesters - Irreversible curing process (impossibility to recycle)
Fiber	Carbon Fiber	<ul style="list-style-type: none"> + high tensile strength + high modulus of elasticity + tolerance to high temperatures + corrosion resistance 	<ul style="list-style-type: none"> - Petroleum based - Greatest environment impact - High energy demand
	Glass Fiber	<ul style="list-style-type: none"> + high strength + tolerance to high temperatures + corrosion resistance 	<ul style="list-style-type: none"> - High temperature needed for manufacturing - High energy demand

Table B2.1 Summary of strengths and weaknesses of the different types of fiber constituents [4].

Appendix C

C1. Micro-Mechanics of a Lamina

Different methods have been developed to account for the orthotropic of composite materials. A first step in doing so is estimating the stiffness of a laminate based on the stiffness/strength values of the reinforcement and resin used as well as the volume fraction. The rules of mixture, either in parallel or series, are often used to approximate the stiffness in the main directions. The parallel model is generally used to approximate the longitudinal stiffness. It assumes that the fibers and the matrix deform compatibly when subjected to uniaxial loading in that direction. Following the rules of mixtures:

$$F = \sigma_c A_c = \sigma_c (A_f + A_m) = F_f + F_m \quad (1a)$$

$$F = \sigma_f A_f + \sigma_m A_m \quad (1b)$$

$$\sigma_c = \frac{\sigma_f A_f + \sigma_m A_m}{A_c} \quad (1c)$$

$$\varepsilon_c = \frac{\sigma_f V_f + \sigma_m V_m}{E_{c1}} \quad (1d)$$

$$E_{c1} = E_f V_f + E_m V_m \quad (1e)$$

Similarly, we can write:

$$\nu_{12} = \nu_{f1} V_f + \nu_{m1} V_m \quad (1f)$$

The series model is generally used to approximate the transverse stiffness. Under uniaxial loading, the transverse normal stress in the fibers is assumed to be equal to the stress in the matrix.

$$\sigma_f = \sigma_m \quad (2a)$$

$$E_c \varepsilon_c = E_m \varepsilon_m = E_f \varepsilon_f \quad (2b)$$

$$\sigma_c = E_c (\nu_m \varepsilon_m + \nu_f \varepsilon_f) \quad (2c)$$

$$\frac{1}{E_{c2}} = \frac{V_f}{E_{f2}} + \frac{V_m}{E_m} \quad (2d)$$

$$E_{c2} = \frac{E_{f2} E_m}{E_{f2} V_m + E_m V_f} \quad (2e)$$

The same applies to the in-plane shear stress in the fibers and that in the matrix. The in-plane shear modulus of lamina can be given by:

$$G_{c2} = \frac{G_{f2} E_m}{G_{f2} V_m + E_m V_f} \quad (3)$$

Experimental studies show that the rules of mixture are more precise in determining the longitudinal modulus of the composite material using a parallel system (equation 1). The rules of mixture assuming a system in series is less reliable: the accuracy in evaluating the transverse elastic modulus and (equations 2 and 3). Research shows that the assumptions of equal transverse stresses adopted in deriving equations 2 oversimplify the real behavior at the interface between a fiber and the matrix. Indeed, the equations are derived on the assumption that the fibers are uniformly distributed in matrix; in practice, fibers are often randomly distributed with some in contact and others not (Jones, 1999). Another issue is the non-uniformity of stress of the matrix when a lamina is subjected to transverse loading. More complicated models have been developed to take these complexities in account.

Appendix D

D1. Pareto Optimality

The concept of optimum is changed in multi-objective optimization problems. Unlike single-objective optimization problems that often result in a unique optimal solution, multi-objective optimization problems result in multiple solutions. No longer unique, the optimum in multi-objective optimization problems is seen as a trade-off or compromise between the different objective function. The most commonly adopted notion of optimum is known as the Pareto optimality, first introduced by Francis.Y.Edgeworth in 1881 and generalized by Vilfredo Pareto in 1906 [5]. Notions of Pareto optimality are elaborated in short to better understand how to select the optimal solutions of a multi-objective optimization.

The following definitions are based on definitions of Pareto notions applied to structural optimization, from the authors' initial applications in political economy [5].

1. Pareto optimality

A solution is considered Pareto optimal within if there exists no feasible vector for a certain variable in the entire variable design space which would improve some criterion without negatively affecting at least another criterion. The vector refers to the objective vector as defined in equation (2). Pareto optimal solutions are referred to as non-inferior, admissible, or efficient; their vectors referred to as non-dominated. They form the Pareto Optimal Set . In mathematical terms, a vector is considered to dominate another vector if and only if is partially less than ; it is written as:

$$\begin{aligned} u &= (u_1, \dots, u_k) \\ v &= (v_1, \dots, v_k) \\ \forall i \in \{1, \dots, k\}, u_i &\leq v_i \wedge \exists i \in \{1, \dots, k\} : u_i < v_i \end{aligned} \quad (4)$$

Pareto optimality is the written as:

$$\mathcal{P}^* := \{x \in \Omega \mid \exists x' \in F(x') \leq F(x)\} \quad (5)$$

When plotted in the solution space, the non-dominate vectors form the Pareto front . It is often very difficult if not impossible to determine it analytically. As such, the Pareto front is often computed through generating as many points of the design space as possible. When a sufficient number of solution is generated, non-dominated objective vectors are produced by evaluating every possible solution.

In mathematical terms, Pareto optimal front is written as:

$$\mathcal{PF}^* := \{u = F(x) \mid x \in \mathcal{P}^*\} \quad (6)$$

Multi-objective optimization problems provide the decision maker with a significant but limited number of solutions. These solutions reveal non-dominated vectors in the objective space and their corresponding variables (parameters) in the decision space. They correspond to the Pareto optimal solutions and thus define the Pareto front. They must maintain a certain diversity in the objective and design space to allow the decision maker a judgment.

Comparisons of different multi-objective optimization solutions have revealed that evolutionary algorithms (EA) are particularly suited to capture the multiple Pareto-optimal solutions. Research has complexified such a statement by generating a hierarchy of the different evolution-based techniques: algorithms incorporating elitism become more favorable in capturing multiple Pareto-optimal solutions, and generating the Pareto Front [6].

Appendix E

E1. Lamination Parameters

The constitutive relations presented in the classical lamination theory discussed in section 2 include the design variables defining a laminate behavior in the term, whether it is the orientation angle or the thickness of layers. [A], [B], and [D] matrices are very important in assessing a laminate's behavior in an optimization problem. With the numerous variables included in these matrices, Tsai and Hahn introduced in 1980 a more convenient way in representing the matrices: lamination parameters (LP) [7]. Laminations parameters are non-dimensional through-the-thickness integration of the layer orientation. Lamination parameter allow to parametrize a composite material: 12 lamination parameters and 1 thickness are sufficient to fully describe any laminate layup. Since stiffness matrices are most important in describing a laminate behavior, lamination parameters can be used as design variables. This simplification will become particularly useful in the optimization process of laminate behavior.

$$LP = \begin{bmatrix} V_{1A} & V_{2A} & V_{3A} & V_{4A} \\ V_{1B} & V_{2B} & V_{3B} & V_{4B} \\ V_{1D} & V_{2D} & V_{3D} & V_{4D} \end{bmatrix}^T \quad (7)$$

The lamination parameters related to the laminate in-plane, out-of-plane and couples responses are respectively denoted by V_{kA} , V_{kB} , V_{kD} with $k=1,2,3,4$. LPs can also be calculated for a N-ply laminate as show below; they are defined as the integral of the layer angles over the thickness z .

In-plane	Coupled	Out-of-Plane
$V_{1A} = \frac{1}{N} \sum_{i=1}^N \cos(2\theta_i)$	$V_{1B} = \frac{2}{N^2} \sum_{i=1}^N (Z_i^2 - Z_{i-1}^2) \cos(2\theta_i)$	$V_{1D} = \frac{4}{N^3} \sum_{i=1}^N (Z_i^3 - Z_{i-1}^3) \cos(2\theta_i)$
$V_{2A} = \frac{1}{N} \sum_{i=1}^N \sin(2\theta_i)$	$V_{2B} = \frac{2}{N^2} \sum_{i=1}^N (Z_i^2 - Z_{i-1}^2) \sin(2\theta_i)$	$V_{2D} = \frac{4}{N^3} \sum_{i=1}^N (Z_i^3 - Z_{i-1}^3) \sin(2\theta_i)$
$V_{3A} = \frac{1}{N} \sum_{i=1}^N \cos(4\theta_i)$	$V_{3B} = \frac{2}{N^2} \sum_{i=1}^N (Z_i^2 - Z_{i-1}^2) \cos(4\theta_i)$	$V_{3D} = \frac{4}{N^3} \sum_{i=1}^N (Z_i^3 - Z_{i-1}^3) \cos(4\theta_i)$
$V_{4A} = \frac{1}{N} \sum_{i=1}^N \sin(4\theta_i)$	$V_{4B} = \frac{2}{N^2} \sum_{i=1}^N (Z_i^2 - Z_{i-1}^2) \sin(4\theta_i)$	$V_{4D} = \frac{4}{N^3} \sum_{i=1}^N (Z_i^3 - Z_{i-1}^3) \sin(4\theta_i)$

Table D1.1 Lamination parameters. Numerical evaluation for constant ply thickness.

Since layer orientations in laminates do not vary in laminates, the laminate stiffness matrices can be expressed as linear functions (summations) of the materials invariants, as follows:

$$A = h (\Gamma_0 + \Gamma_1 V_{1A} + \Gamma_2 V_{2A} + \Gamma_3 V_{3A} + \Gamma_4 V_{4A}) \quad (8)$$

$$B = \frac{h^2}{4} (\Gamma_1 V_{1B} + \Gamma_2 V_{2B} + \Gamma_3 V_{3B} + \Gamma_4 V_{4B}) \quad (9)$$

$$D = \frac{h^3}{12} (\Gamma_0 + \Gamma_1 V_{1D} + \Gamma_2 V_{2D} + \Gamma_3 V_{3D} + \Gamma_4 V_{4D}) \quad (10)$$

We can define the material invariants as:

$$\Gamma_0 = \begin{bmatrix} U_1 & U_4 & 0 \\ U_4 & U_1 & 0 \\ 0 & 0 & U_5 \end{bmatrix}$$

$$\Gamma_1 = \begin{bmatrix} U_2 & 0 & 0 \\ 0 & -U_2 & 0 \\ 0 & 0 & 0 \end{bmatrix}$$

$$\Gamma_2 = \begin{bmatrix} 0 & 0 & U_2/2 \\ 0 & 0 & U_2/2 \\ U_2/2 & U_2/2 & 0 \end{bmatrix}$$

$$\Gamma_3 = \begin{bmatrix} U_3 & -U_3 & 0 \\ -U_3 & U_3 & 0 \\ 0 & 0 & -U_3 \end{bmatrix}$$

$$\Gamma_4 = \begin{bmatrix} 0 & 0 & U_3 \\ 0 & 0 & -U_3 \\ U_3 & -U_3 & 0 \end{bmatrix}$$

Lamination parameters are bound by the values of -1 and +1.

$$-1 \leq V_{iA} \leq 1 \quad (i=1, \dots, 4) \quad (11)$$

In order to generate meaningful laminate stiffness matrices, lamination parameters are constrained by an allowable combination of and . The acceptable domain for the in-plane lamination parameters was defined in 1997 by Hammer et al. The feasible region of arbitrary set of lamination parameters is a convex and closed surface in (Grenestedt 1991).

$$2V_{1A}^2(1 - V_{3A}) + 2V_{2A}^2(1 + V_{2A}) + V_{3A}^2 + V_{4A}^2 - 4V_{1A}V_{2A}V_{4A} \leq 1 \quad (12)$$

Design problems, as the one of the Wilhelminaberg Viewpoint, require the optimization of a both extensional and flexural structural behavior. Limiting our design to balanced and symmetric laminates, the equation above becomes:

$$V_{2A} = V_{4A} = 0 \quad (13)$$

$$V_{3A} \geq 2V_{1A}^2 - 1 \quad (14)$$

$$V_{3D} \geq 2V_{1D}^2 - 1 \quad (15)$$

The allowable combination domains of lamination parameters can be depicted graphically in the form of the following diagrams. While ply orientations can take any value from -90° to $+90^\circ$, practical applications often limit orientations angles to the following angle sets 0° , 30° , 45° , 60° , and 90° . This results in laminates not being the most optimal applications from a structural point of view but reflect an approach more aware of manufacturing limits.

While the diagram represents the convex and closed surface of lamination parameters, either in-plane or out-of-plane, further feasible domains for the lamination parameters can be defined within that surface for specific combination of the lamina orientation. Points along the parabola correspond to laminates made of a single fiber orientation. A line between two points then refers to the lamination parameters that result from the combination of the two corresponding fiber orientation. Similarly, any point in an area defined by 3 or more points must correspond to lamination parameters of laminates with fiber orientations of the vertices of the area. These sub-domains for laminate designs composed of laminae of $[0^\circ, \pm 45^\circ, \pm 90^\circ]$, $[0^\circ, \pm 30^\circ, \pm 60^\circ]$, $[\pm 30^\circ, \pm 45^\circ, \pm 60^\circ]$, and even $[0^\circ, \pm 30^\circ, \pm 45^\circ, \pm 60^\circ, \pm 90^\circ]$ are illustrated in the figure D1.1.

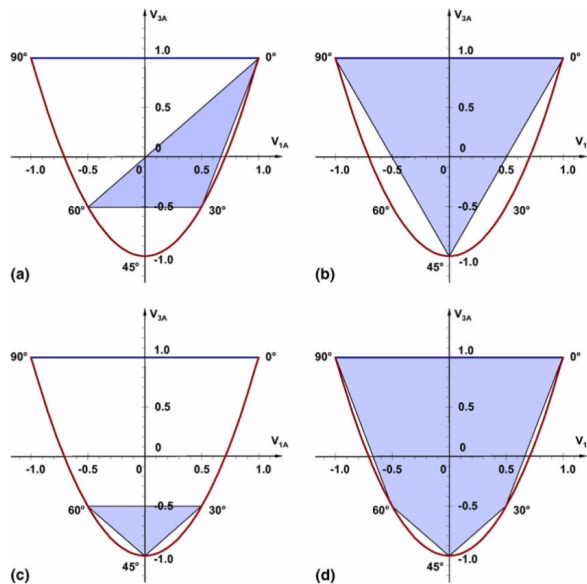


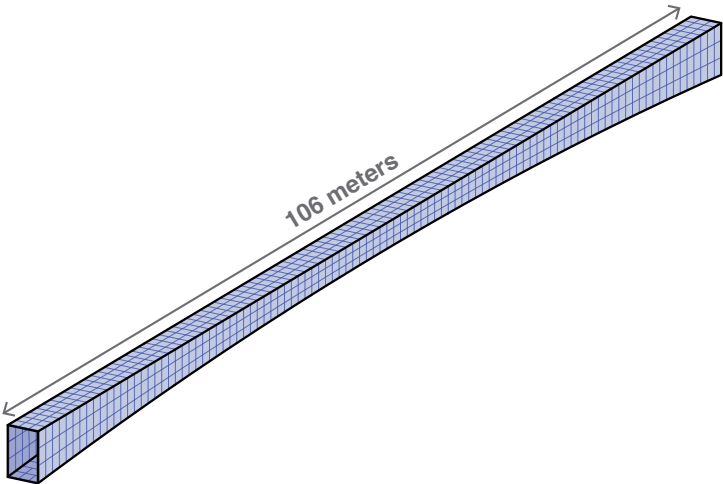
Figure D1.1 In-plane lamination parameter diagrams and feasible domains for discrete angle ply laminates. (a) Laminates from 0° , 30° and 60° angle plies, (b) laminates from 0° , 90° and 45° angle plies, (c) laminates from 30° , 45° and 60° angle plies, and (d) laminates from 0° , 30° , 45° , 60° and 90° angle plies [8]

Appendix F

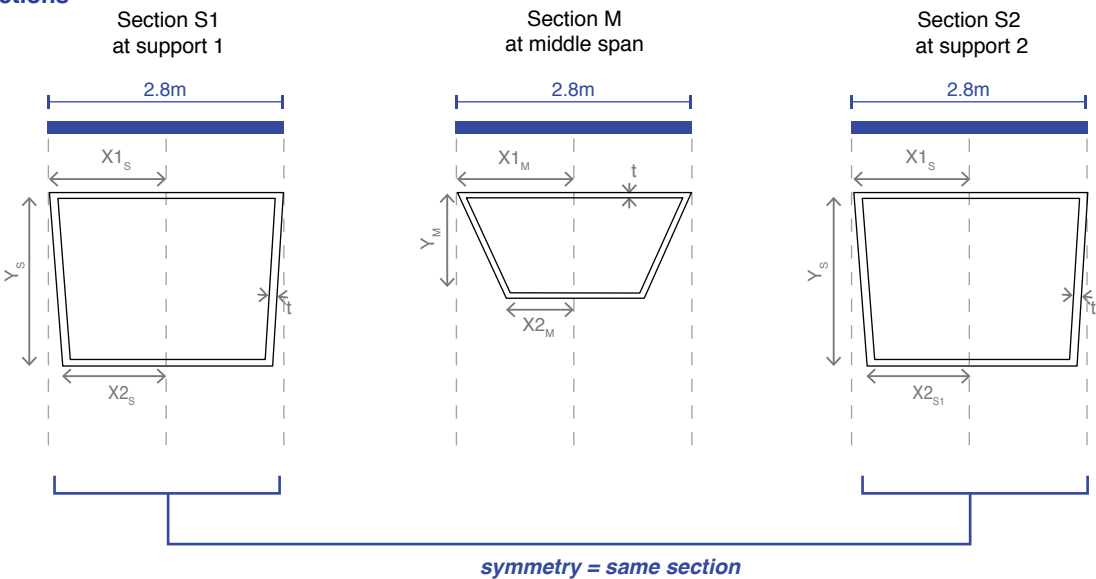
F1. Tool Development: Multi-objective Optimization

Initial definitions of the framework used a multiple objective optimization. In order to test the efficiency of a multi-objective optimization, the structure was simplified with an unrolled straight structure of also 106m. The two defined objectives are strain energy and weight.

3D Impression



Sections



Parameters

$X1_s$	Top width at sections S1 & S2	1.4	(m)
$X2_s$	Bottom width at sections S1 & S2	[0.1 - 1.4]	(m)
Y_s	Depth at sections S1 & S2	[0.1 - 8.0]	(m)
$X1_M$	Top width at section M	1.4	(m)
$X2_M$	Bottom width at section M	[0.1 - 1.4]	(m)
Y_M	Depth at section M	[0.1 - 4.0]	(m)
t	Thickness	[5.0 - 10.0]	(cm)

Figure F1.1 (top) Unrolled straight structure, L=106m in length. (bottom) Parameters defining the geometry.

As shown in figure F.2, the multi-objective optimization results in many optimal solutions at the Pareto-front for one scenario. Each scenario requires significant amount of processing in order to rank their structure once the multi-objective optimization is run.

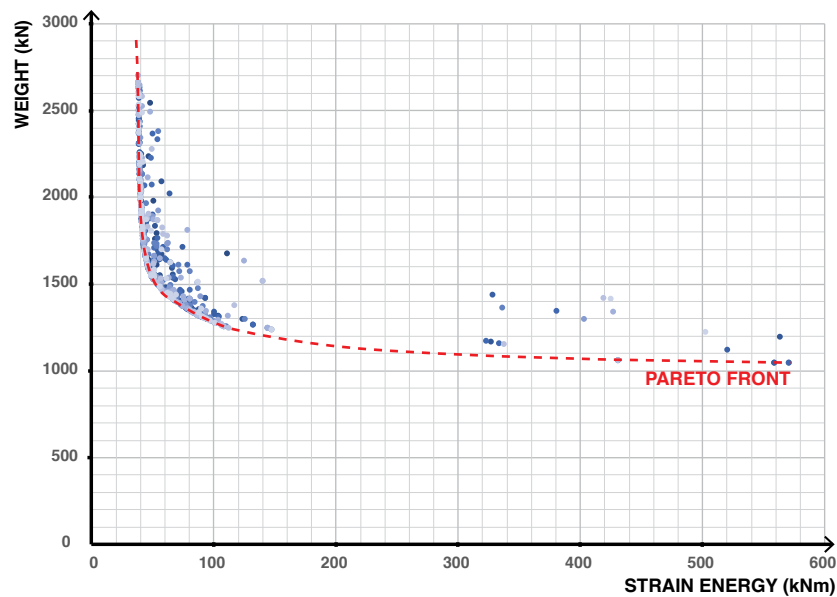


Figure F1.2 Pareto-front generated in the multi-objective optimization of the straight quadrilateral beam.

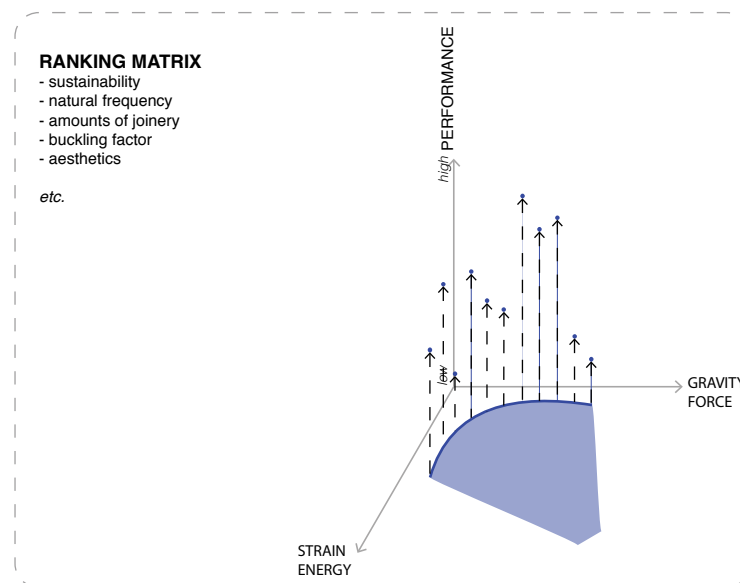


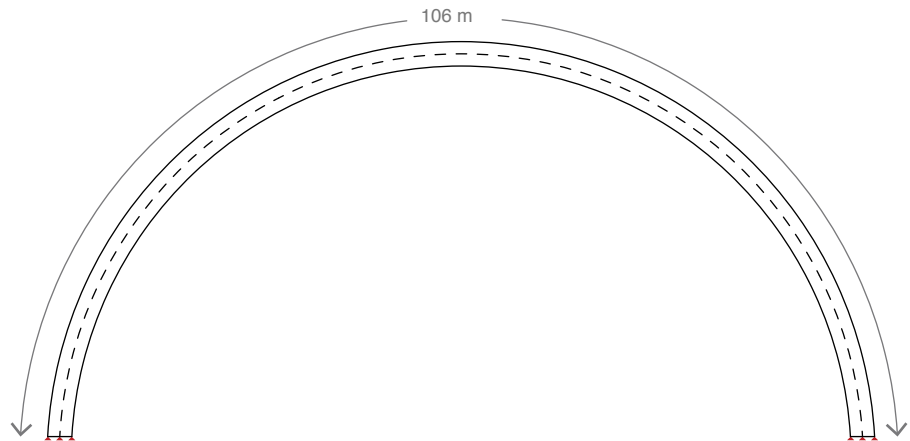
Figure F1.3 Significant post-processing required to rank the “optimal” solutions on the Pareto Front.

Considering the scope of this research is to encourage formal exploration in FRP, multi-objective optimization is dropped in favor of single-objective optimization. The explication of the rational is closely described in chapter 5 of the research.

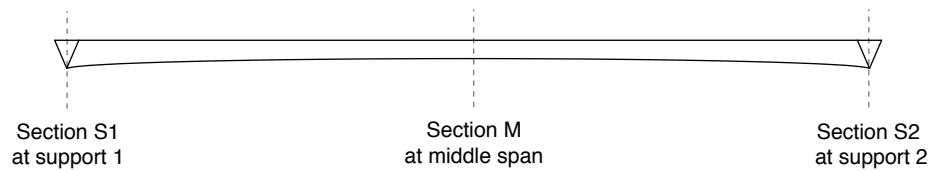
Appendix G

G1. Parameters of Scenario 1: Triangular Symmetric Fixed-width Deck (TSF)

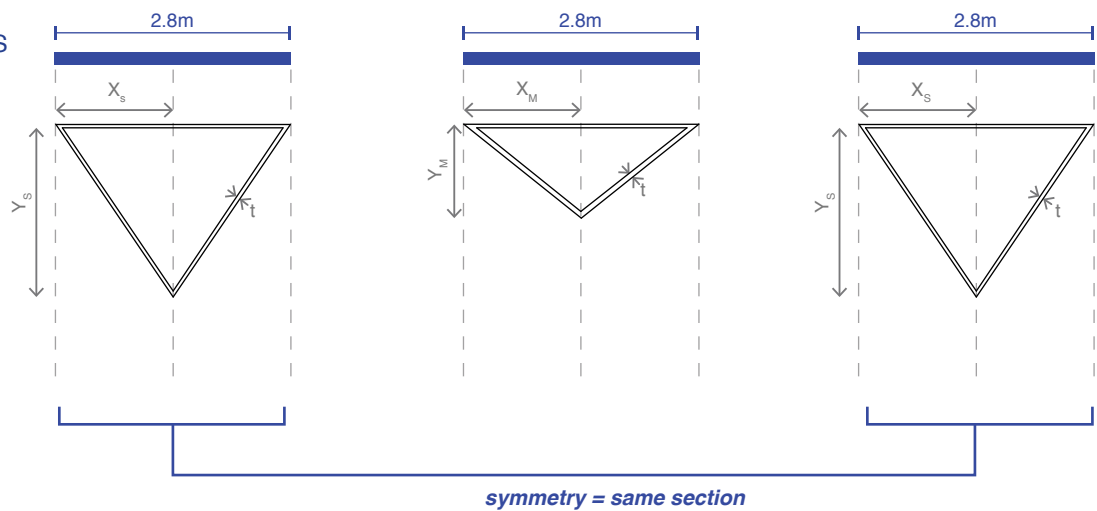
PLAN VIEW



SIDE VIEW



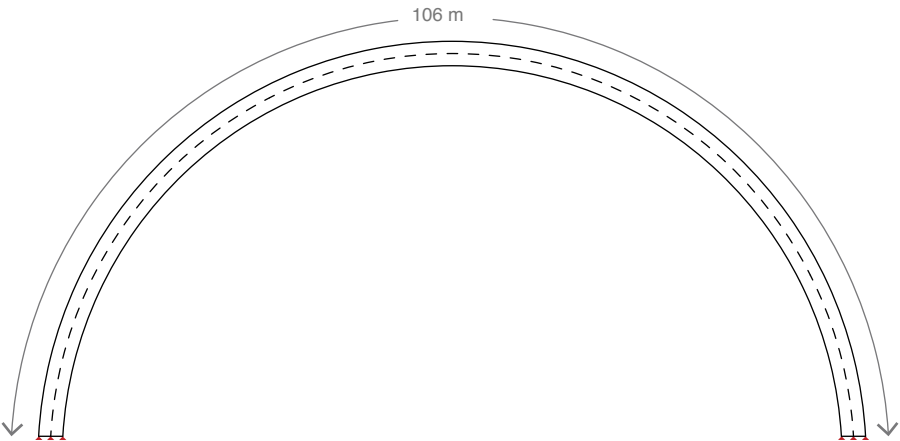
SECTIONS



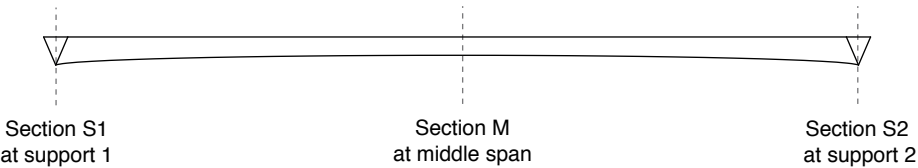
PARAMETERS	VARIABLES	DEFINITION	VALUE/BOUNDARY	UNITS
	X_s	Width at sections S1 & S2	1.4	(m)
	Y_s	Depth at sections S1 & S2	[0.1 - 8.0]	(m)
	X_M	Width at section M	1.4	(m)
	Y_M	Width at section M	[0.1 - 4.0]	(m)
	t	Thickness	[5.0 - 10.0]	(cm)

G2. Parameters of Scenario 2: Triangular Symmetric Cantilevering Deck (TSC)

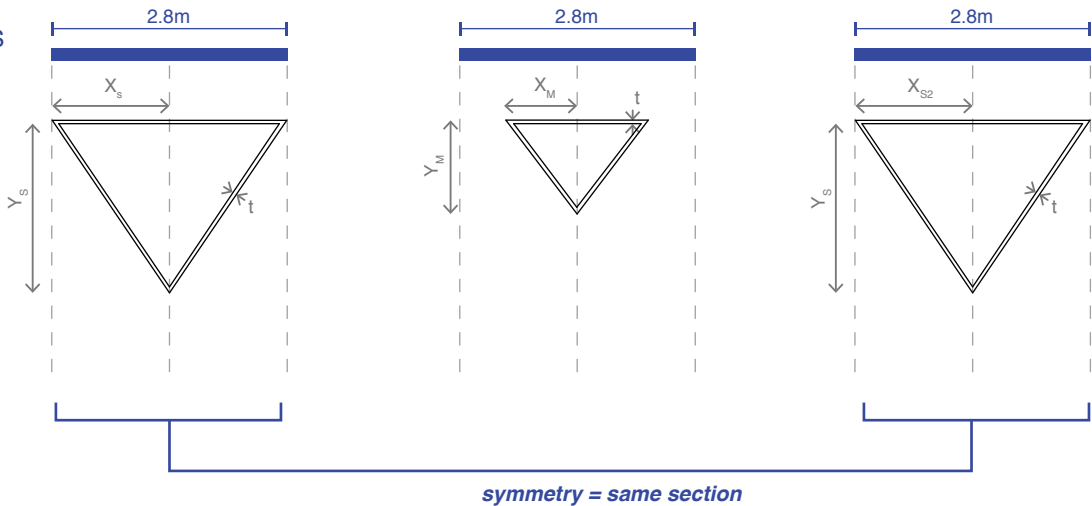
PLAN VIEW



SIDE VIEW



SECTIONS

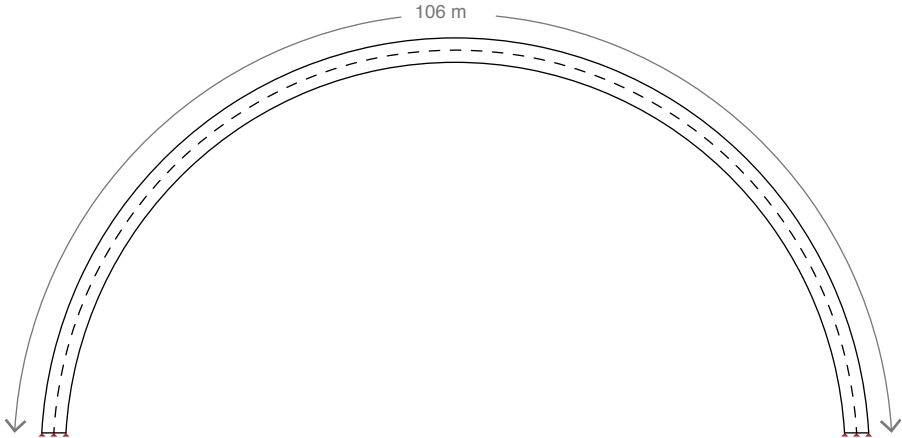


PARAMETERS

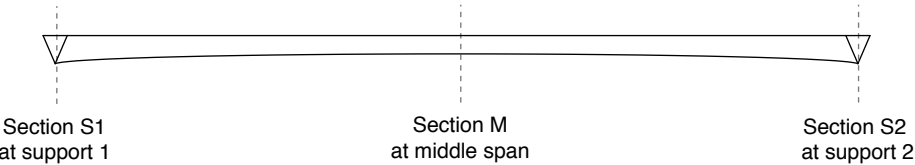
VARIABLES	DEFINITION	VALUE/BOUNDARY	UNITS
X_s	Width at sections S1 & S2	[0.5 - 1.4]	(m)
Y_s	Depth at sections S1 & S2	[0.1 - 8.0]	(m)
X_M	Width at section M	[0.5 - 1.4]	(m)
Y_M	Depth at section M	[0.1 - 4.0]	(m)
t	Thickness	[5.0 - 10.0]	(cm)

G3. Parameters of Scenario 3: Triangular Asymmetric Fixed-width Deck (TAF)

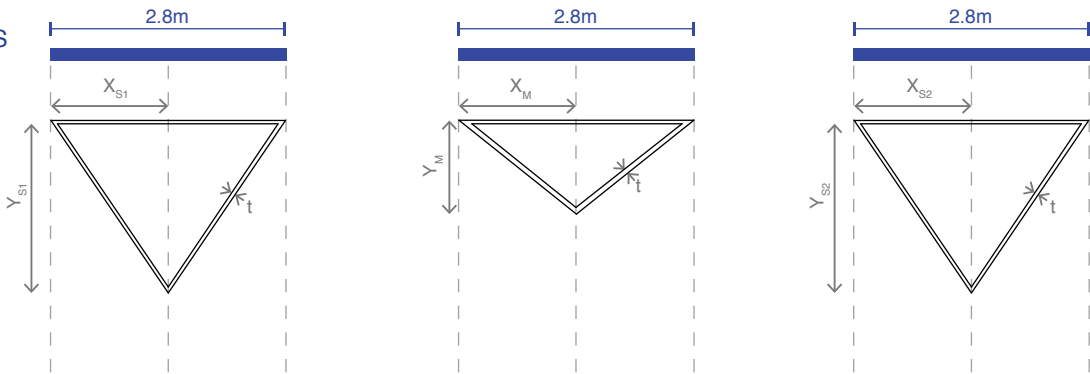
PLAN VIEW



SIDE VIEW

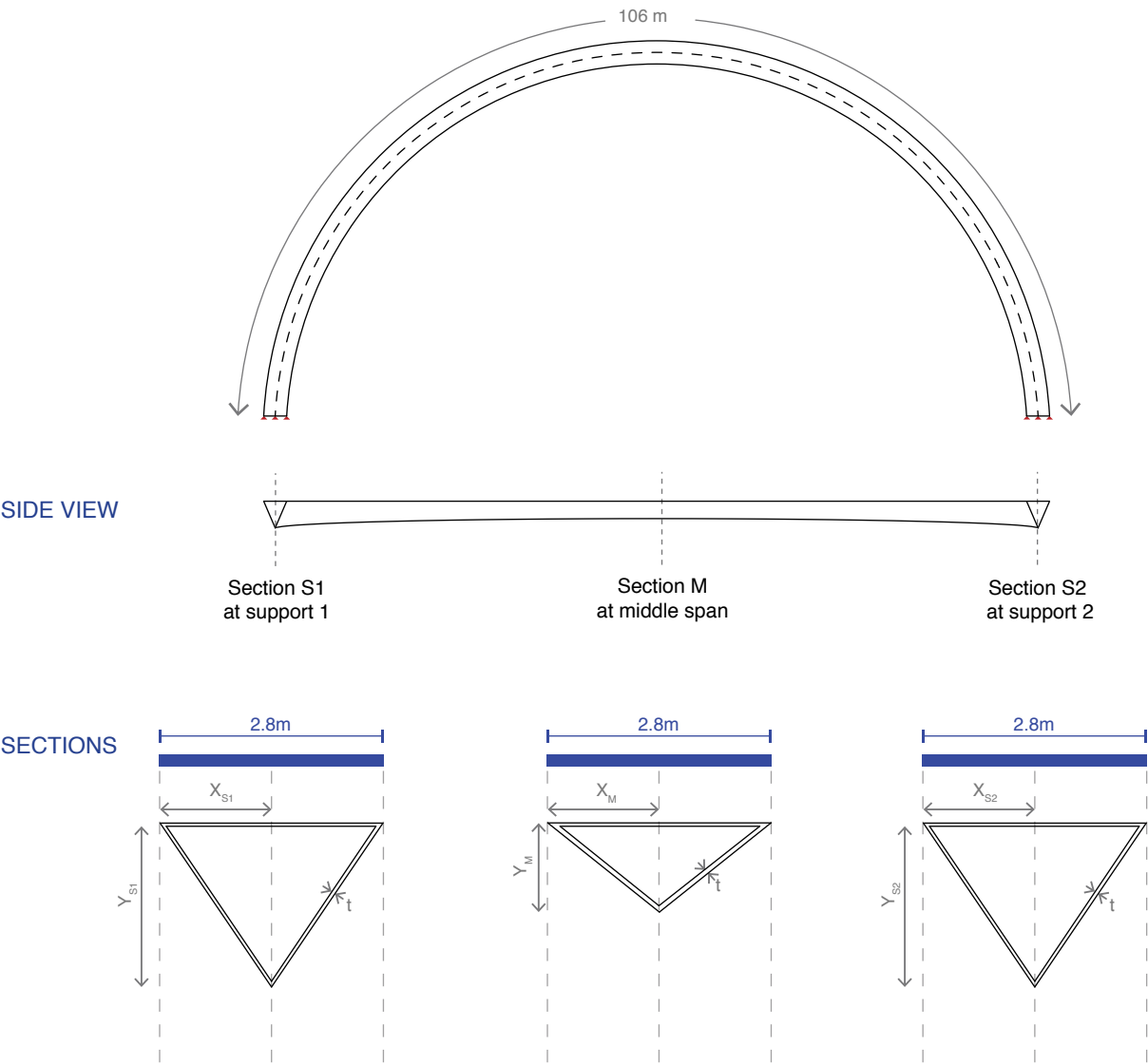


SECTIONS



PARAMETERS	VARIABLES	DEFINITION	VALUE/BOUNDARY	UNITS
	X_s	Width at section S1	1.4	(m)
	Y_s	Depth at section S1	[0.1 - 8.0]	(m)
	X_s	Width at section S2	1.4	(m)
	Y_s	Depth at section S2	[0.1 - 8.0]	(m)
	X_M	Width at section M	1.4	(m)
	Y_M	Depth at section M	[0.1 - 4.0]	(m)
	f_{S1}	Asymmetric factor at S1	[-1.0 - 1.0]	(m)
	f_{S2}	Asymmetric factor at S2	[-1.0 - 1.0]	(m)
	f_M	Asymmetric factor at M	[-1.0 - 1.0]	(m)
	t	Thickness	[5.0 - 10.0]	(cm)

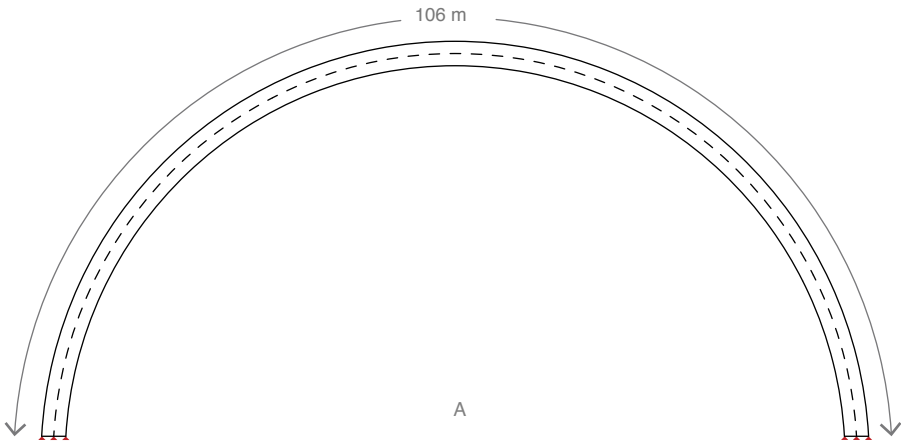
G4. Parameters of Scenario 1: Triangular Asymmetric Cantilevering Deck (TAC)



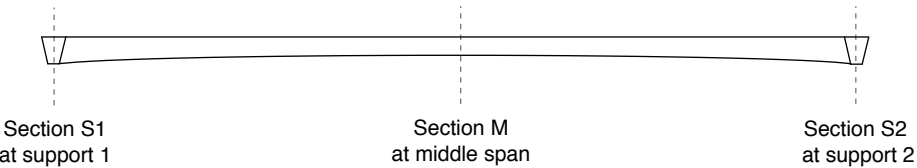
PARAMETERS	VARIABLES	DEFINITION	VALUE/BOUNDARY	UNITS
	X_s	Width at section S1	[0.5 - 1.4]	(m)
	Y_s	Depth at section S1	[0.1 - 8.0]	(m)
	X_s	Width at section S2	[0.5 - 1.4]	(m)
	Y_s	Depth at section S2	[0.1 - 8.0]	(m)
	X_M	Width at section M	[0.5 - 1.4]	(m)
	Y_M	Depth at section M	[0.1 - 8.0]	(m)
	f_{S1}	Asymmetric factor at S1	[-1.0 - 1.0]	(m)
	f_{S2}	Asymmetric factor at S2	[-1.0 - 1.0]	(m)
	f_M	Asymmetric factor at M	[-1.0 - 1.0]	(m)
	t	Thickness	[5.0 - 10.0]	(cm)

G5. Parameters of Scenario 1: Quadrilateral Symmetric Fixed-width Deck (QSF)

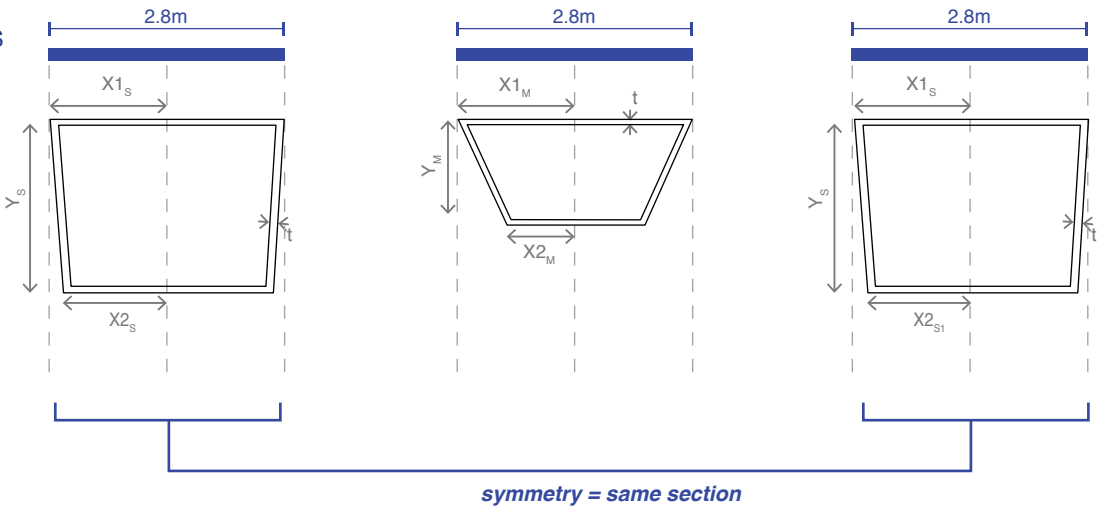
PLAN VIEW



SIDE VIEW

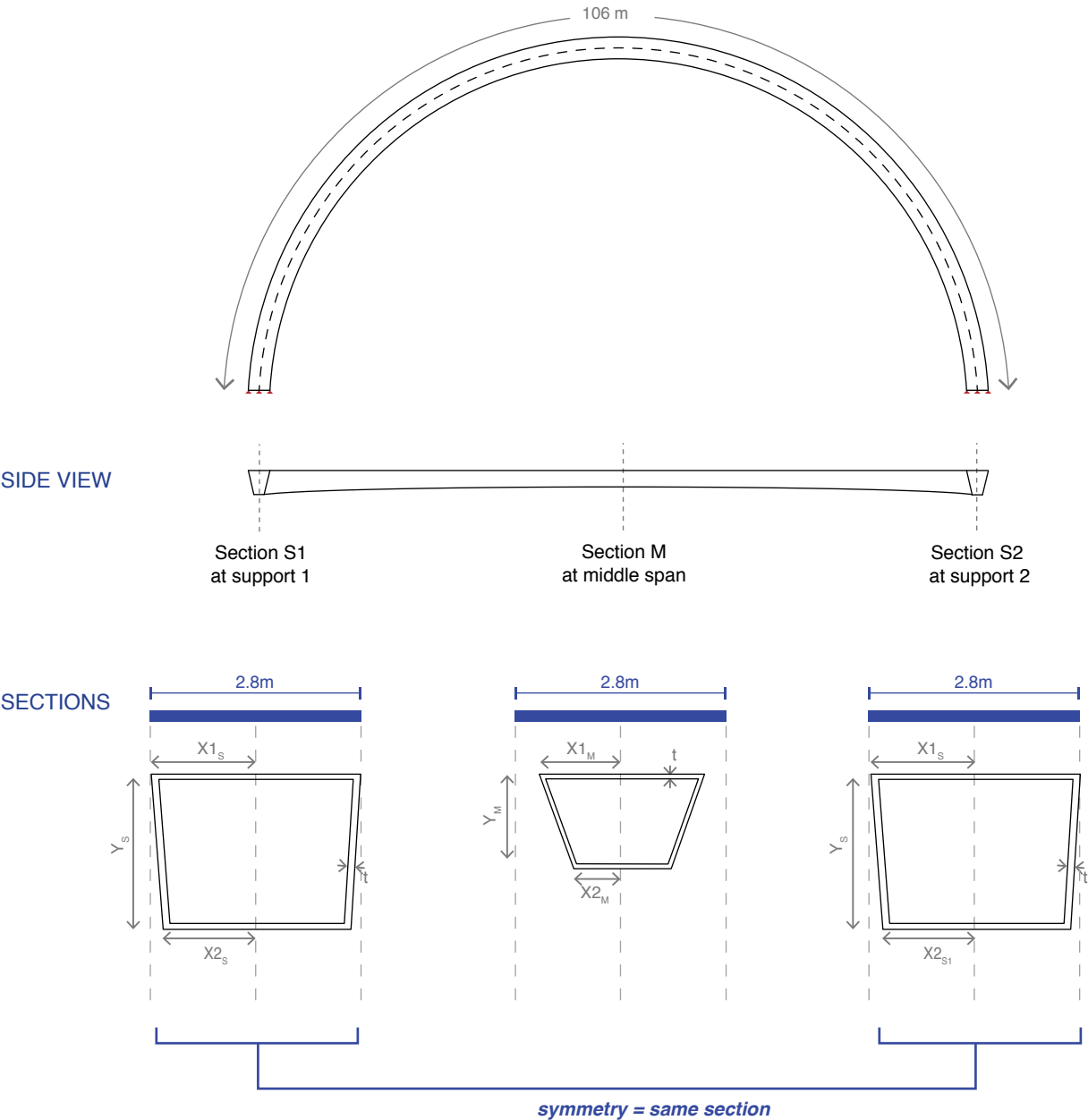


SECTIONS



PARAMETERS	VARIABLES	DEFINITION	VALUE/BOUNDARY	UNITS
	$X1_s$	Top width at sections S1 & S2	1.4	(m)
	$X2_s$	Bottom width at sections S1 & S2	[0.1 - 1.4]	(m)
	Y_s	Depth at sections S1 & S2	[0.1 - 8.0]	(m)
	$X1_M$	Top width at section M	1.4	(m)
	$X2_M$	Bottom width at section M	[0.1 - 1.4]	(m)
	Y_M	Depth at section M	[0.1 - 4.0]	(m)
	t	Thickness	[5.0 - 10.0]	(cm)

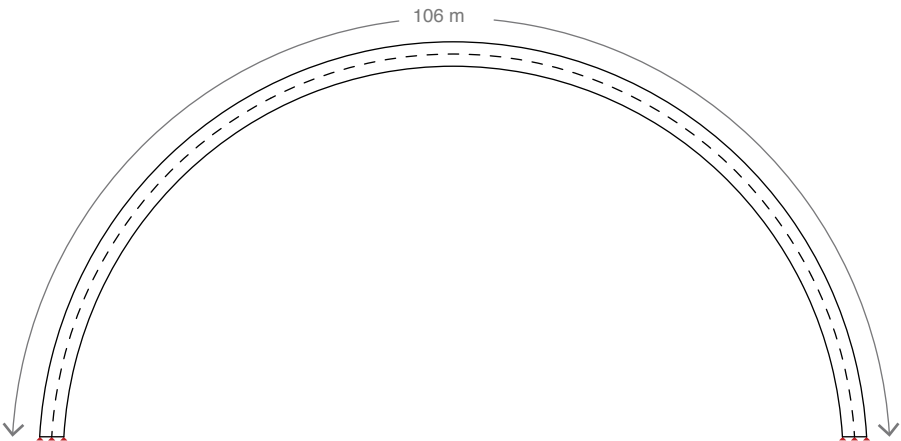
G6. Parameters of Scenario 1: Quadrilateral Symmetric Cantilevering Deck (QSC)



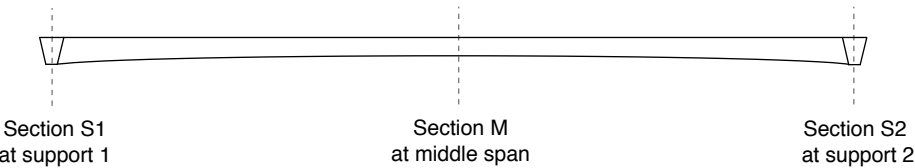
PARAMETERS	VARIABLES	DEFINITION	VALUE/BOUNDARY	UNITS
	$X1_s$	Top width at sections S1 & S2	[0.5 - 1.4]	(m)
	$X2_s$	Bottom width at section S1 & S2	[0.1 - 1.4]	(m)
	Y_s	Depth at section S1	[0.1 - 8.0]	(m)
	$X1_M$	Top width at section M	[0.5 - 1.4]	(m)
	$X2_M$	Bottom width at section M	[0.1 - 1.4]	(m)
	Y_M	Depth at section M	[0.1 - 4.0]	(m)
	f_{S1}	Asymmetric factor at S1	[-1.0 - 1.0]	(m)
	f_{S2}	Asymmetric factor at S2	[-1.0 - 1.0]	(m)
	f_M	Asymmetric factor at M	[-1.0 - 1.0]	(m)
	t	Thickness	[5.0 - 10.0]	(cm)

G7. Parameters of Scenario 1: Quadrilateral Asymmetric Fixed-width Deck (QAF)

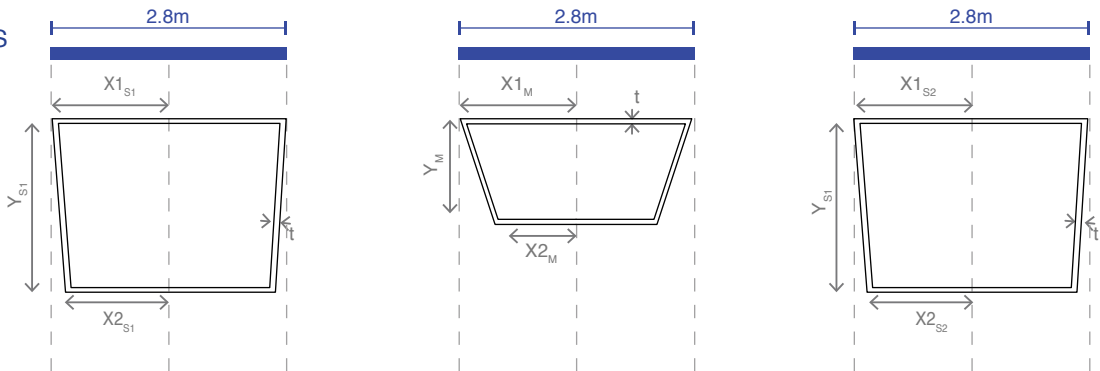
PLAN VIEW



SIDE VIEW

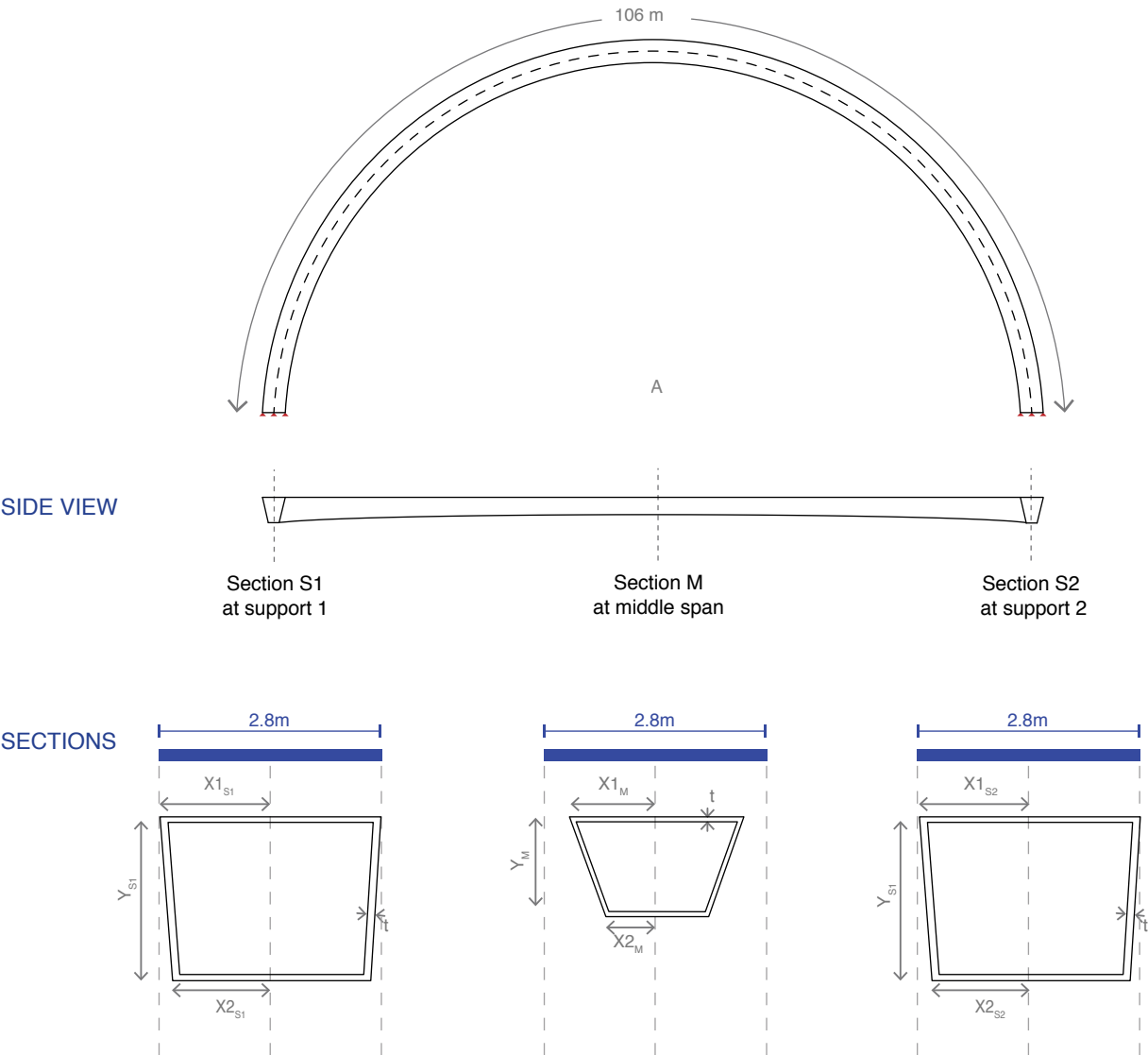


SECTIONS



PARAMETERS	VARIABLES	DEFINITION	VALUE/BOUNDARY	UNITS
	$X1_{S1}$	Top width at section S1	1.4	(m)
	$X2_{S1}$	Bottom width at section S1	[0.1 - 1.4]	(m)
	Y_{S1}	Depth at section S1	[0.1 - 8.0]	(m)
	$X1_{S2}$	Top width at section S2	1.4	(m)
	$X2_{S2}$	Bottom width at section S2	[0.1 - 1.4]	(m)
	Y_{S2}	Depth at section S2	[0.1 - 8.0]	(m)
	$X1_M$	Top width at section M	1.4	(m)
	$X2_M$	Bottom width at section M	[0.1 - 1.4]	(m)
	Y_M	Depth at section M	[0.1 - 4.0]	(m)
	f_{S1}	Asymmetric factor at S1	[-1.0 - 1.0]	(m)
	f_{S2}	Asymmetric factor at S2	[-1.0 - 1.0]	(m)
	f_M	Asymmetric factor at M	[-1.0 - 1.0]	(m)
	t	Thickness	[5.0 - 10.0]	(cm)

G8. Parameters of Scenario 1: Quadrilateral Asymmetric Cantilevering Deck (QAC)



PARAMETERS	VARIABLES	DEFINITION	VALUE/BOUNDARY	UNITS
	$X1_{S1}$	Top width at section S1	[0.5 - 1.4]	(m)
	$X2_{S1}$	Bottom width at section S1	[0.1 - 1.4]	(m)
	Y_{S1}	Depth at support S1	[0.1 - 8.0]	(m)
	$X1_{S2}$	Top width at section S2	[0.5 - 1.4]	(m)
	$X2_{S2}$	Bottom width at section S2	[0.1 - 1.4]	(m)
	Y_{S2}	Depth at section S2	[0.1 - 8.0]	(m)
	$X1_M$	Top width at section M	[0.5 - 1.4]	(m)
	$X2_M$	Bottom width at section M	[0.1 - 1.4]	(m)
	Y_M	Depth at middle span M	[0.1 - 4.0]	(m)
	f_{S1}	Asymmetric factor at section S1	[-1.0 - 1.0]	(m)
	f_{S2}	Asymmetric factor at section S2	[-1.0 - 1.0]	(m)
	f_M	Asymmetric factor at section M	[-1.0 - 1.0]	(m)
	t	Thickness	[5.0 - 10.0]	(cm)

Appendix H

H1. Material Properties: Summary

1. Material Selection

The material for a specific laminate will be chosen for either low, medium, or high performance. Value for E_{11} , E_{22} , G_{12} , G_{13} , G_{23} , and ν_{12} are specified. Material options are the high performing carbon/epoxy options shown in table H1.1.

	AS4	IM6	IM7
Longitudinal Modulus (E_1 , GPa)	142	172	156
Transverse Modulus (E_2 , GPa)	10.3	10.0	10.8
Shear Modulus (G_{12} , GPa)	7.2	6.2	6.0
Poisson's Ratio (ν_{12})	0.27	0.29	0.30
Longitudinal Tensile Strength (X_t , MPa)	2280	2760	2860
Longitudinal Compressive Strength (X_c , MPa)	1440	1540	1875
Transverse Tensile Strength (Y_t , MPa)	57	50	49
Transverse Compressive Strength (Y_c , MPa)	228	152	246
Shear Strength (S , MPa)	71	124	83

Table H1.1 Composite Materials and their corresponding properties. Tabulated material properties for the materials options to conduct this research. AS4/APC2: carbon-PEEL; IM6/3501-6: carbon-epoxy; IM7/8552: carbon-epoxy [9], [10].

2. Laminate Selection

IM6 is chosen: it has a $V_f = 60\%$, appropriate for vacuum infusion production. Using the layups shown in figure H1.1, the following laminate layup combinations (figure H1.2) are designed. The derived properties are summarized in table H1.2. They are derived in the next section using the CLT online tool.

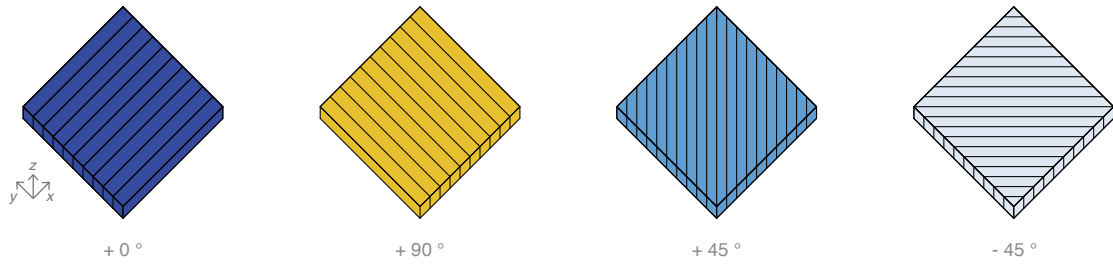


Figure H1.1 The considered laminate layouts (0° , $\pm 45^\circ$, and 90°), widely available in structural applications.

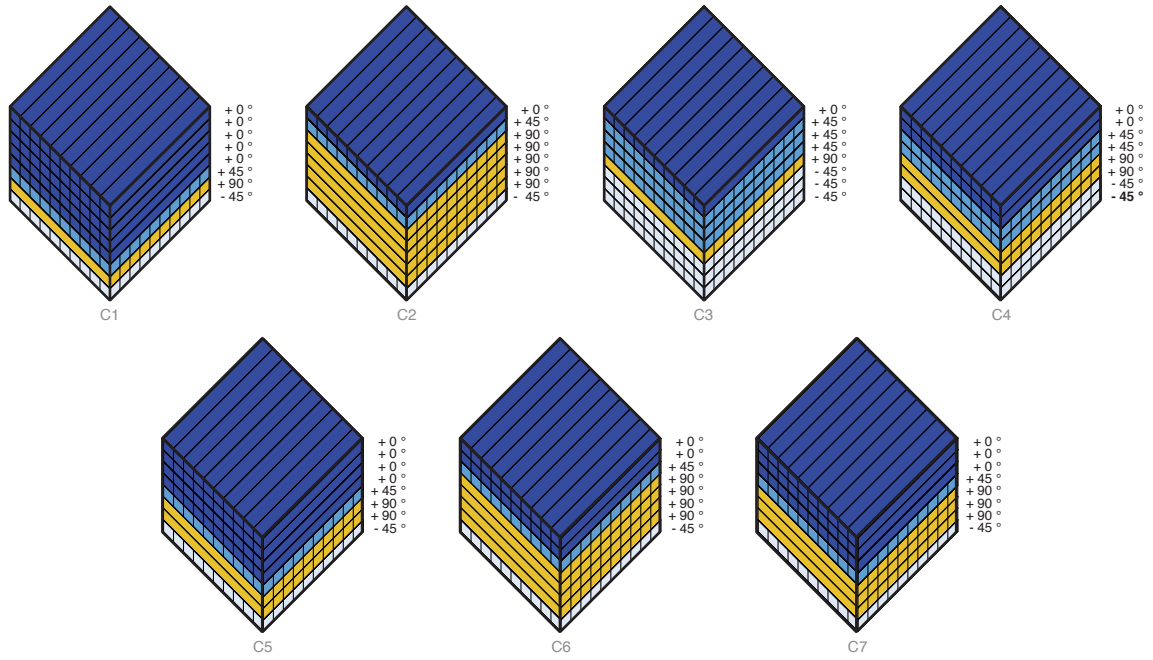


Figure H1.2 Sections of the different considered laminate layout combinations.

Laminate Layup Combinations	E_1 (GPa)	E_2 (GPa)	G_{12} (GPa)	ν_{12}	σ_1 (MPa)	σ_2 (MPa)	τ_{12} (MPa)
C1 $0^\circ/62.5\%;45^\circ/12.5\%; 90^\circ/12.5\%; -45^\circ/12.5\%$	118.7	40	15.6	0.3	1425	480	250
C2 $0^\circ/12.5\%; 45^\circ/12.5\%; 90^\circ/62.5\%; -45^\circ/12.5\%$	40	118.7	15.6	0.1	480	1425	250
C3 $0^\circ/12.5\%; 45^\circ/37.5\%; 90^\circ/12.5\%; -45^\circ/37.5\%$	47.7	47.7	35	0.5	572	572	560
C4 $0^\circ/25\%; 45^\circ/25\%; 90^\circ/25\%; -45^\circ/25\%$	65.9	65.9	25	0.3	791	791	400
C5 $0^\circ/50.0\%; 45^\circ/12.5\%; 90^\circ/25.0\%; -45^\circ/12.5\%$	100	60.4	15.6	0.2	1200	724	250
C6 $0^\circ/25.0\%; 45^\circ/12.5\%; 90^\circ/50.0\%; -45^\circ/12.5\%$	60.4	100	15.6	0.12	724	1200	250
C7 $0^\circ/37.5\%; 45^\circ/12.5\%; 90^\circ/37.5\%; -45^\circ/12.5\%$	80	80	15.6	0.15	960	960	250

Table H1.2 Properties of the different laminate layout combinations.

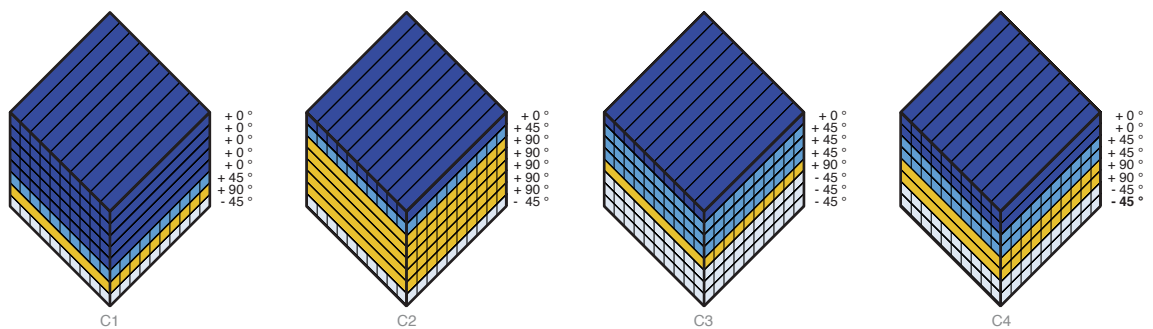


Figure H1.3 The four chosen laminate layout combinations with the extreme values for E_1 , E_2 and G_{12} .

H2. Material Properties: Derivation

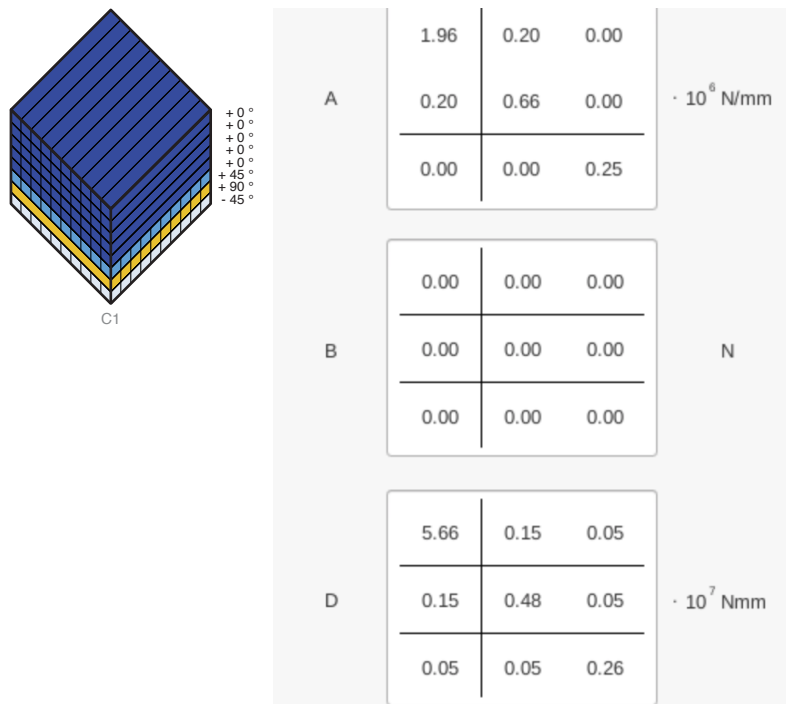


Figure H2.1 Screenshot from the online tool generating the [A], [B], [D] matrices for a laminate using the online CLT tool [11].

C1	0°	45°	90°	45°
%	62.5	12.5	12.5	12.5

A_{11}	1.96E+06	N/mm
A_{22}	6.60E+05	N/mm
A_{12}	2.00E+05	N/mm
A_{66}	2.50E+05	N/mm

E_1	118.7	Gpa
E_2	40.0	GPa
G_{12}	15.6	GPa
ν_{12}	0.30	
ν_{21}	0.10	

σ_1	1425	MPa
σ_2	480	MPa
τ	250	MPa

Table H2.1 Properties of the laminate layup combinations C1.

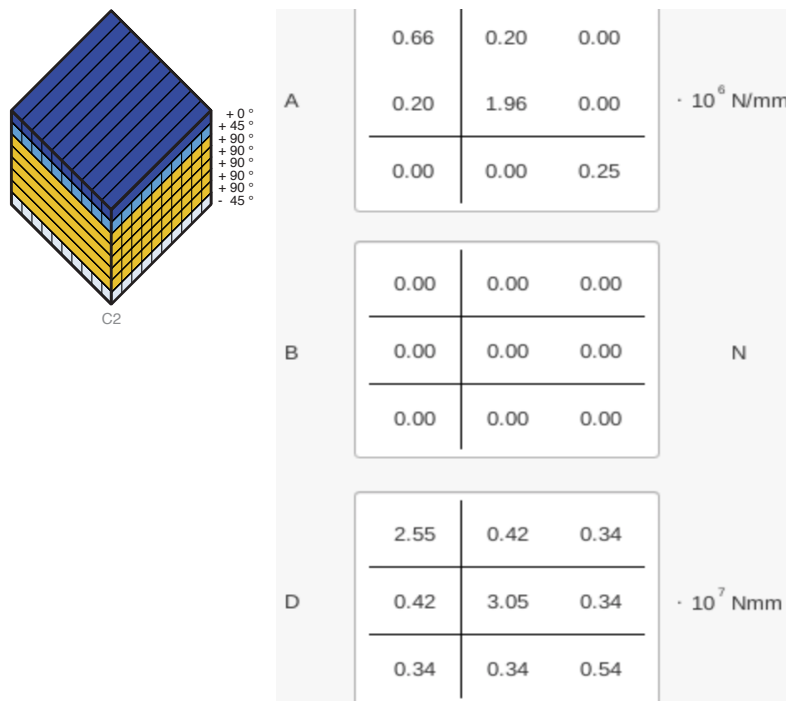


Figure H2.2 Screenshot from the online tool generating the [A], [B], [D] matrices for a laminate using the online CLT tool [10].

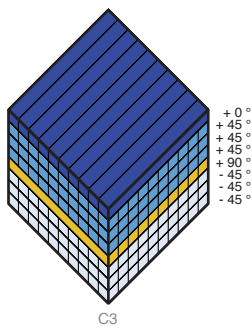
C2	0°	45°	90°	45°
%	12.5	12.5	62.5	12.5

A_{11}	6.60E+05	N/mm
A_{22}	1.96E+06	N/mm
A_{12}	2.00E+05	N/mm
A_{66}	2.50E+05	N/mm

E_1	40.0	GPa
E_2	118.7	GPa
G_{12}	15.6	GPa
ν_{12}	0.10	
ν_{21}	0.30	

σ_1	480	MPa
σ_2	1425	MPa
τ	250	MPa

Table H2.2 Properties of the laminate layup combinations C2.



A	1.01	0.50	0.00	$\cdot 10^6$ N/mm
	0.50	1.01	0.00	
	0.00	0.00	0.56	
B	0.00	0.00	0.00	N
	0.00	0.00	0.00	
	0.00	0.00	0.00	
D	3.06	0.88	0.68	$\cdot 10^7$ Nmm
	0.88	1.63	0.68	
	0.68	0.68	0.99	

Figure H2.3 Screenshot from the online tool generating the [A], [B], [D] matrices for a laminate using the online CLT tool [10].

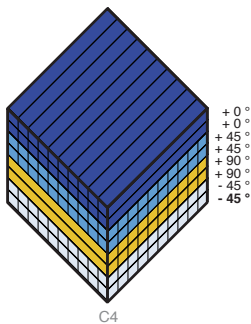
C3	0°	45°	90°	45°
%	12.5	37.5	12.5	37.5

A_{11}	1.01E+06	N/mm
A_{22}	1.01E+06	N/mm
A_{12}	5.00E+05	N/mm
A_{66}	5.60E+05	N/mm

E_1	47.7	GPa
E_2	47.7	GPa
G_{12}	35.0	GPa
ν_{12}	0.50	
ν_{21}	0.50	

σ_1	572	MPa
σ_2	572	MPa
τ	560	MPa

Table H2.3 Properties of the laminate layup combinations C3.



A	1.16	0.35	0.00	$\cdot 10^6$ N/mm
	0.35	1.16	0.00	
	0.00	0.00	0.40	
B	0.00	0.00	0.00	N
	0.00	0.00	0.00	
	0.00	0.00	0.00	
D	4.02	0.51	0.39	$\cdot 10^7$ Nmm
	0.51	1.41	0.39	

Figure H2.4 Screenshot from the online tool generating the [A], [B], [D] matrices for a laminate using the online CLT tool [10].

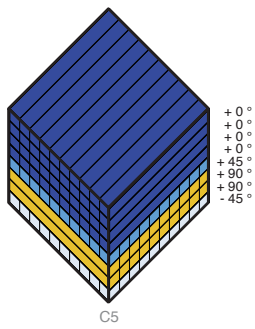
C4	0°	45°	90°	45°
%	25	25	25	25

A_{11}	1.16E+05	N/mm
A_{22}	1.16E+05	N/mm
A_{12}	3.50E+05	N/mm
A_{66}	4.00E+05	N/mm

E_1	65.9	GPa
E_2	65.9	GPa
G_{12}	25.0	GPa
ν_{12}	0.30	
ν_{21}	0.30	

σ_1	791	MPa
σ_2	791	MPa
τ	400	MPa

Table H2.4 Properties of the laminate layup combinations C4.



A	1.64	0.20	0.00	$\cdot 10^6 \text{ N/mm}$
	0.20	0.99	0.00	
	0.00	0.00	0.25	
B	0.00	0.00	0.00	N
	0.00	0.00	0.00	
	0.00	0.00	0.00	
D	5.31	0.20	0.10	$\cdot 10^7 \text{ Nmm}$
	0.20	0.73	0.10	
	0.10	0.10	0.31	

Figure H2.5 Screenshot from the online tool generating the [A], [B], [D] matrices for a laminate using the online CLT tool [10].

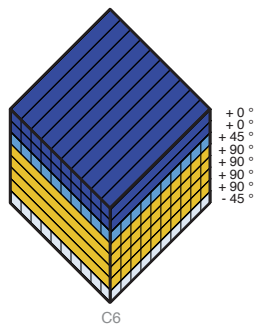
C5	0°	45°	90°	45°
%	50	12.5	25	12.5

A_{11}	1.64E+06	N/mm
A_{22}	9.90E+05	N/mm
A_{12}	2.00E+05	N/mm
A_{66}	2.50E+05	N/mm

E_1	100.0	GPa
E_2	60.4	GPa
G_{12}	15.6	GPa
ν_{12}	0.20	
ν_{21}	0.12	

σ_1	1200	MPa
σ_2	724	MPa
τ	250	MPa

Table H2.5 Properties of the laminate layup combinations C5.



A	0.99	0.20	0.00	$\cdot 10^6 \text{ N/mm}$
	0.20	1.64	0.00	
	0.00	0.00	0.25	
B	0.00	0.00	0.00	N
	0.00	0.00	0.00	
	0.00	0.00	0.00	
D	3.82	0.33	0.24	$\cdot 10^7 \text{ Nmm}$
	0.33	1.95	0.24	
	0.24	0.24	0.45	

Figure H2.6 Screenshot from the online tool generating the [A], [B], [D] matrices for a laminate using the online CLT tool [10].

C2	0°	45°	90°	45°
%	25	12.5	50	12.5

A_{11}	9.90E+05	N/mm
A_{22}	1.64E+06	N/mm
A_{12}	2.00E+05	N/mm
A_{66}	2.50E+05	N/mm

E_1	60.4	GPa
E_2	100.0	GPa
G_{12}	15.6	GPa
ν_{12}	0.12	
ν_{21}	0.20	

σ_1	724	MPa
σ_2	1200	MPa
τ	250	MPa

Table H2.6 Properties of the laminate layup combinations C6.

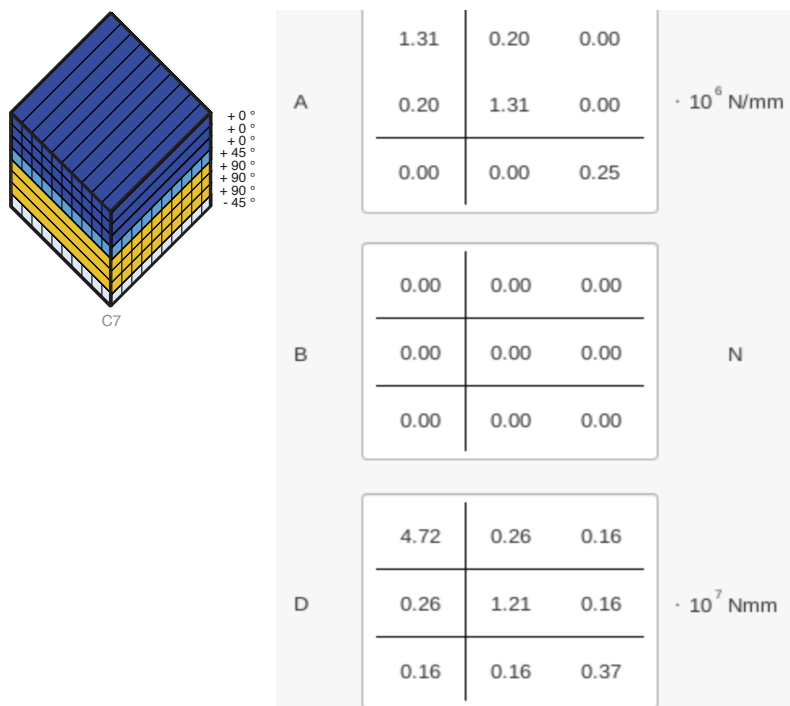


Figure H2.7 Screenshot from the online tool generating the [A], [B], [D] matrices for a laminate using the online CLT tool [10].

C3	0°	45°	90°	45°
%	37.5	12.5	37.5	12.5

A_{11}	1.31E+06	N/mm
A_{22}	1.31E+06	N/mm
A_{12}	2.00E+05	N/mm
A_{66}	2.50E+05	N/mm

E_1	80.0	GPa
E_2	80.0	GPa
G_{12}	15.6	GPa
ν_{12}	0.15	
ν_{21}	0.15	

σ_1	960	MPa
σ_2	960	MPa
τ	250	MPa

Table H2.7 Properties of the laminate layup combinations C7.

Appendix I

I1. Determining Load-Areas

Defining the corresponding load areas is equally important. A study of all possible load-area combinations was conducted in order to find the most critical situation. The most critical load-area is defined as the one that renders the smaller buckling factor, least stiff (maximum strain energy), and largest deflection.

The load areas are tested with 5 different geometries. Consistently, the most critical load was found for the load over the entire structure, load area 32. In the following, the ranking of the load areas are presented for the geometry with $X_s = 1.7\text{m}$; $X_m = 0.6\text{m}$; $Y_s = 1.8\text{m}$; $Y_m = 1.8\text{m}$; $t = 10\text{cm}$.

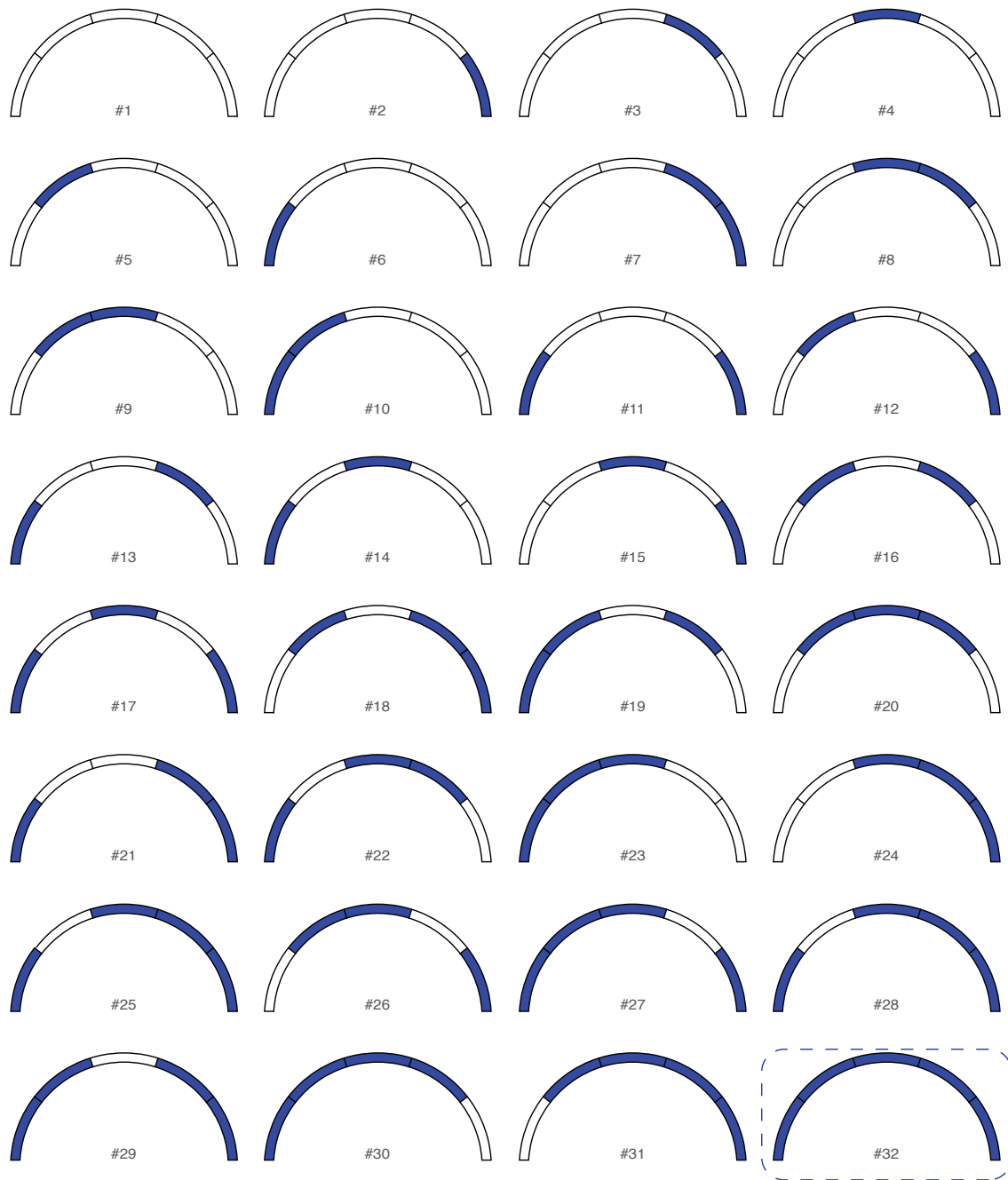


Figure I1.1 The different load-areas tested to find the most critical load-area.

RANK	Buckling factor (ranked from smallest to largest)	Number of corresponding load area
1	8.86	32
2	8.91	30
3	9.19	27
4	9.23	23
5	9.27	31
6	9.33	20
7	9.59	29
8	9.63	26
9	9.65	19
10	9.69	9
11	9.81	25
12	9.86	24
13	9.87	22
14	9.97	28
15	10.04	10
16	10.07	18
17	10.14	16
18	10.21	17
19	10.28	14
20	10.38	8
21	10.50	12
22	10.57	5
23	10.61	21
24	10.66	7
25	10.76	15
26	10.78	13
27	10.83	4
28	11.19	11
29	11.27	6
30	11.30	3
31	11.85	2
32	11.94	1

Table I1.1 Ranked Load areas for buckling load factor, small smallest to largest.

RANK	Deflection (cm) (ranked from smallest to largest)	Number of corresponding load area
1	26.78	32
2	26.53	30
3	26.53	31
4	26.27	20
5	25.87	27
6	25.84	25
7	25.61	23
8	25.61	26
9	25.59	24
10	25.59	22
11	25.44	29
12	25.35	9
13	25.33	8
14	25.19	19
15	25.19	18
16	24.93	16
17	24.92	17
18	24.67	14
19	24.66	15
20	24.53	28
21	24.51	21
22	24.41	4
23	24.28	10
24	24.27	12
25	24.25	13
26	24.25	7
27	24.02	5
28	23.99	3
29	23.58	11
30	23.33	6
31	23.33	2
32	23.07	1

Table I1.2 Ranked Load areas for occurring deflection, small smallest to largest.

RANK	Strain Energy (kNm) (ranked from smallest to largest)	Number of corresponding load area
1	1471.50	32
2	1459.43	31
3	1459.11	30
4	1447.10	20
5	1422.57	25
6	1421.60	27
7	1411.69	24
8	1410.60	22
9	1410.45	23
10	1409.95	26
11	1405.25	29
12	1399.78	8
13	1398.86	9
14	1394.10	18
15	1393.80	19
16	1382.72	16
17	1375.06	17
18	1364.61	15
19	1364.33	14
20	1360.88	21
21	1359.95	28
22	1353.94	4
23	1350.93	7
24	1349.85	13
25	1349.74	10
26	1349.23	12
27	1339.97	3
28	1339.09	5
29	1317.97	11
30	1308.45	2
31	1308.19	6
32	1298.73	1

Table I1.3 Ranked Load areas for occurring deflection, small least stiff to stiffest.

I2. Approximating Cable-effect in the case study

The Wilhelminaberg Viewpoint presents a complex-structural system combining the rings (originally designed in steel) and pre-stressed cables. The effect of the cables must be incorporated in the structural analysis. The pre-stress of the cables cannot be simplified to the effect of forces; the cables contribute to the global stability of the structure. These cables will be pre-stressed and participate in increasing the stiffness of the structure.

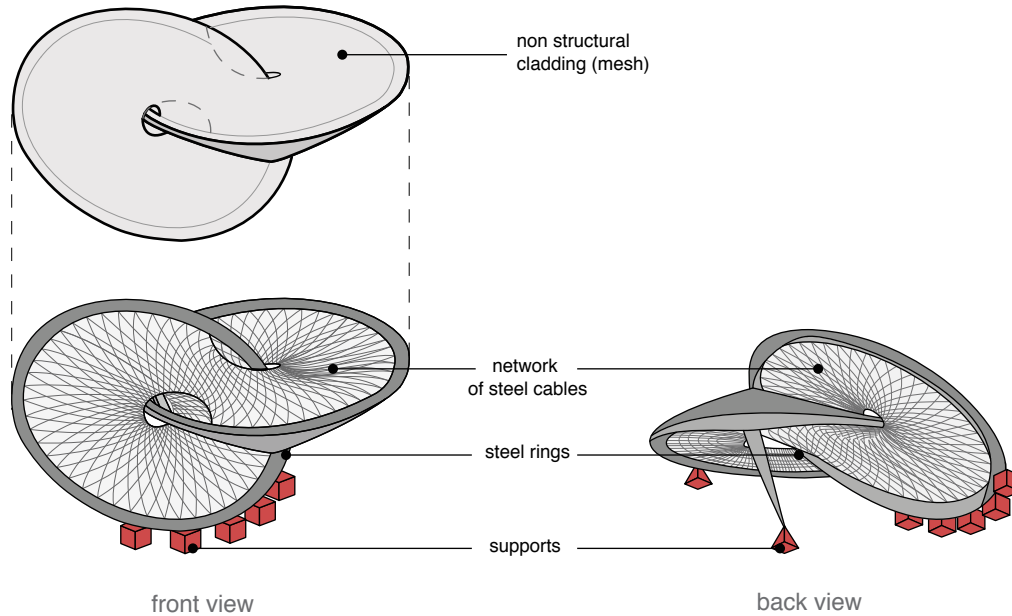


Figure I2.1 Structural system of the Wilhelminaberg Viewpoint.

The values of the tension in the cables under ULS and SLS are taken from the Ney & Partners. Significant experimentation took place in order to model the effect of the cables as close as possible to reality. The experimentation proved first the effect of the cables on the stability of a structure. A grasshopper code was developed to simplify the many cables over the considered span into a smaller number of cables with equivalent pre-stress loads. Eventually, modeling 7 cables was found to accurately model the effect of the cables over the considered span: an error less than 10% in both ULS and SLS (Table I2.3). This allows to expedite the modeling process significantly.

In Grasshopper, the stress in each cable is input manually, then the cables are divided in 7 groups and for each group a cable with an equivalent force and moment are generated. This is done twice for the ULS and SLS load cases. While this approximation saves time, it leads to some discrepancy between the real situation and the equivalent one.

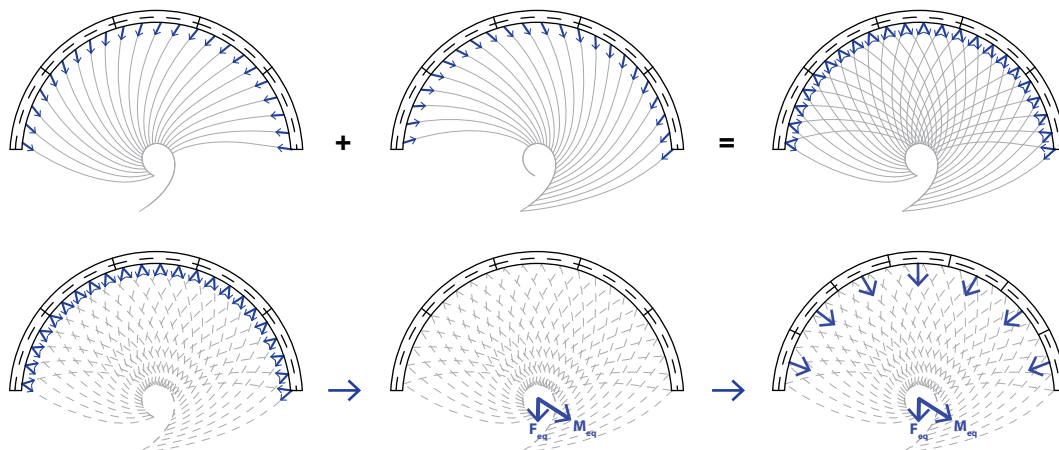


Figure I2.3 Simplification of the cables into groups of 7 cables.

	Vector magnitude	Vector coordinates
VECTOR 1	3246.65	{1509.17, -2687.18, 1020.88}
VECTOR 2	3779.58	{388.07, -3708.61, 617.16}
VECTOR 3	5866.55	{-1635.81, -5633.039819, -96.79}
VECTOR 4	4866.91	{-3093.47, -3618.69, -1011.10}
VECTOR 5	4948.21	{-4157.00, -2118.06, -1648.60}
VECTOR 6	5049.68	{-4619.81, -588.01, -1952.14}
VECTOR 7	7353.42	{-6401.07, 2300.05, -2794.43}

Table I2.1 Equivalent vector coordinates in ULS.

	Vector magnitude	Vector coordinates
VECTOR 1	2561.142	{1195.67, -2116.00, 807.70}
VECTOR 2	2946.612	{301.43, -2891.51, 480.45}
VECTOR 3	4507.149	{-1244.44, -4331.43, -67.26}
VECTOR 4	3750.759	{-2368.257988, -2805.159764, -768.521418}
VECTOR 5	3956.781	{-3322.983149, -1697.68689, -1315.962622}
VECTOR 6	4034.190	{-3689.523941, -489.957171, -1556.29174}
VECTOR 7	6175.053	{-5394.116019, 1874.853372, -2349.407835}

Table I2.2 Equivalent vector coordinates in ULS.

	x	y	z
Error ULS (%)	10.140	4.820	5.650
Error SLS (%)	6.080	4.610	6.940

Table I2.3 Equivalent error between equivalent loads and errors, (x,y,x) are the coordinate of the vector.

Appendix K

K1. Determining Mesh Size

Mesh size is an important aspect of finite element analysis. Defining the mesh density of an analysis is thus a compromise between accuracy of results and computational time. Bigger mesh elements lead to results with large errors while smaller elements increase significantly the computational time. Furthermore, it is hard to predict where exactly a chosen mesh size is on that scale but it can be estimated. Running a mesh density analysis is thus central to determine the mesh size and obtain accurate enough results with an acceptable computational time [12], [13] .

A mesh density analysis requires to perform a chosen analysis multiple times for different mesh sizes. The data of each should be recorded: number of elements, number of nodes, the computation time, the outcome (deflection, buckling factor, etc.) of the model. A similar mesh analysis is run to determine the mesh size of this framework. In order to determine the mesh size, a singular geometry under a load is run multiple time with decreasing mesh size.

The mesh density analysis is run for multiple geometries. Comparing the values of the buckling load factor, the accuracy of the mesh size is evaluated. Taking a structure with an unrolled length of 106m, the mesh sizes vary between 0.25m and 1.25m. For each mesh analysis, graph visualizing the buckling load factor in function of $1/N$ are plotted. The buckling load factor is determined as $1/N$ approaches 0. Then the error in % is plotted in function of mesh size and time of calculation. This allows to visualize the compromise of accuracy and computational efficiency. It is found that the mesh size of 0.5m gives a good enough accuracy, evaluated at 10%.

Mesh Analysis 1:

Parameters	Mesh Size Res. (m)	Number of Elements E	Number of Nodes N	Time (ms)	Buckling Factor	Buckling error (%)
(Xs=18; Xm=9; Ys=2.5; Ym=2.5; t=7.5)	0.50	8501.00	4283.00	8134.00	5.81	8.10
(Xs=18; Xm=9; Ys=2.5; Ym=2.5; t=7.5)	0.60	6061.00	3065.00	3416.00	5.81	8.12
(Xs=18; Xm=9; Ys=2.5; Ym=2.5; t=7.5)	0.70	4309.00	2177.00	2177.00	6.18	15.14
(Xs=18; Xm=9; Ys=2.5; Ym=2.5; t=7.5)	0.80	3742.00	1890.00	2454.00	6.12	13.99
(Xs=18; Xm=9; Ys=2.5; Ym=2.5; t=7.5)	0.90	2645.00	1342.00	-	6.60	22.81
(Xs=18; Xm=9; Ys=2.5; Ym=2.5; t=7.5)	1.00	2377.00	1206.00	1235.00	6.69	24.62

Table K1.1 Mesh analysis 1.

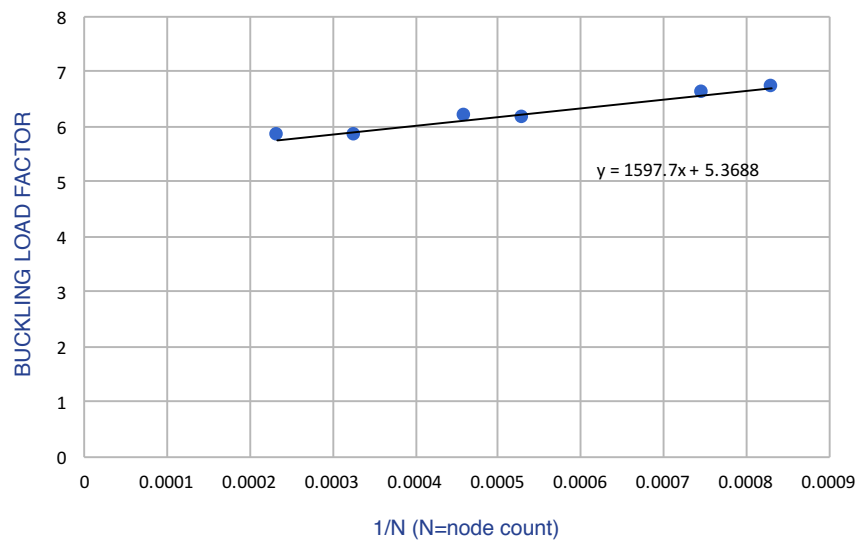


Figure K1.1 Buckling Load-factor vs. 1/N.

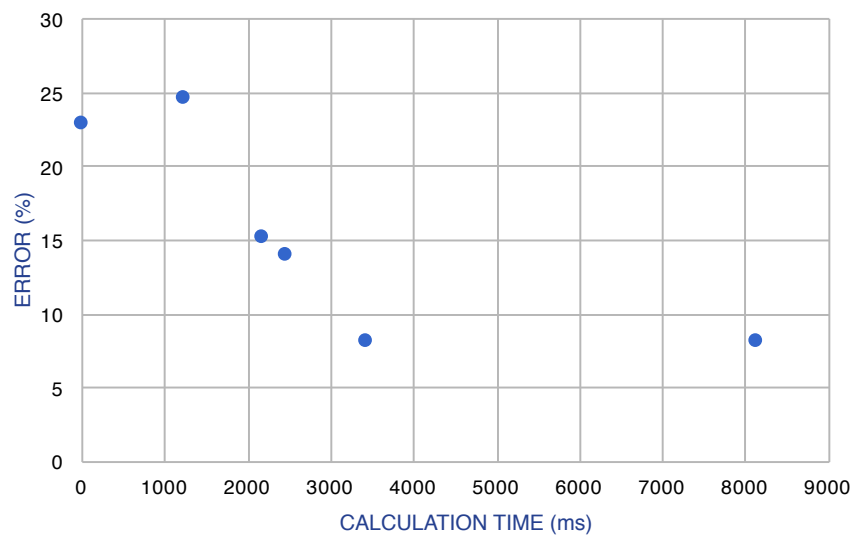


Figure K1.2 Buckling Load-factor error vs. calculation time (ms).

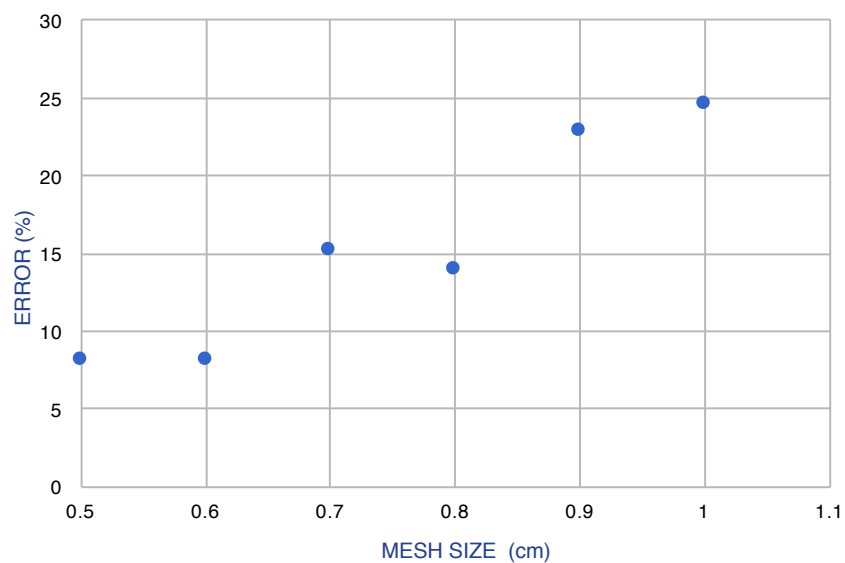


Figure K1.3 Buckling Load-factor error vs. calculation size (cm).

Mesh Analysis 2:

Parameters	Mesh Size Res. (m)	Number of Elements E	Number of Nodes N	Time (ms)	Buckling Factor	Buckling error (%)
(Xs=18; Xm=9; Ys=2.5; Ym=2.5; t=7.5)	25	4.928	4.928	4.928	4.928	1.0442
(Xs=18; Xm=9; Ys=2.5; Ym=2.5; t=7.5)	50	5.272	5.272	5.272	5.272	5.8635
(Xs=18; Xm=9; Ys=2.5; Ym=2.5; t=7.5)	75	5.639	5.639	5.639	5.639	13.2329
(Xs=18; Xm=9; Ys=2.5; Ym=2.5; t=7.5)	100	6.0084	6.0084	6.0084	6.0084	20.6506
(Xs=18; Xm=9; Ys=2.5; Ym=2.5; t=7.5)	125	6.546	6.546	6.546	6.546	31.4458

Table K1.2 Mesh analysis 1.

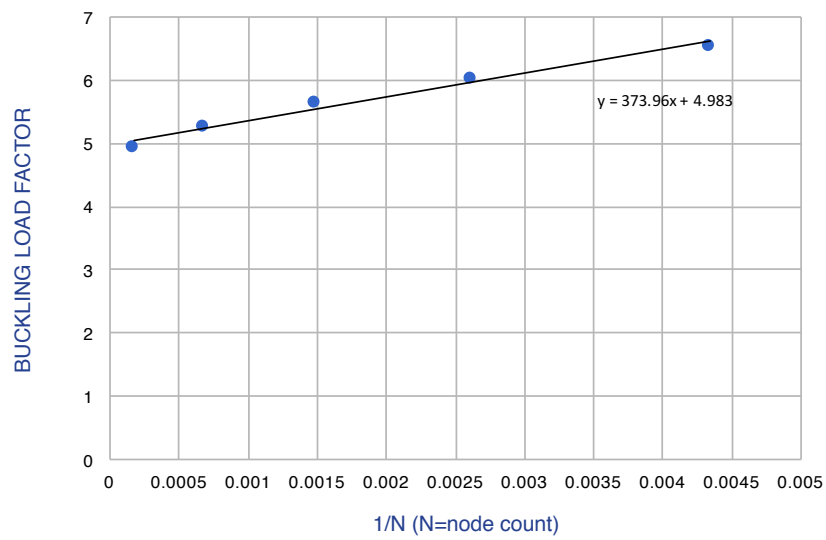


Figure K1.4 Buckling Load-factor vs. 1/N.

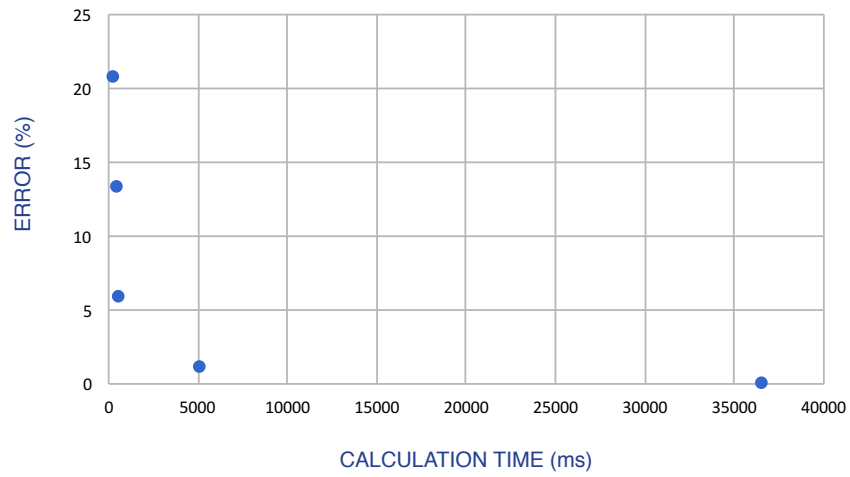


Figure K1.5 Buckling Load-factor error vs. calculation time (ms).

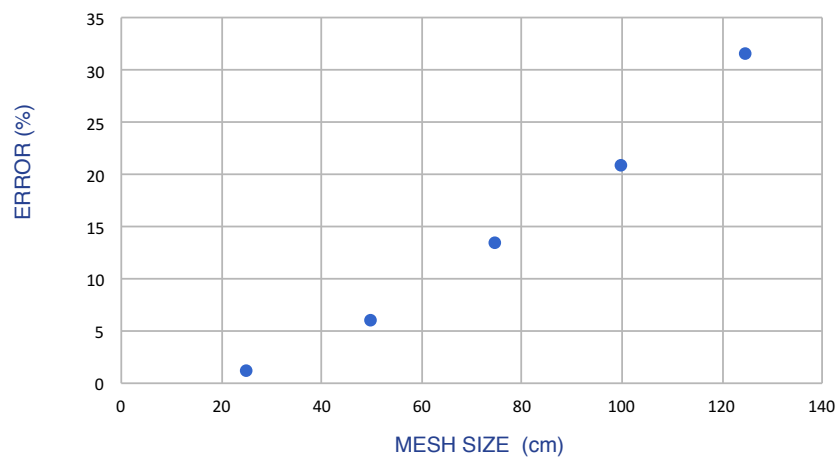


Figure K1.6 Buckling Load-factor error vs. calculation time (cm).

Appendix L

L1. Search Spaces for the 8 Scenarios

The search space corresponds to all the values that a variable can take. For each scenario, the following tables presents the number of values that a parameter can take to finally compute the total search space. In case

TSF	X_s	X_M	Y_s	Y_M	t
MIN	1.4	1.4	0.1	0.1	5
MAX	1.4	1.4	8	4	10
INTERVAL	0	0	7.9	3.9	5
POSSIBILITY	-	-	79	39	50

SEARCH SPACE: 1.54 E+05

Table L1.1 Parameters of the TSF, with the corresponding search space.

TSC	X_s	X_M	Y_s	Y_M	t
MIN	0.1	0.1	0.1	0.1	5
MAX	1.4	1.4	8	4	10
INTERVAL	1.3	1.3	7.9	3.9	5
POSSIBILITY	13	13	79	39	50

SEARCH SPACE: 2.60E+07

Table L1.2 Parameters of the TSC, with the corresponding search space.

TAF	X_{s1} (m)	X_{s2} (m)	X_M (m)	Y_{s1} (m)	Y_{s2} (m)	Y_M (m)	F₁ (m)	F₂ (m)	F₃ (m)	t (cm)
MIN	1.4	1.4	1.4	0.1	0.1	0.1	-1	-1	-1	5
MAX	1.4	1.4	1.4	8	8	4	1	1	1	10
INTERVAL	0	0	0	7.9	7.9	3.9	2	2	2	5
POSSIBILITY	-	-	-	79	79	39	20	20	20	50

SEARCH SPACE: 9.74E+10

Table L1.3 Parameters of the TAF, with the corresponding search space.

TAC	X_{s1} (m)	X_{s2}	X_M (m)	Y_{s1} (m)	Y_{s2} (m)	Y_M (m)	F₁ (m)	F₂ (m)	F₃ (m)	t (cm)
MIN	0.5	0.5	0.5	0.1	0.1	0.1	-1	-1	-1	5
MAX	1.4	1.4	1.4	8	8	4	1	1	1	10
INTERVAL	0.9	0.9	0.9	7.9	7.9	3.9	2	2	2	5
POSSIBILITY	9	9	9	79	79	39	20	20	20	50

SEARCH SPACE: 7.10E+13

Table L1.4 Parameters of the TAC, with the corresponding search space.

QSF	$S_{1.X1}$	$S_{1.X2}$	M_{X1}	M_{X2}	S_Y	M_Y	t
MIN	1.4	0.1	1.4	0.1	0.1	0.1	5
MAX	1.4	1.4	1.4	1.4	8	4	10
INTERVAL	0	1.3	0	1.3	7.9	3.9	5
POSSIBILITY	-	13	-	13	79	39	50

SEARCH SPACE: 2.60E+07

Table L1.5 Parameters of the QSF, with the corresponding search space.

QSC	$S_{1.X1}$	$S_{1.X2}$	M_{X1}	M_{X2}	S_{1-Y}	M_Y	t
MIN	0.5	0.1	0.5	0.1	0.1	0.1	5
MAX	1.4	1.4	1.4	1.4	8	4	10
INTERVAL	0.9	1.3	0.9	1.3	7.9	3.9	5
POSSIBILITY	9	13	9	13	79	39	50

SEARCH SPACE: 2.11E+09

Table L1.6 Parameters of the QSC, with the corresponding search space.

QAF	$S_{1.X1}$	$S_{1.X2}$	$S_{2.X1}$	$S_{2.X2}$	M_{X1}	M_{X2}	S_{1-Y}	S_{2-Y}	M_Y	F_{S1}	F_{S2}	F_M	t (cm)
MIN	1.4	0.1	1.4	0.1	1.4	0.1	0.1	0.1	0.1	-1	-1	-1	5
MAX	1.4	1.4	1.4	1.4	1.4	1.4	8	8	4	1	1	1	10
INTERVAL	0	1.3	0	1.3	0	1.3	7.9	7.9	3.9	2	2	2	5
POSSIBILITY	-	13	-	13	-	13	79	79	39	20	20	20	50

SEARCH SPACE: 2.14E+14

Table L1.7 Parameters of the QAF, with the corresponding search space.

QAC	$S_{1.X1}$	$S_{1.X2}$	$S_{2.X1}$	$S_{2.X2}$	M_{X1}	M_{X2}	S_{1-Y}	S_{2-Y}	M_Y	F_{S1}	F_{S2}	F_M	t (cm)
MIN	0.5	0.1	0.5	0.1	0.5	0.1	0.1	0.1	0.1	-1	-1	-1	5
MAX	1.4	1.4	1.4	1.4	1.4	1.4	8	8	4	1	1	1	10
INTERVAL	0.9	1.3	0.9	1.3	0.9	1.3	7.9	7.9	3.9	2	2	2	5
POSSIBILITY	9	13	9	13	9	13	79	79	39	20	20	20	50

SEARCH SPACE: 1.56E+17

Table L1.8 Parameters of the QAC, with the corresponding search space.

	Number of Genes	Search Space	Number of generations before convergence
T1	3	1.54E+05	44
T2	5	2.60E+07	54
T3	7	9.74E+10	122
T4	10	7.10E+13	335
Q1	5	2.60E+07	73
Q2	7	2.11E+09	83
Q3	10	2.14E+14	291
Q4	13	1.56E+17	279

Table L1.9 Variables to evaluate the computational efficiency of the generated geometries.

L2. Convergence of Graphs

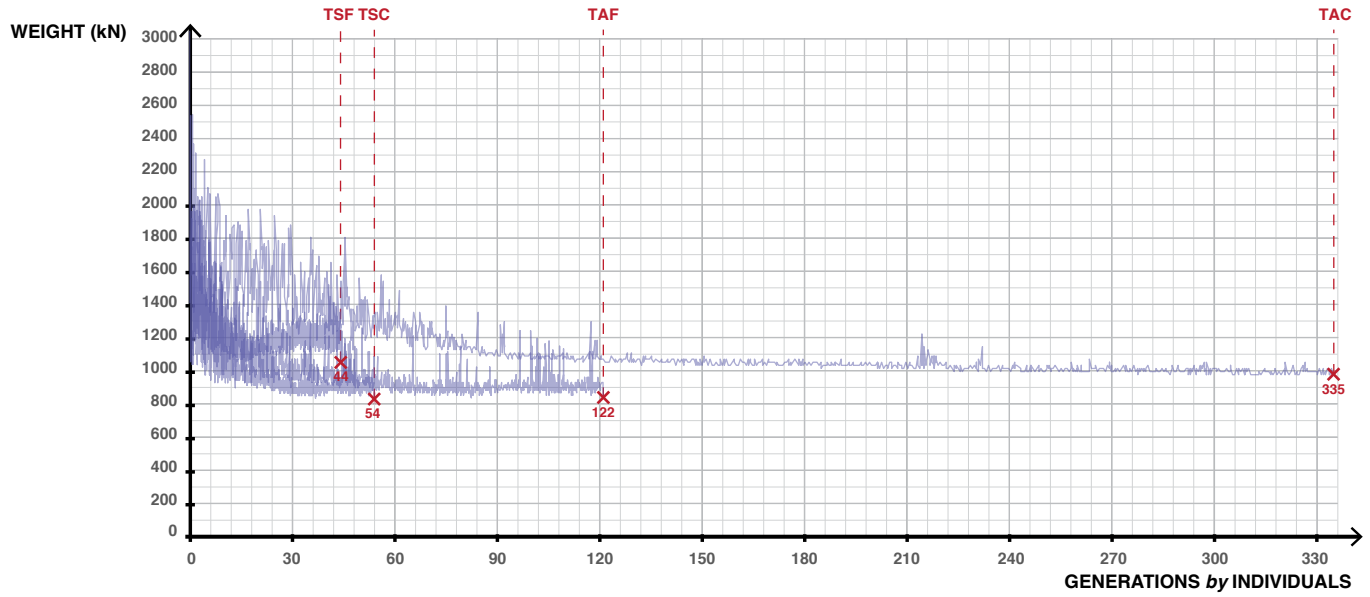


Figure L2.1 Convergence of the genetic algorithms for the triangular geometries.

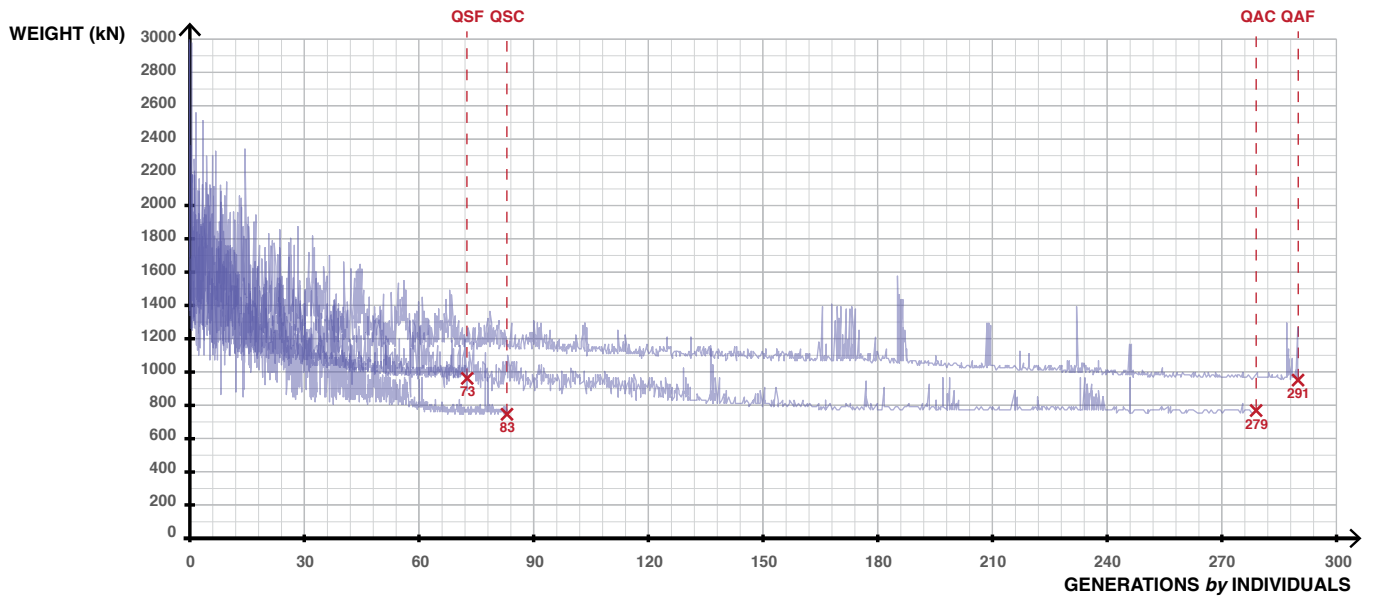


Figure L2.2 Convergence of the genetic algorithms for the quadrilateral geometries.

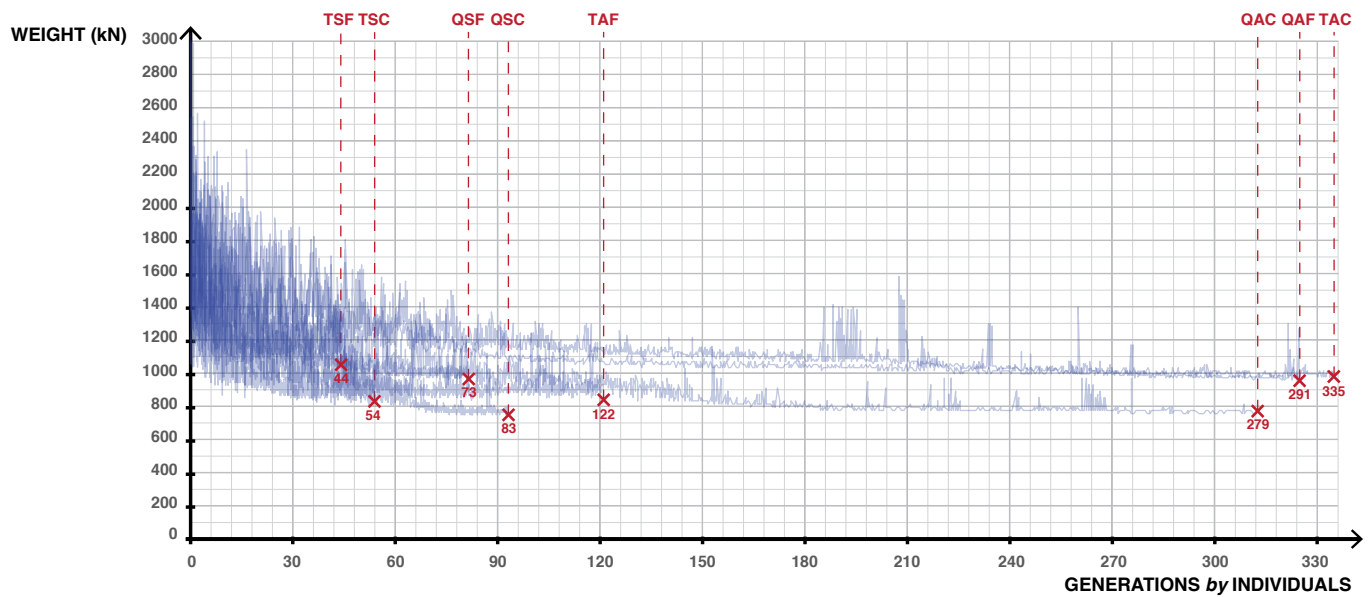


Figure L2.3 Convergence of the genetic algorithms for the eight generated geometries.

L3. Natural Frequency of the 8 structures.

Initial investigations within the design space revealed that minimizing the weight of the structure lead to the significant reduction of the natural frequency of the structure. As the Wilhelminaberg Viewpoint structure is classified as a pedestrian bridge, it is important to avoid resonance and verify comfort requirements. According to paragraph 5.7 in EN 1991-2:2003, *Eurocode 1: Actions on Structures, Part 2: Traffic Loads on Bridges*, a minimum natural frequency of at least 3 Hz is required [14]

Initial investigations reveal that imposing a minimum frequency of 3 Hz as a design constraint reduces significantly the solution space, with some iterations not returning any results. Research as well as discussions with the engineers and designers revealed that the problem of resonance and comfort levels can be solved with tuned mass damper. Another approach is thus adopted for the issue of vibration. The design constraint for natural frequency is relaxed. Natural frequency will be incorporated in evaluating the optimal design in the post-optimality analysis.

There is no scenario that present significant advantage in natural frequency (<3Hz) over the other. They will all require significant attention to solve the vibration issue.

	Natural Frequency (Hz)
TSF	1.804
TSC	2.228
TAF	1.776
TAC	2.118
QSF	1.792
QSC	2.108
QAF	1.766
QAC	2.074

Table L3.1 Natural frequency of the 8 generated geometries.

L4. Cost Estimates

Estimating the cost price of a structure is a complex process. It requires to take in consideration materiel, labor, transportation, and assembly costs. In the suggested design, carbon-fibers are used for the reinforcement. That will be the driving cost of the structure. In order to gage a general idea, the following suggests cost estimates based only on materials, specifically the reinforcement.

The material price of the reinforcement alone in FRP (carbon-fiber) is of 20€ per kilogram [15], [16]. The total price of used reinforcement will thus be calculated by multiplying V_f , the fiber volume fraction, by the unit price of carbon fiber. The cost of the resin can be neglected in comparison to the price carbon fiber. The price of the carbon fiber required for each structure is summarized in table L4.1.

It is worth noting that this pricing does not include the price of manufacturing, transportation, or assembly. It becomes clear that the 35% difference between the best of the eight geometries and the worst of the eight might become very important and a determining factor in choosing a single structure.

While carbon-fiber is still not as cost-competitive as traditional building methods, it is becoming more and more cost-efficient. Cost-effective production methods and form-resistant structures only are means to render the material more widespread. Furthermore, increased use of carbon-fibers renders the material more competitive.

	Force of Gravity (kN)	Weight (tons)	Carbon-Fiber Weight (tons)	Price in millions of Euro
TSF	1069.85	109.09	65.46	1.31
TSC	831.39	84.77	50.87	1.02
TAF	1025.41	104.56	62.74	1.25
TAC	812.041	82.80	49.68	0.99
QSF	968.57	98.76	59.26	1.19
QSC	753.08	76.79	46.07	0.92
QAF	953.98	97.28	58.37	1.17
QAC	750.20	76.50	45.90	0.92

Table L4.1 Cost estimates of the required carbon-fiber, with a fiber volume fraction =60%.

L5. Production Methods

For comparison purposes, the following attempts at estimating the number of mold each scenario would require.

The following assumptions are made:

- Triangular sections have less shell-like element to produce (5 sub-spans with 3 walls, 15 pieces to produce and connect).
- Quadrilateral sections have less shell-like element to produce (5 sub-spans with 5 walls, 20 pieces to produce and connect).
- Top piece of the section:
 - For symmetric and asymmetric sections with a fixed-width deck of 2.8m (T1, T3, Q1, Q3), **1** mold is required the 5 top pieces.
 - For symmetric sections with a cantilevering deck (T2 and Q2), **3** mold are required the 5 top pieces.
 - For symmetric sections with a cantilevering deck (T4 and Q4), **5** mold are required the 5 top pieces.
- For the side pieces:
 - For shape symmetric triangular sections (T1, T3), **6** molds are required for the side pieces.
 - For shape symmetric quadrilateral sections (Q1, Q3), **10** molds are required for the side pieces.
- Bottom piece of the section:
 - Triangular sections have no bottom piece.
 - For symmetric quadrilateral sections (T1 and T2), **3** mold are required the bottom 5 pieces.
 - For asymmetric quadrilateral sections (T3 and T4), **5** mold are required the bottom 5 pieces

	Number of mold-top piece	Number of mold-side pieces	Number of mold-bottom pieces	Total number of mold
TSF	1	6	-	7
TSC	3	6	-	9
TAF	1	10	-	11
TAC	5	10	-	15
QSF	1	6	3	10
QSC	3	6	3	12
QAF	1	10	5	16
QAC	5	10	5	20

Table L5.1 Number of molds for each design scenario.

L6. Joint Design

Bonding is an important aspect of designing in FRP. The main principles of FRP connections are elaborated hereinafter as it will become important to configure viable connections between the different FRP elements. Further research and analysis will be required past the preliminary study phase. Two categories are distinguished in FRP: adhesive and mechanical.

1. Joint Design

Adhesive joints depend strongly on the design as well as good preparation. Examples of good and bad designs are shown in figure E1.1.

- A good adhesive is thus parallel and symmetrical to the line of action of the force acting on it, avoiding eccentricity.
 - Good adhesive joints are generally loaded in shear.
 - Stresses perpendicular to the adhesive joint, known as peel stresses, are to be prevented. Caused by perpendicular forces or secondary bending moment, they rely on the limited tensile strength of the joint.
- An adhesive joint depends on the length of the joint: the larger the design, the better.
- An adhesive joint also depends on the thickness. Generally, a fraction of millimeter thin, thicker adhesive layers ($t > 0.5\text{mm}$) can be used for bridges or wind turbine blades. A thicker layer allows to distribute stress concentration better internally. They are however more difficult to apply because of low viscosity of adhesives. Thicker adhesive joints can be a weakness in the design rendering the structure weaker.
- Peak stresses often occur at the edges of the adhesive joint because of the stiffness transition from the adhesive to the structural members. Such stiffness transitions can be reduced by matching the stiffness of the adhesive to the laminate as closely as possible. However, a flexible adhesive has the advantage of redistributing peak stresses faster [3].

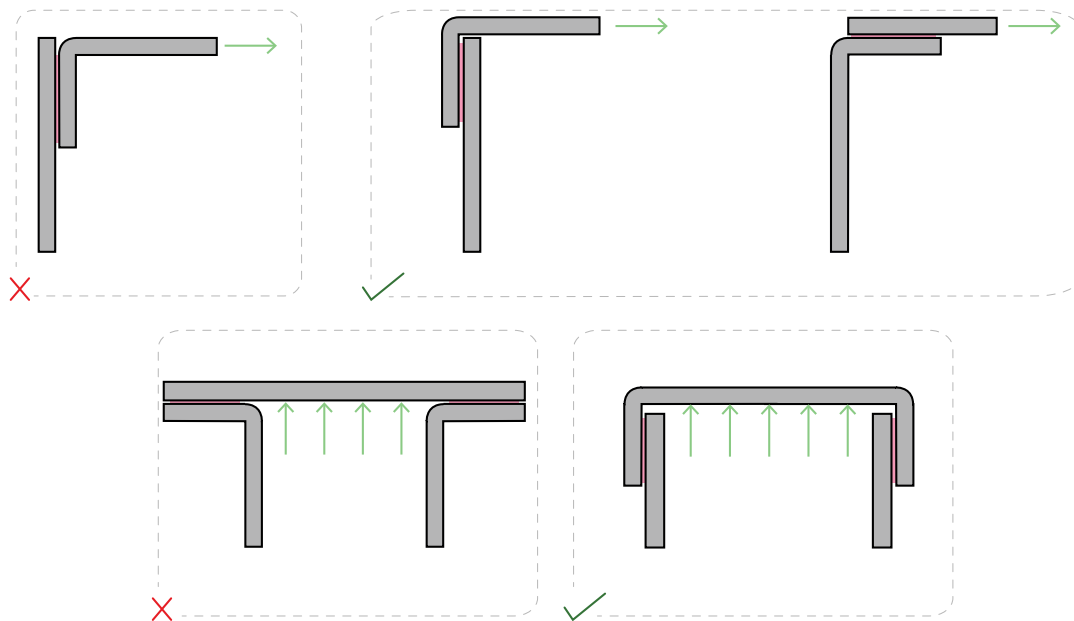


Figure L6.1 Schemes illustrating good and bad joint designs [3].

2. Failure of adhesive joints

The failure of an adhesive mechanism is either related to high stresses occurring or poor design. A distinction is made between adhesive and cohesive failure. It is however often that a mix of failures occurs.

- Adhesive failure occurs at the level of bonding, between the adhesive and the structural components to be bonded. An adhesive failure is identified if the connected components do not show any residual adhesive upon failure. Preventive measures can be applied to the adhesive layer, they include cleaning, drying, and degreasing the adhesive layer.
- A cohesive failure fracture occurs in the adhesive itself. The cohesion strength of a joint is determined by the type of adhesive, curing shrinkage, porosity of the adhesive layer due to solvent evaporation, entrapped air, and homogeneity and correct ratio of components. A cohesive failure indicates that the adhesive is weaker than the joint connecting the adhesive and structural component.

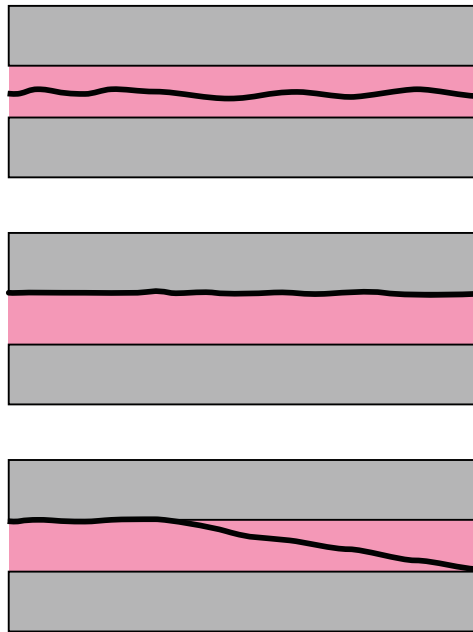


Figure L6. 2 Failure Types (from top to bottom) cohesive, adhesive, cohesive-adhesive [3].

3. Choice of adhesive joint:

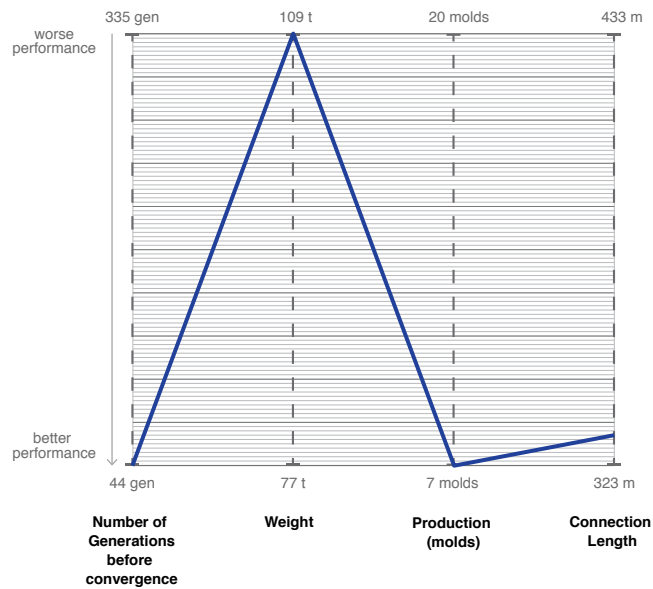
Important factors in deciding types of adhesive are: mechanical properties, processing methods, costs, and whether the adhesive is suited to the surfaces to be bonded.

- Three adhesive types are identified:
 - Thermoplastic adhesives
 - Mixed or two-component adhesives
 - Adhesive solutions

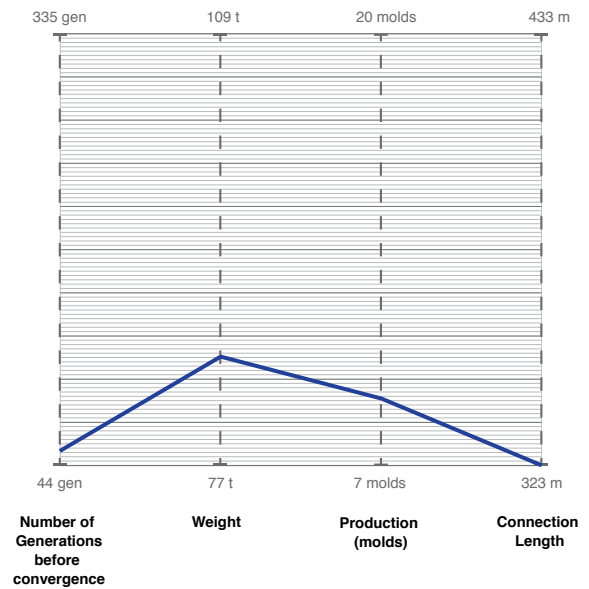
Referred to as “pin-loaded hole,” mechanical loaded joints require no adhesive. The introduction of holes in composite structures is consequential. This is mostly due to the surface pressure the pin can exert on the hole edge when loaded in the plane of the laminate. Stress concentrations also occur in the laminate, by a factor from 1.5 and as high as 7.

Appendix M

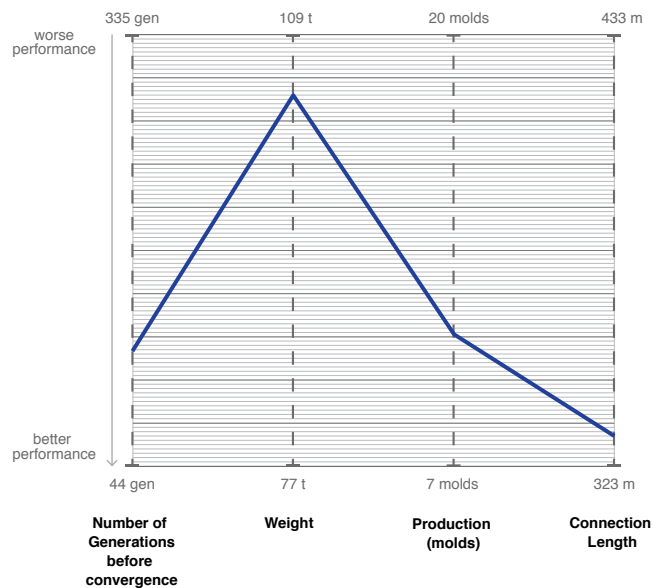
M1. Performance Graphs



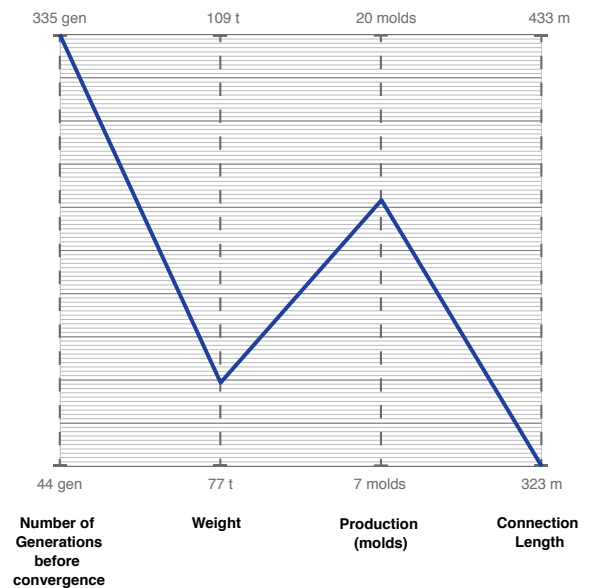
TSF



TSC

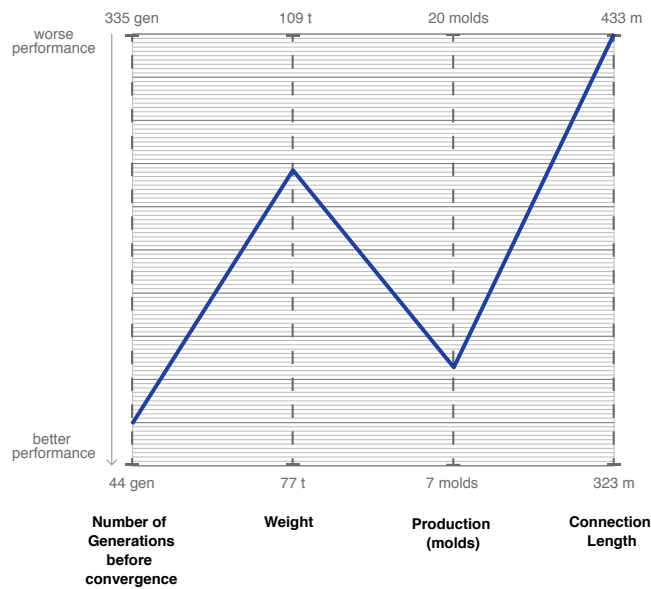


TAF

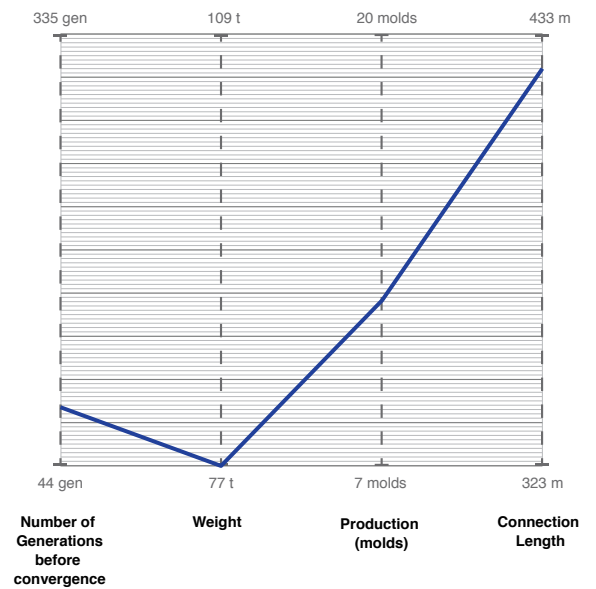


TAC

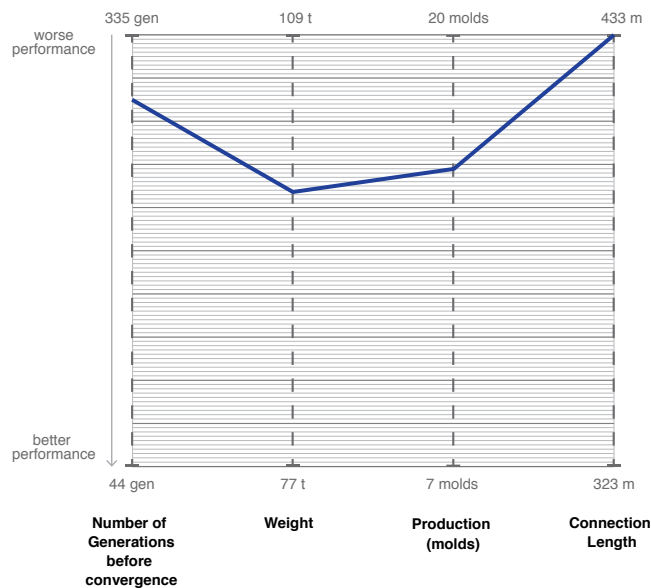
Figure M1.1 Graph summarizing the performance of the triangular cross-section geometries.



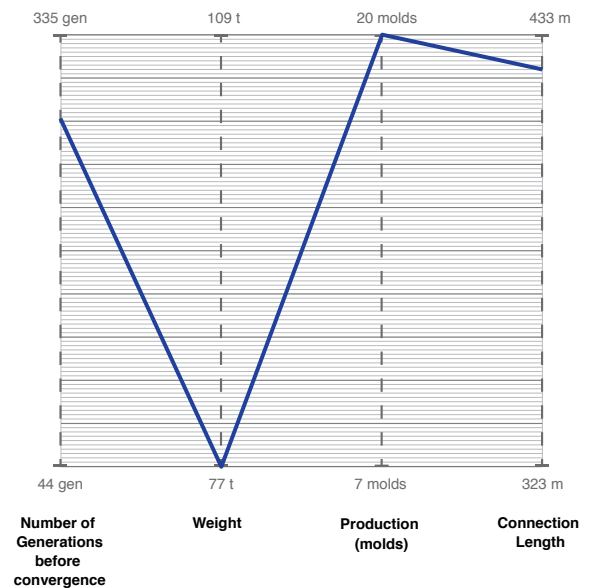
QSF



QSC



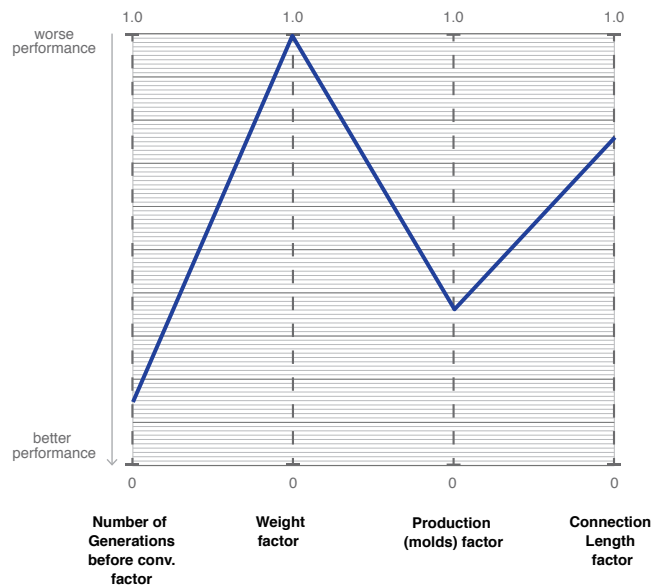
QAF



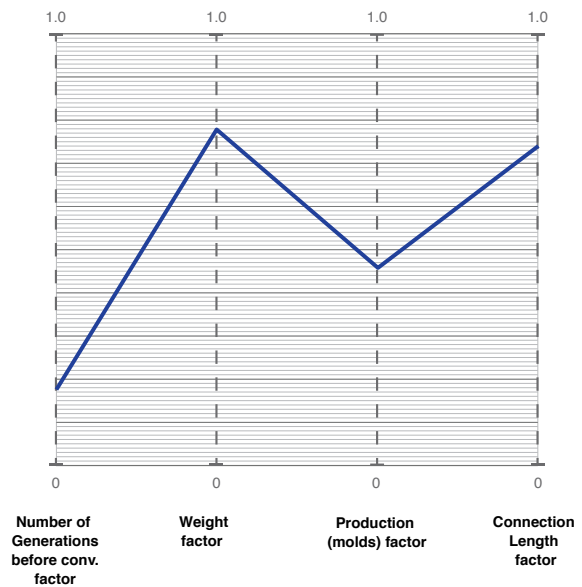
QAC

Figure M1.2 Graph summarizing the performance of the quadrilateral cross-section geometries.

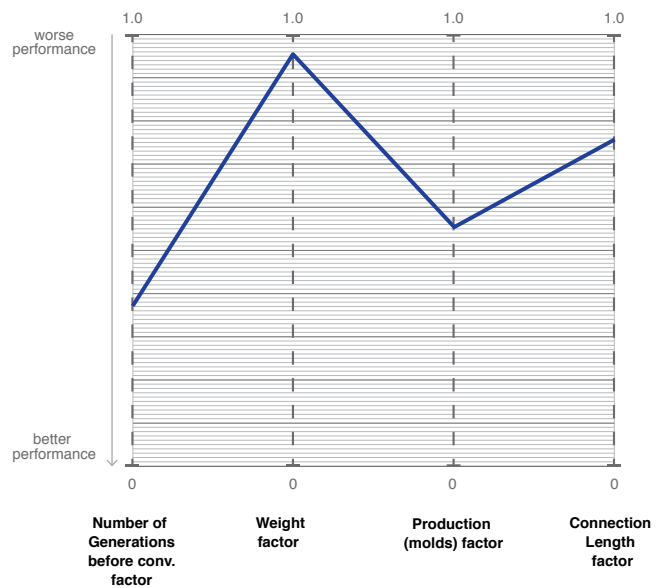
M2. Performance Graphs, using improvement factor



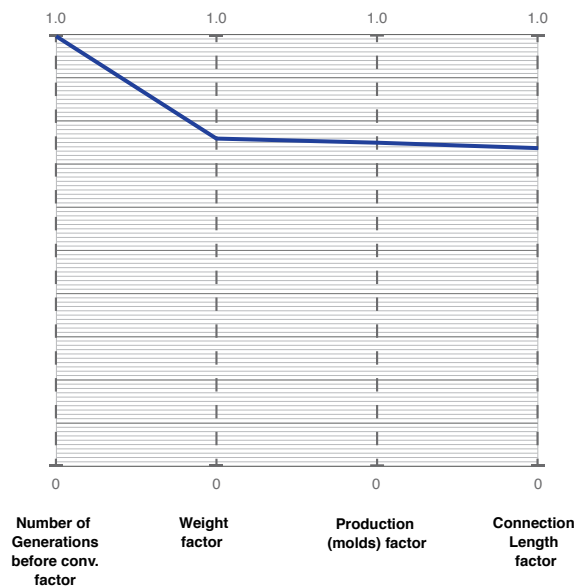
TSF



TSC

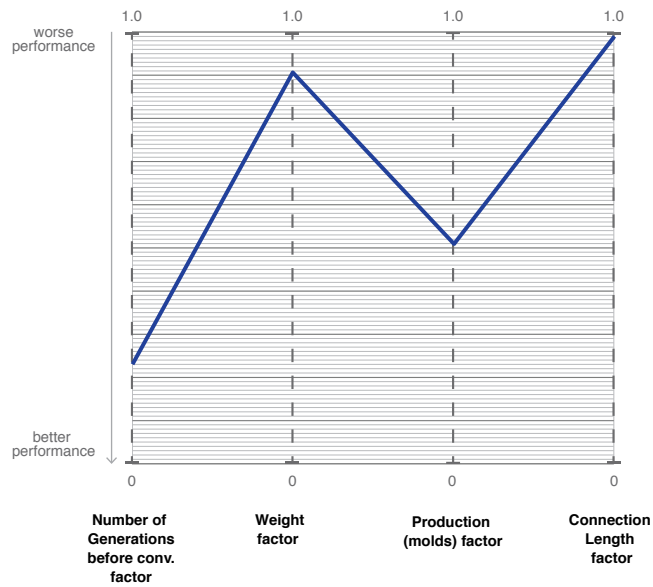


TAF

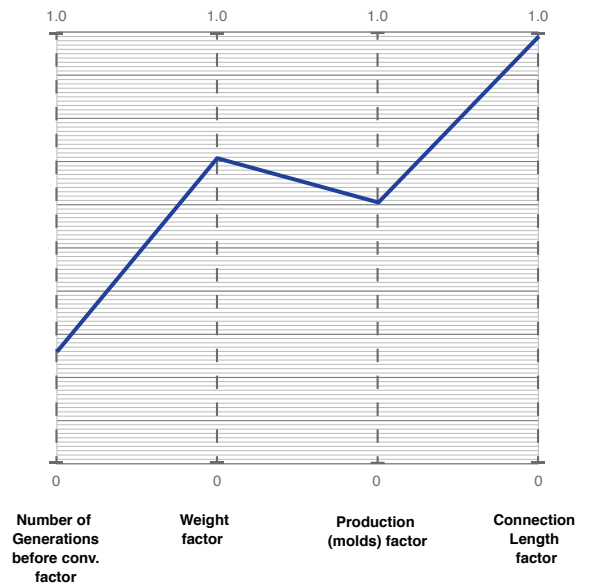


TAC

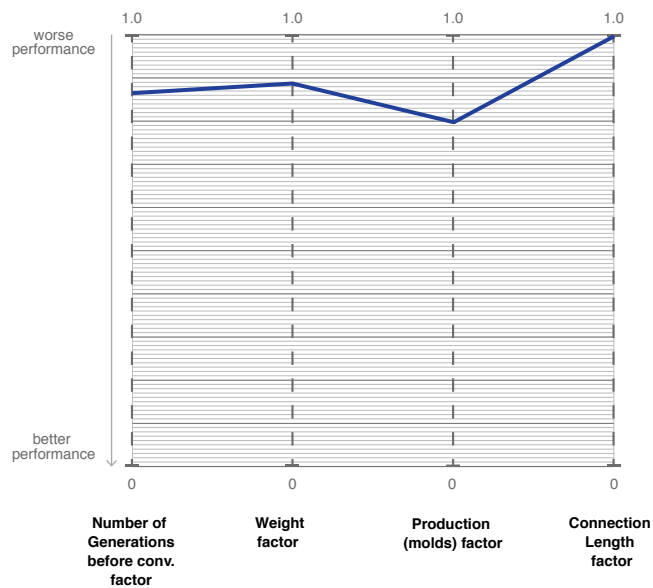
Figure M2.1 Graph summarizing the performance of the triangular cross-section geometry, using improvement factor.



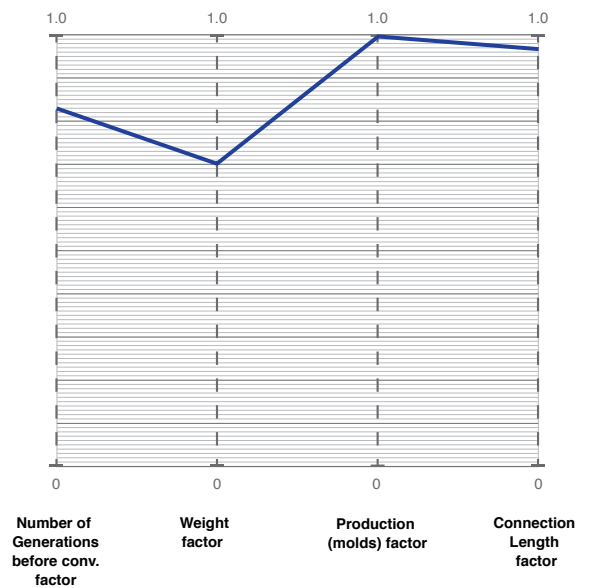
QSF



QSC



QAF



QAC

Figure M2.2 Graph summarizing the performance of the quadrilateral cross-section geometry, using improvement factor.